ANALYTICA CHIMICA ACTA

International monthly devoted to all branches of analytical chemistry
Revue mensuelle internationale consacrée à tous les domaines de la chimie analytique
Internationale Monatsschrift für alle Gebiete der analytischen Chemie

ELSEVIER PUBLISHING COMPANY
AMSTERDAM

Anal. Chim. Acta, Vol. 40, No. 1, 1–172, January 1968
Published monthly

ANALYTICA CHIMICA ACTA

GENERAL INFORMATION

Languages

Papers will be published in English, French or German.

Submission of papers

Papers should be sent to: Prof. PHILIP W. WEST, Coates Chemical Laboratories, College of Chemistry and Physics, Louisiana State University, Baton Rouge 3, La. 70803 (U.S.A.) or to

Dr. A. M. G. MACDONALD, Department of Chemistry, The University, P.O. Box 363, Birmingham 15 (Great Britain)

Manuscripts

Authors should submit two copies in double-spaced type with adequate margins on pages of uniform size. Acknowledgements, summary and references should be placed at the end of the paper.

Tables should be typed on separate pages and numbered in Roman numerals in the order in which they are mentioned in the text. All Tables should have descriptive titles. The use of chemical formulae and conventional abbreviations is encouraged in Tables and Figures but chemical formulae should not be used in the text unless they are necessary for clarity. Units of weight, volume, etc., when used with numerals should be abbreviated and unpunctuated (*e.g.*, 2%, 2 ml, 2 g, 2 μl, 2 μg, 2 ng, 2 cm, 200 mμ).

Figures should be drawn in Indian ink on drawing or tracing paper with all lettering in **thin** pencil. Standard symbols should be used in line drawings; the following are available to the printers:

▼ ▽ ■ □ ● ◎ ■ ◘ ⊖ ⧈ ▪ + ×

Photographs should be submitted as clear black and white glossy prints. Figures and photographs should be of the same size as the typed pages. Legends for figures should be **typed on a separate page**. Figures should be numbered in Arabic numerals in the order in which they are mentioned in the text.

References should be given at the end of the paper and should be numbered in the order of their appearance in the text (**not** arranged alphabetically). Abbreviations of journal titles should conform to those adopted by the *Chemical Abstracts List of Periodicals*, 1961 Edition and supplements. The recommended form for references to journal papers and books is as follows:

1. J. J. LINGANE AND A. M. HARTLEY, *Anal. Chim. Acta*, 11 (1954) 475.
2. F. FEIGL, *Spot Tests in Organic Analysis*, 7th Ed., Elsevier, Amsterdam, 1966, p. 516.

For multi-author references, **all** authors must be named, and initials given, in the reference list, although the use of, for example, SMITH *et al.*, is desirable in the text.

Summaries are published in English, French and German; authors must always provide a summary in the language of the paper, and are encouraged to supply translations where convenient. No summaries are needed for Short Communications.

Reprints

Fifty reprints will be supplied free of charge. Additional reprints (minimum 100) can be ordered at quoted prices. They must be ordered on order forms which are sent together with the proofs.

Publication

In 1968, Analytica Chimica Acta will have three issues to the volume, and four volumes will appear. Subscription prices: $ 17.50 or £ 6.6.— or Dfl. 63.— per volume; $70.00 or £ 25.4.0 or Dfl. 252.— per year, plus postage Additional cost for copies by airmail available on request. For subscribers in the U.S.A. and Canada, 2nd class postage paid at Jamaica, N.Y. For advertising rates apply to the publishers.

Subscriptions

Subscriptions should be sent to:

ELSEVIER PUBLISHING COMPANY, P.O. Box 211, Amsterdam, The Netherlands

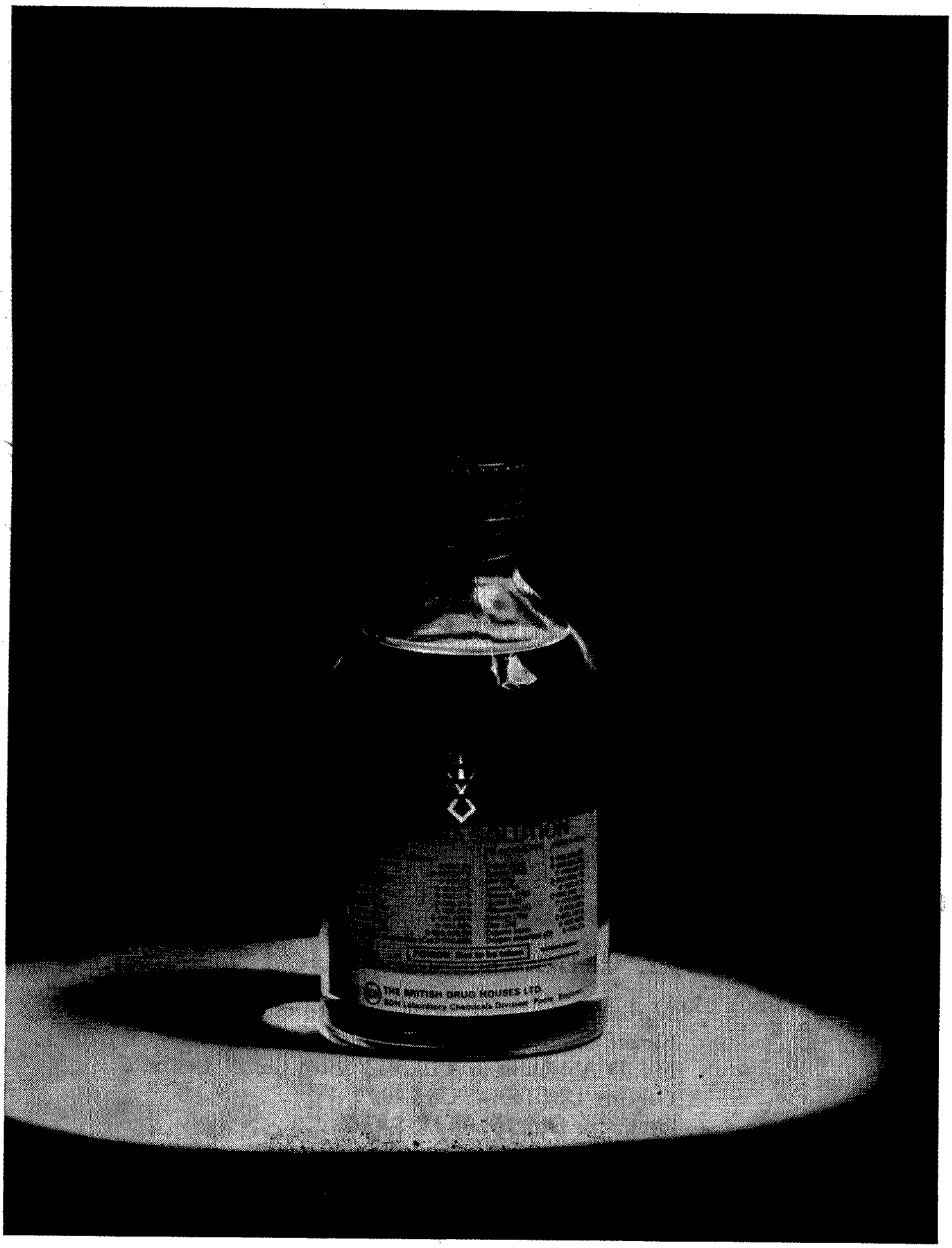
THE BRITISH DRUG HOUSES LTD.
BDH Laboratory Chemicals Division Poole England

PUBLISHER'S NOTE

Beginning with the present issue, North American subscribers to Analytica Chimica Acta will receive their copies by airmail. This step has been taken in order to ensure that publication is virtually simultaneous in Europe and in North America.

Combined with the fact that four volumes are to be published in 1968, this will mean that the "publication delay" will be drastically reduced.

SUMMARIES OF PAPERS PUBLISHED IN ANALYTICA CHIMICA ACTA

Vol. 40, No. 1, January 1968

SPECTROPHOTOMETRIC DETERMINATION OF TRACES OF PHOSPHORUS BY AN EXTRACTION METHOD

A general method is presented for the spectrophotometric determination of phosphorus at trace levels. It involves extraction of the yellow molybdophosphoric acid with isobutyl acetate and subsequent reduction to heteropoly blue. The method covers the range 0.2–20 μg of phosphorus. A comprehensive study of interferences using standard additions of 10 and 20 μg of phosphorus was carried out and modifications are described to permit the determination of phosphorus in a wide variety of metals and salts.

P. Pakalns,
Anal. Chim. Acta, 40 (1968) 1–12

A STUDY OF THE DIRECT SPECTROPHOTOMETRIC DETERMINATION OF FLUORIDE ION WITH THE CERIUM(III)–ALIZARIN FLUORINE BLUE COMPLEX

(in French)

Several workers have observed that the sensitivity of the cerium(III)–alizarin fluorine blue method for the spectrophotometric determination of microgram amounts of fluoride may be enhanced by addition of certain solvents. The present study proves that the use of an aqueous 25% v/v solution of dimethylsulfoxide, the most polar aprotic solvent, enhances to a maximum the sensitivity of the reaction and increases its speed. Two procedures, allowing the determination of 1–25 μg fluoride ion, are described: the best pH value is 4.1 and the spectrophotometric measurements are carried out at 625 or 630 nm. The interferences of 12 ions were studied.

M. Hanocq and L. Molle,
Anal. Chim. Acta, 40 (1968) 13–25

A VOLTAMMETRIC METHOD FOR FLUORIDE

A voltammetric method for the determination of micro amounts of fluoride is described. It is based on the measurement of the amount of free alizarin red S liberated by the fluoride ion from a zirconium–alizarin red S complex. The free dye measurement carried out at 0.7 V *vs.* S.C.E. depends on the anodic reaction of alizarin red S at the rotating pyrolytic graphite electrode. The method is simple, sensitive and suffers from relatively few interferences.

H. E. Zittel and T. M. Florence,
Anal. Chim. Acta, 40 (1968) 27–32

POTENTIOMETRIC TITRATIONS OF ORGANOTIN CHLORIDES WITH TETRAPHENYLARSONIUM CHLORIDE IN ACETONITRILE MEDIA

Tetraphenylarsonium chloride was used for the potentiometric titration of $R_{4-n}SnCl_n$ compounds (R = Me, Et, Pr, Bu, Ph; $n = 2,3$) in acetonitrile media. Evidence for penta-coordinated $R_{4-n}SnCl_{n+1}^-$ complexes was obtained. A stability scale as a function of R groups is given.

G. Tagliavini and P. Zanella,
Anal. Chim. Acta, 40 (1968) 33–39

THE SIMULTANEOUS DETERMINATION OF ALKALI AND ALKALINE-EARTH METALS BY PRECIPITATION TITRATION IN NON-AQUEOUS MEDIUM

(in German)

The precipitation titration of mixtures of alkali and alkaline-earth metals in ketonic media was investigated; the titrant was a solution of lithium chloride in ethanol or the ketone and the end-points were detected oscillometrically. Analyses of barium–sodium, barium–potassium and strontium–potassium mixtures were possible in methyl isobutyl ketone or acetone media. Acetone is the preferred medium because the precipitation equilibrium is reached very quickly, whereas a period of 15 min is needed in the case of methyl isobutyl ketone.

G. Henrion and E. Pungor,
Anal. Chim. Acta, 40 (1968) 41–48

TITRATIONS OF WEAK ACIDS IN 1,1,3,3-TETRAMETHYLGUANIDINE

The use of 1,1,3,3-tetramethylguanidine (TMG) as a medium for the titrations of weak acids has been investigated. The hydrogen electrode behaves reversibly in this solvent and can serve as an indicator electrode in titration reactions. The titrant was a 0.1 *M* solution of tetrabutylammonium hydroxide in a 90–10% mixture of TMG and methanol. A hydrogen electrode dipping into a TMG solution saturated with benzoic acid served as reference electrode. Potentiometric titrations of a number of weak acids gave results accurate to at least ±0.5%. It was found that in most cases curcumin could be used as an end-point indicator with an accuracy comparable to that of the potentiometric titration.

J. A. Caruso, G. G. Jones and A. I. Popov,
Anal. Chim. Acta, 40 (1968) 49–54

A POTENTIOMETRIC STUDY OF THE WATER-SOLUBLE SILVER(I) COMPLEXES OF N,N′-BIS(2-HYDROXYETHYL)DITHIO-OXAMIDE (HEDTO)

PART I. APPLICATION OF THE "CORE + LINKS" METHOD

Silver(I) forms with N,N′-bis(2-hydroxyethyl)dithio-oxamide (HEDTO) water-soluble complexes in acidic medium. The composition of these complexes may be represented by the following formula: $B(AB)_n$ in which B is the ligand and A the metal ion. There is some indication that complexes with general formula $(AB)_n$ also are formed.

L. C. van Poucke, M. A. Herman and Z. Eeckhaut,
Anal. Chim. Acta, 40 (1968) 55–63

QUANTITATIVE ELECTROCHEMICAL FORMATION OF PHOSPHOTUNGSTATE HETEROPOLYANION BLUES

The optical and ESR spectra of electrochemically reduced phosphotungstate and polyphosphotungstate anions in phosphoric acid were examined as quantitative functions of W^{5+} concentration. The optical spectra obey Beer–Lambert laws and are similar to the spectra of reduced silicotungstate anions, indicating the secondary nature of the central cluster in the KEGGIN structure with regard to interactions with the reducing electron. ESR spectra indicate an equivalent correspondence for the W^{5+} concentration and unpaired spins for the reduced polyphosphotungstate anion but for the reduced phosphotungstate anion monomer the unpaired spin concentration estimated by ESR was much lower than the W^{5+} concentration. Reacting reduced phosphotungstate anions with oxygen showed a 1-electron reduction of the oxygen molecule with concomitant oxidation of W^{5+} to W^{6+} and possibly production of high-molecular-weight, polyanion clusters.

P. STONEHART, J. G. KOREN AND J. S. BRINEN,
Anal. Chim. Acta, 40 (1968) 65–75

INTERPRETATION OF POLAROVOLTRIC AND BIPOTENTIOMETRIC CURVES: A NEW NOTATION SYSTEM

(in French)

The interpretation of titration curves is simplified by the concept of electrochemical electrode transitions with which are associated the symbols $\Delta E^{J \to L}_{A,e}$ for the anode, and $\Delta E^{J' \to L'}_{C,e}$ for the cathode. These transitions are derived from the Z–E plots, and represent the variation in potential at the electrode in passing from the family of curves J to the family of curves L in the case of the anode, or in passing from the family of curves J' to the family of curves L' in the case of the cathode. In addition, by using a numerical description of the electrode transitions where the variation in potential is represented by a sign and a relative magnitude given by the combination of two numbers and where the form of the curve at the equivalence point is described by simple formulae corresponding to reference curves, it is possible to classify the form of titration curves and their interpretation. The possible correlations among the members of a given family of compounds are simplified by the use of this new language. Examples are given in the case of the titration of dibasic organic acids in N,N-dimethylformamide.

J. E. DUBOIS ET P. C. LACAZE,
Anal. Chim. Acta, 40 (1968) 77–91

DETERMINATION OF EXTRACTION CONSTANTS OF METAL DIETHYLDITHIOCARBAMATES

The extraction of metal diethyldithiocarbamates (Mn, Fe, Co, Ni, Pd, Cu, Ag, Zn, Cd, Hg, In, Tl, Pb and Bi) into carbon tetrachloride was investigated in order to establish the extraction constants and two-phase stability constants. The order of extractability of these chelates was determined.

J. STARÝ AND K. KRATZER,
Anal Chim. Acta, 40 (1968) 93–100

FRACTIONAL SUBLIMATION OF THE β-DIKETONE CHELATES OF THE LANTHANIDE AND RELATED ELEMENTS

Various β-diketone chelates of Sc(III), Y(III), Th(IV), U(IV), U(VI), Zr(IV) and the lanthanides have been prepared, characterized and investigated to determine if they were volatile and stable. The ligands employed were acetylacetone(AA), trifluoroacetylacetone-(TFAA), hexafluoroacetylacetone(HFAA), and dipivaloylmethane-(DPM). The chelates were sublimed in a fractional vacuum sublimator and the recrystallization temperature zones recorded for individual chelates. None of the lanthanide acetylacetonates are volatile but the Sc(III), Th(IV), U(IV) and dioxouranium(VI) acetylacetonates are thermally stable and quite volatile below 150° at 1 mm mercury pressure. The lanthanide, Sc(III), Y(III), and dioxouranium(VI) trifluoroacetylacetonates are volatile and can be vacuum-sublimed below 150°, but are thermally unstable; only the Th(IV) chelate is sufficiently stable to be quantitatively recovered by sublimation. The Sc(III), Y(III), Th(IV), and lanthanide hexafluoroacetylacetonates are thermally stable and easily sublimed below 125° *in vacuo* or at atmospheric pressure. All the dipivaloylmethanates studied were thermally stable and volatile and could be quantitatively recovered by vacuum sublimation below 140°.

The volatility of the HFAA and DPM lanthanide chelates increased with an increase in atomic weight (a decrease in ionic radii) of the lanthanides. The lack of volatility observed for the lanthanide AA and TFAA chelates is attributed to the fact that only hydrates of the chelates were formed, which decomposed at elevated temperatures *in vacuo* to form basic polymeric compounds.

Separations are proposed for numerous binary mixtures of the β-diketone chelates of the lanthanide and related elements. Recrystallization temperature zones are given for the following binary mixtures which were quantitatively resolved by the fractional sublimation technique: 118–88° for Nd(DPM)$_3$ and 84–48° for Tm(DPM)$_3$; 72–49° for Sc(DPM) and 120–88° for Pr(DPM); 128–79° for La(DPM)$_3$ and 79–47° for Yb(DPM)$_3$; 70–47° for Th(TFAA)$_4$ and 116–96° for Gd-(TFAA)$_3$; 52–42° for Th(HFAA)$_4$ and 120–80° for La(HFAA)$_3$.

E. W. Berg and J. J. Chiang Acosta,
Anal. Chim. Acta, 40 (1968) 101–113

DETERMINATION OF ZIRCONIUM IN ZIRCONIUM-BEARING SAND AND ZIRCONIUM CONCENTRATES BY A NONDISPERSIVE X-RAY FLUORESCENCE METHOD

A nondispersive X-ray fluorescence method for the rapid, nondestructive determination of zirconium in zirconium-bearing sands and zirconium concentrates is described. A ^{109}Cd source of primary radiation and compact geometry for measurements were used. The matrix effect from iron and titanium in sands was eliminated by measuring the fluorescent radiation of zirconium and the scattered primary radiation, and interpreting the data with nomograms. For concentrates, dilution with pure sand and measurement of the ratio of fluorescence to scattered radiation were used to reduce a matrix effect; a calibration curve was then satisfactory. Particle size effects were avoided by grinding to below 70 μ.

B. Holyńska and L. Langer,
Anal. Chim. Acta, 40 (1968) 115–121

THE PRECISE DETERMINATION OF ^{239}Np FOR THE EVALUATION OF ^{238}U CAPTURE CROSS-SECTIONS AT VARYING NEUTRON ENERGIES IN A ZERO-ENERGY FAST REACTOR

A method is described for the determination of ^{239}Np in natural uranium metal foils irradiated in a zero-energy reactor. The foils are dissolved in nitric acid in the presence of ^{237}Np used for the determination of the yield of ^{239}Np. Neptunium is co-precipitated with lanthanum fluoride; lanthanum and thorium are removed by anion exchange in hydrochloric acid solution, and the neptunium is further purified by anion exchange in nitric acid solution. Sources for counting are prepared by direct evaporation of an aqueous solution onto a stainless steel disc. No corrections are necessary to the ^{237}Np α-count for absorption in the source. The method does not necessitate prior separation of daughter ^{233}Pa from the ^{237}Np tracer and gives sources of high purity in good yield.

R. S. LARGE AND L. P. O'CONNOR,
Anal. Chim. Acta, 40 (1968) 123–130

DETERMINATION OF THORIUM AND URANIUM IN BIOLOGICAL MATERIALS

An activation method for the determination of traces of thorium and uranium in various biological samples after wet digestion is described. The (n, γ) and β-decay products of both thorium and uranium were separated and measured. Modified radiochemical separation procedures for protactinium and neptunium activities are described. The method was applied to determination of thorium and uranium in urine, faeces, bone, blood, water and some chemicals.

M. PICER AND P. STROHAL,
Anal. Chim. Acta, 40 (1968) 131–136

DETERMINATION OF SUBMICROGRAM AMOUNTS OF SELENIUM(IV) BY MEANS OF THE CATALYTIC REDUCTION OF 1,4,6,11-TETRAAZANAPHTHACENE

In the presence of glyoxal and hypophosphorous acid 1,4,6,11-tetraazanaphthacene is reduced to 1,6-dihydro-1,4,6,11-tetraazanaphthacene. The reaction is catalyzed by selenium(IV). By means of this catalytic reaction, submicrogram amounts of selenium(IV) can easily be determined. The method is simple and sensitive, and there are few interferences.

T. KAWASHIMA AND M. TANAKA,
Anal. Chim. Acta, 40 (1968) 137–143

SEPARATION OF ALKALINE EARTH ELEMENTS BY CATION-EXCHANGE CHROMATOGRAPHY IN AMMONIUM MALONATE MEDIA

Be(II), Mg(II), Ca(II), Sr(II) and Ba(II) can be separated by elution from a cation-exchange column in the ammonium form with increasing concentrations of ammonium malonate. A typical elution sequence for a 60-ml column (volume in H^+-form) of AG50-X8 resin is: 200 ml of 0.20 N ammonium malonate plus 0.10 N malonic acid for Be(II); 300 ml of 0.50 N, 450 ml of 0.70 N, 350 ml of 1.10 N ammonium malonate for Mg(II), Ca(II) and Sr(II), respectively, and 200 ml of 3.0 N nitric acid for Ba(II). Separations are sharp and quantitative for element pairs in weight ratios from 1:1000 to 1000:1. Distribution coefficients, elution curves and quantitative separations are presented.

F. W. E. Strelow, C. R. Van Zyl and C. R. Nolte,
Anal. Chim. Acta, 40 (1968) 145–153

CHROMATOGRAPHY OF LEAF CHLOROPLAST PIGMENTS ON ION-EXCHANGE PAPERS

For the separation of leaf carotenoid pigments, some ion-exchange papers are more effective than pure cellulose papers. Separations of the major pigments on ion-exchange paper are superior to those obtained by uni-dimensional paper chromatography. For green-leaf extracts, ion-exchange papers offer no advantage. Ion-exchange columns do not separate the chloroplast pigments. On ion-exchange paper, there is no major yellow pigment in addition to neoxanthin, violaxanthin, lutein, and carotene.

J. Sherma and H. H. Strain,
Anal. Chim. Acta, 40 (1968) 155–159

SEPARATION AND DETERMINATION BY THIN-LAYER CHROMATOGRAPHY OF URONIC ACIDS AND THEIR LACTONES

(in German)

A new method for the separation of galacturonic, glucuronic, mannuronic and guluronic acid and the corresponding lactones by thin-layer chromatography is described. The determination of mixtures of galacturonic and glucuronic acid (1–50 μg) is described. Neutral monosaccharides up to 100 μg and lower concentrations of inorganic materials do not interfere with the separation.

W. Ernst,
Anal. Chim. Acta., 40 (1968) 161–166

ON THE FORM OF THE CURVES OF CONTINUOUS VARIATION

(Short Communication)

K. S. Klausen and F. J. Langmyhr,
Anal. Chim. Acta, 40 (1968) 167–169

THE SPECTROPHOTOMETRIC DETERMINATION OF HYPONITRITE

(Short Communication)

C. N. Polydoropoulos and S. D. Voliotis,
Anal. Chim. Acta, 40 (1968) 170–172

ANALYTICA CHIMICA ACTA

Vol. 40 (1968)

ANALYTICA CHIMICA ACTA

International monthly devoted to all branches of analytical chemistry
Revue mensuelle internationale consacrée à tous les domaines de la chimie analytique
Internationale Monatsschrift für alle Gebiete der analytischen Chemie

Editors
Philip W. West *(Baton Rouge, La., U.S.A.)*
A. M. G. Macdonald *(Birmingham, Great Britain)*

ELSEVIER PUBLISHING COMPANY
AMSTERDAM

Anal. Chim. Acta, Vol. 40 (1968)

PRINTED IN THE NETHERLANDS

Analytica Chimica Acta
Elsevier Publishing Company, Amsterdam
Printed in The Netherlands

SPECTROPHOTOMETRIC DETERMINATION OF TRACES OF PHOSPHORUS BY AN EXTRACTION METHOD

P. PAKALNS
Australian Atomic Energy Commission Research Establishment, Lucas Heights, N.S.W. (Australia)

(Received June 16th, 1967)

Reviews by BOLTZ AND LUECK[1] and RIEMAN AND BEUKENKAMP[2] show that many methods have been proposed for the determination of traces of phosphorus by extracting the yellow molybdophosphoric acid with an immiscible solvent, and then reducing to the heteropoly blue by shaking the extract with a reductant. These methods have been primarily concerned with the determination of traces of phosphorus in biological or needle-biopsy samples where the concentration of interfering ions is negligible and the salt effect is low. An extraction method for the determination of phosphorus in carbon steels was proposed by LUECK AND BOLTZ[3] and subsequently LOUNAMAA AND FUGMANN[4] modified the method to permit the determination of phosphorus in alloy steels. Both methods require that all salts be converted to perchlorates, and that silicon and arsenic be volatilised as the tetrafluoride and bromide, respectively.

Alcohols or alcohol–solvent mixtures have been used for the extraction of the yellow molybdophosphoric acid. PAUL[5,6] has shown that a selective separation from the yellow silicomolybdate and the yellow arsenomolybdate can be carried out by extracting the yellow molybdophosphoric acid with isobutyl acetate.

UMLAND AND WUENSCH[7] have described a very sensitive method for the indirect spectrophotometric determination of phosphorus by determining the molybdenum in the dodecamolybdatophosphoric acid. This method is limited to aqueous solutions having an acidity of 0.4 N with respect to hydrochloric acid.

The present paper describes a detailed investigation of the determination of phosphorus at trace levels in many metals and their salts, involving a preliminary extraction of the yellow molybdophosphoric acid with isobutyl acetate and subsequent reduction to heteropoly blue. This procedure permits the determination of phosphorus without a preliminary separation from silicon or arsenic, and is simpler and more precise than the standard molybdate-magnesia or alkalimetric methods. Hydroxylamine hydrochloride was used when oxidizing acids were present or when phosphorus had to be determined in certain oxidizing agents (e.g. dichromate, permanganate and ceric salts). The method is applicable to the determination of phosphorus in waters and in many metals, salts or alloys.

EXPERIMENTAL

Apparatus and reagents

A Unicam SP 600 spectrophotometer with 2-cm glass cuvettes was used.

pH meter. E.I.L. Model 23A direct reading pH meter. For low pH work new glass electrodes must be left in 1 *N* hydrochloric acid for 24 hours.

Distilled water. Demineralized water, further purified by a single distillation in the presence of permanganate, was used throughout.

Standard phosphorus solution. Prepare a stock solution containing 0.1 mg P/ml by dissolving 0.4395 g of potassium dihydrogen phosphate in 1000 ml of water. Prepare a working solution (2 µg P/ml) by diluting 5 ml of stock solution to 250 ml.

Ammonium molybdate solution (5%). Prepare from $(NH_4)_6Mo_7O_{24}\cdot 4H_2O$ and store in a polythene bottle.

Acid ammonium molybdate solution (pH 0.5). Add 11.6 ml of 9 *N* sulphuric acid to 100 ml of ammonium molybdate solution.

Tin(II) chloride solution. Dissolve 10 g of $SnCl_2\cdot 2H_2O$ in 25 ml of hydrochloric acid.

Reducing solution. Dissolve 1.3 g of ascorbic acid in 20 ml of water, add 1.3 ml of tin(II) chloride solution and 15 ml of 9 *N* sulphuric acid and dilute to 100 ml.

Isobutyl acetate (May and Baker Ltd.). Boiling range 115°–120°.

Recommended procedure

Transfer an aliquot of the acidic sample solution (0–15 µg P) to a 200-ml polythene beaker. Dilute with water to 25 ml. Adjust the pH to 0.35 using 9 *N* sulphuric acid or ammonia. Add 10 ml of 5% ammonium molybdate solution and let stand for 10 min. Add 2.5 ml of 9 *N* sulphuric acid. Transfer to a 100-ml separating funnel and adjust the volume to 50 ml with water. Add 8 ml of isobutyl acetate, shake for 1 min and let stand for 5 min. Run the aqueous layer into a beaker and transfer the organic phase to a 50-ml separating funnel. Repeat the extraction with 5 ml of isobutyl acetate shaking only for 30 sec. Swirl the combined organic extracts to dislodge any water droplets, then remove aqueous phase, taking care that it is also removed from the bore of the stopcock. Add 3 ml of reducing solution to the organic phase, shake for 45 sec and let stand for 5 min.

Run the contents of the funnel into a dry 25-ml volumetric flask, wash the funnel with methanol, and add the washings to the flask. Mix and dilute to volume with methanol. Measure the absorbance after 10 min against a blank at 725 nm in 2-cm cells.

Always make a standard addition of 10 µg of phosphorus.

DISCUSSION

Solvent extraction

Isoamyl acetate and isobutyl acetate were considered as solvents for the extraction of the yellow molybdophosphoric acid. Isobutyl acetate was selected, because isoamyl acetate extracted less of the yellow complex at higher phosphorus concentrations than at lower levels.

It is necessary to do two extractions, one with 8 ml and one with 5 ml of isobutyl acetate, because one extraction with 13 ml of solvent extracts only 95% of the yellow complex. The total amount of isobutyl acetate should not exceed 13 ml, otherwise it is not miscible with 3 ml of reducing solution when diluted to 25 ml with methanol.

Sensitivity and stability of the method

The heteropoly blue complex formed in the isobutyl acetate phase gives an absorbance peak at 725 nm, when measured against a blank. The molar absorptivity of the blue complex is 1.63×10^4, corresponding to 0.0019 μg P/cm^2 on the Sandell scale, but the molar absorptivity rises to 2.05×10^4 when phosphorus is determined in iron(III) nitrate solutions. Even submilligram amounts of iron in sample aliquots enhance the absorbance, and amounts of iron above 1 mg lead to a constant absorbance of 0.520 for 10 μg of phosphorus. Beer's law is obeyed to 1.2 μg P/ml. Solutions containing up to 20 μg of phosphorus were used, but the range can be extended to 30 μg of phosphorus by using 1-cm cells.

The heteropoly blue complex in isobutyl acetate–methanol solution is stable in the investigated temperature range 22°–28° for at least 24 h. The colour of heteropoly blue, separated from copper solutions, is stable for 1 h, but the absorbance increases slowly when sample aliquots containing iron(III) have been used, and the absorbance must be measured within 30 min of mixing. Hydroxylamine hydrochloride, being a relatively weak reducing agent compared to tin(II) chloride, does not interfere with the colour development.

The absorbance of the extracted blue complex does not change in the investigated temperature range 22°–28°.

Choice of pH and the effect of varying reagent concentrations

A constant absorbance for the heteropoly blue was obtained when the yellow molybdophosphoric acid was formed in the investigated range of pH 0.1–4.0. After pH adjustment a development time of 5 min was sufficient, but if larger amounts of salts or boric acid are present a waiting time of 10 min is recommended. A final pH of 0.45, after ammonium molybdate addition, was found satisfactory even in the presence of large amounts of sulphates (Fig. 1).

Varying amounts of 9 *N* sulphuric acid were added to the solutions before extraction, and it was found that constant recoveries were obtained when the total amount of 9 *N* sulphuric acid was between 5.0 and 8.0 ml in a 50-ml volume. When the volume before extraction was 65 ml, the total amount of 9 *N* sulphuric acid necessary for constant recoveries was between 6.5 and 9.0 ml. Large numbers of experiments with different salts and acids indicated the correct amounts of 9 *N* sulphuric acid which had to be added before extraction, and the relationship between the measured pH after ammonium molybdate addition and the required amount of 9 *N* sulphuric acid is given in Table I. The correct results were also obtained when the amounts of sulphuric acid recommended in Table I were added to solutions containing no sulphates (e.g. brass and steel samples).

It is important that all of the aqueous phase be removed, even from the bore of the stopcock, otherwise metal ions, when present in higher concentrations, especially iron and copper, will interfere with the reduction.

The reducing solution was carefully balanced with respect to the ascorbic acid and total acidity. The specified amounts of ascorbic acid and sulphuric acid in the reducing solution were found experimentally to complex trace amounts of iron and copper contained in the organic phase. Without the addition of ascorbic acid to the reducing solution varying trace amounts of iron and copper interfered by reducing the stability of the heteropoly blue complex causing a gradual drop in the absorbance.

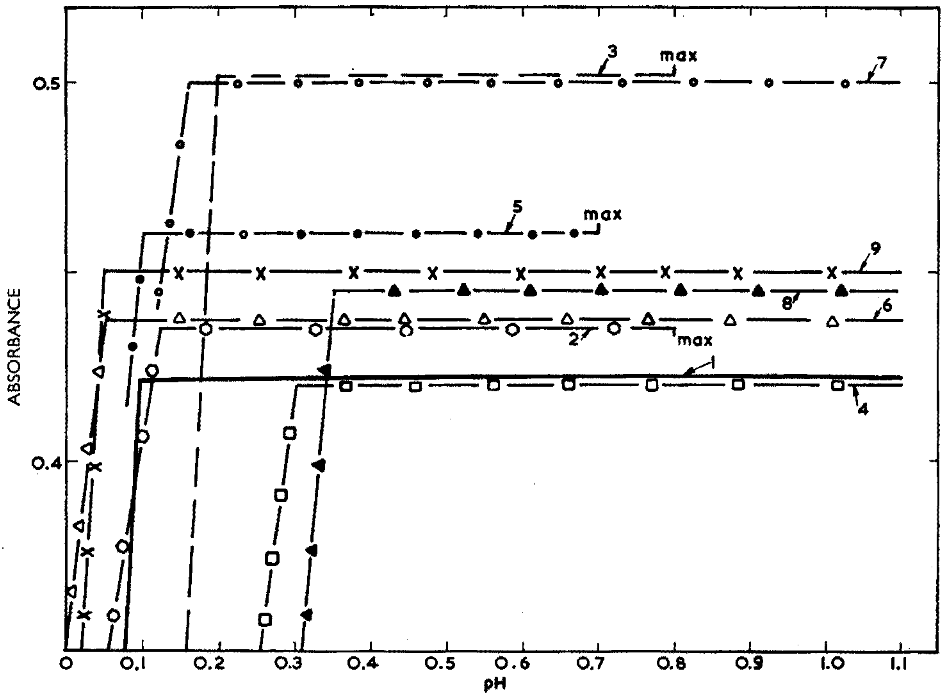

Fig. 1. Effect of salts and pH after ammonium molybdate addition on the absorbance (10 µg P/25 ml). Salts added: (1) standard curve; (2) NH_4Cl, 2.0 g; (3) NH_4NO_3, 2.0 g; (4) $(NH_4)_2SO_4$, 1.0 g; (5) NH_4ClO_4, 2.0 g; (6) NaCl, 2.0 g; (7) $NaNO_3$, 2.0 g; (8) Na_2SO_4, 1.5 g; (9) $NaClO_4$, 2.0 g.

TABLE I

THE RELATIONSHIP OF pH, AFTER AMMONIUM MOLYBDATE ADDITION, AND THE AMOUNT OF 9 *N* H_2SO_4 ADDED BEFORE EXTRACTION

pH	*Required volume of 9 N H_2SO_4 (ml)*^{a,b,c}	
	25 ml initial volume, 50 ml final volume	*40 ml initial volume, 65 ml final volume*
0.9–4.0	5.5	6.5
0.8	4.5	5.5
0.7	4.0	4.5
0.6	3.5	3.5
0.5	3.0	2.5
0.4	2.5	1.0
0.3	1.5	nil
0.25	0.5	nil
0.10	nil	nil

[a] For sulphates, except for $(NH_4)_2SO_4$, add 0.5 ml less.

[b] For $(NH_4)_2SO_4$ add less 9 *N* H_2SO_4 to compensate for the sulphate in the salt.

[c] Add 0.5 ml less of 9 *N* H_2SO_4 for each 0.1 ml of 40% HF in excess of 0.1 ml of 40% HF.

Although it was found that a reducing solution prepared wholly in the hydrochloric acid media gave higher absorbance, the stability of the heteropoly blue was very low.

Standard addition

The change in absorbance depended on the cations or anions added. Figure 1 and Table II show that nitrates gave the highest absorbance of all anions and that iron and copper enhanced the colour of the heteropoly blue. Therefore, it is impossible to use a standard curve, but a standard addition must be made for each determination,

TABLE II

EFFECT OF VARIOUS ELEMENTS

(Standard addition of 10 and 20 μg of P)

Foreign ion	*Amount taken (g)*	*As salt*[b]	*Absorbance (10 μg P)*	*pH after $(NH_4)_2MoO_4$ addition*	*P as PO_4^{3-} in salt (p.p.m.)*
None	—	—	0.420	0.1–4.0	
Al^{3+}	0.5	$Al(NO_3)_3 \cdot 9\ H_2O$	0.520	0.4	0.05
BO_3^{3-}	0.3	H_3BO_3	0.420	min.0.12	
Be^{2+}	0.2	$BeSO_4 \cdot 4\ H_2O$	0.425	0.45	
Ce^{4+} [c]	0.5	$(NH_4)_2Ce(NO_3)_6$	0.530	0.45	2.6
Co^{2+}	0.1	$CoCl_2 \cdot 6\ H_2O$	0.410	0.5	30.5
Cr^{3+}	0.5	$CrCl_3 \cdot 6\ H_2O$	0.445	0.5	
Cu^{2+} [d]	0.5	$Cu(NO_3)_2 \cdot 3\ H_2O$	0.530	0.45	1.3
Cu^{2+}	0.25[a]	$CuSO_4 \cdot 5\ H_2O$	0.470	0.45–0.8	
Cu^{2+}	0.5[e]	$CuSO_4 \cdot 5\ H_2O$	0.470	0.45–0.8	
F^- [f]	0.040	HF	0.420	min.0.17	
F^- [f]	0.080	HF	0.420	min.0.23	
F^- [f]	0.120	HF	0.420	min.0.26	
Fe^{3+} [g]	0.5	$FeCl_3$(60% soln.)	0.530	0.3–0.5	0.8
Fe^{3+}	0.1	$Fe(NO_3)_3 \cdot 9\ H_2O$	0.520	0.4	
Fe^{3+} [g]	0.5	$Fe(NO_3)_3 \cdot 9\ H_2O$	0.485	0.3–0.5	1.0
Mn^{2+} [h]	0.25	$KMnO_4$	0.420	0.5	0.3
Ni^{2+}	0.25[a]	$NiSO_4 \cdot 6\ H_2O$	0.415	0.45–0.8	
Ni^{2+}	0.5[e]	$NiSO_4 \cdot 6\ H_2O$	0.415	0.45–0.8	
Th^{4+}	0.5	$Th(NO_3)_4 \cdot 4\ H_2O$.	0.480	0.45	4.1
Ti^{4+} [i]	0.0005[a]	$Ti(SO_4)_2$ soln.	0.400	0.4	
U(VI)	0.5	$UO_2(NO_3)_2 \cdot 6\ H_2O$	0.490	0.25–0.7	0.4
V(V)[j]	0.01	NH_4VO_3	0.460	min.0.35	
W(VI)	0.0005[a]	$Na_2WO_4 \cdot 2\ H_2O$	0.440	0.45	
Zr^{4+} [k]	0.2	$ZrOCl_2 \cdot 8\ H_2O$	0.390	0.45	3.0
NaCl	2.0	—	0.435	min.0.05	
$NaClO_4$	2.0	—	0.450	min.0.05	
$NaNO_3$	2.0	—	0.500	min.0.17	
Na_2SO_4	1.5[a]	—	0.445	min.0.35	
NH_4Cl	2.0	—	0.435	0.12–0.8	
NH_4ClO_4	2.0	$NH_4OH + HClO_4$	0.460	0.10–0.7	
NH_4NO_3	2.0	—	0.500	0.10–0.8	
$(NH_4)_2SO_4$	1.0[a]	—	0.420	min.0.3	
$H_2C_4H_4O_6$	0.20[a]	—	0.430	0.45	
$NH_2OH \cdot HCl$	0.5	—	0.435	min.0.3	
As(V)	1 mg	$Na_3AsO_4 \cdot 12\ H_2O$	1.0 μg P[l]	0.3–0.7	
Si(IV)	1 mg	Na_2SiO_3	0.1 μg P[l]	0.5	
Si(IV)	5 mg	Na_2SiO_3	0.1 μg P[l]	0.3	

[a] Maximum permissible amount of ion per determination. [b] Add 1 ml 10% $NH_2OH \cdot HCl$ to all salts when as nitrates or perchlorates. [c] Add 1 ml 10% $NH_2OH \cdot HCl$. [d] Add 11.6 ml of acid $(NH_4)_2MoO_4$. [e] Initial volume 40 ml (before ammonium molybdate addition). [f] Add 7.5 ml 4% H_3BO_3. [g] Initial volume 30 ml. Adjust pH to 0.3. Add 20 ml $(NH_4)_2MoO_4$. [h] Add 5 ml 10% $NH_2OH \cdot HCl$. [i] Add 0.1 ml 40% HF, boil and add 7.5 ml 4% H_3BO_3. [j] Adjust pH to 3.5, add 1 ml 10% $NH_2OH \cdot HCl$, boil, cool and add $(NH_4)_2MoO_4$. [k] Add 0.2 ml of 40% HF for every 0.1 g of Zr, acidify with 9 *N* H_2SO_4, bring to boil and add 7.5 ml 4% H_3BO_3. [l] Absorbance equivalent to μg of P.

with a provision that the pH for the formation of the yellow complex be strictly controlled. The proportionality of the absorbances for the standard addition of 10 and 20 μg of phosphorus was the criterion used to establish the feasibility of the method under various conditions. Tolerance levels were established for various ions and salts using the standard addition procedure. For reasons explained above, the results were not expressed as per-cent recoveries, but as absorbance per 10 μg of phosphorus (Table II).

Blanks and corrections

The absorbance of the blanks was about 0.018 and this could be attributed to the isobutyl acetate and reducing solution. Inorganic acids used for dissolution (hydrofluoric acid, and boric acid) all caused only a slight increase in blank values.

Study of interferences

Few modifications were necessary for determining phosphorus in the presence of many of the cations and anions, because of the low pH range selected for the formation of the yellow molybdophosphoric acid. However, some modifications are necessary when the following ions are present: Ce^{4+}, Cu^{2+}, F^-, Fe^{3+}, Ti^{4+}, Th^4, V^{5+}, Zr^{4+}.

Sodium salts in excess of 2 g can be tolerated in the aqueous phase. However, when ammonia salts are analysed, an acid-insoluble precipitate forms, and the maximum pH is 0.7 for 2 g of ammonium perchlorate, 0.8 for 2 g ammonium chloride or 2 g of ammonium nitrate but the range can be extended to at least 1.5 for 1 g of ammonium sulphate (Fig. 1).

Arsenic interferes slightly, and in the investigated pH range (pH 0.3–0.7) 1 mg of arsenic(V) produced a colour equivalent to 1 μg of phosphorus.

Cerium must be present in the reduced state (cerium(III)) which can be accomplished by means of hydroxylamine hydrochloride.

Copper sulphate interferes with the determination of phosphorus when the amount of copper ion exceeds 250 mg, and the optimum pH after ammonium molybdate addition is between 0.45 and 0.8. The initial volume must be increased to 40 ml when sample aliquots containing larger amounts of copper sulphate are used. When hydroxylamine hydrochloride has been added to solutions containing copper, the preliminary pH must be adjusted so that after acid ammonium molybdate addition (from a pipette, with stirring) the correct pH is obtained. When ammonia is used to adjust the pH, hydroxylamine hydrochloride must be added after the ammonia addition.

Hydrofluoric acid may be necessary for dissolution of some metal samples and to hold cations in solution during the formation of the yellow phosphomolybdate (zirconium, tungsten, titanium and niobium). Boric acid is added to complex any free fluoride before the use of glass electrodes for the pH adjustment. The effect of varying amounts of hydrofluoric and boric acids and salts on the pH, after ammonium molybdate addition, is shown in Table III.

Iron does not form a visible precipitate with ammonium molybdate, but the amount of ammonium molybdate must be increased to 20 ml when more than 100 mg of iron(III) is present in the sample aliquot. When hydroxylamine hydrochloride has been added to solutions containing iron, the preliminary pH adjustment must be such that after ammonium molybdate addition the correct pH is obtained. A delay of 15 min must be allowed after mixing before the absorbance is read.

Silicon interference is negligible because the yellow molybdophosphoric acid is formed at a much lower pH than is necessary for the formation of the yellow silicomolybdate complex[8].

TABLE III

MINIMUM pH REQUIRED TO OBTAIN MAXIMUM ABSORBANCE, AFTER AMMONIUM MOLYBDATE ADDITION, IN THE PRESENCE OF VARYING CONCENTRATIONS OF HF, H_3BO_3 AND SALTS

40% HF (ml)	*4% H_3BO_3 (ml)*	*Salt added*	*Min. pH*	*Absorbance (10 µg P)*
—	7.5	—	0.10	0.420
0.1	7.5	—	0.17	0.420
0.1	7.5	2.0 g NH_4NO_3	0.25	0.500
0.1	7.5	1.0 g $(NH_4)_2SO_4$	0.35	0.420
0.2	7.5	—	0.23	0.420
0.3	7.5	—	0.26	0.420

Tartaric acid causes an interference which increases with increasing pH. At a pH of 0.45 a maximum amount of 200 mg of tartaric acid can be present in the sample aliquot.

Thorium solutions containing no sulphate ion form precipitates during the adjustment of the pH. This can be overcome by adding 1 g of sodium sulphate to the sample aliquot for each 0.25 g of thorium.

Titanium interferes seriously, and only 500 µg of titanium can be tolerated. Hydrofluoric acid (0.1 ml of 40% HF) must be added to mask titanium. The addition of larger amounts of hydrofluoric acid is recommended when sample aliquots containing other cations are analysed.

Tungsten interferes seriously and only 500 µg of tungsten can be tolerated in a sample aliquot.

Vanadium(V) must be reduced to vanadium(IV) to overcome the formation of vanadophosphoric acid. Add 1 ml of 10% hydroxylamine hydrochloride solution and bring the solution to the boil. Then cool, add ammonium molybdate with stirring, and continue as in the recommended procedure.

Zirconium can be held in solution with fluoride ion (0.2 g of zirconium requires 0.4 ml of 40% HF). Solutions containing phosphate and zirconium must be boiled with hydrofluoric acid in a Teflon beaker to form zirconium fluoride complex and thus release phosphate for the reaction with molybdate.

Hydroxylamine hydrochloride was used in the modified procedure to allow the determination of phosphorus in the presence of cerium and vanadium, in solutions containing nitrates, perchlorates or oxidizing agents, and in oxidizing reagents such as potassium permanganate and potassium dichromate. It is recommended that 1 ml of 10% hydroxylamine hydrochloride be used as a general reducing agent to reduce any oxidizing agents in solution.

Reproducibility of the method

Readings on a series of 10 standards showed the relative standard deviation at the 0.4 µg P/ml level to be ± 0.8%.

APPLICATIONS

The results obtained for a variety of materials are shown in Table IV.

General precautions

The pH after ammonium molybdate addition should be noted; and the amount of 9 *N* sulphuric acid to be added before extraction is as given in Table I.

Aluminium metal or alloys must be dissolved in sodium hydroxide, because dissolution in mixed acid produces low results.

TABLE IV

SPECTROPHOTOMETRIC DETERMINATION OF PHOSPHORUS IN VARIOUS MATERIALS

Sample	*Certificated P (%)*	*P found (%)*	*Absorbance on standard addition (10 μg P)*
Aluminium alloy "A" BCS 181	—	0.0012	0.520
Manganese brass BCS 179	0.06 (one value)	0.0575	0.510
Bronze "A" BCS 183	0.25 (Range 0.22–0.26)	0.244	0.440
Cupro Nickel "A" BCS 180	—	0.0014	0.485
Pure iron BCS 149/2	0.006 (Range 0.004–0.007)	0.0050	0.510
Ni–Cr–Mo–steel BCS 225/1	0.019 (Range 0.018–0.020)	0.0180	0.530
Cr–V–steel BCS 224	0.012 (Range 0.010–0.013)	0.0106	0.445
"18-8" stainless steel + Ti BCS 235/1	0.020 (Range 0.018–0.022)	0.0196	0.505
High speed steel (6W–1.9V) SAA 101	0.037–0.038	0.0368	0.470
Turbine steel (6W–3Nb) SAA 125	0.033	0.0322	0.465
Permanent magnet alloy BCS 233	—	0.0137	0.405
Ferro–molybdenum	0.08	0.0960	0.455
BCS 231/2	(Range 0.08–0.09)	0.0968	0.455[a]
Ferro–manganese BCS 208	0.237 (Range 0.230–0.248)	0.248	0.430
Ferro–vanadium BCS 205	0.055 (one value)	0.0349	0.445
Nickel crucible (pure)	—	0.0009	0.515[b]
Thorium metal	—	$<$ 0.0004	0.470[c]
Thoria (precipitated)	—	$<$ 0.0003	0.475[c]
U_3O_8 (comm.)	—	0.0003	0.485[d]
Uranium metal	—	0.0002	0.520[d]
Zirconium metal (comm.)	—	$<$ 0.0003	0.510[e]
Zircaloy	—	$<$ 0.0004	0.515[e]

---

[a] Determined after double ammonia separation; analysed to ASTM E 31-47 para. 79 (1956).

[b] Dissolve 1 g in 15 ml (1:1) HNO_3, 0.5 ml 40% HF, and oxidize with $KMnO_4$.

[c] Dissolve 1 g in 20 ml H_2O, 5 ml HNO_3, 0.1 ml 40% HF, and oxidize with $KMnO_4$. Add 1 g Na_2SO_4 per 0.25 g Th.

[d] Dissolve 2 g in 20 ml H_2O, 5 ml HNO_3, 5 ml HCl, 0.5 ml 40% HF, and oxidize with 1 ml sat. $KMnO_4$.

[e] Dissolve 1 g in 20 ml H_2O, 2 ml 40% HF, 4 ml HNO_3, 1 ml H_2SO_4, and oxidize with $KMnO_4$. Initial volume 40 ml, max. 0.2 g Zr. Blank max. 0.2 ml 40% HF.

When ammonia is used to adjust the pH of solutions containing copper and iron a modified procedure must be followed (see Study of interferences).

It is necessary to dissolve alloy steels in fuming perchloric acid to oxidize any metal carbides and separate any tungsten as oxide, otherwise the results are low.

Niobium interferes seriously and a special procedure was developed to permit the determination of phosphorus in steels containing niobium. It is necessary to add a minimum amount of 2.5 ml of 40% hydrofluoric acid to 0.5 g of tungsten–niobium steel to complex niobium and tungsten. The amount of 40% hydrofluoric acid can vary between 0.25 and 0.5 ml. However, 40 mg of iron(III) as chloride must be introduced to complex the free fluoride when more than 0.25 ml of 40% hydrofluoric acid is present in the sample aliquot. For 6W–3Nb steel when 10-ml sample aliquots were taken the recoveries on standard addition were lower (10 μg P $\equiv$ 0.415 abs. units) because of the higher concentration of tungsten and niobium. Standard additions were made to reagent blanks containing varying amounts of hydrofluoric acid, and it was found that a maximum 0.25 ml of 40% hydrofluoric acid can be tolerated without causing any decrease in the recovery. Boiling for 4 min was necessary, otherwise low recoveries were obtained.

A modified procedure had to be used when steels containing vanadium were taken for analysis. The solution, after the addition of perchloric acid and hydroxylamine hydrochloride, was brought to the boil, to ensure that all vanadium(V) was reduced to vanadium(IV), and the whole procedure was carried out at a lower pH in perchloric acid solution where the recoveries on standard addition were higher. Even sample aliquots containing small amounts (more than 20 μg) of vanadium must be brought to the boil to ensure the reduction of vanadium(V), otherwise reproducible results could not be obtained (chromium–vanadium steel).

The maximum amount of titanium per aliquot is limited to 500 μg and it can be complexed in steel samples by 0.3 ml of 40% hydrofluoric acid.

Aluminium

Weigh 0.25 g of sample into a 250-ml Teflon beaker, add 20 ml of 10% sodium hydroxide. Cover the beaker and dissolve the sample with gentle heating. Add 10 ml of nitric acid and boil until any metallic sponge is dissolved. Add 1 ml of saturated potassium permanganate solution and boil for 5 min. Dissolve the precipitate by adding 10% hydroxylamine hydrochloride solution. Cool, dilute to 50 ml with water and mix. Pipette an aliquot containing 7–12 μg of phosphorus into a polythene beaker, add 1 ml of 10% hydroxylamine hydrochloride solution, dilute to 25 ml and adjust the pH to 0.35. Add 10 ml of ammonium molybdate solution and continue as in the recommended procedure. Prepare a blank and make a standard addition of 10 μg of phosphorus.

Brass, bronze and cupro–nickel

Weigh 0.2 g of sample into a 250-ml Teflon beaker, add 10 ml of water, 8 ml of nitric acid, 3 ml of hydrochloric acid and 0.5 ml of 40% hydrofluoric acid. After dissolution add 30 ml of water and 1 ml of saturated potassium permanganate solution, and boil for 5 min. Transfer the sample to a 100-ml polythene cylinder containing 30 ml of saturated boric acid, dilute to 100 ml with water and mix. Pipette an aliquot containing 7–12 μg of phosphorus into a polythene beaker and add boric acid to increase the total volume of boric acid to 7.5 ml. Add 1 ml of 10% hydroxylamine hydrochloride solution, dilute to 25 ml and let stand for 10 min. Adjust the pH to 0.4 with 9 *N* sulphuric acid, add 11.6 ml of acid ammonium molybdate solution from a pipette with stirring and continue as in the recommended procedure. Prepare a blank and make a standard addition of 10 μg of phosphorus.

Pure iron

Weigh 1 g of sample into a 250-ml Teflon beaker, add 30 ml of water, 10 ml of nitric acid and 0.5 ml of 40% hydrofluoric acid. After dissolution add 3 ml of saturated potassium permanganate solution and boil for 5 min. Dissolve the precipitate by adding 10% hydroxylamine hydrochloride solution. Cool, transfer the sample to a 100-ml polythene cylinder containing 30 ml of saturated boric acid, dilute to 100 ml with water, and mix. Pipette an aliquot containing 7–12 μg of phosphorus into a polythene beaker; add boric acid and hydroxylamine hydrochloride as in the case of brass, dilute to 30 ml and let stand for 10 min. Adjust the pH to 0.3 and add 20 ml of ammonium molybdate solution from a pipette with stirring. Continue as in the recommended procedure and adjust the total aqueous volume before extraction to 65 ml. Prepare a blank, and make a standard addition of 10 μg of phosphorus.

Carbon and alloy steels containing neither titanium nor vanadium

Weigh 0.5 g of sample into 250-ml beaker and add 5 ml of water, 8 ml of nitric acid, 8 ml of hydrochloric acid and 0.5 ml of 40% hydrofluoric acid. After dissolution add 12 ml of perchloric acid and evaporate to fumes. Fume so that the perchloric acid refluxes on the sides of the beaker for 10 min. Cool, add 40 ml of water, boil for 5 min and add 10% hydroxylamine hydrochloride to reduce any dichromate. Dilute to 100 ml and pipette an aliquot containing 7–12 μg of phosphorus into a polythene beaker. Add 1 ml of 10% hydroxylamine hydrochloride and dilute to 25 ml. Adjust the pH to 0.35 and add 10 ml of ammonium molybdate solution from a pipette with stirring. Continue as in the recommended procedure. Prepare a blank and make a standard addition of 10 μg of phosphorus.

Steels containing vanadium

Weigh 0.5 g of sample and treat it as in the case of carbon steel. Reduce vanadium and dichromate with 10% hydroxylamine hydrochloride. Continue as for ferro–vanadium.

Steels containing tungsten and vanadium

Weigh 0.5 g of sample and treat it as in the case of carbon steel. Reduce vanadium and dichromate with 10% hydroxylamine hydrochloride and filter off the tungstic acid. Dilute to 100 ml and continue as for ferro–vanadium.

Steels containing tungsten and niobium

Weigh 0.5 g of sample and treat it as in the case of carbon steel. Transfer the contents of the beaker, after fuming with perchloric acid, to a Teflon beaker, add 10% hydroxylamine hydrochloride to reduce dichromate and add 2.5 ml of 40% hydrofluoric acid. Boil to dissolve tungstic acid, cool, transfer into a 100-ml polythene cylinder, dilute to 100 ml with water and mix. Pipette exactly 5 ml into a Teflon beaker, add

1.75 ml of perchloric acid, 1 ml of 10% hydroxylamine hydrochloride and dilute to 25 ml. (When 10 ml is taken, add 40 mg of iron as iron(III) chloride and only 1.25 ml of perchloric acid.) Boil the solution for 4 min, cool and add 10 ml of ammonium molybdate with stirring. Continue as in the recommended procedure, but do not add any 9 *N* sulphuric acid before extraction. Prepare a blank and make a standard addition of 10 μg of phosphorus.

Steel containing titanium and permanent magnet alloy

Weigh 0.5 g of sample into a 250-ml beaker, dissolve and fume with perchloric acid as for carbon steel. Add 40 ml of water and transfer to a Teflon beaker. Add 3 ml of 40% hydrofluoric acid, boil for 5 min and add 10% hydroxylamine hydrochloride to reduce any dichromate. Transfer the sample to a 100-ml polythene cylinder containing 30 ml of saturated boric acid, dilute to 100 ml and mix. Pipette an aliquot containing not more than 12 μg of phosphorus and not more than 500 μg of titanium into a polythene beaker and add boric acid to increase the total volume of boric acid to 7.5 ml. Add 1 ml of 10% hydroxylamine hydrochloride solution, dilute to 25 ml and let stand for 10 min.

For steels adjust the pH to 0.35 and add 10 ml of ammonium molybdate solution with stirring. For permanent magnet alloy adjust the pH to 0.4 with 9 *N* sulphuric acid and add 11.6 ml of acid ammonium molybdate solution. Continue as in the recommended procedure. Prepare a blank and make a standard addition of 10 μg of phosphorus.

Ferro–molybdenum

Weigh 0.25 g of sample into a 250-ml Teflon beaker and add 8 ml of nitric acid, 8 ml of hydrochloric acid, and 0.5 ml of 40% hydrofluoric acid. Continue as for brass, except for the adjustment of pH to 0.35 and the addition of 10 ml of ammonium molybdate solution.

Ferro–manganese

Weigh 0.2 g of sample into a 250-ml beaker and continue as for carbon steel. Reduce any manganese dioxide with 10% hydroxylamine hydrochloride.

Ferro–vanadium

Weigh 0.35 g of sample into a 250-ml beaker and dissolve the sample as for carbon steel, but add 4 ml of 40% hydrofluoric acid, and reduce vanadium pentoxide, precipitated after fuming, with 10% hydroxylamine hydrochloride. Dilute to 100 ml. Pipette an aliquot containing no more than 12 μg of phosphorus and not more than 20 mg of vanadium into a Teflon beaker and dilute to 25 ml. Adjust the pH to 0.4 with perchloric acid, add 1.7 ml of perchloric acid, 1 ml of 10% hydroxylamine hydrochloride and boil the solution for 4 min. Cool and add 10 ml of ammonium molybdate with stirring. Continue as in the recommended procedure, but do not add any 9 *N* sulphuric acid before extraction. Prepare a blank and make a standard addition of 10 μg of phosphorus.

It is a pleasure to acknowledge the assistance given by Mrs. B. MCALLISTER with the experimental work.

SUMMARY

A general method is presented for the spectrophotometric determination of phosphorus at trace levels. It involves extraction of the yellow molybdophosphoric acid with isobutyl acetate and subsequent reduction to heteropoly blue. The method covers the range 0.2–20 μg of phosphorus. A comprehensive study of interferences using standard additions of 10 and 20 μg of phosphorus was carried out and modifications are described to permit the determination of phosphorus in a wide variety of metals and salts.

RÉSUMÉ

Une méthode générale est proposée pour le dosage spectrophotométrique du phosphore, à l'état de traces (0.2–20 μg). Elle consiste en une extraction de l'acide molybdophosphorique jaune dans l'acétate d'isobutyle, suivie de la réduction en bleu de molybdène. On examine l'influence d'autres substances et on décrit des modifications permettant le dosage du phosphore dans divers métaux et sels.

ZUSAMMENFASSUNG

Es wird eine allgemeine Methode zur spektralphotometrischen Bestimmung von Spuren Phosphor angegeben. Sie schliesst ein die Extraktion der gelben Molybdophosphorsäure mit Isobutylacetat und nachfolgender Reduktion zum Heteropolyblau. Die Methode überdeckt den Bereich von 0.2–20 μg Phosphor. Eine zusammenfassende Untersuchung der Störungen unter Verwendung von Standardzugaben von 10 und 20 μg Phosphor wurde durchgeführt und einige Modifikationen werden beschrieben, die die Bestimmung von Phosphor in zahlreichen verschiedenen Metallen und Salzen erlaubt.

REFERENCES

1 D. F. Boltz and C. H. Lueck, in D. F. Boltz (Ed.), *Colorimetric Determination of Non-metals*, Interscience, New York, 1958, p. 29.
2 W. Rieman III and J. Beukenkamp, in I. M. Kolthoff and P. J. Elving (Eds.), *Treatise on Analytical Chemistry*, Part II, Vol. 5, Interscience, New York, 1961, p. 349.
3 C. H. Lueck and D. F. Boltz, *Anal. Chem.*, 28 (1956) 1168.
4 N. Lounamaa and W. Fugmann, *Z. Anal. Chem.*, 199 (1963) 352.
5 J. Paul, *Mikrochim. Acta*, (1965) 830.
6 J. Paul, *Mikrochim. Acta*, (1965) 836.
7 F. Umland and G. Wuensch, *Z. Anal. Chem.*, 213 (1965) 186.
8 P. Pakalns and W. W. Flynn, *Anal. Chim. Acta*, 38 (1967) 403.

Analytica Chimica Acta
Elsevier Publishing Company, Amsterdam
Printed in The Netherlands

ETUDE SUR LE DOSAGE SPECTROPHOTOMETRIQUE DIRECT DE L'ION FLUORURE A L'AIDE DU COMPLEXE CERIUM(III)-ALIZARINE COMPLEXON

M. HANOCQ ET L. MOLLE
Laboratoires de Chimie Analytique et de Chimie pharmaceutique inorganique, Institut de Pharmacie, Université libre de Bruxelles, Bruxelles (Belgique)

(Reçu le 26 juin 1967)

La plupart des méthodes de dosage de faibles quantités d'ions fluorures sont basées sur l'affaiblissement, proportionnel à la concentration de ces derniers, de la coloration de certains chélates métalliques tels que les complexes thorium(IV)-alizarine sulfonate de sodium, zirconium(IV)-ériochromecyanine R, etc.; la diminution de la densité optique permet alors de déterminer la quantité d'ions fluorures présents. Si ces procédés se révèlent très sensibles et rendent toujours de précieux services dans les laboratoires d'analyse, ils pèchent cependant par un manque de spécificité, de nombreux autres ions provoquant le même phénomène.

La première réaction, directe et spécifique, des ions fluorures a été préconisée en 1959 par BELCHER *et al.*[1]: en opérant en milieu tamponné vers pH 4.5 au moyen d'une solution acide acétique-acétate de sodium, le complexe rouge foncé formé entre les sels de cérium(III) et l'alizarine complexon (ou acide aminométhyl-3-alizarine diacétique) vire au bleu en présence d'ions fluorures. Dans ces conditions, ceux-ci n'éliminent pas le cation métallique du complexe cation-colorant pour libérer le colorant, comme c'était le cas lors de la réaction indirecte, mais entrent eux-mêmes dans la structure du chélate pour donner une coloration bleue; celle-ci est donc nettement différente de celle soit du réactif libre (jaune), soit du chélate céreux (rouge). La sensibilité absolue de cette réaction est de 0.2 μg de fluorure et sa concentration limite est de 0.6 p.p.m. Les complexes que forme l'alizarine complexon soit avec le lanthane(III), soit avec le praséodyme(III) se comportent de la même manière, mais c'est le chélate céreux qui est le plus utilisé jusqu'à présent.

Cette réaction, qui n'est présentée par aucun autre anion, a été appliquée à la détermination quantitative de petites quantités d'ions fluorures ainsi qu'au dosage du fluor dans les composés organiques et divers milieux complexes[2-7].

La méthode originale préconisée par BELCHER, LEONARD ET WEST[2,3] prescrit d'opérer, en milieu aqueux tamponné à pH 4.3, à l'aide d'un réactif composé de quantités équimoléculaires d'alizarine complexon et d'ions cérium(III). En portant sur graphique les mesures de la densité optique, effectuées à 610 nm en fonction de diverses concentrations en ions fluorures, on obtient une droite pour des quantités de fluor comprises entre 5 et 30 μg, mais celle-ci ne passe pas par l'origine; suivant les auteurs, la déviation standard de la méthode est de ±0.27%.

La principale critique formulée contre cet élégant procédé vise la lenteur de la formation du complexe ternaire cérium(III)-alizarine complexon-fluorure. On n'aboutit à un équilibre qu'après 60 min[3] et la vitesse d'établissement de ce dernier dépendrait surtout de l'ordre d'addition des réactifs, les meilleurs résultats étant obtenus lorsque la solution tampon et l'alizarine complexon sont ajoutées avant le sel céreux. C'est en partie pour pallier cet inconvénient que Yamamura et ses collaborateurs[8] suggèrent d'opérer en présence d'acétonitrile ou d'acétone: dans ces conditions, non seulement l'équilibre de la réaction est atteint après 20 min, mais comme l'avaient déjà souligné Belcher et West[9], la sensibilité est nettement accrue.

Pour interpréter ce renforcement de la sensibilité de la réaction, trouvé empiriquement, il est nécessaire de s'en rapporter au schéma réactionnel proposé par Leonard et West[3]: à pH 4.3, l'alizarine complexon réagit avec toute une série de cations, et notamment avec le cérium(III) pour former un complexe coloré en rouge.

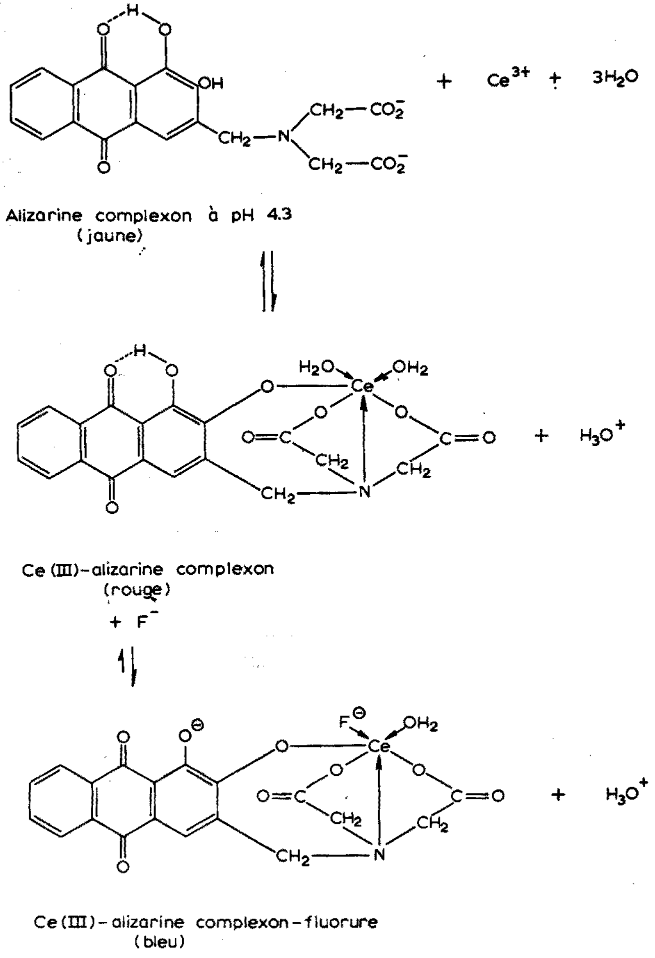

Alizarine complexon à pH 4.3
(jaune)

Ce(III)-alizarine complexon
(rouge)

Ce(III)-alizarine complexon-fluorure
(bleu)

C'est en prenant la place d'une des molécules d'eau attachées au cérium(III) par des covalences de coordination que l'ion fluorure, plus électronégatif que l'oxygène de l'eau, s'intègrerait dans le complexe binaire, donnant ainsi naissance à un composé coloré en bleu.

La spécificité de la réaction est donc liée aux propriétés électrophiles exceptionnellement fortes de l'anion fluorure; c'est, en effet, en raison de ce caractère que cet ion provoquerait un déplacement des électrons aux dépens du noyau aromatique voisin et, par suite, de la fonction phénolique dont il cause la déprotonisation.

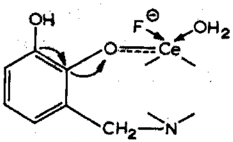

Ces mêmes chercheurs ont aussi démontré la possibilité d'extraire le complexe ternaire de sa solution aqueuse au moyen de solvants organiques non miscibles, notamment en utilisant l'alcool amylique, additionné d'une amine. Mais ils constatent alors qu'indépendamment du facteur concentration, la sensibilité de la réaction est accrue; ce phénomène serait attribuable[3] au remplacement de la molécule d'eau fixée sur le cérium(III) par une molécule d'amine. Poursuivant cette étude, BELCHER ET WEST[9] étudièrent l'effet de quatre solvants miscibles à l'eau (le méthanol, l'éthanol, le dioxane et l'acétone) sur la sensibilité de la réaction et constatèrent que, parmi ceux-ci, l'acétone agit le plus efficacement en raison, selon ces chercheurs, de sa basicité relativement élevée et de sa faible constante diélectrique, cette dernière circonstance étant, d'après eux, favorable à l'association du complexe ternaire.

L'interprétation formulée par BELCHER, LEONARD ET WEST ne nous semble cependant pas entièrement satisfaisante. Il est en effet théoriquement possible d'accroître à la fois la vitesse de formation du complexe ternaire et la sensibilité de la réaction, en opérant en présence d'un solvant aprotique, c'est-à-dire ne disposant pas d'atome hydrogène susceptible de participer à une liaison hydrogène avec les molécules ou les ions dissous. Dans les solvants protiques, tels que l'eau, les anions sont solvatés par des interactions ion-dipôle, renforcées par des liaisons hydrogène d'autant plus intenses que l'anion est petit; il s'ensuit que dans l'eau, l'ion fluorure est très fortement solvaté: son pouvoir réactionnel est donc relativement faible[10-15]. Par contre, dans les solvants aprotiques et plus particulièrement dans ceux qui possèdent une forte constante diélectrique et un moment dipolaire élevé, les cations sont notablement solvatés alors que les anions le sont peu ou même pas du tout; il en résulte que ces derniers sont beaucoup plus réactifs que dans les solvants protiques. Il n'est donc pas étonnant que l'emploi d'un solvant polaire aprotique facilite grandement les réactions faisant intervenir un anion. S'il en est bien ainsi, l'utilisation d'un solvant tel que le diméthylsulfoxyde qui est le plus polaire d'entre eux ($\varepsilon = 48.9$; $\mu = 4.03$) s'impose: en sa présence, l'ion fluorure devient un agent nucléophile puissant et une base forte[10,11].

L'étude qui suit a pour but de démontrer que l'utilisation d'une solution aqueuse à 25% de diméthylsulfoxyde, en lieu et place d'eau seule, accroît la vitesse de formation du complexe ternaire cérium(III)-alizarine complexon-fluorure et augmente la sensibilité de la réaction.

PARTIE EXPÉRIMENTALE

Appareillage

Spectrophotomètre Cary 14, avec cellule de 1 cm*.

Spectrophotomètre Zeiss M4Q, avec cellule soit de 1 cm, soit de 5 cm.

pH-mètre Radiometer 22, équipé du système d'électrodes verre–calomel.

Reactifs

Solution tampon de pH 3.5: dissoudre 15 g d'acétate de sodium trihydraté (Merck P.A.) dans environ 250 ml d'eau bidistillée; ajouter ensuite 117 g d'acide acétique cristallisable 99–100% (Merck P.A.) et compléter à 500 ml à l'aide d'eau bidistillée.

Solution tampon de pH 3.8: dissoudre 20 g d'acétate de sodium trihydraté (Merck P.A.) dans environ 250 ml d'eau bidistillée; ajouter ensuite 78 g d'acide acétique cristallisable 99–100% (Merck P.A.) et compléter à 500 ml à l'aide d'eau bidistillée.

Solution tampon de pH 4.3: dissoudre 50 g d'acétate de sodium trihydraté (Merck P.A.) dans environ 250 ml d'eau bidistillée; ajouter ensuite 50 g d'acide acétique cristallisable 99–100% (Merck P.A.) et compléter à 500 ml à l'aide d'eau bidistillée.

Solutions étalonnées d'ions fluorures. Solution-mère: dissoudre exactement 1.1050 g de fluorure de sodium (Merck P.A.), préalablement desséché, dans 100 ml d'eau bidistillée. Préparer les solutions dont 1 ml = 10 μg de F^- et dont 1 ml = 1 μg de F^- par dilution à l'aide d'eau bidistillée. Toutes les solutions de fluorure sont conservées dans des récipients en polyéthylène.

Solution d'alizarine complexon (AC) 10^{-3} M. A 5 ml d'une solution d'hydroxyde de sodium environ 0.5 *N*, ajouter 385.2 mg d'alizarine complexon (B.D.H.) et agiter jusqu'à dissolution complète. Après avoir dilué à environ 900 ml au moyen d'eau bidistillée, ajouter 400 mg d'acétate de sodium trihydraté (Merck P.A.) et ajuster le pH entre 5.0 et 5.5 par addition d'une solution approximativement normale d'acide chlorhydrique (la coloration passe du violet au rouge). Compléter à 1 litre à l'aide d'eau bidistillée et, après filtration sur papier Whatman no. 1, conserver cette solution dans un flacon en verre brun.

Solution de nitrate de cérium(III) 10^{-3} M. Préparer une solution environ 0.02 *M* de nitrate de cérium(III): $Ce(NO_3)_3 \cdot 6\ H_2O$ (Merck tout pur) par dissolution de 2.167 g de ce réactif dans 250 ml d'eau bidistillée. Le titre exact de cette solution est déterminé à pH 6 au moyen d'une solution 0.05 *M* d'éthylènediamine tétracétate disodique, en présence de xylénol-orange comme indicateur.

A un volume correctement calculé de la solution (environ 50 ml), ajouter 0.1 ml d'acide nitrique concentré (minimum 65% et densité approximative = 1.40; Merck P.A.) et 50 mg de chlorhydrate d'hydroxylamine (Merck P.A.), puis compléter à 1 litre à l'aide d'eau bidistillée.

Solution aqueuse à 50% v/v de diméthylsulfoxyde (DMSO). A préparer par dilution du diméthylsulfoxyde Merck, pour synthèse.

---

* Nous remercions vivement notre Collègue, Monsieur le Professeur MAURICE ERRERA, d'avoir bien voulu mettre cet appareil à notre disposition.

Mode opératoire

Méthode A. Dans un ballon jaugé de 50 ml, on introduit une quantité déterminée de solution contenant de 5 à 25 μg d'ions fluorures. On ajoute alors successivement et en agitant après addition de chaque réactif, 2 ml de la solution tampon à pH 3.5, 5 ml de la solution de nitrate de cérium(III) 10^{-3} *M*, 25 ml de la solution aqueuse à 50% de diméthylsulfoxyde, 5 ml de la solution d'alizarine complexon 10^{-3} *M* et enfin, on complète à 50 ml au moyen d'eau bidistillée. Après 10 min, on mesure l'absorption à 625 nm dans une cuvette en verre de 1 cm d'épaisseur, par comparaison avec une solution contenant les mêmes quantités de réactifs, mais exempte de fluorure.

Méthode B. Dans un ballon jaugé de 100 ml, on introduit une quantité déterminée de solution contenant 1–15 μg d'ions fluorures. On ajoute alors successivement et en agitant après addition de chaque réactif, 4 ml de la solution tampon de pH 3.5, 5 ml de la solution de nitrate de cérium(III) 10^{-3} *M*, 50 ml de la solution aqueuse à 50% de diméthylsulfoxyde, 5 ml de la solution d'alizarine complexon 10^{-3} *M* et enfin, on complète à 100 ml au moyen d'eau bidistillée. Après 10 min, on mesure l'absorption à 630 nm dans une cuvette en verre de 5 cm d'épaisseur, par comparaison avec une solution contenant les mêmes quantités de réactifs, mais exempte de fluorure.

RÉSULTATS ET DISCUSSION

Choix de la concentration en diméthylsulfoxyde

Afin de déterminer la concentration la plus favorable en solvant organique, la méthode A décrite ci-dessus a été appliquée en opérant chaque fois sur une solution

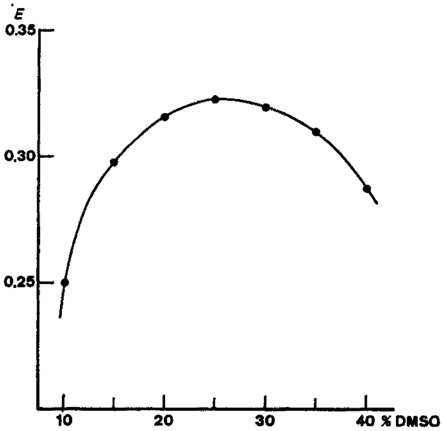

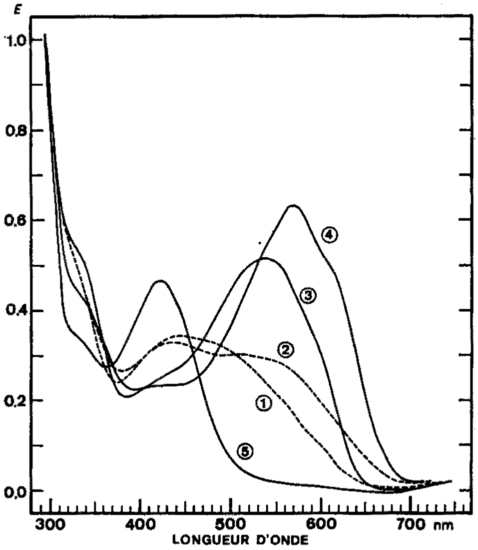

Fig. 1. Etude de l'influence de la concentration en diméthylsulfoxyde (DMSO) sur la sensibilité de la réaction (méthode A; 20 μg de F^-).

Fig. 2. Etude spectrale des complexes, réalisée à l'aide d'un spectrophotomètre Cary-14 (cellules de 1 cm): (1) Ce(III)–AC; (2) Ce(III)–AC–F^- (20 μg); (3) Ce(III)–AC + 25% DMSO; (4) Ce(III)–AC–F^- (20 μg) + 25% DMSO; (5) AC + 25% DMSO.

contenant 20 μg d'ions fluorures, mais en utilisant des concentrations en diméthylsulfoxyde variant de 10–40%, les autres conditions restant identiques. La figure 1, qui résume ces expériences, indique clairement que le maximum d'absorption du complexe ternaire est atteint en opérant dans un milieu contenant 25% de diméthylsulfoxyde.

Une étude identique réalisée en suivant la méthode B aboutit au même résultat.

Etudes spectrales. Choix de la longueur d'onde

Les courbes d'absorption des complexes binaires et ternaires ont été réalisées d'abord en présence d'eau seule, puis en présence de 25% de diméthylsulfoxyde, en opérant par comparaison à de l'eau distillée.

En suivant le mode opératoire A et en terminant l'opération par une exploration du spectre de 375–780 nm, on obtient les courbes d'absorption rassemblées à la figure 2. L'examen de ces dernières permet de constater que l'addition de diméthylsulfoxyde provoque un déplacement des maxima d'absorption aussi bien du chélate binaire (450–535 nm) que du chélate ternaire (435–570 nm). D'autre part, puisque la différence maximum d'absorption existant entre le complexe fluoré (spectre 4) et le complexe du cérium(III) non fluoré (spectre 3) se situe à 625 nm, cette longueur d'onde a été utilisée pour effectuer les mesures spectrophotométriques dans la suite de ce travail, lors de l'application de la méthode A.

Les spectres d'absorption des complexes ternaires, mesurés par comparaison au complexe binaire cérium(III)–alizarine complexon et rassemblés à la figure 3,

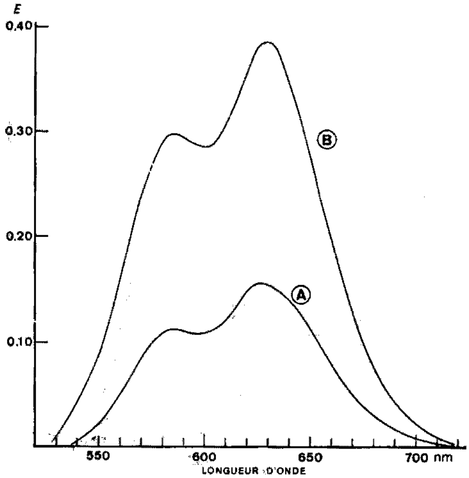

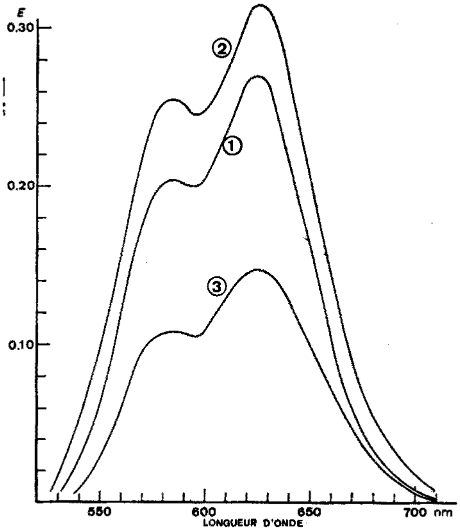

Fig. 3. Spectres d'absorption des complexes Ce(III)–AC–F⁻ (10 μg) par comparaison au complexe Ce(III)–AC, réalisés à l'aide d'un spectrophotomètre Zeiss M4Q (cellules de 1 et 5 cm): (A) Suivant la méthode A; (B) Suivant la méthode B.

Fig. 4. Etude spectrale du complexe ternaire Ce(III)–AC–F⁻ (20 μg) par comparaison au complexe Ce(III)–AC réalisée à l'aide d'un spectrophotomètre Zeiss M4Q (cellules de 1 cm): (1) Eau–acétone 4:1 (pH = 4.3); (2) Eau–DMSO 4:1 (pH = 4.1); (3) Eau seule (pH = 5.2).

confirment la nécessité d'opérer à 625 nm pour la méthode A et justifient, en outre, le choix de la longueur d'onde de 630 nm lors de l'application de la méthode B.

Enfin, les courbes d'absorption du chélate ternaire formé soit dans l'eau seule, soit dans un mélange eau–acétone 4:1, soit dans un mélange eau–diméthylsulfoxyde 4:1 et réalisées par comparaison avec les réactifs blancs dans les conditions de pH les plus favorables indiquent que l'introduction de solvants, tels que l'acétone ou le diméthylsulfoxyde ne déplace pas le maximum d'absorption (figure 4).

Choix du pH

Les extinctions des complexes binaire et ternaire, mesurées par comparaison à de l'eau distillée, augmentent avec le pH du milieu comme l'indiquent les résultats rassemblés dans le tableau I. Pour dresser celui-ci, la méthode A a été suivie en opérant sur 10 µg d'ions fluorures, mais en ajoutant 2 ml d'une solution tampon variant de 3.0–3.9. Il convient de souligner que le pH du milieu final, prêt à être soumis à la lecture spectrophotométrique, est supérieur d'environ 0.5 unité au pH du tampon choisi en raison de la basicité relativement élevée du diméthylsulfoxyde.

TABLEAU I

EFFETS DU pH SUR LES EXTINCTIONS DES COMPLEXES BINAIRE ET TERNAIRE, MESURÉES À 625 nm, PAR COMPARAISON À DE L'EAU BIDISTILLÉE

(Concentration en ions fluorures = 10 µg)

pH de la solut. tampon utilisée	*pH final du milieu*	*Extinctions*		
		Complexe binaire	*Complexe ternaire*	*Différence*
3.0	3.7	0.101	0.253	0.152
3.3	3.9	0.139	0.299	0.160
3.4	4.0	0.160	0.323	0.163
3.5	4.1	0.164	0.330	0.166
3.6	4.15	0.178	0.340	0.162
3.7	4.2	0.192	0.352	0.160
3.8	4.3	0.202	0.360	0.158
3.9	4.4	0.217	0.375	0.158

La différence maximum entre les extinctions des complexes ternaire et binaire s'obtient en utilisant la solution tampon de pH 3.5; dans ces conditions, le pH final du milieu est de 4.1. C'est celui-ci qui a été utilisé au cours de cette étude.

Choix de la concentration la plus favorable en ions fluorures

Le tracé A de la figure 5, obtenu en suivant le mode opératoire A est linéaire pour des quantités de fluorures variant de 3–25 µg, mais la droite ne passe pas par l'origine. D'autre part, le tracé linéaire B obtenu en suivant le mode opératoire B ne passe pas par l'origine, mais permet de déterminer des quantités de fluorures variant de 1–15 µg. Dans les deux cas, le coefficient d'extinction molaire s'élève à $1.53 \cdot 10^4$.

Toutefois, il est bien connu qu'une sensibilité élevée et un tracé linéaire de la relation extinction–concentration ne sont pas les seuls facteurs permettant de choisir les meilleures conditions expérimentales d'un dosage spectrophotométrique. Dans de tels cas, la méthode de RINGBOM[16] permet de calculer les concentrations les plus favorables à une analyse précise. On trouvera à la figure 6 des courbes de Ringbom, obtenues en suivant soit le mode opératoire A, soit le mode opératoire B. Dans le premier cas, les résultats les plus précis seront obtenus en opérant sur des concentrations en fluorures variant de 11–25 µg et, dans le second cas, sur des concentrations en fluorures variant de 3–15 µg.

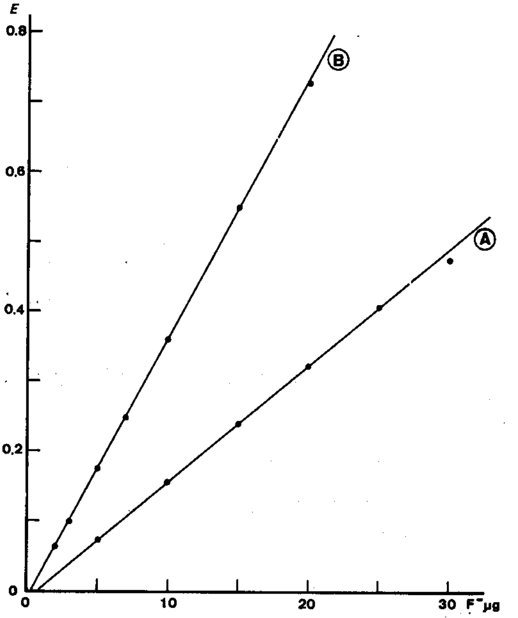

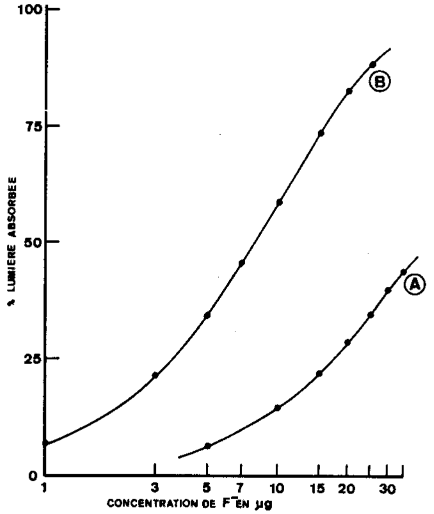

Fig. 5. Courbes d'étalonnage de solutions d'ions fluorures: (A) Suivant la méthode A; (B) Suivant la méthode B.

Fig. 6. Courbes de Ringbom: (A) Suivant la méthode A; (B) Suivant la méthode B.

Influence de la présence de diméthylsulfoxyde sur la sensibilité de la réaction

Comme la théorie le laissait prévoir, la présence de diméthylsulfoxyde, solvant aprotique très polaire, exerce une influence extrêmement favorable sur la sensibilité de la réaction: la figure 7 qui rassemble diverses courbes d'étalonnage réalisées aux pH les plus favorables, en présence de quelques solvants de polarité et de basicité différentes, l'illustre à suffisance.

Les résultats rassemblés dans le tableau II démontrent d'une manière plus quantitative cet accroissement de la sensibilité. Signalons que, dans ce domaine, d'autres auteurs[8] ont démontré que l'acétonitrile possède un effet pratiquement équivalent à celui de l'acétone.

Influence de la présence de diméthylsulfoxyde sur la vitesse de la réaction

Afin d'établir le temps nécessaire à la stabilisation définitive de la réaction, nous avons mesuré les variations de l'extinction en fonction du temps soit du complexe binaire, soit du complexe ternaire, en présence d'eau seule ou d'un mélange eau–diméthylsulfoxyde 4:1. Les complexes ternaires ont été réalisés en opérant sur 20 µg d'ions fluorures suivant le mode opératoire A. Les résultats rassemblés dans le tableau III démontrent qu'en présence d'eau seule, l'équilibre de la réaction n'est atteint qu'au bout de trois heures, alors qu'en milieu eau–diméthylsulfoxyde 4:1, il suffit de dix minutes pour aboutir à la stabilisation.

D'autres auteurs[8] ont démontré qu'en utilisant un mélange eau–acétone 5:1 comme solvant, un temps de vingt minutes est nécessaire pour atteindre l'équilibre.

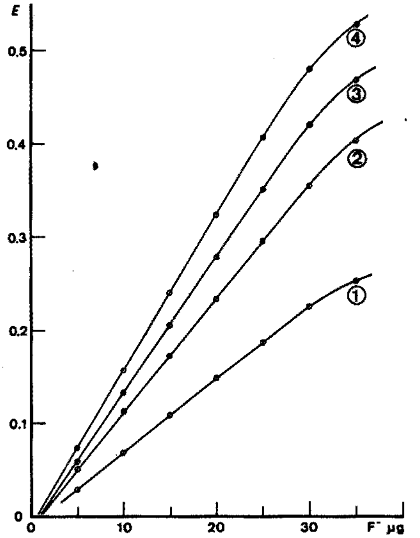

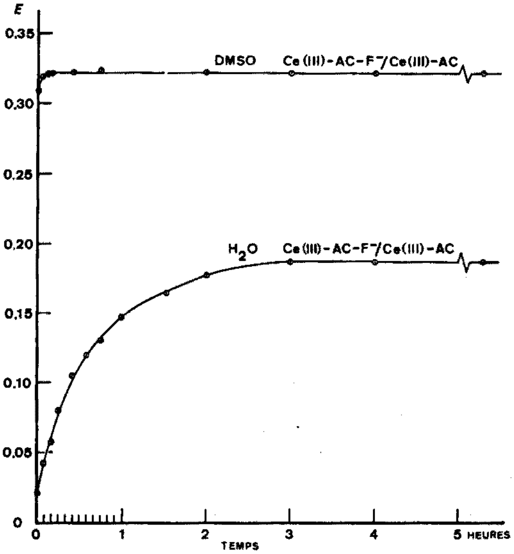

Fig. 7. Accroissement de la sensibilité par l'utilisation de solvants aprotiques polaires: (1) Eau (pH = 5.2); (2) Eau–alcool isopropylique 4:1 (pH = 4.2); (3) Eau–acétone 4:1 (pH = 4.2); (4) Eau–DMSO 4:1 (pH = 4.1), Méthode A.

Fig. 8. Accroissement de la vitesse de réaction par l'utilisation d'une solution aqueuse à 25% de DMSO (v/v).

TABLEAU II

ACCROISSEMENT DE LA SENSIBILITÉ PAR L'UTILISATION DE SOLVANTS APROTIQUES POLAIRES

Solvant	ΔE*	*Coefficient d'extinction molaire* $(\cdot 10^{-4})$
eau	0.0079	0.73
eau–alcool isopropylique 4:1	0.0120	1.10
eau–acétone 4:1	0.0146	1.32
eau–DMSO 4:1		
méthode A	0.0170	1.53
méthode B	0.0545	1.54

* ΔE = variation de l'extinction que provoque 1 µg d'ion fluorure.

Les graphiques de la figure 8, traductions d'une partie des résultats du tableau III, illustrent d'une manière plus nette encore le fait que la présence de diméthylsulfoxyde accroît la vitesse de la réaction ainsi d'ailleurs que sa sensibilité. Notons aussi que, dans les conditions préconisées, les différents complexes restent stables pendant au moins 24 h.

TABLEAU III

VARIATIONS DE L'EXTINCTION DES COMPLEXES BINAIRES ET TERNAIRES EN FONCTION DU TEMPS

Temps en minutes	*Eau*			*Eau–Diméthylsulfoxyde 4:1*		
	Ce–AC/eau	*Ce–AC–F/eau*	*Ce–AC–F/Ce–AC*	*Ce–AC/eau*	*Ce–AC–F/eau*	*Ce–AC–F/Ce-*
0	0.2168	0.2628	0.0200	0.1549	0.4645	0.308
3				0.1543	0.474	0.319
5	0.2197	0.2774	0.0419			
6				0.158	0.476	0.321
10	0.2190	0.2890	0.0560	0.1586	0.4775	0.322
15	0.2153	0.2997	0.0809			
25	0.2104	0.313	0.1057	0.1586	0.4775	0.322
35	0.2062	0.3215	0.1203			
45	0.2033	0.330	0.1308	0.1586	0.4775	0.322
60	0.2007	0.339	0.1463			
90	0.1986	0.350	0.1643			
120	0.1972	0.354	0.1765	0.1586	0.4775	0.322
180	0.1952	0.358	0.1858	0.1586	0.4775	0.322
240	0.1952	0.358	0.1858	0.1586	0.4775	0.322

Influence de divers ions sur la méthode de dosage proposée

Théoriquement, il est possible de concevoir six modes d'interférence par les cations et anions:

1) Par une compétition entre certains anions suffisamment électronégatifs, comme les halogénures, et l'ion fluorure, inhibant ainsi partiellement l'intégration de ce dernier dans le complexe binaire et provoquant une diminution de l'absorption du complexe coloré.

2) Par une compétition entre le cérium(III) et certains cations comme l'aluminium(III), le fer(III), etc..., ceux-ci étant susceptibles de former des complexes plus stables que le chélate cérium(III)–alizarine complexon. Il en résulte alors, suivant les cas, soit une augmentation, soit une diminution de l'absorption.

3) Par formation d'un complexe stable avec l'ion fluorure, empêchant ainsi ce dernier de réagir avec le complexe binaire; les cations calcium(II), magnésium(II), aluminium(III), étain(II), fer(III), etc... agissent de cette manière.

4) Par formation d'un complexe stable avec l'ion cérium(III), empêchant ainsi ce dernier de former le complexe binaire et provoquant alors invariablement une diminution de l'absorption du complexe coloré; cette interférence peut se manifester en présence des anions oxalates et phosphates.

5) Par une variation importante du pH du milieu réactionnel, cas présenté par les anions hydrogénocarbonates et carbonates.

6) Par une modification de la coloration du complexe ternaire due au pouvoir oxydant ou réducteur de certains ions, comme le nitrite par exemple.

Il va sans dire qu'un même ion peut agir en même temps suivant plusieurs modalités différentes, l'erreur résultante étant tantôt positive, tantôt négative, de sorte qu'il est possible que toutes les erreurs se compensent et qu'il semble n'y avoir aucune interférence.

Nous avons étudié l'influence de quelques ions en dosant le fluorure suivant la méthode A dans une solution contenant une quantité constante d'ions fluorures (20 μg) à laquelle les cations ont été ajoutés sous forme de chlorures et les anions

TABLEAU IV

INFLUENCE DE DIVERS IONS SUR LE DOSAGE DES IONS FLUORURES

(La quantité d'ions fluorures reste constante (20 µg) et la méthode A a été suivie)

Ion		*X/F*[a]	*Extinction*[e]	*Interférence (%)*[b]	*Ion*		*X/F*[a]	*Extinction*[e]	*Interférence (%)*[b]
Nature	*Quantité ajoutée (en mg)*				*Nature*	*Quantité ajoutée (en mg)*			
Cl^-	10	500	0.321	−0.31	NO_2^-	0.02	1	0.320	−0.62
	30	1500	0.320	−0.62		0.1	5	0.317	−1.55
	50	2500	0.318	−1.25		25	250	0.114	−64.59
	100	5000	0.313	−2.79		50	500	0.107	−66.77
						100[d]	1000	0.320	−0.62
SO_4^{2-}	0.5	25	0.320	−0.62					
	1	50	0.318	−1.25	Ca^{2+}	5	250	0.318	−1.25
	3	150	0.316	−1.86		10	500	0.312	−3.10
	6	300	0.309	−4.03		20	1000	0.302	−6.21
						30	1500	0.298	−7.45
PO_4^{3-}	0.020	1	0.321	−0.31					
	0.040	2	0.319	−0.93	Mg^{2+}	1	50	0.321	−0.31
	0.080	4	0.317	−1.55		3	150	0.329	+2.17
	0.160	8	0.306	−4.96		4	200	0.335	+4.03
HCO_3^-	10	500	0.325	+0.93	Sn^{2+}	0.04	2	0.317	−1.55
	30	1500	0.336	+4.34		0.1	5	0.305	−5.28
	50	2500	0.347	+7.76					
	50[c]	2500	0.323	+0.31	Al^{3+}	0.02	1	0.202	−37.88
						0.06	3	Interférence	
CO_3^{2-}	10	500	0.334	+3.73		0.1	5		
	30	1500	0.350	+8.69					
	50	2500	0.356	+10.56	Fe^{3+}	0.02	1	0.327	+1.55
	50[c]	2500	0.325	+0.93		0.06	3	0.335	+4.03
						0.1	5	0.348	+8.07
NO_3^-	30	1500	0.321	−0.31					
	60	3000	0.319	−0.93					
	100	5000	0.312	−3.10					

[a] X/F représente le rapport entre la quantité d'ions X ajoutés et la quantité d'ions fluorures présents, toutes deux étant exprimées dans les mêmes unités de poids.
[b] L'interférence a été calculée à l'aide de la relation 100 $\Delta E/E_0$ dans laquelle E_0 représente l'extinction correspondant à 20 µg d'ions fluorures et ΔE, la variation d'extinction provoquée par la même quantité d'ions fluorures, additionnée d'ions étrangers.
[c] Echantillon acidifié par HCl 0.1 *N* avant le développement de la coloration.
[d] Echantillon additionné de chlorhydrate d'hydroxylamine avant le développement de la coloration.
[e] $E_0 = 0.322$.

sous forme de sels de sodium. L'examen du tableau IV qui rassemble les résultats de cette étude permet de conclure que, dans la majorité des cas envisagés, la méthode préconisée se révèle très souple: mise à part celle de l'aluminium(III), les interférences rencontrées sont minimes ou peuvent être corrigées assez aisément.

Les anions phosphates gênent d'une manière assez importante: ainsi, en opérant en présence d'une quantité huit fois plus grande en phosphate par rapport au fluorure, l'erreur atteint près de 5% par défaut. Par contre, des concentrations élevées en chlorure ou en nitrate ont très peu d'influence sur les résultats du dosage.

Parmi les cations examinés, le fer(III) provoque un accroissement assez important de l'extinction tandis que la présence d'étain(II) entraîne une diminution de cette mesure. C'est toutefois l'aluminium(III) qui manifeste l'interférence la plus notable puisqu'en présence de quantités égales des deux ions, l'erreur atteint déjà près de 38% par défaut.

L'interférence observée pour des quantités relativement grandes d'ions hydrogénocarbonates ou carbonates peut être facilement éliminée par acidification préalable des échantillons à analyser à l'aide d'une solution décinormale d'acide chlorhydrique.

Les ions nitrites n'interfèrent pratiquement pas lorsqu'ils sont présents en très faibles quantités, mais dès que le rapport NO_2^-/F^- atteint 250, le complexe ternaire est détruit et sa coloration s'altère au cours du temps. L'addition d'une quantité adéquate de chlorhydrate d'hydroxylamine à la prise d'essai permet toutefois de pallier cet inconvénient: la méthode permet alors d'opérer en présence de fortes concentrations en nitrites ($NO_2^-/F^- = 1000$).

CONCLUSIONS

Suivant BELCHER ET WEST[9], la sensibilité de la méthode de dosage des ions fluorures, basée sur la formation du complexe cérium(III)–alizarine complexon–fluorure, est accrue lorsqu'on opère en présence d'acétone, en raison de la basicité relativement élevée de ce solvant et de sa faible constante diélectrique. La présente étude semble démontrer que cette dernière circonstance est plutôt défavorable à la réaction puisqu'elle prouve que l'utilisation de diméthylsulfoxyde, le plus polaire de tous les solvants aprotiques, augmente la vitesse de la réaction et exalte sa sensibilité au maximum.

La méthode de dosage préconisée permet de déterminer des quantités d'ions fluorures variant de 1 à 25 μg; la déviation standard est de 0.17%. Elle a déjà été appliquée avec succès à l'analyse pharmaceutique.

RÉSUMÉ

Plusieurs chercheurs ont observé que la sensibilité de la méthode de dosage de faibles quantités d'ions fluorures, basée sur la formation du complexe cérium(III)–alizarine complexon–fluorure peut être accrue en opérant en présence de certains solvants. La présente étude démontre que l'utilisation d'une solution aqueuse à 25% v/v de diméthylsulfoxyde, le plus polaire de tous les solvants aprotiques, exalte au maximum la sensibilité de la réaction et en augmente sensiblement la vitesse. Deux modes opératoires, permettant de déterminer des quantités d'ions fluorures variant de 1 à 25 μg sont décrits: le pH le plus favorable est de 4.1 et la mesure s'effectue soit à 625 nm, soit à 630 nm. L'interférence éventuelle de 12 ions a été étudiée.

SUMMARY

Several workers have observed that the sensitivity of the cerium(III)–alizarin fluorine blue method for the spectrophotometric determination of microgram amounts of fluoride may be enhanced by addition of certain solvents. The present study proves that the use of an aqueous 25% v/v solution of dimethylsulfoxide, the most polar aprotic solvent, enhances to a maximum the sensitivity of the reaction and increases its speed. Two procedures, allowing the determination of 1–25 µg fluoride ion, are described: the best pH value is 4.1 and the spectrophotometric measurements are carried out at 625 or 630 nm. The interferences of 12 ions were studied.

ZUSAMMENFASSUNG

Es wurde von anderen beobachtet, dass die Empfindlichkeit der Cer(III)–Alizarinfluoridblau-Methode zur spectralphotometrischen Bestimmung von Mikrogrammen Fluorid durch Zugabe bestimmter Lösungsmittel angeregt werden kann. Die vorliegende Untersuchung bestätigt, dass die Verwendung einer wässrigen Lösung von Dimethylsulfoxid die Reaktion zu einer maximalen Empfindlichkeit anregt und ihre Geschwindigkeit steigert. Zwei Verfahren, die die Bestimmung von 1–25 µg Fluorid erlauben, werden beschrieben. Ein pH-Wert von 4.1 ist günstig. Die Messungen wurden bei 625 oder 630 nm durchgeführt. Die Störungen von 12 Ionen wurden untersucht.

BIBLIOGRAPHIE

1 R. Belcher, M. A. Leonard et T. S. West, *Talanta,* 2 (1959) 92.
2 R. Belcher, M. A. Leonard et T. S. West, *J. Chem. Soc.,* (1959) 3577.
3 M. A. Leonard et T. S. West, *J. Chem. Soc.,* (1960) 4477.
4 C. A. Johnson et M. A. Leonard, *Analyst,* 86 (1961) 101.
5 P. C. Jeffery et D. Williams, *Analyst,* 86 (1961) 590.
6 H. N. S. Shafek, *Anal. Chem.,* 35 (1963) 53.
7 J. M. Ross, R. H. Wade et H. M. Benedict, *J. Assoc. Offic. Agr. Chemists,* 46 (1963) 907.
8 S. S. Yamamura, M. A. Wade et J. H. Sikes, *Anal. Chem.,* 34 (1962) 1308.
9 R. Belcher et T. S. West, *Talanta,* 8 (1961) 863.
10 J. Miller et A. J. Parker, *J. Am. Chem. Soc.,* 83 (1961) 117.
11 A. J. Parker, *Quart. Rev.,* 16 (1962) 163.
12 C. Agami, *Bull. Soc. Chim. France,* (1965) 1021.
13 B. Tchoubar, *Bull. Soc. Chim. France,* (1964) 2069.
14 F. Madaule-Aubry, *Bull. Soc. Chim. France,* (1966) 1456.
15 J. N. Butler, *J. Electroanal. Chem.,* 14 (1967) 89.
16 A. Ringbom, *Z. Anal. Chem.,* 115 (1939) 332.

Anal. Chim. Acta, 40 (1968) 13–25

Analytica Chimica Acta
Elsevier Publishing Company, Amsterdam
Printed in The Netherlands

A VOLTAMMETRIC METHOD FOR FLUORIDE*

H. E. ZITTEL AND T. M. FLORENCE**
Analytical Chemistry Division, Oak Ridge National Laboratory, Oak Ridge, Tenn. (U.S.A.)

(Received April 22nd, 1967)

Most of the procedures used currently for the determination of micro amounts of fluoride are colorimetric. Generally they entail the bleaching of a metal–organic complex by the formation of a stronger metal–fluoride complex. One widely used method of the above type is the determination of fluoride by its effect on the zirconium–alizarin red S complex. The method has been the subject of many studies and is run under a variety of conditions[1]. It has been reported recently that both alizarin red S and its zirconium complex exhibit anodic reactions at the rotating pyrolytic graphite electrode (RPGE)[2]. A voltammetric method for micro amounts of fluoride, based upon the anodic reaction of alizarin red S at the RPGE, has been developed. The procedure is simple, rapid and as little as 20 p.p.b. of fluoride may be determined with good accuracy and precision.

EXPERIMENTAL

Apparatus

Voltammeter. ORNL Model Q-2792[3] controlled-potential D. C. Polarographic voltammeter. The first derivative function was used exclusively throughout this study.

X-Y Recorder. Mosely Model 2D-2A, F. L. Mosely Co., Pasadena, Calif.

Electrodes. The RPGE has been described previously[4] and was used in conjunction with a Beckman 39270 S.C.E. and a platinum wire counter electrode.

Reagents and solutions

Alizarin red S (National Aniline Division, Allied Chemical and Dye Corp.) was recrystallized from 50% ethanol, then dried in an air oven at 100°. Elemental analysis showed a purity of 99.7% as the monohydrate, $C_{14}H_7O_7SNa \cdot H_2O$. The recrystallized dye was weighed directly to make up standard solutions.

Zirconium perchlorate, a pure grade of zirconyl chloride (A. D. MACKAY) was analyzed gravimetrically for zirconium content. This material was then used to prepare a standard solution of zirconium perchlorate by fuming a weighed amount of zirconyl chloride with perchloric acid. The standard solution was made 5 M in perchloric acid to prevent hydrolysis of the zirconium.

---

* Research sponsored by the U.S. Atomic Energy Commission under contract with the Union Carbide Corp.

** Attached to Oak Ridge National Laboratory from the Australian Atomic Energy Commission, N. S. W., Australia.

All other reagents used were of reagent grade and, where necessary, were standardized by conventional methods.

Stock solution of reagent. To 500 ml of 2 N perchloric acid in a 1-l volumetric flask, add 50 ml of aqueous $3 \cdot 10^{-4}$ M alizarin red S and 10 ml of a $3.5 \cdot 10^{-3}$ M solution of $Zr(ClO_4)_4$ in 5 M perchloric acid. Dilute to volume with distilled water. Such a stock solution is stable for several weeks with less than a 3% change in the blank current, *i.e.* the current due to the free alizarin red S present when no fluoride is present. The concentrations given are such that when diluted 1:1, the concentration of the Zr–ligand complex in the resulting solution will be 85–90% of that of the limiting reagent alizarin red S added initially. For further details see RESULTS AND DISCUSSION.

Sample procedure

To 25 ml of the reagent stock solution in a 50-ml volumetric flask add an aliquot, preferably not more than several ml, of the sample solution containing *ca.* 4–40 μg of fluoride. Dilute to volume and heat in a water bath at 60–70° for 15 min. Cool, transfer to the voltammetric cell and record the derivative current–voltage curve between +0.4 and 1.0 V *vs.* S.C.E. The increase in the height of the free alizarin red S anodic wave at *ca.* 0.7 V *vs.* S.C.E. is proportional to the amount of fluoride present. The results should be compared to a standard curve obtained by carrying standard fluoride solutions through the same procedure using the same stock reagent solution. After each potential scan, clean the RPGE by allowing it to rotate briefly in warm 1 N sodium hydroxide followed by 5 M perchloric acid.

Notes

If the amount of fluoride in the sample aliquot is outside the range given, use a proportionately adjusted reagent solution. The stock reagent solution should always be prepared so that, upon making the desired dilution, the limiting reagent (alizarin red S) will be 85–90% complexed by the zirconium, always present in excess. The amount of zirconium necessary to achieve this may be calculated from the equilibrium constant for eqn. (1).

The standard curve may be plotted as $[F^-]$ *vs.* i or as $[F^-]$ *vs.* Δi, *i.e.*, the change in current due to the fluoride present referred to the current of the solution with no fluoride present. It is normally easier to use the first method.

In this study only derivative voltammetry was used because of its greater sensitivity and ease of current measurement. Normal voltammetry may be used but the same degree of precision should not be expected since the low current levels obtained are difficult to measure.

RESULTS AND DISCUSSION

The method for fluoride determination discussed in this paper is based upon the voltammetric measurement of the free alizarin red S liberated from the zirconium–alizarin red S complex by the fluoride present. The increase in the anodic current resulting from the oxidation of alizarin red S at *ca.* 0.7 V *vs.* S.C.E. is a measure of the amount of fluoride. The chemical equilibria involved may be represented by the following equations.

$$Zr^{4+} + 2\,H_2O + H_2A \rightleftarrows Zr(OH)_2A + 4\,H^+ \tag{1}$$

$$Zr^{4+} + 4\,F^- \rightleftarrows ZrF_4 \tag{2}$$

$$Zr(OH)_2A + 4\,F^- + 4\,H^+ \rightleftarrows ZrF_4 + H_2A + 2\,H_2O \tag{3}$$

where H_2A represents the free alizarin red S and $Zr(OH)_2A$ represents the complex. This is not to imply that other reactions do not occur since very probably a series of zirconium fluoride complexes results, depending on the relative amounts of zirconium and fluoride present. However, for the purposes at hand, the above equations adequately describe the system. Of the equations given (1) and (2) are the more important since the zirconium ion will always be present in excess. Equation (2) represents the fast reaction taking place on the addition of fluoride to the complex solution. This in turn disturbs the equilibrium of eqn. (1) which is fairly slow. Equation (3) probably plays a very small role in the generation of the electroactive H_2A from the complex since it is also a slow reaction. The equilibrium constant for eqn. (1) has been established previously[2] as being $4.2 \cdot 10^4$.

In order to establish the optimum conditions for the method various parameters were studied. In Fig. 1 is shown the effect of varying acid concentrations on the Δi resulting from the presence of a fixed amount of fluoride. At each acid concentration level the reagent solution was scanned both with and without fluoride present. The difference in the current measured, Δi, was assumed to be free of error due to ionizaation of the complex itself. As can be seen the Δi value increases almost linearly with acid concentration up to *ca.* 0.5 *N* at which point it begins to level out. From the data

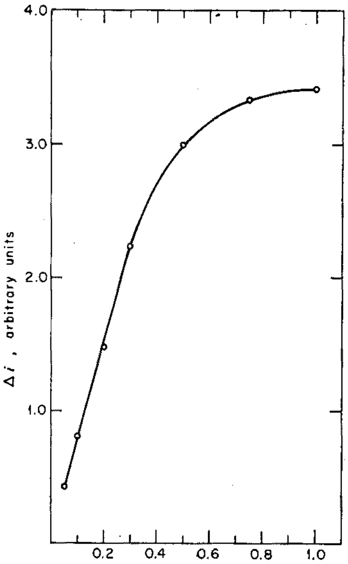

Fig. 1. Effect of acid concentration on Δi. Test conditions: [Zr] = $2.5 \cdot 10^{-5}$ *M*; [Aliz] = $2.5 \cdot 10^{-5}$ *M*; $[F^-]$ = 380 p.p.b.; ionic strength to 1 *M* with $NaClO_4$.

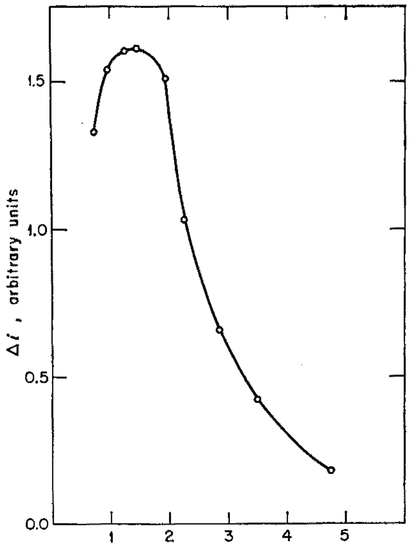

Fig. 2. Effect of [Zr] on Δi. Test conditions: [Aliz] = $7.4 \cdot 10^{-6}$ *M*; $[HClO_4]$ = 0.5 *N*; $[F^-]$ = 190 p.p.b.

presented it is apparent that the reaction to determine fluoride is more sensitive at the higher acid concentrations and that the exact acid concentration is least critical between 0.5 and 1 N. The exact reason for the increase in sensitivity at the higher acid concentrations was not established but the data would seem to indicate an increased difference in the stabilities of the two complex compounds involved as the test solution becomes more acid.

In order to determine the optimum concentrations of zirconium and alizarin red S for use in the reagent solution a series of tests was carried out. In Fig. 2 are shown the results of one of this series of tests. This illustrates the effect of excess zirconium in the reagent solution, the alizarin red S concentration being held constant at a value equal to or less than the zirconium concentration. The organic ligand is therefore the limiting reagent. In each case a fixed amount, 9.5 μg, of fluoride was added to 25 ml of the reagent solution. After dilution to a volume of 50 ml, the Δi was measured. As the zirconium concentration was increased the Δi increased until a maximum was reached. At this point a further increase in zirconium concentration caused a decrease in the Δi. Similar results were obtained when the zirconium was the limiting reagent, *i.e.* the concentration of zirconium was held constant and the concentration of alizarin red S varied. Using the equilibrium constant for eqn.(1), it was determined that the maximum Δi per unit of fluoride added occurred, in all cases studied, at essentially the same point. At the Δi maximum, 85–90% of the limiting reagent is present as the zirconium–alizarin red S complex before any fluoride is added. This was found to be true, regardless of whether zirconium or alizarin red S was the limiting reagent, over several ranges of zirconium–alizarin red S and fluoride concentrations.

The question as to whether alizarin red S or zirconium should be used as the limiting reagent was resolved by determining the percent change in current per unit of fluoride, the Δi caused by a given amount of fluoride divided by the blank current, *i.e.* the current of the reagent solution with no fluoride present. The solutions containing excess of alizarin red S exhibited a large blank current and thus the percent change per unit of fluoride was fairly small. On the other hand, those test solutions containing

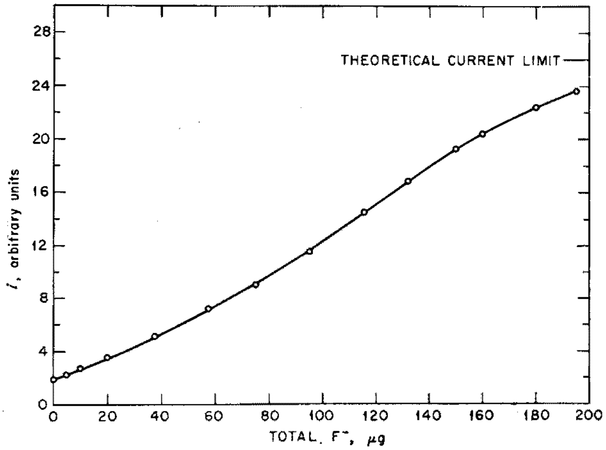

Fig. 3. Calibration curve of total fluoride *vs.* i. Test conditions: [Zr] = $6.6 \cdot 10^{-5}$ M; [Aliz] = $5.9 \cdot 10^{-5}$ M; [$HClO_4$] = 0.5 N. Sample volume = 50 ml. Theoretical current limit = current exhibited by $5.9 \cdot 10^{-5}$ M alizarin red S.

excess of zirconium while exhibiting $\Delta i/[F^-]$ values not quite so large as those containing excess of alizarin, exhibited a low blank current and the percent change per unit of fluoride present was much larger than in the reverse case. Therefore it was decided that the stock reagent solutions should be made up with an excess of zirconium such that in the final test solution 85–90% of the alizarin red S present is complexed.

In Fig. 3 is shown a calibration curve of $[F^-]$ *vs.* i over a fairly wide range of concentrations. The upward curvature of the lower position of the curve is probably due to the fact that the $i/[\text{aliz}]$ factor is not a constant but increases with increasing concentration of alizarin red S. The upper portion of the curve shows the influence of the equilibria involved. The current due to the alizarin red S released by increasing concentrations of fluoride should approach asymptotically the current of pure alizarin red S in a concentration equal to that in the reagent. The calibration curve reflects this more strongly as the fluoride concentration increases. In practice it is advisable to use only the central portion of the curve excluding the higher and lower 20%. Over a narrower range of fluoride concentration such as would ordinarily be used following the prescribed procedure, the inflection of the curve is much less prominent.

In Table I is shown a precision study over two ranges of reagent concentration. The data indicate the method to be highly sensitive and comparable to the best colorimetric methods for trace quantities of fluoride.

TABLE I

PRECISION STUDY

$[F^-]$*(p.p.m.)*	*Relative standard deviation*[a]
(A) $[\text{Zr}] = 1.7 \cdot 10^{-5}$ *M*; $[\text{Aliz}] = 7.5 \cdot 10^{-6}$ *M*; $[\text{HClO}_4] = 0.5$ *N*.	
0.038	3.7
0.190	3.1
0.380	2.2
(B) $[\text{Zr}] = 4.1 \cdot 10^{-5}$ *M*; $[\text{Aliz}] = 2.9 \cdot 10^{-5}$ *M*; $[\text{HClO}_4] = 0.5$ *N*.	
0.76	3.1
1.14	2.6
1.52	2.2

[a] Seven determinations.

TABLE II

INTERFERENCE STUDY

(Test conditions: $[\text{Zr}] = 1.7 \cdot 10^{-5}$ *M*; $[\text{Aliz}] = 7.5 \cdot 10^{-6}$ *M*; $[\text{HClO}_4] = 0.5$ *N*; $[F^-] = 200$ p.p.b. Ionic strength to 1 *M* with sodium perchlorate)

No interference—Metals

40 p.p.m. of Ag(I), Al(III), Bi(III), Ca(II), Cd(II), Co(II), Cu(II), Hg(II), Li(I), Mo(VI), Mg(II), Ni(II), Pr(III), Pb(II), Th(IV), Tl(I), U(VI) or Zn(II).

10 p.p.m. of Be(II), Fe(III) or V(V)[a].

No interference—Anions

$5 \cdot 10^{-1}$ *M* NO_3^-, $1 \cdot 10^{-1}$ *M* Cl^-, $3 \cdot 10^{-3}$*M* acetate, or $1 \cdot 10^{-4}$ *M* SO_4^{2-}[b]

Interference at any level—PO_4^{3-}

[a] Slight interference at 40 p.p.m. but none measurable at 10 p.p.m.

[b] Interferes above this level.

Table II shows some interference studies carried out. The method is relatively free from interferences, phosphate being the only interfering ion at all levels studied. Strong oxidizing agents such as chromium(VI) also interfere by oxidation of the reagent but reduction with a hydroxylamine salt before the addition of the sample to the reagent eliminates this interference. Since the work is carried out at anodic potentials, oxygen does not interfere and deaeration is unnecessary.

SUMMARY

A voltammetric method for the determination of micro amounts of fluoride is described. It is based on the measurement of the amount of free alizarin red S liberated by the fluoride ion from a zirconium–alizarin red S complex. The free dye measurement carried out at 0.7 V *vs.* S.C.E. depends on the anodic reaction of alizarin red S at the rotating pyrolytic graphite electrode. The method is simple, sensitive and suffers from relatively few interferences.

RÉSUMÉ

Une méthode voltammétrique est décrite pour le dosage de microquantités de fluorure. Elle est basée sur la détermination du rouge d'alizarine S libéré du complexe zirconium-rouge d'alizarine S par le fluorure. La mesure effectuée à 0.7 V *vs.* ECS dépend de la réaction anodique du rouge d'alizarine S à l'électrode tournante en graphite pyrolytique. La méthode est simple, sensible et peu perturbée par des ions étrangers.

ZUSAMMENFASSUNG

Eine voltametrische Methode für die Bestimmung von Mikromengen Fluorid wird beschrieben. Sie beruht auf der Messung des Anteils freien Alizarinrot S, das durch das Fluorid-Ion aus einem Zirkoniumalizarinrot S in Freiheit gesetzt wurde. Die Messung des freien Farbstoffs, welche bei 0.7 V gegen eine Standard-Kalomel-Elektrode ausgeführt wurde, hängt von der anodischen Reaktion des Alizarinrot S an der rotierenden pyrolytischen Graphitelektrode ab. Die Methode ist einfach, empfindlich und besitzt relativ wenig Störungen.

REFERENCES

1 I. M. Kolthoff and P. J. Elving, *Treatise on Analytical Chemistry*, Part II, Vol. 7, Interscience Publishers, New York, 1961.
2 H. E. Zittel and T. M. Florence, *Anal. Chem.*, 39 (1967) 320.
3 M. T. Kelley, *U. S. At. Energy Comm. Rept. ORNL-3750*, 1964, p. 4.
4 T. M. Florence, F. J. Miller and H. E. Zittel, *Anal. Chem.*, 38 (1966) 1065.

Analytica Chimica Acta
Elsevier Publishing Company, Amsterdam
Printed in The Netherlands

POTENTIOMETRIC TITRATIONS OF ORGANOTIN CHLORIDES WITH TETRAPHENYLARSONIUM CHLORIDE IN ACETONITRILE MEDIA

GIUSEPPE TAGLIAVINI AND PIERINO ZANELLA*
Institute of Analytical Chemistry, University of Padua, Padua (Italy)

(Received May 13th, 1967)

In recent years, interest in the coordination chemistry of organotin compounds has increased, but although much work has been devoted to organometallic species in aqueous solutions or crystals[1,2] only a few papers have dealt with complexes in non-aqueous solvents[3].

In this laboratory, attention has already been given to the formation of chloride complexes of organometallic compounds of the type $R_{4-n}SnCl_{n+1}^-$ ($n=2,3$). The formation of the negatively charged complexes $RSnCl_4^-$ and $R_2SnCl_3^-$ (R=Bu and Ph) in acetonitrile and acetone solution has been studied[4]; evidence for these species has also been obtained from their precipitation from aqueous solution as tetraphenylarsonium salts[5].

In the present paper, the formation of organotin halo-complexes (R = Me, Et, Pr, Bu, Ph) by titration of organotin compounds in acetonitrile media with tetraphenylarsonium chloride or tetraethylammonium chloride or bromide is described. The experimental methods employed were very similar to those described by GUTMANN AND MAIRINGER,[6] and have been used by many workers for potentiometric titrations of inorganic acids such as MCl_n (M = Metal) with tetraethylammonium chloride, triphenylmethylchloride, etc., in solvents such as $SOCl_2$[7], C_6H_5COCl[8], $POCl_3$[9], $PhPOCl_2$[9] and CH_3COCl[10].

EXPERIMENTAL

Materials and solutions

Phenyltin and butyltin trichlorides (Fluka AG) were distilled before use. All the other organotin compounds were prepared and purified by the methods reported in the literature[11].

Tetraethylammonium chloride was obtained by neutralization of an aqueous solution of tetraethylammonium hydroxide with hydrochloric acid and was purified by two crystallizations from anhydrous acetone. Tetraethylammonium bromide (C. Erba, Milan) was dried under vacuum at 80° before use. Tetraphenylarsonium chloride (K. K. Labs. Inc., New York) was purified by precipitating it from an ethanolic solution by addition of absolute ether (m.p. 260°; reported values 261–263°[12] and 256–257°[13]). Commercial acetonitrile (C. Erba) was purified as described by

---

[*] Ricercatore incaricato aggiunto C.N.R. (Roma).

WALDEN AND BIRR[14]. The specific conductance of the purified solvent varied from 0.8 to $1 \cdot 10^{-7}$ Ω^{-1} cm^{-1}.

Solutions of organotin compounds, tetraethylammonium chloride and bromide, and tetraphenylarsonium chloride were prepared by adding weighed quantities to a known volume of acetonitrile. The molarities were checked by potentiometric titration of halide ion with silver nitrate. Solutions of the required concentrations were prepared by dilution of the stock solutions. All operations were carried out in a dry box under a nitrogen atmosphere.

Procedure and apparatus

Potentiometric titrations of organotin compounds with halogen bases, as well as the reverse titrations, were performed at 25° in a cell (Fig. 1), which is a modification of the cell described by GUTMANN AND MAIRINGER[6].

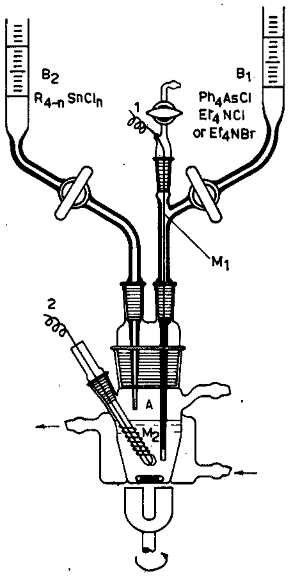

Fig. 1. Cell assembly.

A known volume of the halogen base was transferred to vessel A from burette B_1 (10-ml capacity) containing a molybdenum wire M_1 (*cf.* ref. 4); the tip of the burette was immersed in the sample solution, so that wire M_1 formed one electrode of a concentration cell, the other one being the molybdenum wire M_2. The titration was performed by adding the organotin solution from burette B_2.

In all cases the reference electrode was the wire M_1 inside burette B_1. Leads 1 and 2 were jointed to an Electronic Digital Voltmeter LM 1420 Solartron so that e.m.f. measurements could be carried out.

The molybdenum electrodes were appropriately treated before measurements were made, by placing them as anodes in an electrolytic solution of acetonitrile containing 0.5 *M* tetrabutylammonium perchlorate and 0.1 *M* tetraethylammonium chloride. This treatment allowed the electrodes to be used as indicators for tetraphenylarsonium chloride solutions. The e.m.f. values of tetraphenylarsonium chloride concentration cells are related by the following equation

$$E_{\mathrm{exp}} = 0.0591 \log \{[\mathrm{Ph_4AsCl}]_r/[\mathrm{Ph_4AsCl}]_x\} + C \qquad (1)$$

where $[\mathrm{Ph_4AsCl}]_r$ represents the tetraphenylarsonium chloride concentration of the reference electrode and $[\mathrm{Ph_4AsCl}]_x$ that in which the concentration of this salt is changed. The validity of eqn. (1) was verified for a range of tetraphenylarsonium chloride concentrations from 10^{-2} to $5 \cdot 10^{-5}\,M$, and the C value, determined by putting $[\mathrm{Ph_4AsCl}]_r = [\mathrm{Ph_4AsCl}]_x$, represents a constant e.m.f. depending on the intrinsic nature of the two electrodes. This value was always subtracted from each E_{exp}-value.

Since the salt is completely dissociated[12,15] for the above-mentioned concentration range, *i.e.*

$$[\mathrm{Cl}] = [\mathrm{Ph_4AsCl}], \quad \text{and } K = \frac{[\mathrm{R_{4-n}SnCl_{n+1}}^-]}{[\mathrm{R_{4-n}SnCl_n}][\mathrm{Cl}^-]},$$

the following equation may be written:

$$E = 0.0591 \log K + 0.0591 \log \frac{[\mathrm{R_{4-n}SnCl_n}]}{[\mathrm{R_{4-n}SnCl_{n+1}}^-]} + 0.0591 \log [\mathrm{Cl}^-]_r \qquad (2)$$

This equation can be used in the part of the potentiometric plots in which $x \geqslant 1$.

RESULTS AND DISCUSSION

The results of the potentiometric titrations of tetraphenylarsonium chloride (see Fig. 2), tetraethylammonium chloride and tetraethylammonium bromide with the selected organotin chlorides, are listed in Tables I, II and III respectively. Reverse titrations of organotin compounds with these bases were also possible and gave the same results (*cf.* ref. 4).

All titration plots gave an equivalence point at ratio $x = \{[\mathrm{R_{4-n}SnCl_n}]/[\mathrm{Ph_4AsCl}]\}$ equal to 1 (within the experimental error), indicating that the acid–base systems consist of the conjugated couples $\mathrm{R_{4-n}SnCl_n}/\mathrm{R_{4-n}SnCl_{n+1}}^-$.

For the titration with tin(IV) chloride, reported[4] and listed results (Tables I and II) show that two endpoints are found with ratios x of about 0.5 and 1. Anionic chloro-complexes of the type $\mathrm{R_{4-n}SnCl_{n+1}}^-$ seem to be the more probable species in a solvent such as acetonitrile, and the formation of penta-coordinated tin anions may be established in such a solvent.

Species of the type $\mathrm{R_{4-n}SnCl_nBr}^-$ appear to be present in acetonitrile when tetraethylammonium bromide is the -onium base employed.

The acceptor power of tin, when (i) one or more chlorine atoms are substituted by organic groups and (ii) the organic group is changed, can be discussed on the basis of the potentiometric titrations of tetraphenylarsonium chloride with the examined organometallic compounds.

In Fig. 3 the plots of E against $\log\{[\mathrm{R_{4-n}SnCl_n}]/[\mathrm{R_{4-n}SnCl_{n+1}}^-]\}$ are shown. The lines were obtained by computing the potentiometric data from ratio $x = 1$ to

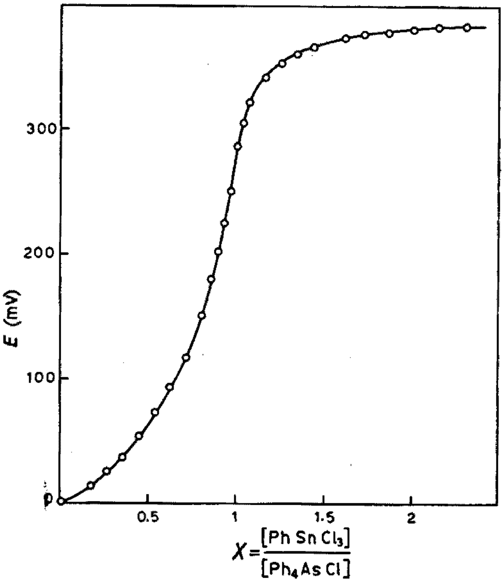

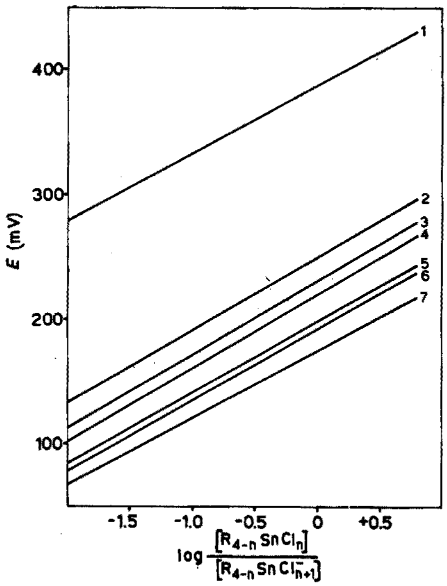

Fig. 2. Potentiometric titration plot of tetraphenylarsonium chloride with phenyltin trichloride in acetonitrile at 25°.

Fig. 3. Plots of E against $\log(R_{4-n}SnCl_n/R_{4-n}SnCl_{n+1}^-)$ (*cf.* eqn. (2)). (1) $PhSnCl_3$, (2) $MeSnCl_3 \cdot EtSnCl_3 \cdot BuSnCl_3$, (3) Ph_2SnCl_2, (4) Me_2SnCl_2, (5) $Et_2SnCl_2 \cdot Pr_2SnCl_2$, (6) Bu_2SnCl_2, (7) Ph_3SnCl.

TABLE I

TITRATION OF TETRAPHENYLARSONIUM CHLORIDE WITH $R_{4-n}SnCl_n$ COMPOUNDS (n = 4,3,2,1) IN ACETONITRILE AT 25°

Concn. Ph_4AsCl ($M \cdot 10^2$)	*Amount Ph_4AsCl titrated (ml)*	*Titrant*	*Concn. $R_{4-n}SnCl_n$ ($M \cdot 10^2$)*	*Titrant added ml at end-point*		$x = \frac{[R_{4-n}SnCl_n]}{[Ph_4AsCl]}$, *at e.p.*
				Calcd.	*Found*	
1.344	10	$SnCl_4$	7.07	1.90	0.93–1.90	0.49–1.000
1.344	10	$MeSnCl_3$	5.00	2.69	2.70	1.002
1.344	12	Me_2SnCl_2	5.00	3.23	3.15	0.975
1.344	10	$EtSnCl_3$	5.00	2.69	2.70	1.002
1.344	12	Et_2SnCl_2	5.40	2.99	2.90	0.970
1.344	12	Pr_2SnCl_2	5.40	2.99	2.95	0.986
1.344	9	$BuSnCl_3$	4.48	2.70	2.70	1.000
1.344	14	Bu_2SnCl_2	5.00	3.77	3.80	1.007
1.344	10	$PhSnCl_3$	4.80	2.80	2.70	0.964
1.344	12	Ph_2SnCl_2	5.00	3.23	3.15	0.975
1.344	10	Ph_3SnCl	2.80	4.80	4.95	1.031

2.3, that is in the range in which the ratio x may be considered equal to the ratio $[R_{4-n}SnCl_n]/[R_{4-n}SnCl_{n+1}^-]$.

Table IV shows for each compound the E-values when the ratio $[R_{4-n}SnCl_n]/[R_{4-n}SnCl_{n+1}^-]$ is equal to 1, (*i.e.*, $x=2$) and the values of the slope of each lines. The slopes (Δ-values) are very near the calculated value: 0.0591 V.

On considering the Δ-values, it may be concluded that in acetonitrile the

TABLE II

TITRATION OF TETRAETHYLAMMONIUM CHLORIDE WITH $R_{4-n}SnCl_n$ (n = 4,3,2) IN ACETONITRILE AT 25°

Concn. Et_4NCl ($M \cdot 10^2$)	*Amount Et_4NCl titrated (ml)*	*Titrant*	*Concn. $R_{4-n}SnCl_n$ ($M \cdot 10^2$)*	*Titrant added ml at end point*		$x = \frac{[R_{4-n}SnCl_n]}{[Et_4NCl]}$, *at e.p.*
				Calcd.	*Found*	
1.344	6.0	$SnCl_4$	5.00	1.61	0.80–1.57	0.497–0.975
1.344	12.0	$MeSnCl_3$	5.00	3.22	3.25	1.009
1.344	12.0	Me_2SnCl_2	5.00	3.22	3.20	0.993
1.344	10.0	$EtSnCl_3$	5.00	2.69	2.70	1.002
1.344	12.0	Et_2SnCl_2	5.00	3.22	3.20	0.993
1.344	12.0	Pr_2SnCl_2	5.00	3.22	3.25	1.009
1.344	6.0	$BuSnCl_3$	5.00	1.61	1.62	1.006
1.344	10.0	Bu_2SnCl_2	4.98	2.70	2.65	0.981
1.344	10.0	$PhSnCl_3$	5.00	2.69	2.70	1.003
1.344	10.0	Ph_2SnCl_2	5.00	2.69	2.50	0.930

TABLE III

TITRATION OF TETRAETHYLAMMONIUM BROMIDE WITH $R_{4-n}SnCl_n$ (n = 3,2) IN ACETONITRILE AT 25°

Concn. Et_4NBr ($M \cdot 10^2$)	*Amount Et_4NBr titrated (ml)*	*Titrant*	*Concn. $R_{4-n}SnCl_n$ ($M \cdot 10^2$)*	*Titrant added ml at end-point*		$x = \frac{[R_{4-n}SnCl_n]}{[Et_4NBr]}$, *at e.p.*
				Calcd.	*Found*	
1.344	6	$BuSnCl_3$	5.00	1.61	1.72	1.068
1.344	6	Bu_2SnCl_2	4.98	1.62	1.60	0.988
1.344	6	$PhSnCl_3$	5.00	1.61	1.68	1.043
1.344	6	Ph_2SnCl_2	5.02	1.61	1.61	1.000

TABLE IV

E-VALUES AT $[R_{4-n}SnCl_n]/[R_{4-n}SnCl_{n+1}^-] = 1$ AND SLOPE VALUES OF THE LINES OF FIG. 2

Compound	*E (mV) at $\frac{[R_{4-n}SnCl_n]}{[R_{4-n}SnCl_{n+1}^-]} = 1$*	*Δ-value (V) (cf. Fig. 2)*
$MeSnCl_3$	255	0.058
$EtSnCl_3$	250	0.058
$BuSnCl_3$	250	0.058
$PhSnCl_3$	380	0.055
Me_2SnCl_2	220	0.059
Et_2SnCl_2	198	0.058
Pr_2SnCl_2	198	0.058
Bu_2SnCl_2	193	0.058
Ph_2SnCl_2	220	0.057
Ph_3SnCl	175	0.054

chloro-complexes of these organotin species possess univalent negative charges. This means that no dimerization occurs in such a solvent in view of the formation of hexa-coordinated chloro-bridge species.

Solvation may be important, and the sixth position of coordination could be ascribed to acetonitrile, which can form adducts with several acceptors. It has been ascertained that tin(IV) chloride forms adducts with acetonitrile; the compound

$SnCl_4 \cdot 2CH_3CN$ has been isolated in solid[16]. However, in the present work, attempts to prepare addition compounds of acetonitrile with the considered organometallic derivatives, under the same experimental conditions as for the tin(IV) chloride adducts[16], failed. In the potentiometric titrations, only tin(IV) chloride showed two equivalence points, indicating that two conjugated acid–base systems can exist: $SnCl_4/SnCl_5^-$ and $SnCl_5^-/SnCl_6^{2-}$ (see also ref. 4). This does not seem to be the case for the organometallic species examined since they gave only one equivalence point at ratio $x=1$.

These results seem to show that chloride has a greater ability than acetonitrile, to coordinate to $SnCl_4$, which has acceptor properties greater than those of $R_{4-n}SnCl_n$ compounds. On the other hand, solvation of chloride in such a solvent is weak[17] and greater stabilization of the formed complexes can arise with chloride as ligand[18,19].

Therefore, penta-coordination of the organotin species with a ligand such as chloride or bromide, seems the more probable configuration in such a solvent; on the other hand, salts of the type $[Ph_4As][RSnCl_4]$ and $[Ph_4As][R_2SnCl_3]$ can be prepared by precipitating the organometallic compounds dissolved in water at high chloride concentration with tetraphenylarsonium chloride[5]. The same compounds can be prepared by crystallization from acetone or acetonitrile[15].

In order to indicate the relative stability of the chloro-complexes, the E-values can be considered (*cf.* Table IV). A comparison of these values shows the following relative order, which indicates the complex-forming ability: $PhSnCl_3 > MeSnCl_3$, $EtSnCl_3$, $BuSnCl_3 > Ph_2SnCl_2 > Me_2SnCl_2 > Et_2SnCl_2$, Pr_2SnCl_2, $Bu_2SnCl_2 > Ph_3SnCl > R_3SnCl$ ($R =$ Me, Et, Pr, Bu). It appears that mono-organotin compounds have a better ability than diorgano-tin and triorgano-tin, to form negatively charged chloro-complexes. Of the triorganotin compounds examined, only triphenyltin chloride gave a good titration plot; with the trialkyltin compounds, it was not possible to carry out potentiometric titrations, certainly because of the lower stability of the complexes.

The high value of E for phenyltin trichloride and consequently the higher stability of the $PhSnCl_4^-$ complex compared to $RSnCl_4^-$ and $R_2SnCl_3^-$ ($R =$ alkyl group), which appeared to have equal stabilities, are probably due to the $-I$ effect of the phenyl group. Together with the four coordinated chlorine atoms, this effect stabilizes the negative charge on the whole complex ion. The method does not allow the stability order of the $R_2SnCl_3^-$ and $RSnCl_4^-$ complexes to be distinguished when the alkyl groups are changed. Spectrophotometric methods are being examined in order to obtain the corresponding stability constants in acetonitrile for analogous series of alkyl- and aryltin chlorides complexes.

The authors express their thanks to Prof. L. RICCOBONI for helpful discussion. The financial support of the Consiglio Nazionale delle Ricerche (Roma, Italy) is gratefully acknowledged.

SUMMARY

Tetraphenylarsonium chloride was used for the potentiometric titration of $R_{4-n}SnCl_n$ compounds ($R =$ Me, Et, Pr, Bu, Ph; $n = 2,3$) in acetonitrile media. Evidence for penta-coordinated $R_{4-n}SnCl_{n+1}^-$ complexes was obtained. A stability scale as a function of R groups is given.

RÉSUMÉ

On utilise le chlorure de tétraphénylarsonium pour le titrage potentiométrique de composés $R_{4-n}SnCl_n$ (R = Me, Et, Pr, Bu, Ph; $n = 2,3$) en milieu acétonitrile. On admet la formation de complexes pentacoordinés $R_{4-n}SnCl_{n+1}^-$. On donne une échelle de stabilité en fonction des groupes R.

ZUSAMMENFASSUNG

Für die potentiometrische Titration von $R_{4-n}SnCl_n$-Verbindungen (R = Me, Et, Pr, Bu, Ph; $n = 2,3$) in Acetonitril wurde Tetraphenylarsoniumchlorid verwendet. Aus diesen Messungen ergaben sich Beweise für $R_{4-n}SnCl_{n+1}^-$-Komplexe mit 5er-Koordination. Eine Stabilitätsskala als Funktion der R-Gruppen wird angegeben.

REFERENCES

1 See R. S. Tobias, *Organometal. Chem. Rev.*, 1 (1966) 93.
2 See M. Gielen and N. Sprecher, *Organometal. Chem. Rev.*, 1 (1966) 455.
3 M. Gielen, J. Nasielski and R. Yernaux, *Bull. Soc. Chim. Belges*, 72 (1963) 594.
4 G. Tagliavini, P. Zanella and M. Fiorani, *Coordin. Chem. Rev.*, 1 (1966) 249.
5 G. Tagliavini and P. Zanella, *J. Organometal. Chem.*, 5 (1966) 299.
6 V. Gutmann and F. Mairinger, *Z. Anorg. Allgem. Chem.*, 289 (1957) 279.
7 H. Spandau and E. Brunneck, *Z. Anorg. Allgem. Chem.*, 278 (1955) 197.
8 V. Gutmann and H. Tannenberger, *Monatsh.*, 88 (1957) 216.
9 V. Gutmann, *Quaderni Chim.*, 1 (1964) 7 and references therein.
10 M. Fiorani, L. Riccoboni and G. Schiavon, *Boll. Sci. Fac. Chim. Ind. Bologna*, 21 (1963) 211.
11 See R. K. Ingham, S. D. Rosemberg and H. Gilman, *Chem. Rev.*, (1960) 459.
12 A. I. Popov and R. E. Humphrey, *J. Am. Chem. Soc.*, 81 (1959) 2043.
13 F. F. Blicke and E. Monroe, *J. Am. Chem. Soc.*, 57 (1935) 720.
14 P. Walden and E. J. Birr, *Z. Physik. Chem. (Leipzig)*, A 144 (1929) 269.
15 Unpublished results.
16 H. J. Coerver and C. Curran, *J. Am. Chem. Soc.*, 80 (1958) 3522.
17 A. J. Parker, *Quart. Rev.*, 16 (1962) 163.
18 J. Coates and E. Taylor, *J. Chem. Soc.*, (1936) 1245.
19 J. F. Coetzee, *Ph. D. Thesis*, Univ. of Minnesota, 1955.

Analytica Chimica Acta
Elsevier Publishing Company, Amsterdam
Printed in The Netherlands

DIE QUANTITATIVE BESTIMMUNG VON ALKALI- UND ERDALKALIIONEN NEBENEINANDER DURCH CHLORIDIMETRISCHE FÄLLUNGSTITRATION IN NICHTWÄSSRIGEN LÖSUNGEN

G. HENRION* UND E. PUNGOR
Universität für die Chemische Industrie, Lehrstuhl für Analytische Chemie, Veszprém (Ungarn)

(Eingegangen den 10. Mai, 1967)

Die im Vergleich zu Wasser oft völlig veränderten Löslichkeitsverhältnisse vieler Salze in nichtwässrigen Solventien können zu quantitativen Fällungsreaktionen ausgenutzt werden, die in wässriger Lösung nicht denkbar sind. So konnten z.B. in verschiedenen Ketonen die dort gut löslichen Jodide[1], Perchlorate und Hexafluoroarsenate[2] des Natriums oder des Kaliums mit einer Lithiumchlorid enthaltenden alkoholischen oder ketonischen Masslösung titriert werden. Dabei fiel das Kation als Chlorid aus. Der Äquivalenzpunkt wurde oszillometrisch oder konduktometrisch indiziert. Die Einzelfehler bewegten sich innerhalb der Grenzen ±1%. In Abhängigkeit von den verwendeten Solventien und vom jeweils vorliegenden Salz war die Gestalt der Titrationsdiagramme unterschiedlich. Sie konnte durch Vergleich der Leitfähigkeit der titrierten Stoffe (MeX) und der dabei gebildeten Stoffe (LiX) bei den gegebenen Konzentrationen erklärt werden.

Lösungen von Bariumjodid oder Bariumperchlorat in Azeton oder Methylisobutylketon wurden ebenfalls chloridimetrisch titriert. Dabei lieferte die oszillometrische Indikation vor dem Äquivalenzpunkt gekrümmte Kurvenäste, die erst bei Vorlagen mit kleinerer Konzentration in Geraden übergingen. Ähnliche Verhältnisse wurden beim Strontium und beim Calzium gefunden. In der vorliegenden Arbeit soll die Möglichkeit der Titration von Alkalien und Erdalkalien nebeneinander geprüft werden. Bezüglich experimenteller Einzelheiten siehe den Lit[1].

ERGEBNISSE

Die simultane Titration von Natriumjodid und Bariumjodid bzw. Natriumperchlorat und Bariumperchlorat in Methyl-isobutylketon

In eine gut gerührte Vorlage von *ca.* 100 ml Methyl-isobutylketon wurden 1180 Val·10^{-6} Natriumjodid und 196 Val·10^{-6} Bariumjodid einpipettiert. Diese Lösung wurde mit Lithiumchlorid in Äthanol (0.2550 *N*) titriert. Die Ablesung der Messwerte vom Oszillotitrator erfolgte jeweils *ca.* 2 min nach der Reagenzzugabe. Das Gleichgewicht bei der Ausfällung von Natriumchlorid oder Bariumchlorid allein stellt sich erheblich schneller ein, so dass diese Zeit ausreichen sollte. Die graphische Darstellung der Messwerte wird durch Diagramm I auf Fig. 1 gezeigt. Der Verlauf

---

[*] I Chemisches Institut der Humboldt-Universität zu Berlin (DDR).

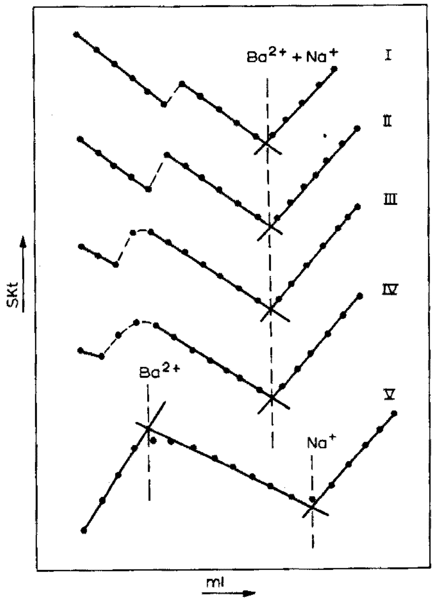

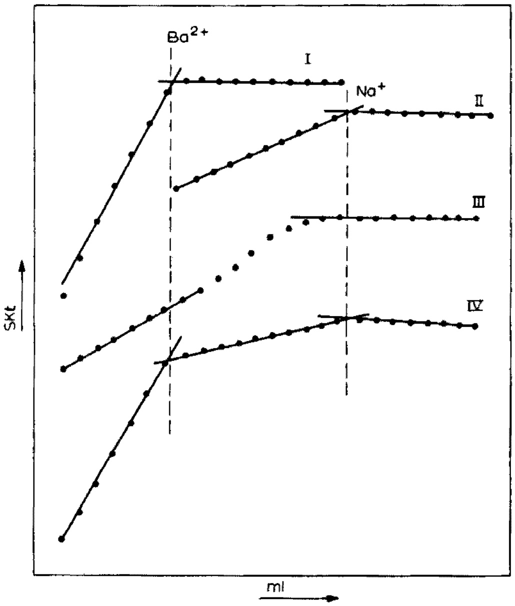

Fig. 1. Titration von NaI und BaI_2 in Methyl-isobutylketon mit LiCl in Äthanol 0.255 *N*. (I) bis (IV) 1180 Val·10^{-6} NaI + 196 Val·10^{-6} BaI_2 (mit abnehmender Geschwindigkeit titriert); (V) 1180 Val·10^{-6} NaI + 490 Val·10^{-6} BaI_2 (langsam titriert).

Fig. 2. Titration von $NaClO_4$ und $Ba(ClO_4)_2$ in Methyl-isobutylketon mit LiCl 0.0824 *N* in Methyl-isobutylketon. (I) 132 Val·10^{-6} $Ba(ClO_4)_2$; (II) 206 Val·10^{-6} $NaClO_4$; (III) die Mischung von I und II schnell titriert; (IV) die gleiche Mischung langsam titriert.

des Diagramms ist anfangs so, wie von der Titration reiner Natriumjodidlösungen her gewohnt. Die Leitwerte nehmen stetig ab. Doch setzt bei ungefähr halbem Umsatz ein Anstieg des Leitwertes an, der sehr langsam erfolgt. Deshalb muss hier mit der Ablesung und weiteren Reagenzzugabe längere Zeit gewartet werden. Ein solcher Anstieg tritt bei der Ausfällung von Bariumchlorid aus Bariumjodid- oder Bariumperchloratlösungen auf, wie früher gezeigt worden ist[2]. Der weitere Verlauf der Titration ist wieder ganz so, als läge nur Natriumjodid vor. Erfolgt die Ablesung und Reagenzzugabe langsamer (in Intervallen von *ca.* 3 min) dann tritt die Unterbrechung der stetigen Abnahme des Leitwertes durch den Anstieg schon bei geringerem Reagenzverbrauch auf (Diagramm II). Hat man die Einstellung des Gleichgewichtes abgewartet, dann kann wieder weitertitriert werden, als läge nur Natriumjodid vor. Die Zeitintervalle wurden auf *ca.* 5 min (Diagramm III) und *ca.* 15 min (Diagramm IV) vergrössert. Dabei zeigte sich, dass bei so langsamer Titration die Ausfällung des Bariumchlorids aus der Mischlösung fast ganz an den Anfang rückt, trotz dem grossen Überschuss von Natriumjodid zu Bariumjodid wie *ca.* 10:1 (Molverhältnis!).

Diagramm V zeigt die analoge Titration einer Mischung von 1180 Val·10^{-6} Natriumjodid und 490 Val·10^{-6} Bariumjodid. Hier tritt trotz dem vierfachen Überschuss von Natriumjodid die Ausfällung des Bariumchlorides ganz an den Anfang.

Analoge Beobachtungen werden bei der Titration von Bariumperchlorat neben Natriumperchlorat in Methyl-isobutylketon mit Lithiumchlorid in Methyl-isobutylketon gemacht. Figur 2 zeigt hierfür Beispiele. Diagramm I entspricht der Titration von Bariumperchlorat allein, Diagramm II der von Natriumperchlorat allein. Wird die Mischung beider schnell titriert (Diagramm III), so fällt zuerst überwiegend Natriumchlorid, später Bariumchlorid, wobei in letzterem Bereich die Streuung der Messwerte daraufhinweist, dass die Gleichgewichtseinstellung nicht erreicht wurde. Titriert man die gleiche Mischung sehr langsam (Wartezeit vor jeder Ablesung *ca.* 15 min), so wird zuerst Bariumchlorid gefällt und dann Natriumchlorid (Diagramm IV). Beide Komponenten sind auf dem Diagramm sauber getrennt, wenn auch der Schnittwinkel am Äquivalenzpunkt des Natriums für eine quantitative Auswertung verhälnismässig ungünstig ist. Aus den geschilderten Ergebnissen kann man zweierlei folgern:

(1) Die Löslichkeit des Bariumchlorids in Methyl-isobutylketon ist deutlich kleiner als die des Natriumchlorids.

(2) Während sich bei der Ausfällung von Alkalichlorid allein oder Bariumchlorid allein das Gleichgewicht sehr schnell einstellt (innerhalb einiger Sekunden), so dass die Durchmischung der Lösung nach der Reagenzzugabe der langsamste Vorgang ist, ist die Gleichgewichtseinstellung bei gleichzeitigem Vorliegen von Alkali- und Bariumionen in Methyl-isobutylketon erheblich verzögert. Demzufolge wäre eine selektive Titration solcher Mischungen nur mit grossem Zeitaufwand möglich.

Kinetische Untersuchungen

Die Vorgänge bei der Fällung und Gleichgewichtseinstellung von festem Natriumchlorid und festem Bariumchlorid in ketonischen Lösungen wurden am System Natriumperchlorat/Bariumperchlorat in Methyl-isobutylketon und in Azeton untersucht. In eine stark gerührte Vorlage von *ca.* 100 ml Methyl-isobutylketon wurden 200 $\mathrm{Val \cdot 10^{-6}}$ Natriumperchlorat und 150 $\mathrm{Val \cdot 10^{-6}}$ Bariumperchlorat gegeben. Der Oszillotitrator wurde an einen Kompensationsbanschreiber angeschlossen. Er zeichnete für diese Mischung zuerst die Grundlinie. Dann wurden 100 $\mathrm{Val \cdot 10^{-6}}$ Lithiumchlorid schnell einpipettiert (Fig. 3, Diagramm I). Es erfolgte steile Zunahme des Leitwertes, dann weiteres immer langsamer werdendes Anwachsen. Das Gleichgewicht war nach *ca.* 10 min erreicht.

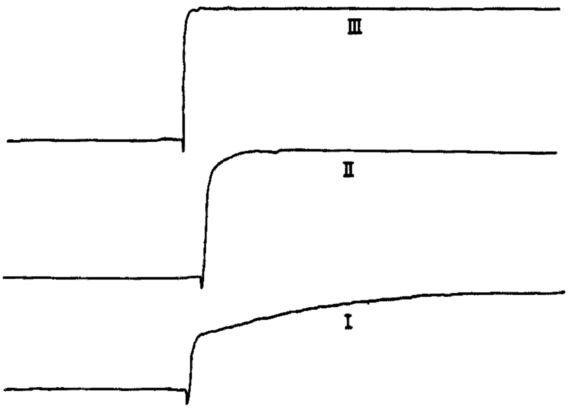

Fig. 3. Zeitlicher Verlauf der Umsetzung in Methyl-isobutylketon. 200 $\mathrm{Val \cdot 10^{-6}}$ $NaClO_4$ + 150 $\mathrm{Val \cdot 10^{-6}}$ $Ba(ClO_4)_2$ und plötzliche Zugabe von (I) 100; (II) 200; (III) 300 $\mathrm{Val \cdot 10^{-6}}$ LiCl.

In eine analoge Mischung von Natriumperchlorat und Bariumperchlorat wurden im nächsten Versuch 200 Val·10^{-6} Lithiumchlorid einpipettiert (Diagramm II). Wieder ist dem anfänglichen steilen Anstieg eine weitere langsame Reaktion angeschlossen. Doch wird hier das Gleichgewicht schon nach *ca.* 2 min erreicht. Zugabe von 300 Val·10^{-6} Lithiumchlorid (Diagramm III) bewirkt schnelle fast vollständige Umsetzung. Der Anteil der langsamen Reaktion ist hier nur noch sehr klein. Das Gleichgewicht wird schon nach *ca.* 30 sec. erreicht.

Wir kamen zu folgender Erklärung: Obwohl die Fällung von Natriumchlorid und die von Bariumchlorid sehr schnell verläuft, muss die Geschwindigkeit beider Vorgänge relativ zueinander deutlich verschieden sein. Natriumchlorid kristallisiert schneller aus, obgleich Bariumchlorid weniger löslich ist. Deshalb werden bei Reagenzzugabe die Chloridionen zuerst überwiegend von den Natriumionen gebunden. Erst anschliessend erfolgt eine Umsetzung von festem Natriumchlorid mit Bariumionen der Lösung zu festem Bariumchlorid, wobei sich das endgültige Gleichgewicht naturgemäss langsam einstellt. Diese Vorstellungen entsprechen auch unseren Beobachtungen bei der Titration der Alkalijodide neben Bariumjodid in Azeton, die weiter unten beschrieben werden. Im ersten Teil der Diagramme, wo Bariumchlorid gefällt wird, beobachtet man nach Reagenzzugabe erst eine Abnahme des Leitwertes wie bei der Titration der reinen Alkalijodide und erst nach einigen Sekunden den dargestellten Anstieg.

Um die Richtigkeit der Annahme zu überprüfen, wurden die auf Fig. 3 dargestellten Versuche unter den gleichen Bedingungen und Konzentrationsverhältnissen wiederholt, nur mit dem einen Unterschied: Es wurde Natriumperchlorat allein vorgelegt, dann Lithiumchlorid einpipettiert und erst danach das Bariumperchlorat (Fig. 4). Dabei wurden nun die Chloridionen zuerst ganz sicher zur Fällung von Natriumchlorid verbraucht. Soweit sich dabei Lithiumchlorid gegenüber Natriumperchlorat im Unterschuss befand (Diagramm I) musste der Angriff des Bariumperchlorats auf das ausgefällte Natriumchlorid sogar gegen einen Überschuss von Natriumionen erfolgen. Das geht entsprechend langsam vonstatten. Bei Diagramm I war das Gleichgewicht erst nach *ca.* 80 min erreicht. Bei Diagramm II hat sich der Gleichgewichts-

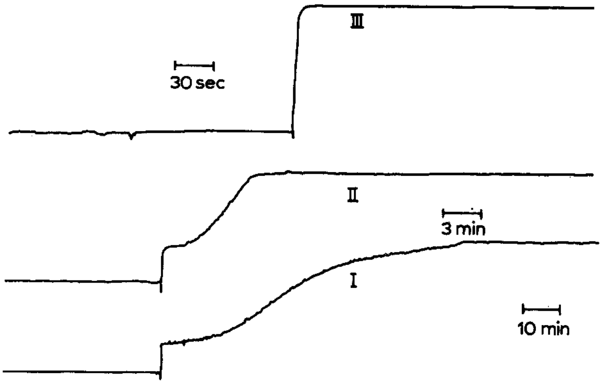

Fig. 4. Zeitlicher Verlauf der Umsetzung in Methyl-isobutylketon bei vorheriger Ausfällung des NaCl. Jeweils 200 Val·10^{-6} $NaClO_4$ + 100 (I); 200 (II); 300 (III) Val·10^{-6} LiCl + jeweils 150 Val·10^{-6} $Ba(ClO_4)_2$.

zustand nach ungefähr 8 min eingestellt. Im Falle III wird das zugesetzte Chlorid nicht vollständig zur Fällung von Natriumchlorid verbraucht. Sein Überschuss kann sofort Bariumchlorid ausfällen. Doch dann muss auch hier die Umsetzung mit dem festen Natriumchlorid folgen. Das Gleichgewicht stellt sich sehr schnell ein. Der S-förmige, im Anfang fast waagerechte Verlauf der Diagramme I und II zeigt, dass der Angriff auf das auskristallisierte Natriumchlorid zuerst gehemmt ist. Möglicherweise ist die Keimbildung des Bariumchlorids bei den hier vorliegenden geringen Chloridionenkonzentrationen erschwert. Naturgemäss sind in den auf Fig. 4 gezeigten Reaktionen die Einstellungszeiten der Gleichgewichte grösser als bei den auf Fig. 3 dargestellten. Im Falle 4 hat die Natriumchloridphase mehr Zeit zu ihrer Ausbildung.

Vergrössert man bei analogen Versuchen den Anteil des Bariums gegenüber dem Natrium, dann wird der Zeitbedarf für die Einstellung des Gleichgewichtes geringer und umgekehrt. Das trifft sowohl für die Fällung aus der Mischlösung wie auch für die Umsetzung mit dem zuvor gefällten Natriumchlorid zu.

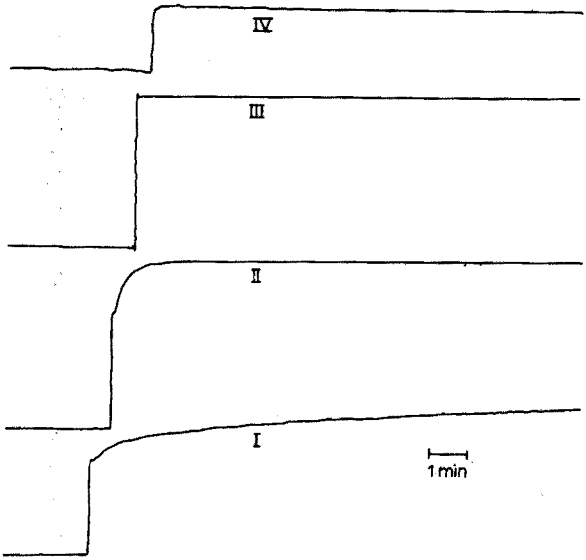

Fig. 5. Zeitlicher Verlauf der Umsetzung in Azeton. 200 Val $\cdot 10^{-6}$ $NaClO_4$ + 100 (I); 200 (II); 300 (III) Val $\cdot 10^{-6}$ LiCl + jeweils 150 Val $\cdot 10^{-6}$ $Ba(ClO_4)_2$. (IV) 200 Val $\cdot 10^{-6}$ $NaClO_4$ + 150 Val $\cdot 10^{-6}$ $Ba(ClO_4)_2$ + 100 Val $\cdot 10^{-6}$ LiCl.

Entsprechende Versuchsreihen wurden in Azeton als Lösungsmittel durchgeführt. Hiervon zeigt Fig. 5 einige Beispiele. Bei Diagramm I wurden 200 Val $\cdot 10^{-6}$ Natriumperchlorat und 100 Val $\cdot 10^{-6}$ Lithiumchlorid einpipettiert und anschliessend 150 Val $\cdot 10^{-6}$ Bariumperchlorat zugesetzt. Das Gleichgewicht wird nach ungefähr 20 min erreicht. Wird der gleiche Versuch mit 200 Val $\cdot 10^{-6}$ Lithiumchlorid durchgeführt, dann stellt sich das Gleichgewicht schon nach 2 min ein (Diagramm II) und bei 300 Val $\cdot 10^{-6}$ Lithiumchlorid praktisch sofort. Wie durch Vergleich mit Fig. 4 folgt, geht der Niederschlagsaustausch des festen Natriumchlorids mit dem Bariumperchlorat der Lösung in Azeton erheblich schneller vonstatten als in Methyl-isobutylketon. Wird in Azeton analog zu den auf Fig. 3 gezeigten Versuchen aus Mischlösungen von Natriumperchlorat und Bariumperchlorat gefällt, dann ist das Gleichgewicht in jedem Falle, unabhängig von der angewandten Menge Lithiumchlorid, bereits nach einigen Sekunden erreicht. Als Beispiel soll das Diagramm IV auf Fig. 5 dienen. Hier wurden 200 Val·10^{-6} Natriumperchlorat und 150 Val·10^{-6} Bariumperchlorat mit 100 Val·10^{-6} Lithiumchlorid umgesetzt.

Die Einzelheiten der Kinetik des Niederschlagsaustausches solcher Reaktionen sollen näheren Untersuchungen vorbehalten bleiben.

Die simultane Titration der Alkalijodide und des Bariumjodids bzw. Strontiumjodids in Azeton

Die schnellere Einstellung des Gleichgewichtes in Azeton ermutigte zu dem Versuch, hier die simultane Titration von Alkalijodid neben Bariumjodid bzw. Strontiumjodid noch einmal zu erproben. In einer gut gerührten Vorlage von 100 ml Azeton wurde reine Bariumjodidlösung (Fig. 6, Diagramm I) und später die gleiche Menge Bariumjodid mit wachsenden Anteilen Kaliumjodid (Diagramme II, III, IV und V) und schliesslich zum Vergleich reine Kaliumjodidlösung (Diagramm VI) mit Lithiumchlorid in Azeton als Masslösung titriert. Die Indikation erfolgte wieder oszillometrisch. Nach jeder Reagenzzugabe wurde vor der Ablesung 2 bis 3 min die Gleichgewichtseinstellung abgewartet. Die gestrichelten Vertikalen deuten die Lage der theoretischen Äquivalenzpunkte an. Die Diagramme zeigen, dass eine saubere

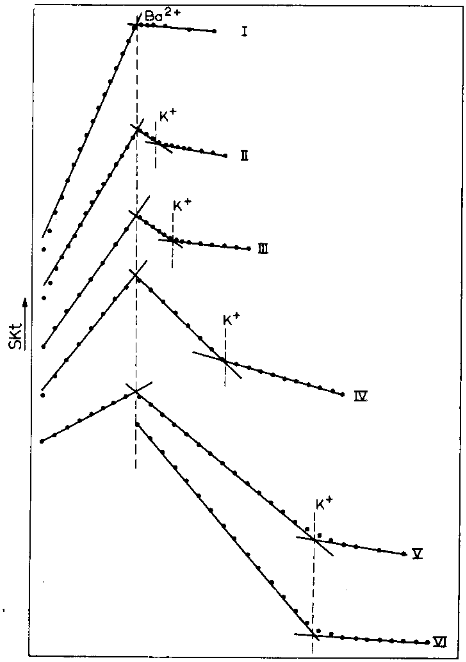

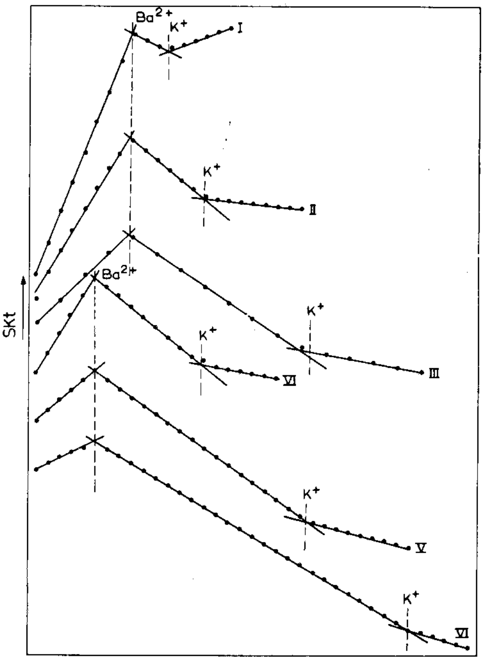

Fig. 6. Titration von BaI_2 und KI in Azeton mit LiCl in Azeton 0.0825 *N.* (I) Vorlage von 322 Val·10^{-6} BaI_2 allein; (II) 322 Val·10^{-6} BaI_2 + 61 Val·10^{-6} KI; (III) 122; (IV) 305; (V) 610 Val·10^{-6} KI bei gleicher BaI_2-Menge; (VI) 610 Val·10^{-6} KI allein.

Fig. 7. Titration von BaI_2 und KI in Azeton mit LiCl in Azeton 0.0825 *N.* (I) bis (III) jeweils 161 Val·10^{-6} BaI_2 + 61 (I); 122 (II); 305 (III) Val·10^{-6} KI. (IV) bis (VI) jeweils 67 Val·10^{-6} BaI_2 + 113 (IV); 226 (V); 340 Val·10^{-6} KI (VI).

Trennung erfolgt. Auch bei weiterer Verkleinerung des Verhältnisses Bariumjodid zu Kaliumjodid werden gute Ergebnisse erzielt (Fig. 7), doch wird der Schnittwinkel am Äquivalenzpunkt des Alkalis ungünstiger. Die Bariumjodidkonzentration kann wegen der bereits erwähnten Tendenz zur Krümmung nicht wesentlich über die hier verwendeten Werte vergrössert werden.

Analoge Diagramme wurden bei der Titration der Systeme Bariumjodid/Natriumjodid und Strontiumjodid/Kaliumjodid erhalten. Allerdings wird im letzteren Falle die Genauigkeit der Bestimmung beider Komponenten deutlich geringer, wenn man das Konzentrationsverhältnis stark von 1 abweichen lässt. Dann ist zu erkennen, dass beide Komponenten teilweise gemeinsam ausfallen. Das tritt ganz deutlich in Erscheinung bei der Kombination Strontiumjodid/Natriumjodid. Hier heben sich beide Tendenzen, nämlich der Anstieg des Leitwertes bei der Fällung des Erdalkalis und das Absinken bei der Fällung des Alkalis wegen gemeinsamer Ausfällung weitgehend auf, so dass keine auswertbaren Schnittpunkte erhalten werden.

Die Titration der Perchlorate nebeneinander wurde ebenfalls untersucht. Doch ist hier nur der Äquivalenzpunkt des Erdalkalis exakt auswertbar, nicht aber der des Natriums. Das erklärt sich aus der äusserst geringen Leitfähigkeitsänderung bei der Titration von Natriumperchlorat mit Lithiumchlorid in Azeton[2]. Werden Mischlösungen von Natriumperchlorat und Calciumperchlorat in Azeton titriert, dann fällt erst Natriumchlorid und anschliessend Calciumchlorid aus. Da die Fällung des Calciumchlorides mit einem starken Anstieg der Leitfähigkeit verbunden ist, wird hier der Äquivalenzpunkt des Natriums gut erkennbar, wogegen der des Calciums schlecht auswertbar ist. Die Titration der Erdalkalien Barium, Strontium und Calcium nebeneinander liefert wegen der grossen Ähnlichkeit der Leitwertsanstiege keine erkennbare Trennung der Komponenten. Dabei sollten sich die Löslichkeiten der Erdalkalichloride stark genug unterscheiden. Denn aus den beschriebenen Ergebnissen folgt die Reihenfolge der Löslichkeiten: Barium, Strontium und Natrium, Kalium und Calcium. Hier werden weitere Untersuchungen, eventuell mit potentiometrischer Indikation, erforderlich sein.

ZUSAMMENFASSUNG

Die chloridimetrische Fällungstitration von Erdalkali- und Alkaliionen nebeneinander in ketonischen Lösungsmitteln wurde untersucht. Als Massreagenz diente eine Lösung von Lithiumchlorid in Äthanol oder den verwendeten Ketonen Azeton bzw. Methyl-isobutylketon. Die Indikation erfolgte oszillometrisch. Die Bestimmungen Barium/Natrium, Barium/Kalium und Strontium/Kalium sind in beiden Ketonen möglich. Doch wird der nach Lage der Löslichkeiten zu erwartende richtige Verlauf der Titrationsdiagramme in Methyl-isobutylketon nur erhalten, wenn man nach jeder Reagenzzugabe mindestens 15 min wartet, bis sich das Fällungsgleichgewicht eingestellt hat. Dieses Gleichgewicht wird dagegen in Azeton sehr schnell erreicht. Deshalb ist bei der Titration von Alkalien und Erdalkalien nebeneinander dem Azeton als Lösungsmittel der Vorzug zu geben.

SUMMARY

The precipitation titration of mixtures of alkali and alkaline-earth metals in ketonic media was investigated; the titrant was a solution of lithium chloride in ethanol or the ketone and the end-points were detected oscillometrically. Analyses of barium–sodium, barium–potassium and strontium–potassium mixtures were possible in methyl isobutyl ketone or acetone media. Acetone is the preferred medium because the precipitation equilibrium is reached very quickly, whereas a period of 15 min is needed in the case of methyl isobutyl ketone.

RÉSUMÉ

On a examiné le titrage par précipitation de mélanges de métaux alcalins et alcalino-terreux en milieu cétonique. Le titrant est constitué par une solution de chlorure de lithium dans l'éthanol ou dans une cétone; le point final est décelé oscillométriquement. Il est possible d'effectuer les analyses des mélanges baryum–sodium; baryum–potassium et strontium–potassium, en milieu méthylisobutylcétone ou acétone. On préfére le milieu acétone: l'équilibre de précipitation est atteint très rapidement tandis qu'une période de 15 minutes est nécessaire dans le cas de la méthylisobutylcétone.

LITERATUR

1 G. HENRION UND E. PUNGOR, *Anal. Chim. Acta*, 38 (1967) 357.
2 G. HENRION UND E. PUNGOR, *Anal. Chim. Acta*, 39 (1967) 195.

Analytica Chimica Acta
Elsevier Publishing Company, Amsterdam
Printed in The Netherlands

TITRATIONS OF WEAK ACIDS IN 1,1,3,3-TETRAMETHYLGUANIDINE

JOSEPH A. CARUSO, GILBERT G. JONES AND ALEXANDER I. POPOV
Department of Chemistry, Michigan State University, East Lansing, Mich. 48823 (U.S.A.)

(Received May 8th, 1967)

While the use of glacial acetic acid as a medium for titrations of weak bases has been firmly established in analytical laboratories and the nature of acid–base equilibria in this solvent has been well elucidated by the work of KOLTHOFF AND BRUCKENSTEIN[1], the use of basic media for the titrations of weak acids has been explored less extensively. Both pyridine and ethylenediamine enhance the proton-donor abilities of weak acids and have been widely used as solvents in non-aqueous titrations[2,3]. In recent years a relatively new solvent, 1,1,3,3-tetramethylguanidine became commercially available. Comparison of basic strengths of substituted guanidines in aqueous solutions showed that TMG is a strong base with $pK_a > 13$[4] and one would expect, therefore, that its solvent properties would be similar to those of ethylenediamine and pyridine. The similarity of the three solvents is also reflected by their dielectric constants, 12.9 for ethylenediamine, 12.3 for pyridine and 11.00 for TMG[5]. This work was initiated, therefore, to study TMG as a non-aqueous solvent particularly with reference to acid–base equilibria and to develop, if possible, a suitable electrode system in TMG for the study of these equilibria.

A literature search indicated that the only mention of TMG as non-aqueous solvent is contained in the two papers of WILLIAMS *et al.*[6]. These authors carried out potentiometric titrations of phenols and substituted phenols in TMG using a glass indicator electrode and either an aqueous SCE or a modified SCE as reference. The titrant was tetrabutylammonium hydroxide in methanol solution. Good analytical results were obtained.

EXPERIMENTAL

Reagents

1,1,3,3-Tetramethylguanidine was obtained from the American Cyanamid Company and was purified by vacuum distillation over granulated barium oxide[5]. Its purity was checked by gas chromatography and a single smooth peak was obtained.

Tetrabutylammonium hydroxide (TBAH) was obtained from Eastman Chemical Company as a 25% solution in methanol. Since preliminary results indicated that pure methanolic solutions could not be used as titrants, a solution of TBAH in TMG–MeOH mixture was prepared by adding *ca.* 13 ml of the stock TBAH solution to 87 ml of TMG. The titrant was unstable over a 24-h period, and it was necessary to standardize it at the onset of each series of titrations. DAHMEN AND VAN DER HEIJDE[7] indicate that TBAH is unstable in pyridine as a consequence of the "Hofmann degradation". This may also be the case for the TBAH–TMG solutions.

Benzoic acid and the substituted benzoic acids were recrystallized from appropriate solvent systems and dried to constant weight *in vacuo*; 5-methyltetrazole was prepared and purified as previously described[5].

Phenol and *p*-chlorophenol, obtained from Eastman, were purified by vacuum distillation in a microdistillation apparatus; *o*-cresol (Eastman) was purified by sublimation.

Curcumin (turmeric), 1,7-bis(3-methoxy-4-hydroxyphenyl)-1,6-heptadiene-3,5-dione, was obtained from Eastman (m.p. 179–181°) and was not further purified. Indicator solutions for the titrations were prepared to a concentration of *ca.* 0.2 mg/ml of TMG.

G. F. SMITH sodium perchlorate was used in the bridging electrolyte solution and was not further purified.

Apparatus

Potentiometric titrations were carried out in a concentration cell using a hydrogen electrode dipping into a saturated solution of benzoic acid in TMG as the reference electrode and a hydrogen indicator electrode. The titration cell was H-shaped with the two electrode compartments separated by two fine-porosity sintered-glass discs from the center compartment filled with saturated solution of sodium perchlorate in TMG. Platinum electrodes were prepared by sealing platinum wires in a narrow-bore, soft-glass tubing. The cell can be represented by

Pt, H_2	Reference soln. Satd. benzoic acid in TMG	Satd. soln. of $NaClO_4$ in TMG	Solution of unknown acid in TMG	H_2, Pt

Before use, the electrodes were cleaned in *aqua regia*, cathodically cleaned in sulfuric acid and rinsed in distilled water. They were platinized at 30 mA for 3 min by the procedure of JONES AND BOLLINGER[8]. Electrodes were replatinized when undue unsteadiness was noted in the meter readings.

A Beckman Expanded Scale pH meter was used to follow the potentiometric titrations. The meter range was extended by recalibrating the scale using the output of a Biddle-Gray Volt Potentiometer, Model No. 605014. The hydrogen bubbling rate did not appear to have a great influence on the potential reading and, therefore, the tank output was set to maintain a slow passage of hydrogen through the solutions throughout the titration. After the solutions had been saturated with hydrogen (usually 15–30 min) the titration was begun. The potential values were taken after the highest scale reading was reached which was usually after about 1 min. Near the equivalence point the potentials were more unsteady and it took somewhat longer to reach the peak reading. After the equivalence point the readings were generally unsteady until a relatively large excess of titrant had been added. Again, the peak scale readings were taken.

When curcumin indicator was used for the detection of the end-point, the titrations were carried out under nitrogen atmosphere because of the high affinity of the solvent for atmospheric moisture and carbon dioxide. To insure that the color change corresponded to the potentiometric equivalence point, preliminary titrations were done potentiometrically with indicator added to the cell. Initially, the solutions to be titrated had a red-violet color (3 or 4 drops of indicator solution per 50 ml of solvent) which then became an intense blue in color upon addition of a small amount of base and turned very sharply to yellow or gold at the equivalence point. Blank corrections were not made in as much as the experimental conditions, volume of solutions, and volume of indicator were kept the same during the standardization of the titrant solution and the titrations of the acids. Fresh indicator solution was prepared before each series of titrations since decomposition over a period of time was noted.

RESULTS AND DISCUSSION

In the initial phases of this investigation an attempt was made to use TBAH solution in methanol as the titrant. The titration curves were erratic and it was evident that methanol was undergoing a slow reaction with TMG. In order to minimize these effects, titrations were performed with TBAH in an approximately 90:10 mixture of TMG with methanol.

Typical titration curves are shown in Fig. 1. As expected, with weak acids a sharp increase in potential is observed in the initial stages of titration. Thus for phenol ($\mathrm{p}K_a^{\mathrm{H_2O}}$ *ca.* 10) a sharp rise at the beginning of the titration is seen, while for *m*-chlorobenzoic acid ($\mathrm{p}K_a^{\mathrm{H_2O}}$ *ca.* 4) no noticeable inflection is observed at the start of the titration. A titration curve similar to that of phenol was observed for *o*-cresol. Likewise, in the case of the substituted benzoic acids, the titration curves are similar to that of *m*-chlorobenzoic acid. While it is difficult to compare directly acid strength in TMG to acid strength in water, it appears that the substituted benzoic acids

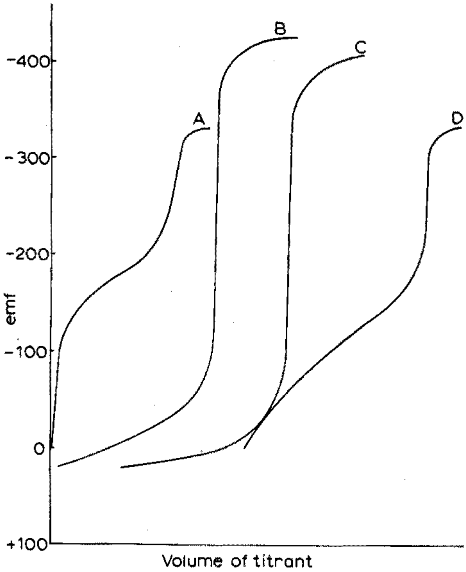

Fig. 1. Titration curves of (A) phenol, (B) *m*-chlorobenzoic acid, (C) 5-methyltetrazole, and (D) *p*-chlorophenol in TMG.

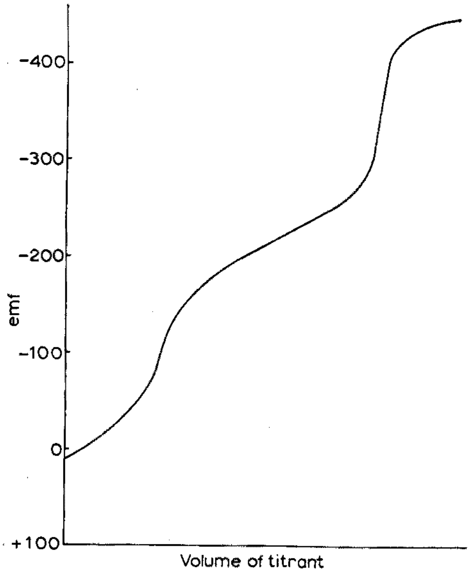

Fig. 2. Titration curve for a *m*-chlorobenzoic acid–phenol mixture in TMG.

titrate in TMG as strong acids do in water, while phenol and the substituted phenols yield titration curves similar to those of weak acids in aqueous solutions.

Because of the relatively low dielectric constant of TMG, it would be expected that most of the electrolytes are present in this solvent as ion-pairs. It has been previously shown[5] from conductance measurements that the "overall" dissociation constant, $K_{HA} = (H^+)\ (A^-)/(HA) + (H^+A^-)$, for picric acid is $5.6 \cdot 10^{-4}$ while the ion-pair dissociation constant for a strong electrolyte, tri(isoamyl)butylammonium tetraphenylborate was $1.8 \cdot 10^{-3}$. It is seen, therefore, that picric acid in TMG is essentially completely ionized, but, because of low dielectric constant of the solvent, it is incompletely dissociated. The same behavior would be expected of the substituted benzoic acids. Thus, as would be expected, the titration curves are indicative of the ionization process rather than of the dissociation. A more detailed study of acid–base equilibria in TMG is presently under investigation.

The results of the titrations are shown in Table I. It is seen that the results are quite acceptable and that the error is always less than 1%. Addition of 0.1% of water did not change significantly the results, but larger amounts produced increasing errors. The results were quite unreliable when 1% or more of water was added.

TABLE I

RESULTS OF POTENTIOMETRIC AND INDICATOR TITRATIONS OF WEAK ACIDS IN TMG

Substance	*Meq. taken*	*Meq. found*	*Recovery (%)*
Phenol[a]	0.659	0.656	99.5
o-Cresol[a]	0.513	0.513	100
p-Chlorophenol	0.475	0.475	100
5-Methyltetrazole	1.215	1.212	99.75
	0.7630	0.7650	100.3
o-Nitrobenzoic acid[b]	0.660	0.660	100
	0.414	0.412	99.4
m-Chlorobenzoic acid	0.6662	0.6667	100.1
p-Chlorobenzoic acid	0.6591	0.6585	99.91
	0.9069	0.9055	99.85
o-Chlorobenzoic acid	0.6853	0.6856	100.0
	0.7798	0.7771	99.65

[a] Potentiometric titrations only.
[b] Indicator titration only.

All titration curves were reproducible. The starting potentials for identical solutions were reproducible to within 10 mV. The blue-to-gold color change of the curcumin indicator occurred in the −170 to −250 mV region. In the case of phenol and *o*-cresol, the break in the titration curve occurred at more negative potentials and, consequently, curcumin indicator is not suitable for the titrations of these two compounds. In all other cases, the equivalence points occurred at higher potentials and, therefore, the indicator method gave the same end-point as the potentiometric titration.

Potentiometric titrations of organic acids with nitro groups, such as picric acid, were unsuccessful due to apparent reduction of the nitro group with hydrogen. The intense yellow color of picric acid obscured the indicator end-point but other nitro-acids, such as *o*-nitrobenzoic acid, yielded clear and sharp end-points with curcumin.

An attempt was made to titrate binary mixtures of acids. Figure 2 illustrates the titration of a mixture of *m*-chlorobenzoic acid and phenol. Similar curves were obtained for other mixtures. Although the titration curves show good resolution, as seen from Table II, only the total acid present could be determined with any degree of accuracy. It is obvious that because of the levelling effect of TMG, the acid strengths are compressed and, for example, in the phenol–benzoic acid mixture, the weaker acid, phenol, is being titrated before all of the benzoic acid is neutralized.

TABLE II

POTENTIOMETRIC TITRATIONS OF BINARY ACID MIXTURES IN TMG

Mixture	*Meq. taken*	*Meq. found*	*Total taken*	*Total found*	*Total recovery (%)*
(1) Benzoic acid	0.200	0.213	0.489	0.491	100
phenol	0.289	0.278			
(2) *m*-Chlorobenzoic acid	0.130	0.163	0.518	0.522	101
phenol	0.388	0.359			
(3) *m*-Chlorobenzoic acid	0.123	0.158	0.391	0.400	102
o-cresol	0.268	0.242			

It can be concluded from the above results that TMG is a suitable solvent for the titrations of weak acids either potentiometrically, with hydrogen indicator electrode or with a visual determination of end-point using curcumin as indicator.

This work was supported by a grant MH-07825 from the Institute of Public Health, U.S. Public Health Service.

SUMMARY

The use of 1,1,3,3-tetramethylguanidine (TMG) as a medium for the titrations of weak acids has been investigated. The hydrogen electrode behaves reversibly in this solvent and can serve as an indicator electrode in titration reactions. The titrant was a 0.1 *M* solution of tetrabutylammonium hydroxide in a 90–10% mixture of TMG and methanol. A hydrogen electrode dipping into a TMG solution saturated with benzoic acid served as reference electrode. Potentiometric titrations of a number of weak acids gave results accurate to at least ±0.5%. It was found that in most cases curcumin could be used as an end-point indicator with an accuracy comparable to that of the potentiometric titration.

RÉSUMÉ

On a examiné l'utilisation de la tétraméthyl-1,1,3,3-guanidine (TMG) comme milieu pour les titrages d'acides faibles. L'électrode d'hydrogène se comporte réversiblement dans ce solvant et peut servir d'électrode indicatrice dans ces réactions de titrage. Titrant: solution d'hydroxyde de tétrabutylammonium 0.1 *M* dans un mélange TMG–méthanol (90–10%). Une électrode d'hydrogène plongeant dans une solution TMG saturée en acide benzoïque sert d'électrode de référence. Des titrages potentiométriques d'un certain nombre d'acides faibles ont donné des résultats avec une précision de ±0.5%. Il est possible dans la plupart des cas d'utiliser la curcumine comme indicateur, donnant une précision comparable à celle obtenue par titrage potentiométrique.

ZUSAMMENFASSUNG

Es wurde die Verwendung von 1,1,3,3-Tetramethylguanidin (TMG) als Medium für die Titration schwacher Säuren untersucht. Die Wasserstoffelektrode verhält sich in diesem Lösungsmittel reversibel und kann als Indikatorelektrode dienen. Titriert wurde mit einer 0.1 *M* Lösung von Tetrabutylammoniumhydroxid in einer 90 : 10 %igen Mischung von TMG und Methanol. Eine in mit Benzoesäure gesättigte TMG-Lösung tauchende Wasserstoffelektrode dient als Bezugselektrode. Potentiometrische Titrationen einer Anzahl schwacher Säuren führten zu Ergebnissen mit Fehlern von weniger als ±0.5%. Es wurde gefunden, dass in den meisten Fällen Curcumin als Endpunktindikator verwendet werden konnte mit einer Genauigkeit, die mit der potentiometrischen Titration vergleichbar ist.

REFERENCES

1 I. M. KOLTHOFF AND S. BRUCKENSTEIN, in I. M. KOLTHOFF AND P. J. ELVING, *Acid–Base Equilibria in Nonaqueous Solvents. Chapter XIII. Treatise on Analytical Chemistry*, Part I, Vol. I, The Interscience Encyclopedia Company, Inc., New York, N. Y., 1959, pp. 499–522 and references cited therein.
2 L. M. MUKHERJEE, S. BRUCKENSTEIN AND F. A. K. BADAWI, *J. Phys. Chem.*, 69 (1965) 2537.
3 R. H. CUNDIFF AND P. C. MARKUNAS, *Anal. Chem.*, 30 (1958) 1447.
4 S. J. ANGYAL AND W. K. WARBURTON, *J. Chem. Soc.*, (1951) 2492.
5 J. A. CARUSO, P. G. SEARS AND A. I. POPOV, *J. Phys. Chem.*, 71 (1967) 1756.
6 T. R. WILLIAMS AND J. CUSTER, *Talanta*, 9 (1962) 175; T. R. WILLIAMS AND M. LAUTENSCHLEGER, *Talanta*, 10 (1963) 804.
7 H. B. VAN DER HEIJDE AND E. A. M. F. DAHMEN, *Anal. Chim. Acta*, 16 (1957) 381.
8 G. JONES AND D. M. BOLLINGER, *J. Am. Chem. Soc.*, 57 (1935) 280.

Analytica Chimica Acta
Elsevier Publishing Company, Amsterdam
Printed in The Netherlands

A POTENTIOMETRIC STUDY OF THE WATER-SOLUBLE SILVER(I) COMPLEXES OF N,N'-BIS(2-HYDROXYETHYL)DITHIO-OXAMIDE (HEDTO)

PART I. APPLICATION OF THE "CORE+LINKS" METHOD

L. C. VAN POUCKE, M. A. HERMAN* AND Z. EECKHAUT
Department of General and Inorganic Chemistry, University of Ghent, Ghent (Belgium)

(Received May 15th, 1967)

In preceding papers[1,2] the composition of the water-insoluble complexes of silver(I) with HEDTO was determined; these complexes were found to be polynuclear. In the present paper, soluble complexes are discussed. The complex formation may be represented by the following reaction equation:

$$p\ \mathrm{Ag}^+ + q\ \mathrm{H_2X} \rightleftarrows \mathrm{Ag}_p\mathrm{H}_{2q-r}\mathrm{X}_q + r\ \mathrm{H}^+ \qquad (1)$$

where H_2X is the ligand HEDTO, this being considered as a dibasic acid[3]. It is further assumed that $1 \leqslant p \leqslant P$, $1 \leqslant q \leqslant Q$, and $0 \leqslant r \leqslant 2Q$. Since H_2X is a weak acid ($pK_1^T = 11.07$) the ligand HEDTO will be undissociated in acidic medium. Therefore, from the general reaction eqn. (1), the following equilibrium constant can be written:

$$K_{pqr} = (\mathrm{Ag}_p\mathrm{H}_{2q-r}\mathrm{X}_q)(\mathrm{H}^+)^r/(\mathrm{Ag}^+)^p(\mathrm{H_2X})^q \qquad (2)$$

Several complexes $\mathrm{Ag}_p\mathrm{H}_{2q-r}\mathrm{X}_q$ may be simultaneously present in the solution. For reasons of simplicity, the following symbols are used:

C_A = total concentration of silver ions
C_B = total concentration of ligand
C_H = total concentration of a strong mineral acid
A = $[\mathrm{Ag}^+]$ = concentration of free silver ions
B = $[\mathrm{H_2X}]$ = concentration of free ligand
H = $[\mathrm{H}^+]$ = concentration of hydrogen ions
C_{pqr} = concentration of the complex $\mathrm{Ag}_p\mathrm{H}_{2q-r}\mathrm{X}_q$

Considering the law of concentration of mass, we can write:

$$C_A = A + \text{bound } A = A + \sum_{p=1}^{p=P} \sum_{q=1}^{q=Q} \sum_{r=0}^{r=2Q} pC_{pqr} \qquad (3)$$

$$C_B = B + \text{bound } B = B + \sum_{p=1}^{p=P} \sum_{q=1}^{q=Q} \sum_{r=0}^{r=2Q} qC_{pqr} \qquad (4)$$

Substitution of eqn. (2) in eqns. (3) and (4) gives:

$$C_A = A + \sum_{p=1}^{p=P} \sum_{q=1}^{q=Q} \sum_{r=0}^{r=2Q} pK_{pqr}\, A^p B^q H^{-r} \qquad (5)$$

$$C_B = B + \sum_{p=1}^{p=P} \sum_{q=1}^{q=Q} \sum_{r=0}^{r=2Q} qK_{pqr}\, A^p B^q H^{-r} \qquad (6)$$

---

* Present address: University Centre, Antwerp (Belgium).

In studies of reaction equilibria such as eqn. (1), it seems necessary from eqns. (5) and (6) to know the values of A, B and H.

EXPERIMENTAL

Reagents

HEDTO was obtained and purified as described in an earlier paper[1]. All measurements were carried out with freshly prepared solutions. Silver perchlorate monohydrate (puriss., Fluka) and perchloric acid (Merck, p.a.) were used. Sodium perchlorate monohydrate (puriss., p.a., Fluka) was purified[4] from chloride ions by repeated crystallisation, and separated from the solution at a temperature above 60° in order to obtain the anhydrous product.

Determination of the concentration of free silver(I) ions

The concentration of free silver, A, was measured with the following cell:

calomel electrode | electrolyte bridge | Ag^+-ions; Ag

An electrolyte bridge of the Wilhelm[5] type was filled with a 0.1 M sodium perchlorate solution. The diffusion potentials were cancelled out by measuring the cell potential of solutions with a known concentration of Ag^+ ions and calculating the E_0 value of the cell from following equation:

$$E_0 = \{E - \log(Ag^+)\}/59.16 \qquad t = 25.0^\circ$$

Two series of solutions were used: the first composed of 0.05 M perchloric acid and 0.05 M sodium perchlorate, the second of 0.01 M perchloric acid and 0.09 M sodium perchlorate. In each of these solutions the silver ion concentration was varied between 10^{-5} M and 10^{-4} M. For the apparent E_0 a mean value of 530.1 mV was found for the first series and 547.1 mV for the second series. The mean deviation in the determination of the E_0 value was 0.3 mV. The difference (17 mV) between the two E_0 values agrees well with the experimental relation found by DYRSSEN[6]. The potential measurements were carried out with a Siemens and Halske potentiometer and with a galvanometer of a sensitivity of 10^{-9} Å. The temperature was constant at 25.0°.

Determination of the concentration of free ligand

The concentration of free ligand, B, was calculated by means of the HEDSTRÖM–McKAY equation[7,8]. This equation is not proved for a reaction equation of type (1). It can be shown, however, that the equation holds provided that the pH remains constant.

The GIBBS–DUHEM equation can therefore be written as follows:

$$n_1 d\mu_1 + n_2 d\mu_2 + \ldots + n_n d\mu_n = 0 \tag{7}$$

where n_i and μ_i are the number of moles and the chemical potential respectively of each species.

For each complex compound c_i in solution, the following equilibrium relation holds:

$$p_i\mu_A + q_i\mu_B - r_i\mu_H = \mu_{c_i} \tag{8}$$

Differentiating eqn. (8) gives:

$$p_i \mathrm{d}\mu_{\mathrm{A}} + q_i \mathrm{d}\mu_{\mathrm{B}} - r_i \mathrm{d}\mu_{\mathrm{H}} = \mathrm{d}\mu_{c_i} \tag{9}$$

Introducing eqn. (9) into eqn. (7) and applying eqn. (7) to our case we find:

$$(n_{\mathrm{A}} + \sum_i p_i n_{c_i})\mathrm{d}\mu_{\mathrm{A}} + (n_{\mathrm{B}} + \sum_i q_i n_{c_i})\mathrm{d}\mu_{\mathrm{B}} + (n_{\mathrm{H}} - \sum_i r_i n_{c_i})\mathrm{d}\mu_{\mathrm{H}} + n\mathrm{d}\mu = 0 \tag{10}$$

where n is the number of moles of the solvent and μ is the chemical potential of the solvent.

Equation (10) can be written as follows:

$$a\mathrm{d}\mu_{\mathrm{A}} + b\mathrm{d}\mu_{\mathrm{B}} + n\mathrm{d}\mu + h\mathrm{d}\mu_{\mathrm{H}} = 0 \tag{11}$$

where $a = n_{\mathrm{A}} + \sum_i p_i n_{c_i} =$ the total number of moles of A; $b = n_{\mathrm{B}} + \sum_i q_i n_{c_i} =$ the total number of moles of B, and $h = n_{\mathrm{H}} - \sum_i r_i n_{c_i} =$ the total number of moles mineral acid. For dilute solutions it can be assumed that the number of moles of the solvent n is proportional to the volume V of the solvent:

$$n = k \cdot V$$

From this and eqn. (11) we obtain:

$$-\mathrm{d}\mu' = (a/V)\mathrm{d}\mu_{\mathrm{A}} + (b/V)\mathrm{d}\mu_{\mathrm{B}} + (h/V)\mathrm{d}\mu_{\mathrm{H}} \tag{12}$$

where $\mu' = k\mu$.

Since $a/V = C_{\mathrm{A}}$, $b/V = C_{\mathrm{B}}$, $h/V = C_{\mathrm{H}}$, eqn. (12) becomes:

$$-\mathrm{d}\mu' = C_{\mathrm{A}}\mathrm{d}\mu_{\mathrm{A}} + C_{\mathrm{B}}\mathrm{d}\mu_{\mathrm{B}} + C_{\mathrm{H}}\mathrm{d}\mu_{\mathrm{H}} \tag{13}$$

Application of the properties of the total differential to eqn. (13) gives:

$$\left(\frac{\partial C_{\mathrm{A}}}{\partial \mu_{\mathrm{B}}}\right)_{\mu_{\mathrm{A}}\mu_{\mathrm{H}}} = \left(\frac{\partial C_{\mathrm{B}}}{\partial \mu_{\mathrm{A}}}\right)_{\mu_{\mathrm{B}}\mu_{\mathrm{H}}} \tag{14}$$

At constant ionic strength, it can be assumed with good approximation that the activity coefficients of all reacting species also remain constant.

For dilute solutions it is possible to write:

$$\mu = \mu^\circ + RT \ln C + RT \ln f$$

and consequently eqn. (14) becomes:

$$\left(\frac{\partial C_{\mathrm{A}}}{\partial \ln B}\right)_{\ln A,\, \ln H} = \left(\frac{\partial C_{\mathrm{B}}}{\partial \ln A}\right)_{\ln B,\, \ln H} \tag{15}$$

A Jacobian transformation according to HEDSTRÖM[7] gives eqn. (15) the following form:

$$\left(\frac{\partial \ln A}{\partial C_{\mathrm{B}}}\right)_{C_{\mathrm{A}},\mathrm{pH}} = \left(\frac{\partial \ln B}{\partial C_{\mathrm{A}}}\right)_{C_{\mathrm{B}},\mathrm{pH}} \tag{16}$$

or

$$\left(\frac{\partial \log A}{\partial C_{\mathrm{B}}}\right)_{C_{\mathrm{A}},\mathrm{pH}} = \left(\frac{\partial \log B}{\partial C_{\mathrm{A}}}\right)_{C_{\mathrm{B}},\mathrm{pH}} \tag{17}$$

After integration eqn. (17) becomes:

$$\log C_{\mathrm{B}} - \log B = \left[\int_0^{C_{\mathrm{A}}} \left(\frac{\partial \log A}{\partial C_{\mathrm{B}}}\right)_{C_{\mathrm{A}},\mathrm{pH}} \mathrm{d}\, C_{\mathrm{A}}\right]_{C_{\mathrm{B}},\mathrm{pH}} \tag{18}$$

This is the HEDSTRÖM–MCKAY equation if the additional condition that the pH remains constant is provided. This was realised in sufficiently acidic medium. All measurements were performed twice, once in a medium of 0.05 M perchloric acid and 0.05 M sodium perchlorate and once in a medium of 0.01 M perchloric acid and 0.09 M sodium perchlorate, so that the ionic strength was equal to 0.1 in each case. In these experiments it was found that in each series the pH remained constant. Therefore in each series:

$$K_{pq} = \sum_{r=0}^{r=2Q} K_{pqr} H^{-r} \tag{19}$$

Substitution of eqn. (19) in eqns. (5) and (6) gives:

$$C_A = A + \sum_{p=1}^{p=P} \sum_{q=1}^{q=Q} p\, K_{pq} A^p B^q \tag{20}$$

$$C_B = B + \sum_{p=1}^{p=P} \sum_{q=1}^{q=Q} q\, K_{pq} A^p B^q \tag{21}$$

By this transformation the three-dimensional problem was reduced to a two-dimensional problem. Therefore, the methods for the study of complexes with general formula A_pB_q can be used.

DISCUSSION OF THE EXPERIMENTAL DATA

In the treatment of the experimental data only the figures for the case of $C_H = 0.05\ M$, will be given. A function Z is defined as follows:

$$Z = \frac{C_A - A}{C_B} = \frac{\sum_{p=1}^{p=P} \sum_{q=1}^{q=Q} p\, K_{pq} A^p B^q}{B + \sum_{p=1}^{p=P} \sum_{q=1}^{q=Q} q\, K_{pq} A^p B^q} \tag{22}$$

The function is not defined in the usual way $Z = (C_B - B)/C_A$ for reason of opportunism. Indeed, since A is directly determined by potentiometric measurements, $(C_A - A)/C_B$ is more accurate than $(C_B - B)/C_A$.

The validity of this inversion with regard to the application of the "core + links" method has been discussed by NILSSON[9] and SCHLÄFER[10].

If $q = 1$, Z becomes $\dfrac{\sum_{p=1}^{p=P} p\, K_{p1} A^p}{1 + \sum_{p=1}^{p=P} K_{p1} A^p}$, and only depends on A.

In Fig. 1 log Z *vs.* log A is plotted for different values of C_A. Since all these curves do not coincide, it can be concluded that q has values other than 1. A new function I is defined as follows:

$$I = \frac{C_A - A}{A} = \sum_{p=1}^{p=P} \sum_{q=1}^{q=Q} p\, K_{pq} A^{p-1} B^q \tag{23}$$

If $p=1$, I becomes equal to $\sum_{q=1}^{q=Q} K_{1q} B^q$ and depends only on B. In Fig. 2 the curves for log I as a function of log B are shown for different values of C_B. These curves do not coincide and consequently q has other values in addition to 1. Accordingly, the formation of polynuclear complexes with the general formula A_pB_q must be taken into account.

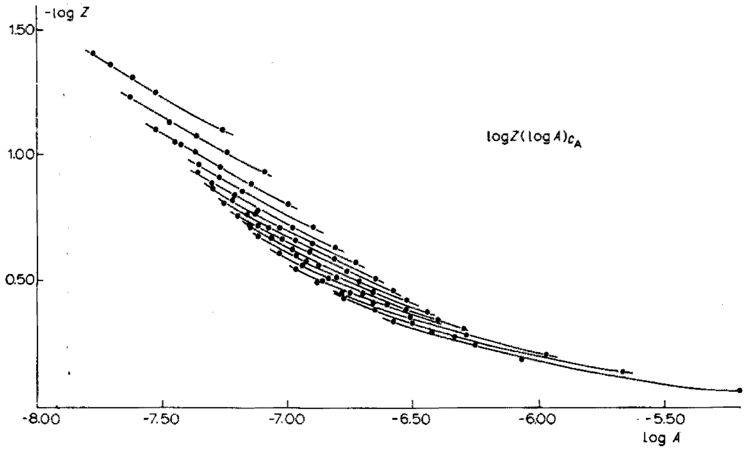

Fig. 1. log Z *versus* log A for different values of C_A.

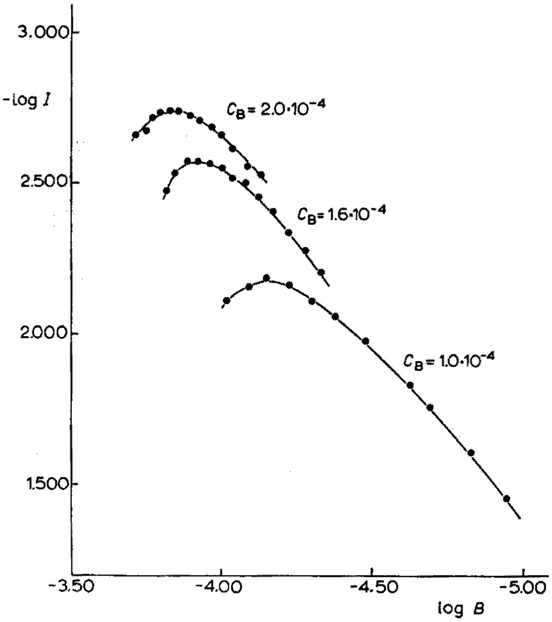

Fig. 2. log I *versus* log B for different values of C_B.

One of the most important methods in treating polynuclear systems is the "core + links" method given by SILLÉN[11,12]. It had been found in a number of cases that the formula of the polynuclear complexes may be represented by $A_r(A_tB)_n$ or

$B_s(A_tB)_n$ where r, s and t have definite values and n varies in such a way that p and q in A_pB_q are positive integers. When complexes with general formula $B(A_tB)_n$ are formed, the $Z(\log A)_{C_B}$ curves are parallel. Moreover

$$\left(\frac{\partial \log C_B}{\partial \log A}\right)_Z = R = C^{te}.$$

In application of the present experimental data R was found to equal -1. As $t = -R = 1$, and as B has a significant value compared to C_B, it follows that complexes with general formula $B(AB)_n$ are formed in this region. According to SILLÉN the general formula is $A_{-1}(A_tB)_n$ when $C_B \gg B$.

Figure 3 shows a plot of Z against log A. It should be noted that Z tends to 0 for decreasing values of log A (the region where B is negligible against C_B), and to the value of 1 for increasing values of log A.

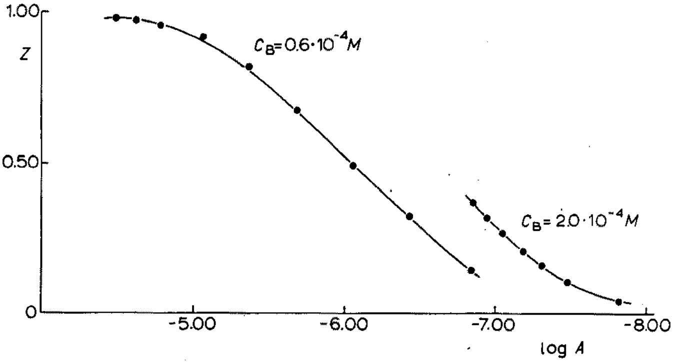

Fig. 3. Limit values of Z for increasing and decreasing values of log A.

SILLÉN has proved that Z tends to $t/(1+s/n_{\max})$ for increasing values of log A. This means for $s=1$, $t=(n_{\max}+1)/n_{\max}$. Substitution of t in $A_{-1}(A_tB)_n$ then gives a complex with formula $(AB)_{n_{\max}}$.

If it is assumed that only complexes with a general formula $B(AB)_n$ are formed, the value of Z becomes only a function of $u = A \cdot B$.

$$Z = \frac{\sum_{n=1}^{n=N} n\, K_{n,n+1}\, u^n}{1 + \sum_{n=1}^{n=N} (n+1)\, K_{n,n+1}\, u^n} \tag{24}$$

All the curves $Z(\log u)_{C_B}$ must coincide according to eqn. (24). From Fig. 4 it can be seen that this is true up to $Z=0.6$. Beyond this value of Z, marked deviations appear.

When $\left(\frac{\partial \log C_B}{\partial \log A}\right)_Z = R = C^{te}$ it can be proved that all the curves $\log Z(A^{-R}C_B)_{C_B}$ must coincide. This is a further proof of the existence of complexes $B(AB)_n$ for all concentrations examined. Figure 5 shows that it is the case for the whole range of observations. The validity of the formula $B(AB)_n$ can further be proved by comparing the experimental data with a few families of theoretical curves, calculated under various simple assumptions.

For this purpose the hypothesis III_a formulated by SILLÉN[12] and summarized below, can be used.

(1) Complexes $B(AB)_n$ with all positive values of n are formed.

(2) $K_{n,n+1}/K_{n-1,n}=k$

$K_{n,n+1}=k_0k^n$

Figures 5 and 6 show the curves log Z (log $A^{-R}\cdot C_B)_{C_B}$ calculated in these conditions, respectively, for $C_H=0.05\ M$ and $C_H=0.01\ M$, together with some experimental data. It can be seen that the agreement between the experimental and theoretical curves is good except for high values of Z. In each of these curves, k_0 was found to be 0.325. For $C_H=0.05\ M$, log $k=10.52$, and for $C_H=0.01\ M$, log $k=10.60$, are found. The stability constants K_{pq}, as defined by eqn. (19) and derived from $K_{n,n+1}=k_0k^n$ for the three first complexes of the series, are given below:

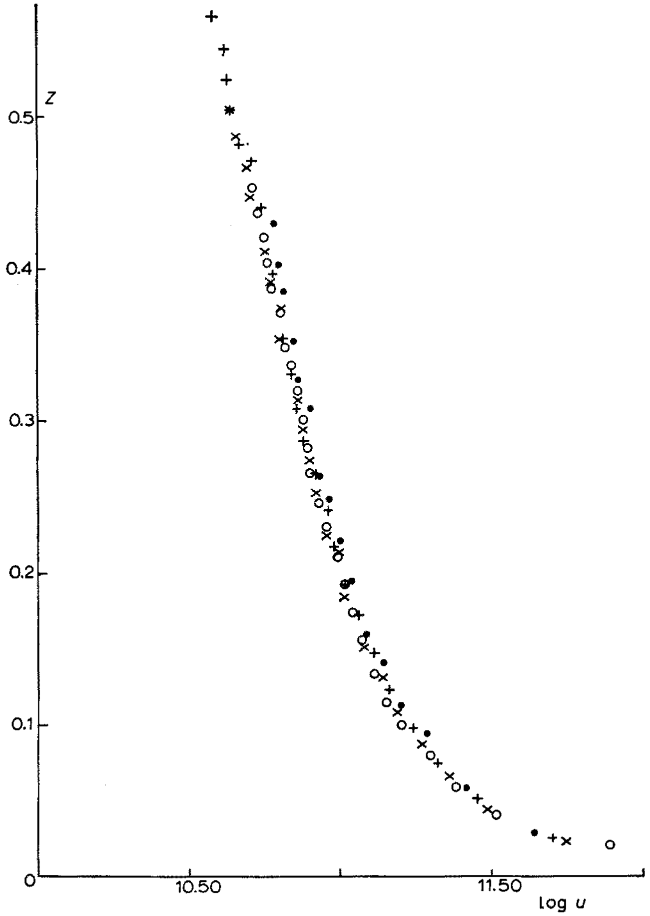

Fig. 4. Z versus log u = log $A\cdot B$ for different values of C_B: (○) $2.0\cdot10^{-4}\ M$, (×) $1.8\cdot10^{-4}\ M$, (+) $1.6\cdot10^{-4}\ M$, (●) $1.4\cdot10^{-4}\ M$.

	$C_H = 0.05\ M$	$C_H = 0.01\ M$
$\log K_{12}$	10.01	10.09
$\log K_{23}$	20.53	20.69
$\log K_{34}$	31.05	31.29

It can be seen that the stability constants vary with the pH. However this variation is much less than could be expected from reaction eqn. (1) with $r = p$. Therefore it can be assumed that $r < p$, showing that complexes are also formed without hydrogen ion displacement.

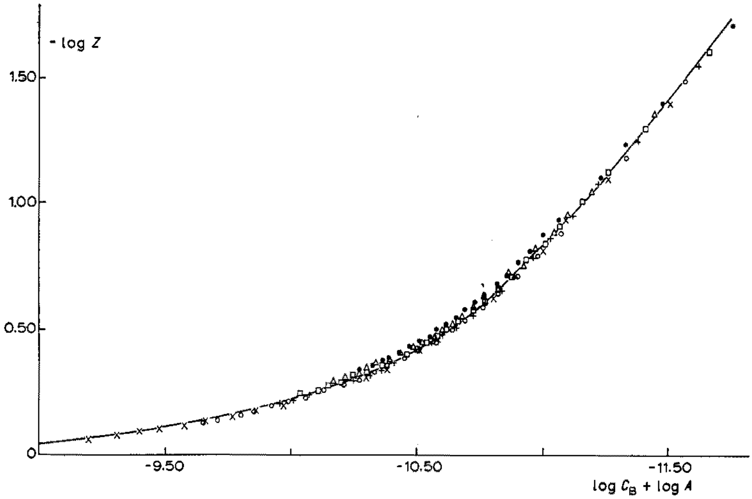

Fig. 5. $\log Z$ in function of $\log A + \log C_B$ for different values of C_B: (●) $2.0 \cdot 10^{-4}\ M$, (△) $1.8 \cdot 10^{-4}\ M$, (□) $1.6 \cdot 10^{-4}\ M$, (+) $1.4 \cdot 10^{-4}\ M$, (○) $1.2 \cdot 10^{-4}\ M$, (×) $1.0 \cdot 10^{-4}\ M$; and for $C_H = 0.05\ M$. The full line is the theoretical calculated.

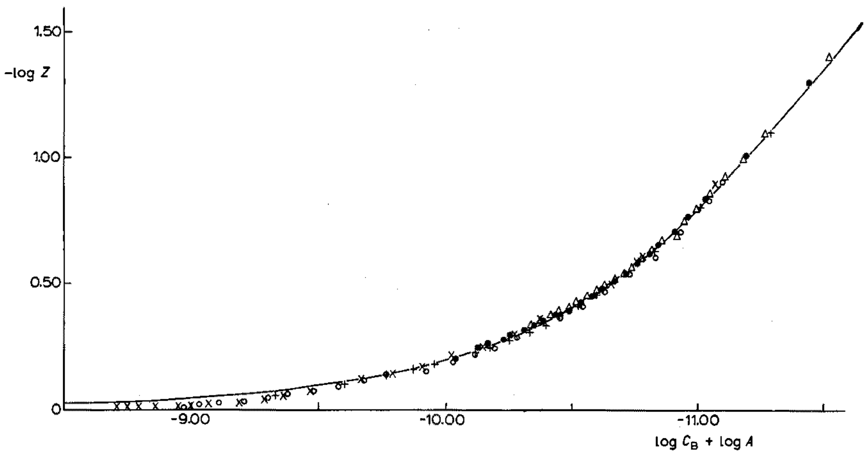

Fig. 6. As Fig. 5 for $C_H = 0.01\ M$. C_B: (△) $2.0 \cdot 10^{-4}\ M$, (●) $1.6 \cdot 10^{-4}\ M$, (+) $1.0 \cdot 10^{-4}\ M$, (○) $0.8 \cdot 10^{-4}\ M$, (×) $0.6 \cdot 10^{-4}\ M$.

CONCLUSIONS

Complexes with the general formula $B(AB)_n$ are formed between silver(I) and HEDTO. Changing $K_{n,n+1}$ as a function of pH can be related to the partial formation of complexes without hydrogen displacement.

Not all the experimental data agree, however, with the presence of only one type of complex $B(AB)_n$. Probably complexes with the general formula $(AB)_n$ are formed in the neighbourhood of $C_A:C_B=1$.

The composition of these complexes cannot be confirmed by the "core + links" method. The complex formation between silver(I) and HEDTO will be treated by other methods and discussed in a later paper.

SUMMARY

Silver(I) forms with N,N′-bis(2-hydroxyethyl)dithio-oxamide (HEDTO) water-soluble complexes in acidic medium. The composition of these complexes may be represented by the following formula: $B(AB)_n$ in which B is the ligand and A the metal ion. There is some indication that complexes with general formula $(AB)_n$ also are formed.

RÉSUMÉ

L'ion argent donne avec le N,N′-bis(2-hydroxyethyl)dithio-oxamide (HEDTO) en milieu acide des complexes qui sont solubles dans l'eau. La composition de ces complexes peut être représentée par la formule générale: $B(AB)_n$ où B est le ligand tandis que A représente l'ion argent. Toutefois les résultats nous révèlent que dans certaines conditions, des complexes avec formule générale $(AB)_n$ sont présents.

ZUSAMMENFASSUNG

Das Silberion gibt mit N,N′-Bis(2-hydroxyethyl)dithio-oxamide (HEDTO) in saurem Medium Komplexverbindungen löslich in Wasser. Die Zusammenstellung dieser Komplexen kann vorgestellt werden durch die allgemeine Formel $B(AB)_n$ ($B =$ ligand, $A = Ag^+$). Die Resultate wiesen darauf dass noch Komplexverbindungen mit Formel $(AB)_n$ in bedingter Umstände vorhanden sind.

REFERENCES

1 M. Herman, L. van Poucke and Z. Eeckhaut, *Bull. Soc. Chim. Belges*, 72 (1963) 385.
2 L. van Poucke, *Ind. Chim. Belge*, 28 (1963) 753.
3 L. van Poucke and M. Herman, *Anal. Chim. Acta*, 30 (1964) 569.
4 I. Leden, *Acta Chem. Scand.*, 3 (1949) 1318.
5 W. Forsling, S. Hietanen and L. G. Sillén, *Acta Chem. Scand.*, 6 (1952) 901.
6 D. Dyrssen, *Svensk Kem. Tidskr.*, 64 (1952) 213.
7 Hedström, *Acta Chem. Scand.*, 9 (1955) 613.
8 H. A. C. McKay, *Trans. Faraday Soc.*, 49 (1953) 237.
9 R. O. Nilsson, *Arkiv Kemi*, 12 (1958) 337.
10 H. L. Schläfer, *Komplexbildung in Lösung*, Springer Verlag, Berlin, 1961, p. 118.
11 L. G. Sillén, *Acta Chem. Scand.*, 8 (1954) 299.
12 L. G. Sillén, *Acta Chem. Scand.*, 8 (1954) 318.

Analytica Chimica Acta
Elsevier Publishing Company, Amsterdam
Printed in The Netherlands

QUANTITATIVE ELECTROCHEMICAL FORMATION OF PHOSPHOTUNGSTATE HETEROPOLYANION BLUES

PAUL STONEHART, JOHN G. KOREN AND JACOB S. BRINEN
American Cyanamid Company, Central Research Division, Stamford, Conn. 06904 (U.S.A.)

(Received April 1st, 1967)

The reduction of tungsten compounds in the presence of water usually gives rise to blue reduction products associated with tungsten(V). BENSON *et al.*[1] have re-examined the gas-phase reduction of WO_3 with hydrogen as a function of temperature, moisture content, and platinum catalyst; both moisture and platinum enhance the reduction of tungsten. Platinum facilitates the dissociation of hydrogen molecules to adsorbed hydrogen atoms and the moisture increases the rate of diffusion of the reduced species. The fully reduced blue compounds showed X-ray patterns characteristic of $H_{0.33}WO_3$ and/or $H_{0.5}WO_3$, being the hydrogen analogues of tungsten bronzes Na_xWO_3.

Reduction of WO_3 at electrodes in aqueous solution was carried out by KOBOSEV AND NEKRASSOV[2] who observed that WO_3 crystals in the vicinity of the cathodic electrode turned blue and postulated the production of free hydrogen atoms in solution. BAGOTSKII *et al.*[3,4] concluded that the reduction mechanism was *via* direct electron transfer to WO_3 crystals in intimate contact with the electrode surface and that production of blue color throughout the WO_3 crystals was facilitated by the increased electronic conductivity of the reduced form[5,6]. BAGOTSKII AND IOFA[3] also pointed out that when pure WO_3 is heated *in vacuo* the crystals turn blue due to loss of oxygen, indicating high oxygen mobilities within the crystal.

Photochemical reduction of tungsten compounds in the presence of organic reducing agents have been shown by various workers[7-12]. Very large degrees of reduction were obtained so that the reduced tungsten complexes appeared "black". The general reaction may be written as

$$W^{6+} + \text{organic} \xrightarrow{h\nu} \underset{\text{blue}}{W^{5+}} + \text{oxidized organic} \tag{1}$$

In the presence of oxygen the reduced tungsten is reoxidized with consequent reduction of the oxygen molecule.

$$W^{5+} + O_2 \rightarrow O_2^- + \underset{\text{colorless}}{W^{6+}} \tag{2}$$

Owing to the low solubility of tungstic acid, H_2WO_4, the electrochemical reduction of tungsten has been examined *via* soluble complexes, *e.g.*, the chloro complex by LINGANE AND SMALL[13] who noted production of blue at the electrode surface, and SPERANSKAYA AND MAMBEEVA[14] who showed the absorption spectrum of the reduction product. Heteropoly complexes of the general formula

$[M^{n+}O_4W_{12}O_{36}]^{(8-n)-}$ where M is P^{5+}, As^{5+}, Si^{4+}, Ge^{4+}, Fe^{3+}, Co^{2+} have been examined for reduction potentials. Pope and Varga[15] have shown that the P^{5+}, Si^{4+}, Fe^{3+}, Co^{2+} complexes and the isopolymetatungstate anion $[H_2W_{12}O_{40}]^{6-}$ each can accept two electrons without decomposition while Stonehart[16] has shown that the addition of the first electron to the P^{5+} complex is extremely rapid and reversible. Spectra of the 1- and 2-electron reduction products of the Si^{4+} complex have been shown by Souchay and Hervé[17].

The heteropoly complexes of tungsten are eminently suitable for studying the electron transfer and rate kinetics for tungsten(VI) reduction at electrodes[18]. These heteropolyanions are quite soluble and well characterized[19] structurally. Since complexes with P^{5+} and Si^{4+} show blue transmission on reduction, the reduction electron must be associated with the tungsten cage. A quantitative examination of the optical absorbance coupled with the tungsten(V) concentration should give a greater understanding of transitions associated with tungsten(V) and tungsten–oxygen–tungsten interactions. Electron spin resonance may indicate the location of the reduction electron within the tungsten cage and the relationship between unpaired spins and tungsten(V) concentration.

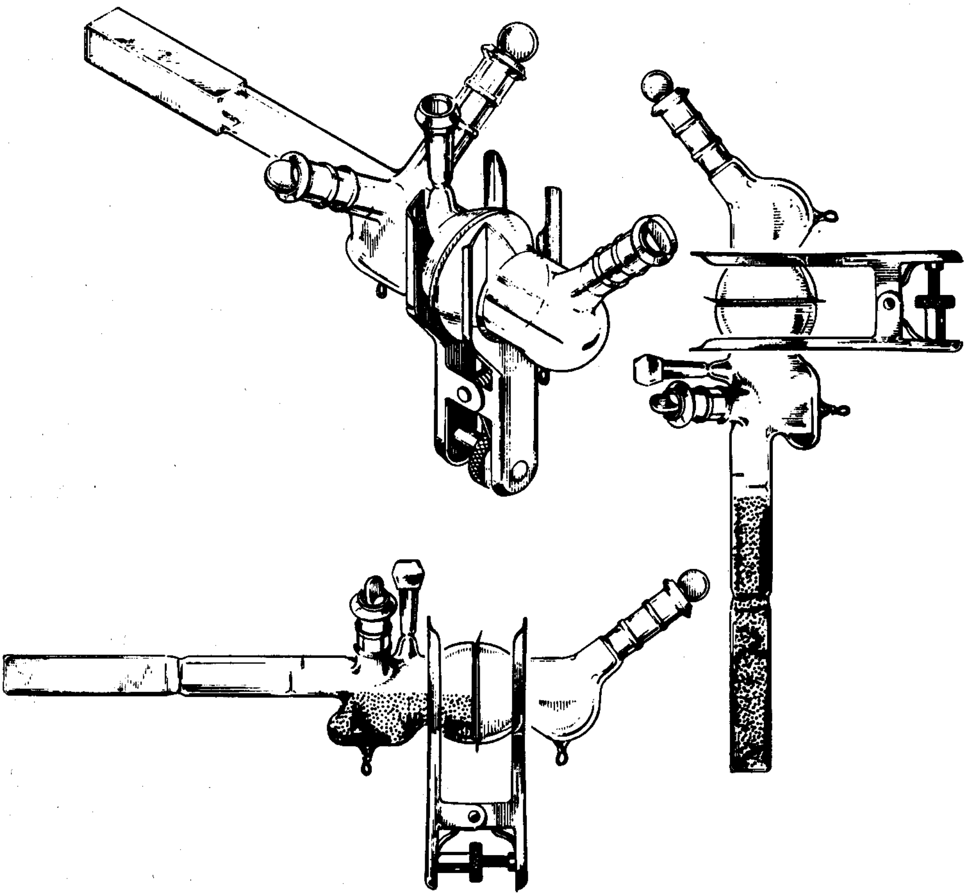

Fig. 1. Electrochemical cell.

EXPERIMENTAL

The potentiostat and current–voltage measuring system have been described previously[16]. The electrochemical cell is shown in Fig. 1; the anode and cathode compartments were separated by a membrane (Permion 1010). Platinum contacts were sealed through the glass, making contact to mercury pool electrodes, while two ground-glass ports enabled positioning of a reference electrode and a gas inlet. A small gas outlet port was also included in the cathode compartment. To measure the absorption spectrum, the cell was rotated through 90° so that the electrolyte was decanted into the quartz cell side-arm (10 mm) with the mercury trapped in a small bulb.

The solutions were flushed with argon, purified by passage over hot copper and through a water saturator. During the electrolysis at a constant potential, argon was bubbled continuously through the solution and samples for ESR were withdrawn under an argon atmosphere and inserted into argon-flushed ESR tubes (3 mm).

Absorption spectra were measured on a Cary 14 spectrophotometer against a 10 mm cell filled with unreduced solution. ESR spectra were measured at 77°K on a Varian V4502 spectrometer with a 9″ magnet and Fieldial.

RESULTS AND DISCUSSION

Production of tungsten blues

The current–voltage parameters with potentiodynamic control for the addition of the first electron to the phosphotungstate heteropolyanion have been discussed previously[16] and are shown in Fig. 2, curve (A). Curve (B) shows the current–voltage parameters obtained by linearly scanning the electrode potential to more negative

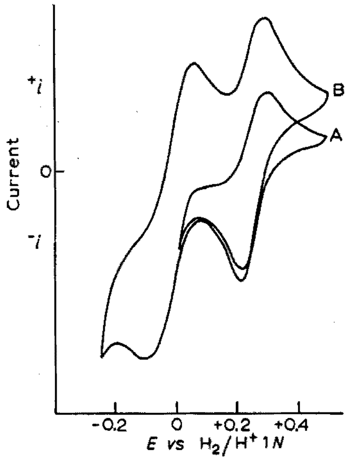

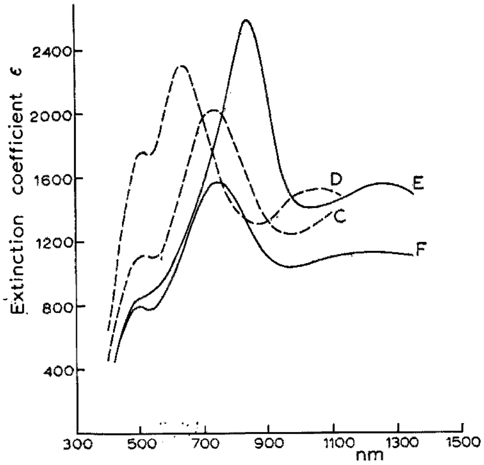

Fig. 2. Cyclic potentiodynamic *i–V* 0.050 *M* WO_4^{2-}/1 *M* H_3PO_4. (A) 54.5 mV·sec^{-1}; (B) 92.5 mV·sec^{-1}.

Fig. 3. Absorption spectra. (C) and (D) Reduced silicotungstate. (E) and (F) Reduced phosphotungstate.

values. An asymmetrical wave shape was produced with a second maximum at −0.1 V, and a reoxidation peak at +0.06 V, both *vs.* H_2/H^+ 1 *N*. Injection and removal of the first electron into the complex anion is certainly shown by the reduction peak at +0.21 V and the reoxidation peak at +0.29 V. It is tempting therefore to assign the second reduction peak at −0.1 V to the addition of a second electron to the complex. Assigning electron numbers is complicated by the presence of specific adsorption of the 1-electron reduction product at the electrode surface at +0.05 V, producing an anomalously high surface concentration; the re-oxidation peak at +0.06 V is not of the same magnitude as the reduction peak at −0.1 V, indicating that the 2-electron (or >1-electron) reduction product is not so strongly adsorbed at the electrode surface. The specific adsorption of the 1-electron reduction product is well defined at +0.05 V and may be characterized by an adsorption step measured with a dropping mercury electrode and an adsorption-desorption peak measured by A. C. impedance. The formation of color and ESR signals were therefore measured for the two situations of injection of one electron into the phosphotungstate anion (electrode potential maintained at +0.15 V) and for the injection of more than one electron (electrode potential maintained at −0.15 V). In addition, it was shown previously[18] that a polyphosphotungstate anion cluster could be formed not greater than a tetramer with a significantly lower diffusion coefficient than the hydrated monophosphotungstate anion. Although the polyphosphotungstate anion was unstable, it was possible to investigate the formation of tungsten blue with this species.

The equivalent absorbances of reduced heteropolyanions are shown in Fig. 3. SOUCHAY AND HERVÉ[17] indicate curve (C) to be the absorption for the 1-electron reduction $[SiW_{12}O_{40}]^{5-}$ and curve (D) for the 2-electron reduction $[SiW_{12}O_{40}]^{6-}$. The curve (E) is an extrapolated magnitude, corrected for the polymer decay with time, obtained for the 1-electron reduction of the polyphosphotungstate and curve (F) for the 1-electron reduction of the solvated monophosphotungstate heteropolyanion. SOUCHAY AND HERVÉ[17] indicate a quantitative conversion from the 1-electron to the 2-electron reduced silicotungstate, showing a spectral shift with isosbestic points at 350, 700, and 900 nm. The present results for the 1- and 2-electron reductions of the phosphotungstate anion show no shift in the absorption peak at 750 nm, but the 2-electron reduction product does show a higher extinction coefficient. No difference was observed between 1-electron and >1-electron for the reduction of the polyphosphotungstate (curve E) but the absorption peak, compared to the monomer, shifts to 850 nm with a higher extinction coefficient than the monomer. This shift would be expected for a larger ion cluster suggesting an increased delocalization of the reduction electron. Comparison of the absorption spectra for the 1-electron reduction of the silicotungstate $[SiW_{12}O_{40}]^{5-}$ in curve (C) and the 1-electron reduction of the phosphotungstate $[PW_{12}O_{40}]^{4-}$ in curve (F) shows a difference only in magnitude and that these two different ions produce an identical "fingerprint". This points to the secondary effect of the central atom in the KEGGIN[19] structure wherein the reduction electron is associated with the $[W_{12}O_{36}]$ shell. Structurally, these two ions have similar configurations and ionic sizes, although the sizes and degree of solvation for a given anion, shown by diffusion coefficients, differ in value depending on the measuring technique used; the differences in value (Table I) must be attributed to fundamental weaknesses in these techniques. The optical spectra of reduced heter-

TABLE I

COMPARISON OF HETEROPOLYANION DIFFUSION COEFFICIENTS

Anion	*D (cm² · sec⁻¹ × 10⁶)*	*Technique*	*Solution*	*Temp(°)*	*Ref.*
$[SiW_{12}O_{40}]^{4-}$	4.51	Ultracentrifuge	CH_3COONa/CH_3COOH $\mu = 0.2$	25	20
$[SiW_{12}O_{40}]^{4-}$	5.9	Radiotracer	$NaClO_4/HClO_4$ 1.0 *M*	30	21
$[SiW_{12}O_{40}]^{4-}$	2.56	D.M.E.	0.9 *M* Na_2SO_4/0.1 *M* H_2SO_4	25	15
$[SiW_{12}O_{40}]^{4-}$	4.2	D.M.E.	0.45 *M* Na_2SO_4/0.05 *M* H_2SO_4	25	22
$[SiW_{12}O_{40}]^{4-}$	2.9 (calc.)	Viscosity and density	CH_3COONa/CH_3COOH $\mu = 0.2$	—	23
$[PW_{12}O_{40}]^{3-}$	3.36	D.M.E.	1 *M* H_2SO_4	25	15
$[PW_{12}O_{40}]^{3-}$	2.48	Rotating disc	1 *M* H_3PO_4	25	18
$[PW_{12}O_{40}]^{3-}$	1.98	Chronopotentiometry	1 *M* H_3PO_4	25	24
$[PW_{12}O_{40}]^{3-}$	4.0	D.M.E.	0.1 *N* H_2SO_4	—	25

opoly acids are characterized by a broad maximum around 1250 nm in the near infrared, a peak between 650 and 850 nm and a shoulder at 500 nm. For the reduction product of the chloro complex, SPERANSKAYA *et al.*[14] show corresponding peaks at 750 nm and 550 nm. If the reduction electron is situated at a particular tungsten atom, it would be in the $5d^1$ configuration and the main interactions would be the local contributions of the 6 tungsten–oxygen bonds. Owing to the probable delocalization of the reduction electron through the conductive tungsten–oxygen skeleton, predictions of absorption maxima and assignments should not be made. The rapid electron transfer[16] indicates a low-energy barrier but due to tungsten–oxygen–tungsten interactions, not more than 1 in 12 W^{5+} is allowed, while the high conductivity of the $[W_{12}O_{36}]$ skeleton has been shown[26] by the rate kinetics for oxidation and reduction of the cobalt in the cobalt tungstate heteropolyanion.

An examination in the ultraviolet for the absorption spectra of the unreduced phosphotungstate anion shows a well-defined peak at 265 nm with an extinction coefficient of $5.13 \cdot 10^4$ which may be attributed[27] to intraligand charge transfer for the $[W_{12}O_{36}]$ skeleton. This peak is not shown for the polyphosphotungstate and therefore the rate of degradation of the polymer was followed at 25° by measuring the rate of rise of the 265 nm peak.

The formation of color as a function of reduction charge for the phosphotungstate heteropolyanions is shown in Fig. 4. Values were recorded for the peak absorbance and line (G) indicates the extrapolated relationship for the polyphosphotungstate without degradation of the polymer. The experimental points yield a curve because of the extremely low diffusion coefficients and hence the long times needed to carry out the reduction, allowing the polymer time to degrade while carrying out the experiment. Line (H) indicates the peak absorbance for color formation when more than one electron is injected into the phosphotungstate monomer (-0.15 V), whereas (J) shows the peak absorbance obtained for injecting one electron into the monomer ($+0.15$ V). The extinction coefficient for the values of (H) and absorption spectra are identical to the 1-electron reduction of silicotungstate shown by SOUCHAY AND HERVÉ[17]. As the absorption spectra of the phosphotungstates are so similar, it was thought that a rearrangement might be taking place:

$$[PW_{12}O_{40}]^{5-} + [PW_{12}O_{40}]^{3-} \rightarrow 2[PW_{12}O_{40}]^{4-} \qquad (3)$$

but this is not so, as there are no changes in the magnitudes for equivalent reduction between (H) and (J) with time. Also, the electrochemical peak for the penultimate reoxidation shown in Fig. 2 certainly indicates a short-term stable entity. Experimental points shown in Fig. 4 are the sums of many individual series performed at different times to estimate the reproducibility of a given set of values.

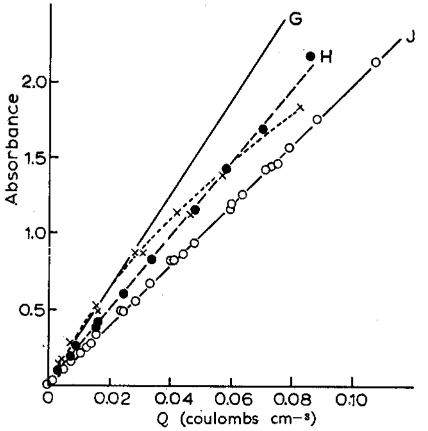

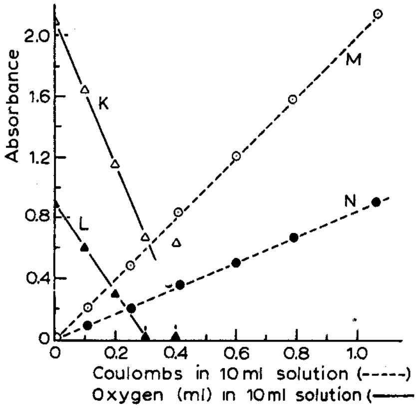

Fig. 4. Peak absorbance of reduced phosphotungstates. (G) Extrapolated value for polyphosphotungstate. Experimental (×) 850 nm. (H) 2-electron reduction of phosphotungstate anion (●) 750 nm. (J) 1-electron reduction of phosphotungstate anion (○) 750 nm.

Fig. 5. Electrochemical formation of color and annihilation of color with oxygen. (K) Peak absorbance after titrating with oxygen. (L) Excess peak height at 750 nm after titrating with oxygen. (M) Peak absorbance for reduction of phosphotungstate. (N) Excess peak height at 750 nm for reduction of phosphotungstate.

Reduction of oxygen

The general reaction of oxygen with tungsten reduction products is shown in eqn. (2). No indications of the mode or stoichiometry of this reaction have been shown previously. Accordingly, it was decided that the blue color could be used as an internal indicator to investigate the quantitative reduction of oxygen with concomitant reoxidation of the phosphotungstate heteropolyanion.

The 1-electron reduction product $[PW_{12}O_{40}]^{4-}$ was generated within the cell until the maximum absorption range of the Cary 14 was reached monitoring the peak at 750 nm and using a 1-cm path length, corresponding to the line (J) in Fig. 4. The electronic control was removed, together with the reference probe and the gas bubbler. The probe ports were sealed with solid glass stoppers and the gas outlet port plugged with a rubber septum. Rigorous precautions were taken to maintain a positive pressure of argon within the cell during these operations. The cell was then allowed to come to equilibrium, in case traces of oxygen had entered during manipulation. Finally, small quantities of pure oxygen gas were injected with a calibrated hypodermic syringe through the rubber septum and into the atmosphere above the $[PW_{12}O_{40}]^{4-}$ solution. The cell was shaken vigorously for 5 min and allowed to come to a steady state and the decreased absorption spectrum recorded. The results are shown in Fig. 5. Line (K) shows the decrease in total peak height for the absorption maximum at 750 nm whereas line (L) shows the decrease at 750 nm using a base line[28] drawn between the shoulder at 1000 nm and the shoulder at 550 nm. This was necessary as it was apparent that although the blue color decreased, so the solution became progressively more cloudy and produced light scattering. Therefore, at the juncture where all of the blue was removed, an apparent absorbance was still measurable. The coulombic formation of color, measuring the total peak height at 750 nm is shown by line (M) and the extrapolated peak height by line (N) to correspond to lines (K) and (L) for color removal. As both of the lines (K) and (L) in Fig. 5 are linear, this indicates that the increase in light scattering was directly proportional to the decrease in absorbance at 750 nm and also directly proportional to the oxygen added.

The reduction of oxygen has been shown[29-31] to proceed in a series of discrete steps

$$O_2 + e^- \rightarrow O_2^- \tag{4}$$

$$O_2^- + H^+ \rightarrow HO_2\cdot \tag{5}$$

$$HO_2\cdot + H^+ + e^- \rightarrow H_2O_2 \tag{6}$$

$$H_2O_2 + 2e^- + 2H^+ \rightarrow 2H_2O \tag{7}$$

with the rate-controlling step, eqn. (4), for the production of hydrogen peroxide as an intermediate and a much higher energy barrier for the reduction of hydrogen peroxide to water involving rupture of the oxygen–oxygen bond (eqn. 7). This process is usually separable into either a 2-electron reduction to peroxide or a 4-electron reduction to water. For the 4-electron reduction, a total of 4 × 96,500 coulombs are required, representing the reduction of 22.4 liters of oxygen at S.T.P. Therefore, 1 ml of oxygen requires 17.23 coulombs for the 4-electron reduction and correspondingly 8.615 coulombs for the 2-electron reduction. The coulombic charge required to generate the reduced $[PW_{12}O_{40}]^{4-}$ color density and the loss in color by oxidation with oxygen being known, the coulombic equivalence for the oxygen reduction was obtained. After correcting to S.T.P. it was apparent that 0.27 ml O_2 was equivalent to 1.07 coulombs; or 3.96 coulombs. ml^{-1} O_2. From the foregoing arguments this corresponds to a 1-electron reduction of the oxygen to the $HO_2\cdot$ free radical (eqns. 4 and 5). This radical was thought to be too unstable in aqueous solutions to be detected under these conditions although evidence for the existence of O_2^- in non-aqueous systems has been given[32]. This interpretation of the data is not unambiguous as it may be postulated that the total reduction charge on the tungsten is not associated with the color centers and that perhaps only 50% is associated with this transition. In this case, the oxygen atoms might attack *only* the color centers giving a 2-electron reduction which is pseudo 1-electron, although this is not very likely so. The linear increase in light scattering with oxygen consumption must be associated with the formation of large molecular weight polymers or anion clusters in the solution due to the attachment of the -HO_2 groups, affecting the anion surface charge or forming bridge links between heteropolyanions.

Electron spin resonance

Samples of solutions containing differing concentrations of reduced phosphotungstate anions were withdrawn from the electrochemical cell and transferred to argon-flushed ESR tubes (3-mm diameter). The tubes were frozen to 77°K in liquid nitrogen for the spectral determinations.

Polyphosphotungstate anion. The ESR spectrum for reduced polyphosphotungstate is shown in Fig. 6a, while the unreduced solution showed no signal. The broad signal shown in Fig. 6a may be interpreted as a species with anisotropic g value, $g_\perp = 1.85$ and $g_\parallel = 1.77$. The magnitude of the signal increased linearly up to spin concentration of *ca.* $65 \cdot 10^{-8}$ M cm^{-3}, with the degree of reduction of the polyphosphotungstate; because of the slow decomposition of the polymer during the electrochemical formation of the reduction product (see Fig. 4), the absorbance at 850 nm was plotted against spin concentration, rather than coulombic charge. When

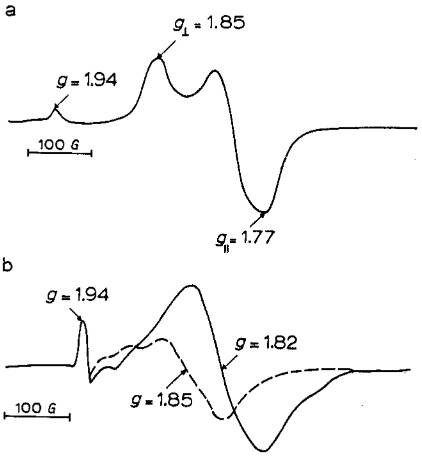

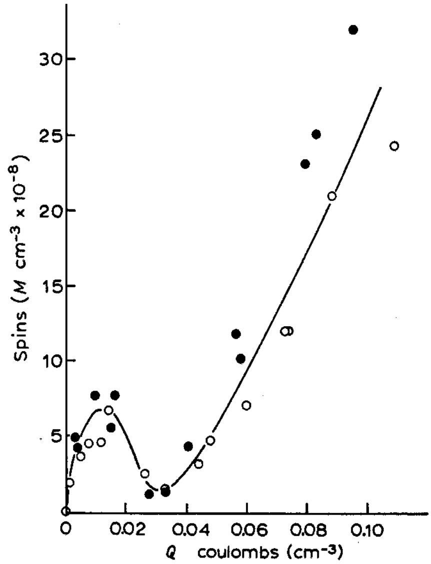

Fig. 6. ESR spectra of reduced phosphotungstate anions. (a) Polyphosphotungstate anion. (b) Monophosphotungstate anion.

Fig. 7. Spin concentration of reduced monophosphotungstate anions *versus* coulombic charge. (○) 1-electron reduction. (●) 2-electron reduction.

the extinction coefficient was calculated from the spin concentration, a value of 4000 ±1000 was obtained, which is in fair agreement with the extrapolated extinction coefficient obtained from the optical spectrum (2,600). It appears, therefore, that for the polymer there is a 1:1 correspondence between the W^{5+} spin concentration determined by ESR and the number of color centers determined from optical spectra.

Phosphotungstate anion monomer. The ESR signals for reduction of the phosphotungstate monomer are quite different from those for the polymer. At low concentrations a broad signal with some structure was observed at $g = 1.85$. With continued reduction the initial signal decreased to a minimum. Further increases of the $[PW_{12}O_{40}]^{4-}$ concentration produced a new ESR signal at $g = 1.82$. The latter signal increased to large values with the increase in reduced phosphotungstate anion $[PW_{12}O_{40}]^{4-}$ concentration. The ESR spectra for the reduced monomer are shown in Fig. 6b and the spin concentration with increasing $[PW_{12}O_{40}]^{4-}$ in Fig. 7. Similar behavior was observed whether one (+0.15 V) or two (−0.15 V) electrons were injected into the heteropolyanion; with the minimum corresponding to $0.31 \cdot 10^{-3}$ M W^{5+}/l. This anomalous behaviour was completely reproducible. Estimation of the extinction coefficient from spin densities at low (< 0.01 coulombs·cm^{-3}) concentrations of $[PW_{12}O_{40}]^{4-}$ gave a value of 2,500±500, which indicates that the ESR technique was seeing similar concentrations of the reduced tungsten as was the optical spectrum. At high (> 0.06 coulombs·cm^{-3}) concentrations of $[PW_{12}O_{40}]^{4-}$ the spin density indicated an extinction coefficient of 11,000, which suggests that the ESR was measuring far lower concentrations of unpaired spins than would have been expected, possibly owing to an exchange phenomenon. It must be noted that the ESR results presented in Fig. 7 should be correlated to the optical data presented in Fig. 4. This is particularly interesting since there is no suggestion from the optical spectra that, with increasing $[PW_{12}O_{40}]^{4-}$ concentration, a structural transition takes place because the absorbance of all species increases linearly with concentration of the reduced anions.

A minor signal was observed with $g = 1.94$ which appeared with initial reduction of the phosphotungstate anion to a small finite value. This signal was also seen in solutions containing the reduced polyphosphotungstate anion and may be due to the presence in the solution of a small concentration of tungsten species that are not complexed as heteropolyanions.

Hyperfine structures for these tungsten complexes are absent, except for a suggestion of shoulders on the $g = 1.82$ signal in Fig. 6b. This may be due to hyperfine components associated with ^{183}W which has nuclear spin 0.5 and is 14% abundant. With this abundance value the hyperfine structure of the ^{183}W isotope is masked by the large signals from the natural tungsten isotopes with nuclear spin zero. Studying the spectra obtained for ^{183}W enriched phosphotungstate anions may give a more definite interpretation for the degree of delocalization of the reduction electron. Such an investigation is now in progress.

CONCLUSIONS

The formation of "blue" color by electrochemical reduction of phosphotungstate heteropolyanions has shown that the color densities increase linearly with the coulombic reduction of these anions, obeying the Beer–Lambert laws. The optical spectra obtained were similar to those shown for reduced silicotungstate, indicating that the central hetero cluster in the KEGGIN structure of the anion affected only the reduction potential and hence free energy of the heteropolyanion, not the optical transition of the reduced anion. This supports the view that the reduction electron is associated only with the $[W_{12}O_{36}]$ skeleton. Assignments for the transitions relating to the optical absorption spectra have not been made at this stage, as the broad absorption peaks are the products of the high conductivity of the W–O–W skeleton, so that the reduction electron may be shared with 12 tungsten atoms.

Reacting the reduced phosphotungstate anions with oxygen gave a quantitative 1-electron reduction of the oxygen molecule, possibly producing high molecular weight, polyanion clusters.

Broad ESR signals were obtained for reduced phosphotungstate heteropolyanions but in the absence of hyperfine structure a definitive answer to the degree of delocalization of the reduction electron in the $[W_{12}O_{36}]$ skeleton was not obtained. A quantitative determination of the unpaired electron spins as a function of W^{5+} concentration showed that for the reduced polyphosphotungstate anion cluster a 1:1

correlation was obtained; for the reduced phosphotungstate anion monomer, apart from very low W^{5+} concentrations, the spin concentration was far lower than the W^{5+} concentration.

We should like to acknowledge the many helpful discussions with Dr. W. G. HODGSON concerning the ESR spectra results.

SUMMARY

The optical and ESR spectra of electrochemically reduced phosphotungstate and polyphosphotungstate anions in phosphoric acid were examined as quantitative functions of W^{5+} concentration. The optical spectra obey Beer–Lambert laws and are similar to the spectra of reduced silicotungstate anions, indicating the secondary nature of the central cluster in the KEGGIN structure with regard to interactions with the reduction electron. ESR spectra indicate an equivalent correspondence for the W^{5+} concentration and unpaired spins for the reduced polyphosphotungstate anion but for the reduced phosphotungstate anion monomer the unpaired spin concentration estimated by ESR was much lower than the W^{5+} concentration. Reacting reduced phosphotungstate anions with oxygen showed a 1-electron reduction of the oxygen molecule with concomitant oxidation of W^{5+} to W^{6+} and possibly production of high-molecular-weight, polyanion clusters.

RÉSUMÉ

On a examiné les spectres optiques et ESR des anions phosphotungstates et polyphosphotungstates électrochimiquement réduits, en fonction de la concentration en W^{5+}. Les spectres optiques obéissent aux lois de Beer–Lambert et sont identiques aux spectres des anions silicotungstates réduits, indiquant la nature secondaire du groupe central dans la structure Keggin à l'égard des interactions avec l'électron réducteur. Les spectres ESR indiquent une correspondance équivalente pour la concentration de W^{5+} et les spins non couplés pour l'anion polyphosphotungstate réduit. Les anions phosphotungstates réduits réagissant avec l'oxygène indiquent une réduction à un électron de la molécule d'oxygène avec oxydation de W^{5+} en W^{6+} et production possible de groupements polyanions de masse moléculaire élevée.

ZUSAMMENFASSUNG

Electrochemisch reduzierte Phosphowolframat- und Polyphosphowolframat-Anionen in Phosphorsäure wurden mit optischen und ESR-Spektren in Abhängigkeit von der W^{5+}-Konzentration geprüft. Die optischen Spektren gehorchen dem Lambert–Beerschen Gesetz und sind den Spektren reduzierter Silicowolframat-Anionen ähnlich. Das weist auf die sekundäre Natur der zentralen Cluster bei der Keggin-Struktur hin in bezug auf die Zwichenwirkungen mit dem reduzierenden Elektron. Die ESR-Spektren zeigen einen äquivalenten Zusammenhang zwischen der W^{5+}-Konzentration und den ungepaarten Spins des reduzierten Polyphosphowolframat-Anions. Jedoch ist für das reduzierte monomere Phosphowolframat-Anion die ungepaarte Spin-Konzentration, geschätzt mit der ESR, niedriger als die W^{5+}-

Konzentration. Reduzierte Phosphowolframat-Anionen, die mit Sauerstoff reagierten, zeigten eine Ein-Elektronen-Reduktion des Sauerstoffmoleküls begleitet von einer Oxydation des W^{5+} zum W^{6+} und eine mögliche Bildung eines hochmolekularen polyanionischen Clusters.

REFERENCES

1 J. E. Benson, H. W. Kohn and M. Boudart, *J. Catalysis*, 5 (1966) 307.
2 V. I. Kobosev and N. I. Nekrassov, *Z. Elektrochem.*, 36 (1930) 529.
3 V. S. Bagotskii and Z. A. Iofa, *Dokl. Akad. Nauk SSSR*, 53 (1946) 439.
4 V. S. Bagotskii, Z. A. Iofa and A. N. Frumkin, *Zh. Fiz. Khim.*, 21 (1947) 241.
5 E. Friederich, *Z. Physik*, 31 (1925) 813.
6 W. Meyer, *Z. Physik*, 85 (1933) 278.
7 L. Chalkley, *J. Phys. Chem.*, 56 (1952) 1084.
8 L. Chalkley, *J. Opt. Soc. Am.*, 44 (1954) 699.
9 L. Chalkley, *U. S. Patents 2,895,892*, 1959; *2,981, 622*, 1961.
10 M. Rindl, *S. African J. Sci.*, 11 (1916) 362.
11 S. E. Sheppard and L. W. Eberlin, *U. S. Patent 1,934,451*, 1933.
12 A. Bollinger and N. T. Hinks, *Australian J. Expl. Biol. Med. Sci.*, 27 (1949) 569.
13 J. J. Lingane and L. A. Small, *J. Am. Chem. Soc.*, 71 (1949) 973.
14 E. F. Speranskaya and D. B. Mambeeva, *Zh. Fiz. Khim.*, 39 (1965) 1837.
15 M. T. Pope and G. M. Varga, Jr., *Inorg. Chem.*, 5 (1966) 1249.
16 P. Stonehart, *Anal. Chim. Acta*, 37 (1967) 127.
17 P. Souchay and G. Hervé, *Compt. Rend.*, 261 (1965) 2486.
18 P. Stonehart, *Anal. Chim. Acta*, 37 (1967) 350.
19 J. F. Keggin, *Proc. Roy. Soc. (London)*, 144A (1934) 75.
20 M. C. Baker, P. A. Lyons and S. J. Singer, *J. Am. Chem. Soc.*, 77 (1955) 2011.
21 L. C. W. Baker and M. T. Pope, *J. Am. Chem. Soc.*, 82 (1960) 4176.
22 A-M. Baticle and P. Vennereau, *Compt. Rend.*, 261 (1965) 4086.
23 T. Kurucsev, A. M. Sargeson and B. O. West, *J. Phys. Chem.*, 61 (1957) 1567.
24 R. Bankert, private communication.
25 J. H. Kennedy, *J. Am. Chem. Soc.*, 82 (1960) 2701.
26 V. E. Simmons-Baker, *Ph.D. Thesis*, Boston University, 1963, p. 396.
27 V. E. Simmons-Baker, *Ph.D. Thesis*, Boston University, 1963, p. 369.
28 *A.S.T.M. Manual on Recommended Practices in Spectrophotometry*, 1966, p. 64.
29 I. M. Kolthoff and C. S. Miller, *J. Am. Chem. Soc.*, 63 (1941) 1013.
30 D. M. H. Kern, *J. Am. Chem. Soc.*, 76 (1954) 4208.
31 J. Kuta and J. Koryta, *Collection Czech. Chem. Commun.*, 30 (1965) 4095.
32 D. L. Maricle and W. G. Hodgson, *Anal. Chem.*, 37 (1965) 1562.

Anal. Chim. Acta, 40 (1968) 65–75

Analytica Chimica Acta
Elsevier Publishing Company, Amsterdam
Printed in The Netherlands

INTERPRETATION ET DESCRIPTION DES COURBES POLAROVOLTRIQUES ET BIPOTENTIOMETRIQUES: SYSTEME DE NOTATIONS SYMBOLIQUES ET NUMERIQUES

J. E. DUBOIS ET P. C. LACAZE

Laboratoire de Chimie Organique Physique, Faculté des Sciences de Paris, Associé au C.N.R.S., 1, rue Guy de la Brosse, Paris 5ème (France)

(Reçu le 15 avril, 1967)

Nous avons montré dans une étude précédente[1] comment l'utilisation de réseaux $i=f(V)$ et $V=f(U)$, où V représente la tension mesurée entre 2 électrodes indicatrices et U la tension appliquée à ces 2 électrodes, avait conduit à un choix optimal des paramètres électriques qui définissent la méthode polarovoltrique.

L'interprétation des variations de tension des courbes polarovoltriques peut être abordée à partir des courbes $i=f(E)$, dans lesquelles E représente la tension d'une électrode indicatrice par rapport à une électrode de référence. Cependant, comme le passage de ce dernier réseau aux courbes de dosages nécessite certaines déterminations graphiques, il nous a paru plus simple de construire des diagrammes intermédiaires Z–E, qui, définis à l'aide de notations symboliques nouvelles et simples, font apparaître directement la liaison entre variations de tension des courbes de dosages et évolution des systèmes électrochimiques au cours de la réaction de titrage.

Cette dernière relation exprimée par une notation dérivée des précédentes, est liée à la notion de transition électrochimique d'électrode, que nous définissons plus loin, et qui est à la base de l'interprétation des courbes de dosages polarovoltriques.

Ce concept, utilisé parallèlement avec un système de représentation numérique, développé par ailleurs[2], permet de répertorier simplement, pour une courbe de dosage polarovoltrique, sa morphologie et aussi d'attribuer à chaque variation de tension une signification électrochimique précise.

Dans un souci d'exposition nous définissons en premier lieu les symboles utilisés, et montrons leur utilisation à l'étude électrochimique des solvants organiques.

La description d'un diagramme Z–E est envisagée ensuite dans le cas particulier d'un dosage d'oxydo-réduction, pour lequel on définit la notion de transition électrochimique et son symbole.

Des exemples d'utilisation de cette notation et du système numérique descriptif de la morphologie sont montrés dans le cas de dosages du type acide–base en milieu organique.

COURBES DE POLARISATION–NOTATION SYMBOLIQUE

L'obtention de courbes polarovoltriques ou bipotentiométriques à partir des courbes courant–tension impose la mesure de valeurs de tension anodique et cathodique pour des densités de courant déterminées. La connaissance simultanée et impérative de ces 2 variables, nous incite à introduire des symboles de base, qui tiennent compte implicitement de ces 2 grandeurs, et qui puissent être utilisés aussi bien pour la description des courbes courant–tension que pour celles des courbes polarovoltriques. Comme par ailleurs la méthode polarovoltrique est très utilisée en milieu organique, nous en avons tenu compte afin que la gamme des définitions et des symboles proposés permette les interprétations des problèmes de l'électrochimie organique.

*Définitions**

	(*i*) *Notations descriptives.*
$\mathscr{M}_S$:	milieu chimique défini par: $S=\Sigma S_i$ solvant pur ou mélange de solvants S_i, électrolyte support à forte concentration, eau résiduelle, impuretés organiques.
e:	nature de l'électrode; A: anode; C: cathode; R: électrode de comparaison (réference).
i:	densité de courant à l'électrode e.
J,L,J',L':	entités électroactives introduites dans $\mathscr{M}_S$, à faible concentration par rapport à l'électrolyte support.
$[\mathrm{N}],[\mathrm{N}']$:	composé ou ensemble de composés correspondant aux réactions électrochimiques (1) $[\mathrm{N}]-nq\rightarrow[\mathrm{P}]$ (2) $[\mathrm{N}']+n'q\rightarrow[\mathrm{Q}']$ (q: charge de l'électron; n,n': nombre d'électrons échangés).
M,M':	espèces électroactives de $\mathscr{M}_S$, donnant lieu aux courbes limites courant–tension $\mathscr{E}^{M}_{A,e}$ (oxydation) et $\mathscr{E}^{M'}_{C,e}$ (réduction). Suivant les cas, M et M' pourront être identifiées à S, à l'anion ou au cation, ou à une impureté résiduelle.
$\mathscr{E}^{J}_{A,e}, \mathscr{E}^{J'}_{C,e}$:	courbes courant–tension d'oxydation et de réduction après introduction de J et J' dans $\mathscr{M}_S$. (Cette notation n'implique pas de mécanisme électrochimique pour J et J' contrairement à la notation suivante.)
$\mathscr{E}^{[\mathrm{N}]-nq}_{A,e}\ \mathscr{E}^{[\mathrm{N}']+n'q}_{C,e}$:	courbes courant–tension d'oxydation et de réduction, correspondant aux réactions électrochimiques (1) et (2).
$\mathscr{D}^{M,M'}_{e,\mathscr{M}_S}$:	domaine d'utilisation du milieu chimique $\mathscr{M}_S$. Région courant–tension limitée par les courbes $\mathscr{E}^{M}_{A,e}$ et $\mathscr{E}^{M'}_{C,e}$. Pour plus de simplicité dans l'écriture nous représenterons $\mathscr{D}^{M,M'}_{e,\mathscr{M}_S}$ par $\mathscr{D}^{M,M'}_{e,S^*}$.
$(\mathscr{D}^{M,M'}_{e,S^*})^{\max}$:	domaine d'utilisation maximal correspondant à une composition optimale de $\mathscr{M}_S$.
	(*ii*) *Notations quantitatives.*
(3) $(E^{J}_{A,e})^{R}_{i}$:	mesure de la tension d'oxydation de J, par rapport à R et pour une valeur i de la densité de courant.
$(E^{J'}_{C,e})^{R}_{i}$:	définition analogue à (3) pour la réduction de J'.

---

* Certaines des notations que nous présentons ici ont reçu de légères modifications par rapport à leur présentation intiale[3,1].

(4) $(E^{J}_{A,e})^{R}_{i=0}$: valeur de la tension extrapolée pour une densité de courant nulle (point d'intersection avec l'axe des tensions de la partie rectiligne de la courbe $\mathscr{E}^{J}_{A,e}$ due à une surtension ohmique résiduelle).
$(E^{J'}_{C,e})^{R}_{i=0}$: définition analogue à (4).
(5) $(E^{[\mathrm{N}]-nq}_{A,e})^{R}_{i}$: valeur de la tension anodique associée à la réaction (1), mesurée par rapport à R et pour une valeur i de la densité de courant.
$(E^{[\mathrm{N'}]+n'q}_{C,e})^{R}_{i}$: définition analogue à (5) pour la réaction (2).
$(E^{[\mathrm{N}]-nq}_{A,e})^{R}_{i=0}$, $(E^{[\mathrm{N'}]+n'q}_{C,e})^{R}_{i=0}$: définitions semblables à (4).
(6) $(D^{M,M'}_{e,S^*})_{i}$: mesure de tension de $\mathscr{D}^{M,M'}_{e,S^*}$ pour la densité de courant i.
$(D^{M,M'}_{e,S^*})_{i}$ $= (E^{M}_{A,e})^{R}_{i} - (E^{M'}_{C,e})^{R}_{i}$.
$(D^{M,M'}_{e,S^*})_{i=0}$ $=$ mesure de tension de $\mathscr{D}^{M,M'}_{e,S^*}$ pour $i=0$.
$(D^{M,M'}_{e,S^*})_{i=0}$ $= (E^{M}_{A,e})^{R}_{i=0} - (E^{M'}_{C,e})^{R}_{i=0}$.
$(D^{M,M'}_{e,S^*})^{\max}_{i}$: mesure de tension de $(\mathscr{D}^{M,M'}_{e,S^*})^{\max}$ pour la valeur i de la densité de courant.
$(D^{M,M'}_{e,S^*})^{\max}_{i=0}$: mesure de tension de $(\mathscr{D}^{M,M'}_{e,S^*})^{\max}$ pour $i=0$.
(7) $\Delta E^{J\to L}_{A,e}$: transition électrochimique à l'anode du système J à L.
$\Delta E^{J\to L}_{A,e}$ $= (E^{L}_{A,e})^{R}_{i} - (E^{J}_{A,e})^{R}_{i}$.
$\Delta E^{J'\to L'}_{C,e}$: définition analogue à (7) (transition cathodique de J' à L').
$\Delta E^{J'\to L'}_{C,e}$ $= -\left[(E^{L'}_{C,e})^{R}_{i} - (E^{J'}_{C,e})^{R}_{i}\right]$.

Des définitions précédentes, on remarque que $(D^{M,M'}_{e,\mathscr{M}_s})_{i=0}$ donne l'étendue globale du domaine d'utilisation du solvant mais ne permet pas de caractériser totalement le solvant sans la connaissance d'au moins une des deux valeurs de tension $(E^{M}_{A,e})^{R}_{i=0}$ ou $(E^{M'}_{C,e})^{R}_{i}$, qui est indispensable pour définir l'étendue possible des domaines d'oxydation et de réduction du solvant.

Remarque

Dans le cas où l'écriture proposée introduirait des difficultés typographiques, on pourra convenir de représenter également les notations telles que $\mathscr{D}^{M,M'}_{e,S}$, $(E^{[\mathrm{N}]-nq}_{A,e})^{R}_{i}$ sous une forme uniligne equivalente:

$$\mathscr{D}(M,M')(e,\mathscr{M}_S);\quad E([\mathrm{N}]-nq)(A,e)(R,i)$$

Applications

Description des caractéristiques électrochimiques d'un solvant. Nous montrons, à titre d'exemple, l'utilisation de cette notation dans la description des propriétés électrochimiques du solvant HMPT (hexaméthylphosphotriamide), étudié sur électrode tournante de platine[1] (Fig. 1).

En zone anodique, la courbe limite est indépendante de l'anion en solution, à condition que celui-ci soit difficilement oxydable comme par exemple ClO_4^-, $C_6H_5SO_3^-$, $C_6H_5CO_2^-$, $CH_3CO_2^-$ ... Cette courbe attribuable à l'oxydation du solvant sera notée $\mathscr{E}^{S}_{A,\mathrm{Pt}}$; il lui correspond la valeur de tension $(E^{S}_{A,\mathrm{Pt}})^{\mathrm{Ag-Ag^+}}_{i=0} = 0.75$ V mesurée par rapport à l'électrode de comparaison Ag–$Ag^+ \cdot 10^{-2}$ M dans le même solvant.

En réduction, les courbes courant–tension dépendent de la nature du cation présent et de la teneur en eau du solvant.

TABLEAU I

DOMAINES D'"ELECTROACTIVITE" COMPARES DE QUELQUES SOLVANTS ORGANIQUES, EN PRESENCE DE SELS A LA CONCENTRATION 0.1 N (VALEURS MESUREES EN VOLTS)

$\mathcal{M}_S$	$(E^{\mathrm{M'}}_{C,\mathrm{Pt}})^R_i$	$(E^{\mathrm{M}}_{A,\mathrm{Pt}})^R_i$	$(D^{\mathrm{M,M'}}_{\mathrm{Pt},S^*})_i$
S = CH_3CN $LiClO_4$ 0.1 M $H_2O < 50$ p.p.m.	$(E^{\mathrm{Li}^+}_{C,\mathrm{Pt}})^{\mathrm{Ag-Ag^+ \cdot 10^{-2}}M}_{i=0} = -3.5$	$(E^{\mathrm{ClO_4^-}}_{A,\mathrm{Pt}})^{\mathrm{Ag-Ag^+ \cdot 10^{-2}}M}_{i=0} = 2.4$	$(D^{\mathrm{ClO_4^-,Li^+}}_{\mathrm{Pt,CH_3CN^*}})_{i=0} = 5.9^{a}$
S = THF NBu_4ClO_4 0.1 M $H_2O < 10$ p.p.m.	$(E^{\mathrm{NBu_4^+}}_{C,\mathrm{Pt}})^{\mathrm{Ag-Ag^+ \cdot 10^{-1}}M}_{i=0} = -4$	$(E^{\mathrm{ClO_4^-}}_{A,\mathrm{Pt}})^{\mathrm{Ag-Ag^+ \cdot 10^{-1}}M}_{i=0} = 1.5$	$(D^{\mathrm{ClO_4^-,NBu_4^+}}_{\mathrm{Pt,THF^*}})_{i=0} = 5.5^{a}$
S = CH_3NO_2 $LiClO_4$ 0.1 M $H_2O < 200$ p.p.m.	$(E^{\mathrm{Li}^+}_{C,\mathrm{Pt}})^{\mathrm{Ag-AgCl}}_{i=0,6\,\mathrm{mA/cm^2}} = -2.4$	$(E^{\mathrm{ClO_4^-}}_{A,\mathrm{Pt}})^{\mathrm{Ag-AgCl}}_{i=0,6\,\mathrm{mA/cm^2}} = 2.95$	$(D^{\mathrm{ClO_4^-,Li^+}}_{\mathrm{Pt,CH_3NO_2^*}})_{i=0,6\,\mathrm{mA/cm^2}} = 5.35^{a}$
S = HMPT $LiClO_4$ 0.1 M $H_2O = 300$ p.p.m.	$(E^{\mathrm{Li}^+}_{C,\mathrm{Pt}})^{\mathrm{Ag-Ag^+ \cdot 10^{-2}}M}_{i=0} = -3.7$	$(E^{S}_{A,\mathrm{Pt}})^{\mathrm{Ag-Ag^+ \cdot 10^{-2}}M}_{i=0} = 0.75$	$(D^{S,\mathrm{Li^+}}_{\mathrm{Pt,HMPT^*}})_{i=0} = 4.45^{b}$
S = AcOH $NaClO_4$ 0.1 M $H_2O = 500$ p.p.m.	$(E^{\mathrm{H}^+}_{C,\mathrm{Pt}})^{\mathrm{Ag-AgCl}}_{i=0} = -0.2$	$(E^{S}_{A,\mathrm{Pt}})^{\mathrm{Ag-AgCl}}_{i=0} = 2.17$	$(D^{S,\mathrm{H^+}}_{\mathrm{Pt,AcOH^*}})_{i=0} = 2.37^{b}$

[a] Electrode de Pt nettoyée par polissage mécanique. [b] Electrode de Pt nettoyée à la flamme d'un bec Bunsen.

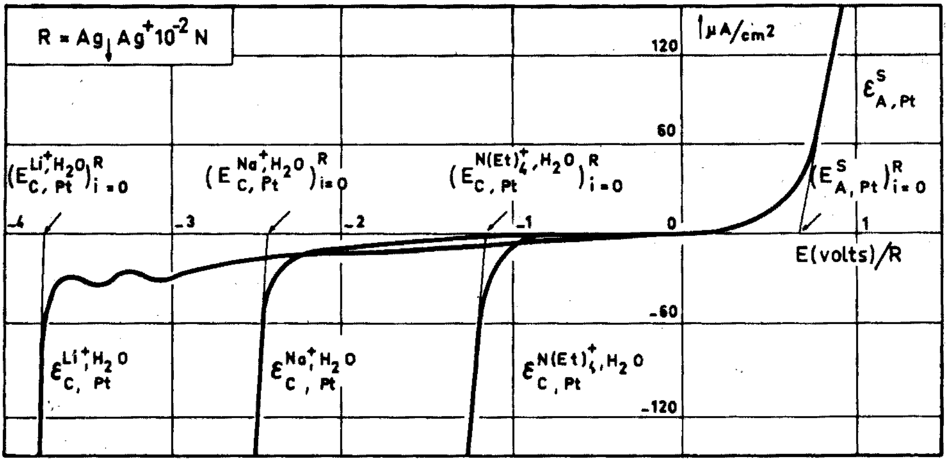

Fig. 1. Description du domaine électrochimique d'utilisation du solvant HMPT. Electrode de platine tournante (1200 t/min) traitée à la flamme d'un bec Bunsen avant chaque tracé de courbe. Vitesse de polarisation: 5.55 mV/sec. Concentration des sels: 0.1 *M*.

Ainsi pour une concentration d'eau équivalente à 0.03‰, on obtient avec les perchlorates de Li^+, Na^+ et $N(Et)_4^+$, les courbes de réduction $\mathcal{E}^{Li^+,H_2O}_{C,Pt}$, $\mathcal{E}^{Na^+,H_2O}_{C,Pt}$, et $\mathcal{E}^{N(Et)_4^+,H_2O}_{C,Pt}$ caractérisées par les valeurs de tension: $(E^{Li^+,H_2O}_{C,Pt})^{Ag-Ag^+}_{i=0} = -3.65$ V, $(E^{Na^+,H_2O}_{C,Pt})^{Ag-Ag^+}_{i=0} = -2.4$ V et $(E^{N(Et)_4^+,H_2O}_{C,Pt})^{Ag-Ag^+}_{i=0} = -1.13$ V.

Il ressort de ces données que la nature du cation détermine les limites cathodiques du domaine d'utilisation du solvant susceptible donc d'une ouverture plus ou moins grande. Ainsi avec les perchlorates de tétraéthylammonium, sodium et lithium, on obtient respectivement

$$(D^{S,N^+(Et)_4}_{Pt,HMPT*})_{i=0} = 1.88 \text{ V}, \quad (D^{S,Na^+}_{Pt,HMPT*})_{i=0} = 3.15 \text{ V},$$

et

$$(D^{S,Li^+}_{Pt,HMPT*})_{i=0} = 4.40 \text{ V},$$

cette dernière valeur correspondant au domaine d'utilisation maximum du solvant en présence de traces d'eau.

Comparaison des caractéristiques électrochimiques de solvants. A partir de données relevées dans la littérature, nous donnons sous forme de tableau les valeurs caractéristiques des domaines d'utilisation et des courbes limites obtenues sur électrodes de platine dans le cas de quelques solvants aprotiques, tels que l'acétonitrile[4], le nitrométhane[5], le tétrahydrofurane[6] (THF), l'hexaméthylphosphotriamide[3] (HMPT), et d'un solvant protolytique tel que l'acide acétique, que nous avons utilisé dans les dosages d'amines au moyen de la méthode polarovoltrique[7].

Ces quelques exemples résumés dans le Tableau I permettent de comparer pour chaque solvant l'étendue relative des zones anodique et cathodique, ainsi que l'étendue totale du domaine.

On remarquera cependant que la seule comparaison des propriétés électrochimiques d'un solvant ne saurait justifier entièrement son choix, et qu'il importe de tenir compte de ses propriétés chimiques qui interviennent également dans les réactions que l'on se propose d'étudier.

RELATIONS SCHEMATIQUES ENTRE COURBES COURANT–TENSION ET COURBES DE DOSAGES: DIAGRAMMES Z–E ET Z–V

Nous proposons de relier les propriétés des courbes de dosages expérimentales Z–V* aux propriétés des réseaux de courbes courant–tension, au moyen de notations symboliques dérivées des notations précédentes, et qui relient les variations de tension observées dans les courbes polarovoltriques et bipotentiométriques à l'évolution des réactions électrochimiques dans le milieu du dosage.

Le principe de cette notation repose sur la notion de transition électrochimique d'une électrode. Soit dans un milieu chimique $\mathscr{M}_S$ la réaction de dosage $\mathrm{D} + \mathrm{T} \rightarrow [\mathrm{D\ T}]$ (D: corps titré, T: réactif titrant, [D T]: composé ou ensemble de corps résultant de la réaction précédente). Pour $Z < 1$ les entités en présence sont D, [D T] et $\mathscr{M}_S$ et pour $Z > 1$, T, [D T] et $\mathscr{M}_S$.

Si D est plus facilement oxydo-réductible que [D T] et S, le réseau des courbes courant–tension de [D T] ou de $\mathscr{M}_S$ se substitue, pour $Z = 1$, à celui des courbes courant–tension de D. De même pour $Z > 1$, le réseau des courbes courant–tension de T remplacera celui de [D T] ou de $\mathscr{M}_S$. Cette substitution entraîne donc pour une seule ou pour les deux électrodes une variation rapide de tension que nous définissons comme une *transition électrochimique d'électrode.* Cela signifie que la tension d'une électrode, initialement contrôlée par un système électrochimique (I), subit au voisinage d'un point équivalent une variation de tension rapide, due à la substitution d'un systeme électrochimique (II).

Afin de faire apparaître plus précisément cette notion de transition électrochimique d'électrode, nous avons défini un diagramme Z–E schématique, déduit de la connaissance des courbes courant–tension, à partir duquel on déduit la courbe de dosage Z–V ($V = E_A - E_C$), et qui permet d'identifier les variations de tension aux transitions d'électrodes.

Nous montrons avec l'exemple d'un dosage d'oxydo–réduction la construction schématique d'un tel diagramme Z–E, et la définition symbolique des transitions électrochimiques d'électrode.

Diagramme Z–E: cas d'un dosage d'oxydo–réduction

Soit l'exemple type d'un dosage d'oxydo–réduction $\mathrm{Ox}_1 + \mathrm{Red}_2 \rightarrow \mathrm{Ox}_2 + \mathrm{Red}_1$, avec Ox_1 la substance dosée, Red_2, le réactif titrant et $\mathrm{Ox}_1/\mathrm{Red}_1$, $\mathrm{Ox}_2/\mathrm{Red}_2$ deux couples de systèmes électrochimiques rapides.

Sur un système d'axes rectangulaires Z–E, portons en ordonnée les valeurs $(E^{M'}_{C,e})^R_i$ et $(E^{M}_{A,e})^R_i$ qui limitent le domaine d'utilisation du milieu chimique $\mathscr{M}_S$.

Nous représentons graphiquement en fonction de Z les variations de chacune des valeurs de tension

$$(E^{\mathrm{Red}_1}_{A,e})^R_i,\ (E^{\mathrm{Red}_2}_{A,e})^R_i,\ (E^{\mathrm{Ox}_1}_{C,})^R_i,\ (E^{\mathrm{Ox}_2}_{C,})^R_i$$

mesurées dans l'intervalle: $0 < Z < 1.10$ et pour une valeur moyenne i de la densité de courant.

Au réseau de la Fig. 2 nous apportons la schématisation suivante:

---

* Z: degré d'avancement de la réaction de dosage, égal au rapport du nombre d'équivalents de réactif titrant versé au nombre d'équivalents de produit à doser.

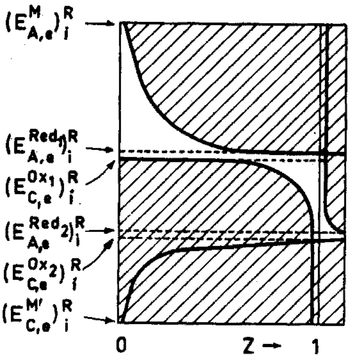

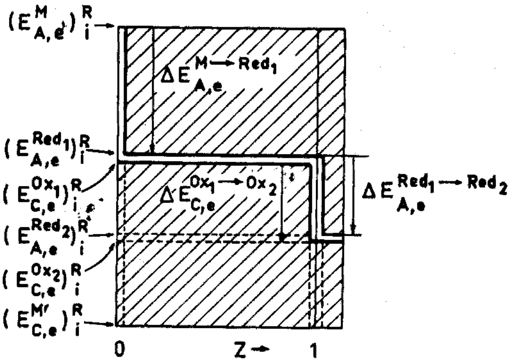

Fig. 2. Diagramme Z–E correspondant à la réaction de dosage $Ox_1 + Red_2 \rightarrow Ox_2 + Red_1$.

Fig. 3. Diagramme Z–E schématique.

(*i*) on considère que le seuil de sensibilité de deux électrodes est le même pour les différentes espèces Ox_1, Ox_2, Red_1, et Red_2, et correspond à une concentration minimale, telle que:

$$\frac{(C_{Ox_1})_{min}}{C_{Ox_1}} = \frac{(C_{Ox_2})_{min}}{C_{Ox_1}} = \ldots = \frac{(C_{Red_2})_{min}}{C_{Ox_1}} = \varepsilon_{(petit)}$$

(*ii*) les transitions électrochimiques d'électrodes se produisent dès que la concentration relative de l'une des espèces par rapport à celle de C_{Ox_1} devient égale à ε.

(*iii*) les valeurs

$$(E^{Red_1}_{A,e})^{R}_{i},\ (E^{Red_2}_{A,e})^{R}_{i},\ (E^{Ox_1}_{C,e})^{R}_{i} \text{ et } (E^{Ox_2}_{C,e})^{R}_{i}$$

sont définies dans un intervalle de Z où leur concentration relative par rapport à celle de Ox_1 est supérieure à ε; dans chacun de ces intervalles, les valeurs $(E^{Red_1}_{A,e})^{R}_{i} \ldots (E^{Ox_1}_{C,e})^{R}_{i}$ restent constantes et égales à la valeur limite atteinte dans l'intervalle $0 \leqslant Z \leqslant 1.10$.

Ainsi $(E^{Red_1}_{A,e})^{R}_{i}$, défini de $Z = \varepsilon$ à $Z = 1.10$, est représentée par un segment de droite dont l'ordonnée correspond à la valeur de

$$(E^{Red_1}_{A,e})^{R}_{i} \text{ pour } Z = 1.10$$

Cette dernière simplification permet de tenir compte uniquement des variations de tension dues aux transitions électrochimiques, en négligeant toute variation de tension entraînée par des changements de concentration à l'intérieur du domaine de définition de chaque espèce.

Courbes de dosage Z–V: transition électrochimique d'une électrode

Soit V la tension mesurée entre les deux electrodes au cours du dosage. Pour $Z = 0$, la différence de tension initiale $V_{(Z=0)}$ entre l'anode et la cathode, est égale à

$$(E^{Red_1}_{A,e})^{R}_{i} - (E^{Ox_1}_{C,e})^{R}_{i}.$$

L'addition du réactif Red_2 conduit à la formation de Red_1 et l'anode acquiert pour $Z = \varepsilon$ la nouvelle valeur de tension $(E^{Red_1}_{A,e})^{R}_{i}$.

La tension mesurée entre les deux électrodes est alors égale à $V_{(Z=\varepsilon)} = (E_{A,e}^{\mathrm{Red}_1})_i^R - (E_{C,e}^{\mathrm{Ox}_1})_i^R$, soit $V_{(Z=\varepsilon)} = V_{(Z=0)} - \Delta E_{A,e}^{\mathrm{M}\to\mathrm{Red}_1}$, *où* $\Delta E_{A,e}^{\mathrm{M}\to\mathrm{Red}_1}$ *représente par définition la transition électrochimique de l'anode, pour* $Z=\varepsilon$.

Cette transition anodique qui résulte de l'apparition de l'espèce Red_1, plus facilement oxydable que M, est caractérisée par une valeur de tension égale à $(E_{A,e}^{\mathrm{Red}_1})_i^R - (E_{A,e}^{\mathrm{M}})_i^R$.

De la même manière pour $Z = 1-\varepsilon$, Ox_1 disparaît, et la tension de la cathode varie donc de $(E_{C,e}^{\mathrm{Ox}_1})_i^R$ à $(E_{C,e}^{\mathrm{Ox}_2})_i^R$. Il en résulte la *transition cathodique*

$\Delta E_{C,e}^{\mathrm{Ox}_1\to\mathrm{Ox}_2}$ égale à $-[(E_{C,e}^{\mathrm{Ox}_2})_i^R - (E_{C,e}^{\mathrm{Ox}_1})_i^R]$

Enfin pour $Z = 1+\varepsilon$, une nouvelle transition anodique se produit

$\Delta E_{A,e}^{\mathrm{Red}_1\to\mathrm{Red}_2}$ égale à $(E_{A,e}^{\mathrm{Red}_2})_i^R - (E_{A,e}^{\mathrm{Red}_1})_i^R$

Nous avons représenté sur la Fig. 4 la courbe de dosage déduite du diagramme précédent en faisant correspondre à chaque variation de tension une transition d'électrode.

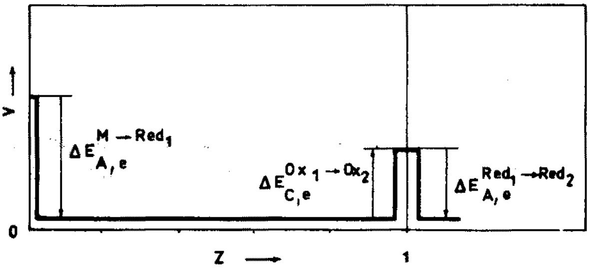

Fig. 4. Courbe de dosage [0,1,0] de la réaction $\mathrm{Ox}_1 + \mathrm{Red}_2 \to \mathrm{Ox}_2 + \mathrm{Red}_1$. Courbe déduite du diagramme *Z–E* de la Fig. 3.

Cette dernière relation peut cependant être établie de façon plus formelle en reliant les transitions d'électrodes au système de représentation numérique de la morphologie des courbes de dosages polarovoltriques.

Ce système qui a été défini par ailleurs[2], permet de représenter sous forme numérique et dans la région d'un point de virage, toute morphologie de courbe polarovoltrique ou bipotentiométrique. Il permet également de représenter de façon non ambiguë chaque variation de tension à l'aide d'une formule numérique simple. *La combinaison de l'écriture symbolique des transitions d'électrode et du système numérique permet donc de décrire complètement une courbe de dosage, tant du point de vue morphologique que de l'interprétation des réactions électrochimiques.*

Représentation complète d'une courbe de dosage: transitions d'électrodes et formule numérique

La courbe de la Fig. 4 est représentée dans la région du point équivalent ($Z=1$), par la formule numérique [0,1,0]. Ceci indique que la courbe comporte une première variation de tension (0,1) positive, et une deuxième variation de tension négative (1,0) opposée à (0,1).

Il en résulte que pour ce type de dosage, la transition $\Delta E_{C,e}^{\mathrm{Ox}_1\to\mathrm{Ox}_2}$ est associée à la variation de tension positive (0,1), et $\Delta E_{A,e}^{\mathrm{Red_1\rightarrow Red_2}}$ à la variation de tension négative (1,0).

Cette correspondance entre transition et variation de tension se conserve pour une même famille de composés dont les formes de courbes, différentes du type [0,1,0], peuvent être [$\frac{1}{4}$,1,0], [$\frac{1}{2}$,1,0], [$\frac{3}{4}$,1,0], [0,1,$\frac{3}{4}$], [0,1,$\frac{1}{2}$], [0,1,$\frac{1}{4}$] ou [0,1] et [1,0] dans le cas où l'un des systèmes $\mathrm{Red_1/Ox_1}$ ou $\mathrm{Red_2/Ox_2}$ n'est pas réversible.

En conclusion, l'utilisation simultanée du système numérique et de la notion de transition électrochimique permet d'interpréter et de répertorier pour une même famille de composés réactionnels, la morphologie des courbes de dosages polarovoltriques dans la région du point équivalent.

Nous montrons, dans ce qui suit, une application de cette théorie aux dosages acides–bases en milieu organique (dosages de diacides organiques dans le N,N-diméthylformamide (DMF)), et aux dosages de bases organiques dans différents types de solvants.

APPLICATION DE LA NOTATION SYMBOLIQUE ET DU SYSTEME NUMERIQUE A LA DESCRIPTION DES COURBES DE DOSAGES POLAROVOLTRIQUES

Dosages de diacides organiques en solution dans le N,N-diméthylformamide

Nous avons décrit précédemment avec l'exemple de l'acide maléique[8] l'origine électrochimique des deux transitions ou sauts de tension, observés au cours d'un dosage par une base organique.

Elles correspondent à une transition cathodique positive $\Delta E_{C,\mathrm{Pt}}^{\mathrm{H^+\rightarrow M'}}$, et à une transition anodique négative $\Delta E_{A,\mathrm{Pt}}^{\mathrm{M\rightarrow OH^-}}$.

La première rend compte de la disparition des ions H^+ en solution par suite de la réaction de neutralisation, la deuxième est liée à l'apparition d'un excès de OH^- ou de MeO^- correspondant soit à l'hydroxyde de tétrabutylammonium, soit au méthylate de sodium.

Suivant les forces relatives des deux acidités il est alors possible de prévoir pour quelles valeurs de Z se produiront les différentes transitions, ce qui conduit à envisager formellement six possibilités distinctes auxquelles il est possible d'assigner des types de courbes précis (Figs. 5 et 6).

(*a*) *Deux acidités très faibles, non dissociées et ne réagissant pas sur la base titrante.* La transition anodique $\Delta E_{A,\mathrm{Pt}}^{\mathrm{M\rightarrow OH^-}}$ apparaît dès $Z=\varepsilon$. La courbe de dosage est du type [0] [0], le dosage est impossible.

(*b*) *Deux acidités faibles et équivalentes, neutralisées par la base titrante.* La transition $\Delta E_{C,\mathrm{Pt}}^{\mathrm{H^+\rightarrow M'}}$ est faible ou inexistante, et peut avoir lieu pour $Z=1-\varepsilon$, la transition anodique se produisant pour $Z=1+\varepsilon$. Les courbes correspondantes seront du type [0] [$\frac{3}{4}$,1,0] ou [0] [1,0].

(*c*) *Première acidité forte, deuxième acidité très faible, non neutralisée par la base titrante.* La transition cathodique $\Delta E_{C,\mathrm{Pt}}^{\mathrm{H^+\rightarrow M'}}$ se produit pour $Z=0.5-\varepsilon$ en même temps qu'un excès de réactif apparaît pour $Z>0.5$, en donnant la transition $\Delta E_{A,\mathrm{Pt}}^{\mathrm{M\rightarrow OH^-}}$. Cette dernière variation de tension peut d'ailleurs être très faible si la base réagit partiellement sur la deuxième acidité. Les courbes de dosages correspondent aux types [0,1,0] [0] ou [0,1,$\frac{3}{4}$] [0].

(*d*) *Première acidité forte, deuxième acidité faible neutralisée par la base titrante.* La transition cathodique a toujours lieu, pour $Z=0.5-\varepsilon$. Le réactif neutralise la

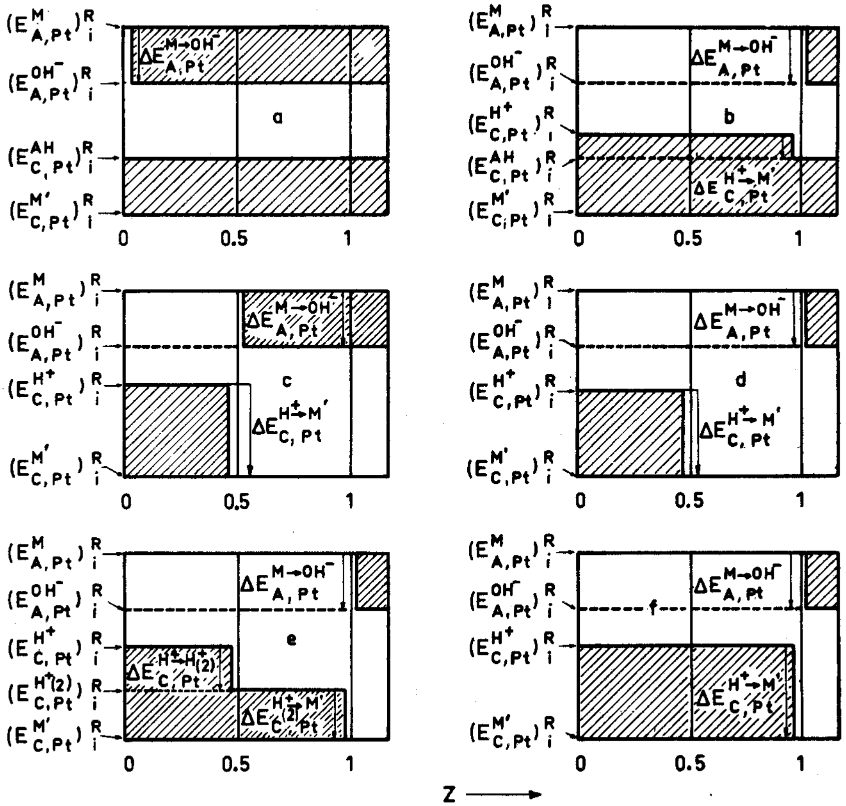

Fig. 5. Diagrammes *Z–E* schématiques correspondant aux dosages de diacides organiques par une base en milieu anhydre. (*a*) deux acidités très faibles, courbe [0] [0]; (*b*) deux acidités faibles, équivalentes, neutralisées par la base titrante, courbe [0] [$\frac{3}{4}$,1,0] ou [0] [1,0]; (*c*) première acidité forte, deuxième acidité ne réagit pas sur la base titrante, courbe [0,1,$\frac{3}{4}$] [0] ou [0,1,$\frac{1}{2}$] [0]; (*d*) première acidité forte, deuxième acidité non dissociée réagit sur la base, courbe type [0,1] [1,0]; (*e*) première et deuxième acidités fortes et différentiées, courbes [0,1] [$\frac{1}{4}$,1,0]; [0,1] [$\frac{1}{2}$,1,0]; [0,1] [$\frac{3}{4}$, 1,0]; (*f*) deux acidités fortes et équivalentes, courbes [0] [0,1,0]; [0] [$\frac{1}{2}$,1,0], et [0] [0,1,$\frac{1}{2}$].

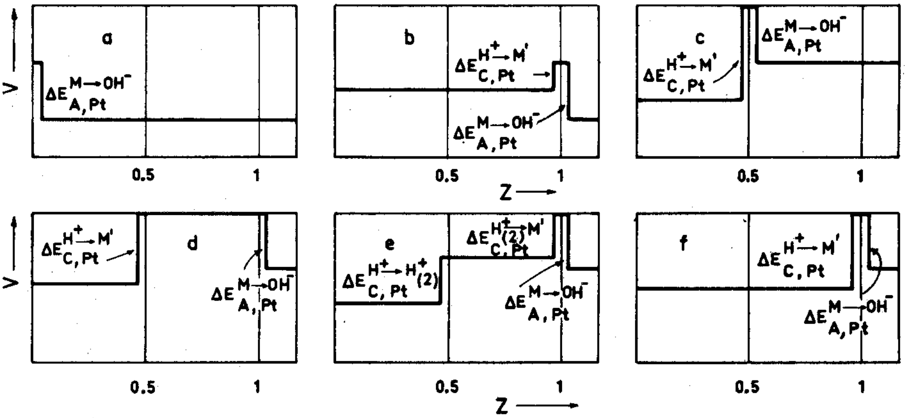

Fig. 6. Schémas types de dosages de diacides. Courbes déduites des diagrammes *Z–E* de la Fig. 5. (a) [0] [0]; (b) [0] [$\frac{3}{4}$,1,0]; (c) [0,1,$\frac{1}{2}$] [0]; (d) [0,1] [1,0]; (e) [0,1] [$\frac{1}{4}$,1,0]; (f) [0] [0,1,$\frac{1}{4}$].

deuxième acidité, cependant trop faiblement dissociée pour qu'apparaisse une transition cathodique nouvelle. L'excès de réactif pour $Z>1$, donne la transition anodique $\Delta E_{A,\mathrm{Pt}}^{\mathrm{M}\to\mathrm{OH}^-}$. Les courbes de dosages sont du type [0,1] [1,0].

(*e*) *Deux acidités fortes et différenciées* ($H^+_{(1)}$ *et* $H^+_{(2)}$). Dans ce cas, deux transitions cathodiques $\Delta E_{C,\mathrm{Pt}}^{\mathrm{H}^+_{(1)}\to\mathrm{H}_{(2)}}$ et $\Delta E_{C,\mathrm{Pt}}^{\mathrm{H}^+_{(2)}\to\mathrm{M}'}$ pourront se produire respectivement pour $Z=0.5-\varepsilon$ et $Z=1-\varepsilon$, la transition anodique continuant d'apparaître pour $Z=1+\varepsilon$. Les courbes de dosages sont intermédiaires entre les types [0,1] [0,1,0] et [0,1] [$\frac{3}{4}$,1,0].

(*f*) *Deux acidités fortes et non différenciées.* Avec cette dernière éventualitè, la transition $\Delta E_{C,\mathrm{Pt}}^{\mathrm{H}^+\to\mathrm{M}'}$ se produit pour $Z=1-\varepsilon$ suivie immédiatement par la transition anodique $\Delta E_{A,\mathrm{Pt}}^{\mathrm{M}\to\mathrm{OH}^-}$ pour $Z=1+\varepsilon$. Les courbes de dosages correspondent aux types [0] [0,1.0], [0] [0,1,$\frac{1}{4}$] ou [0] [$\frac{1}{4}$,1,0].

En résumé nous devrions donc nous attendre à observer 5 types de courbes de dosages, en considérant que le premier cas correspond à une impossibilité, du fait de la trop faible acidité du composé envisagé.

C'est effectivement ce qui est montré expérimentalement avec les diacides choisis: malonique, succinique, adipique, maléique, fumarique et *o*-phtalique[9]. On remarquera cependant, que les courbes du type (*e*) ne sont obtenues que lorsque les deux électrodes dissymétriques ont les polarités indiquées sur le Tableau II (cathode fixe de grande surface et micro-électrode tournante anode). Ainsi avec l'acide maléique en présence de $\mathrm{NaClO_4}$, et dans le cas du réactif MeONa, on passe de la courbe $\frac{1}{2}$[0,1] [$\frac{3}{4}$,1,0] du Tableau II à la courbe [0,1] [1,0] obtenue dans le cas où l'électrode tournante est cathode[8].

TABLEAU II

COURBES DE DOSAGES POLAROVOLTRIQUES DE DIACIDES ORGANIQUES

(Electrode tournante anode, cathode fixe de grande surface[9]; les variations de tension positives telles que (0,1), ($\frac{1}{2}$,1), ($\frac{3}{4}$,1) correspondent à la transition $\Delta E_{C,\mathrm{Pt}}^{\mathrm{H}^+\to\mathrm{M}'}$, et les variations négatives (1,0), (1,$\frac{3}{4}$) à la transition $\Delta E_{A,\mathrm{Pt}}^{\mathrm{M}\to\mathrm{OH}^-}$)

Réactif	*TBA OH*		*MeO Na*	
Milieu	*DMF*	*DMF + NaClO₄*	*DMF*	*DMF + NaClO₄*
Malonique	[0,1,$\frac{3}{4}$] [0]	$\frac{1}{2}$[0,1] [1,0]	[0] [$\frac{3}{4}$,1,0]	[0,1] [1,0]
Succinique	[0,1] [1,0]	[0] [1,0]	[0] [1,0]	[0] [$\frac{3}{4}$,1,0]
Adipique	[0] [1,0]	[0] [1,0]	[0] [$\frac{3}{4}$,1,0]	[0] [1,0]
o-Phtalique	[($\frac{1}{4}$),0,1,$\frac{3}{4}$] [0][a]	$\frac{1}{4}$[0,1] [1,0]	$\frac{1}{2}$[0,1] [$\frac{3}{4}$,1,0]	$\frac{1}{4}$[0,1] [1,0]
Maléïque	[($\frac{1}{4}$),0,1,$\frac{3}{4}$] [0][a]	[($\frac{1}{4}$),0,1] [1,0][a]	[($\frac{1}{4}$),0,1] [$\frac{3}{4}$,1,0][a]	$\frac{1}{2}$[0,1] [$\frac{3}{4}$,1,0]
Fumarique	$\frac{1}{2}$[0,1] [1,0]	[0] [$\frac{1}{2}$,1,0]	[0] [1,0]	[0] [$\frac{1}{2}$,1,0]

[a] La variation de tension notée (($\frac{1}{4}$),0) (classification numérique généralisée) ne doit pas être considérée comme une transition normale mais comme une variation secondaire résultant soit d'une modification de l'état de surface de l'électrode, soit d'une variation de conductivité du milieu chimique (voir référence[2]).

Ceci indique que la transition $\Delta E_{C,\mathrm{Pt}}^{\mathrm{H}^+_{(2)}\to\mathrm{M}'}$, correspondant à la variation de tension ($\frac{3}{4}$,1), se produit en fait pour une très faible dissociation de la 2ème acidité, caractéristique du groupe (*d*) des diacides.

Par ailleurs, pour un même composé, plusieurs types de courbes peuvent être obtenus, correspondant soit au choix du réactif titrant (MeONa ou TBAOH), soit à des modifications du milieu chimique (présence ou non de $NaClO_4$ dans le solvant).

La morphologie relative aux différents diacides est résumée sur le Tableau II. Pour toutes les courbes indiquées, *les variations de tension positives telles que* (0,1), ($\frac{1}{2}$, 1)... *sont attribuables à des transitions cathodiques* $\Delta E_{C,Pt}^{H^+\to M'}$, *alors que les variations de tension négatives, telles que* (1,0) *sont caractéristiques de la transition* $\Delta E_{A,Pt}^{M\to OH^-}$.

Certaines des transitions cependant ne correspondent pas toujours à une valeur quantitative de la réaction de dosage, ce qui explique que l'on ne trouvera pas la même correspondance entre ce Tableau qui résume les différents types de courbes, et celui précédemment publié[9], où nous avions indiqué seulement quelles étaient les acidités pouvant être dosées avec précision.

Dosages de bases organiques à l'aide d'un acide fort

Les dosages de bases organiques au moyen d'un acide fort, peuvent être réalisés en milieu neutre ou en milieu acide suivant la réaction type $B+H^+ \to BH^+$ ou $B+AH \to BH\text{-}A$.

Lorsque le solvant choisi est aprotique et neutre (Fig. 7a), on observe deux

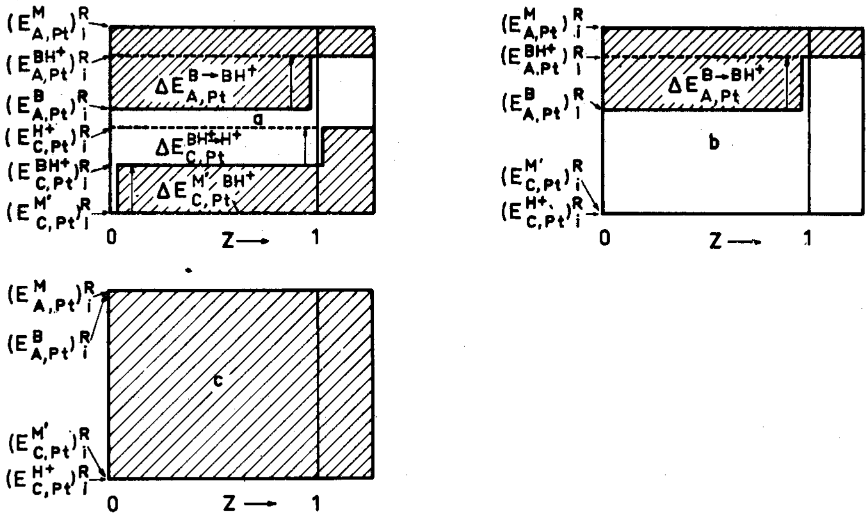

Fig. 7. Diagrammes schématiques *Z–E* correspondant aux dosages de bases organiques par un acide fort en milieu anhydre. (a) solvant aprotique; (b) solvant acide, base électroactive; (c) solvant acide, base non électroactive.

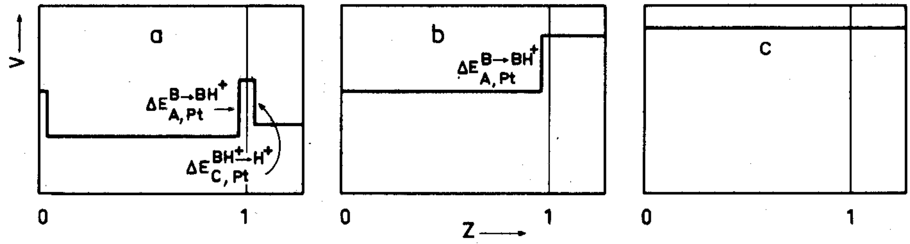

Fig. 8. Schémas types de dosages polarovoltriques de bases organiques. Courbes déduites des diagrammes *Z–E* de la Fig. 7. (a) [0,1,0]; (b) [0,1]; (c) [0].

transitions au voisinage de $Z=1$. La première, $\Delta E_{A,\mathrm{Pt}}^{\mathrm{B}\to\mathrm{BH}^+}$, anodique et positive, se produit pour $Z=1-\varepsilon$, la deuxième, $\Delta E_{C,\mathrm{Pt}}^{\mathrm{BH}^+\to\mathrm{H}^+}$, cathodique et négative, est liée à l'apparition d'un excès de réactif acide pour $Z=1+\varepsilon$. La courbe de dosage correspondante est alors du type [0,1,0] (Fig. 8a).

Avec un solvant aprotique et acide (Fig. 7b), seule la transition anodique $\Delta E_{A,\mathrm{Pt}}^{\mathrm{B}\to\mathrm{BH}^+}$ est conservée, la transition cathodique disparaît par suite de la présence initiale de protons provenant de la dissociation du solvant. Toutes les courbes de dosages sont du type [0,1] (Fig. 8b), et cette variation de tension est due uniquement à l'anode, comme nous avons pu l'observer pour les dosages de certaines amines aromatiques en solution dans l'acide acétique[7].

Enfin, dans le cas où l'amine n'est pas électroactive, (Fig. 7c), la courbe de dosage obtenue est du type [0] (Fig. 8c), et le dosage direct n'est pas possible (cas des amines aliphatiques).

Pour cette famille de composés, il est alors nécessaire d'ajouter un indicateur électrochimique à la solution d'amine aliphatique afin de faire apparaître une transition d'électrode. En particulier le perchlorate de N,N-diéthylanilinium, qui donne lieu à un déplacement de diéthylaniline dans la solution par l'intermédiaire de la réaction équilibrée:

$$\mathrm{B+DEA\ H^+ClO_4^- \to BH^+ClO_4^- + DEA}$$

(B = amine aliphatique, DEA = diéthylaniline)

donne lieu à la transition anodique $\Delta E_{A,\mathrm{Pt}}^{\mathrm{DEA}\to\mathrm{DEA\,H^+ClO_4^-}}$ pour $Z=1-\varepsilon$, ce qui transforme la courbe de dosage initiale [0] en courbe du type [0,1].

En conclusion, nous voyons d'après ces deux types d'exemples qui viennent d'être développés, que l'utilisation de ces définitions nouvelles permet une simplification notable du langage nécessaire à la description et à l'interprétation des courbes de dosages.

A chaque variation de tension, répérée par une combinaison de deux nombres est associée une transition électrochimique précise. Ceci permet de répertorier de façon simple les différents types de courbes (*Z–V*), en même temps que l'interprétation des courbes de dosages appartenant à une même famille de composés devient possible, sans qu'il soit nécessaire d'effectuer une étude complète des diagrammes *Z–E* pour chaque cas particulier.

RÉSUMÉ

L'interprétation des courbes de dosages est simplifiée par la notion de transition électrochimique d'électrode, à laquelle on associe les symboles $\Delta E_{A,e}^{J\to L}$ (transition anodique) et $\Delta E_{C,e}^{J'\to L'}$ (transition cathodique). Ces transitions sont déduites de diagrammes schématiques *Z–E*, et représentent respectivement dans le cas de l'anode (*A*) ou de la cathode (*C*), la variation de tension à l'électrode résultant du passage des réseaux de courbes courant–tension de *J* à *L* ou de *J'* à *L'*. En tenant compte par ailleurs d'un système descriptif numérique, où toute variation de tension est représentée en signe et en grandeur relative par une combinaison de deux nombres, et où la morphologie primaire des courbes de dosages, (région correspondant à un point de neutralisation) est décrite à l'aide de formules numériques simples correspondant à des modèles de courbes, il devient alors possible de répertorier sous forme symbolique et numérique l'interprétation des courbes de dosages et leur morphologie.

Les corrélations permises à l'intérieur d'une même famille de composés sont facilitées par l'utilisation de ce nouveau langage.

Des exemples d'application sont donnés dans le cas de dosages de diacides organiques en milieu N,N-diméthylformamide.

SUMMARY

The interpretation of titration curves is simplified by the concept of electrochemical electrode transitions with which are associated the symbols $\Delta E_{A,e}^{J\to L}$ for the anode, and $\Delta E_{C,e}^{J'\to L'}$ for the cathode. These transitions are derived from the Z–E plots, and represent the variation in potential at the electrode in passing from the family of curves J to the family of curves L in the case of the anode, or in passing from the family of curves J' to the family of curves L' in the case of the cathode. In addition, by using a numerical description of the electrode transitions where the variation in potential is represented by a sign and a relative magnitude given by the combination of two numbers and where the form of the curve at the equivalence point is described by simple formulae corresponding to reference curves, it is possible to classify the form of titration curves and their interpretation. The possible correlations among the members of a given family of compounds are simplified by the use of this new language. Examples are given in the case of the titration of dibasic organic acids in N,N-dimethylformamide.

ZUSAMMENFASSUNG

Titrationskurven können vereinfacht dargestellt und erklärt werden durch Einführung einer "elektrochemischen Übergangselektrode", zu dem die Symbole $\Delta E_{A,e}^{J\to L}$ (Anodenübergang) und $\Delta E_{C,e}^{J'\to L'}$ (Kathodenübergang) gehören. Diese Übergänge können schematischen Diagrammen Z–E entnommen werden. Diese Symbole beschreiben für die Anode (A) bzw. die Kathode (C) die Spannungsänderung der Electrode e, die ihren Ursprung in der Änderung von J nach L bzw. J' nach L' der Strom–Spannungs-Kurven hat. Die Schematisierung der Titrationskurven erlaubt es, die Spannungsänderungen durch relative Grössen welche sich durch Kombination zweier Zahlenwerte ergeben, zu kennzeichnen. Das Gebiet um den Neutralisationspunkt, kann durch einfache numerische Formeln dargestellt werden. Dadurch wird es möglich, Titrationskurven in einer symbolischen und numerischen Form auszudrücken und sie in ein Schema einzuordnen. Diese neue Beziehungen gestatten es, Zusammenhänge innerhalb einer Familie von Verbindungen leichter zu darzustellen. Für zweibasische organischen Säuren in N,N-Dimethylformamid werden Beispiele gegeben.

BIBLIOGRAPHIE

1 J. E. Dubois et P. C. Lacaze, *Anal. Chim. Acta*, 33 (1965) 403.
2 P. C. Lacaze et J. E. Dubois, *Bull. Soc. Chim. France*, (1967) 1702.
3 J. E. Dubois, P. C. Lacaze et A. Marie de Ficquelmont, *Compt. Rend.*, 262 (1966) 181, 249.

4 J. P. BILLON, *J. Electroanal. Chem.*, 1 (1959–1960) 486.
5 G. CAUQUIS ET D. SERVE, *Bull. Soc. Chim. France*, (1966) 302.
6 J. PERICHON, *Thèse*, Paris, 1967.
7 J. E. DUBOIS ET P. C. LACAZE, à paraître.
8 J. E. DUBOIS ET P. C. LACAZE, *Anal. Chim. Acta*, 33 (1965) 503.
9 J. E. DUBOIS ET P. C. LACAZE, *Anal. Chim. Acta*, 33 (1965) 602.

Analytica Chimica Acta
Elsevier Publishing Company, Amsterdam
Printed in The Netherlands

DETERMINATION OF EXTRACTION CONSTANTS OF METAL DIETHYLDITHIOCARBAMATES

JIŘÍ STARÝ AND KAREL KRATZER
Department of Nuclear Chemistry, Faculty of Technics and Physics, Praha 1, Břehová 7 (Czechoslovakia)

(Received May 3rd, 1967)

Cupral (the sodium salt of diethyldithiocarbamic acid) is one of the best known organic reagents which form extractable chelates with many metals. Although many qualitative data of the extraction of metal diethyldithiocarbamates have been published[1,2], no information on the extraction constants is available. The low stability of diethyldithiocarbamic acid and the high values of the extraction constants make the determination of these constants rather difficult.

In the work described below the extraction of 14 metal diethyldithiocarbamates into carbon tetrachloride was investigated in order to find their extraction constants and two-phase stability constants. These values can be used for prediction of optimum conditions for separation of various metals and for the substoichiometric determination of traces of metals.

THEORY

The solvent extraction of metals by a solution of diethyldithiocarbamic acid (HA) in carbon tetrachloride can be in general described by the following equation:

$$M^{N+} + N\,(HA)_{org} = (MA_N)_{org} + N\,H^+ \qquad (1)$$

with the equilibrium constant K (extraction constant)

$$K = [MA_N]_{org}[H^+]^N/[M^{N+}]\,[HA]_{org}^N \qquad (2)$$

In this work the following methods for determination of extraction constants were used.

The first method consisted of determining the distribution of the metal in question between two phases at various pH values and equilibrium concentrations of HA in the organic phase. In the case when metal is present in the aqueous phase exclusively as the metal ion (the formation of hydroxocomplexes or other complexes can be neglected) the extraction constant can be easily calculated from equation:

$$K = q_0[H^+]^N/[HA]_{org}^N \qquad (3)$$

where q_0 is the distribution ratio of the metal. This method can be used only for the case when the extraction constant is not very high and q_0 can be determined with sufficient precision.

If a suitable masking agent H_nB which forms with the metal in question a nonextractable chelate MB_s, is used, it is possible to determine even very high extraction constants according to the equation:

$$K = q\,(1 + \beta_s[B^{n-}]^s)\,[H^+]^N/[HA]_{org}^N \tag{4}$$

where q is the distribution ratio of the metal in the presence of the masking agent, and β_s is the stability constant of the metal complex MB_s.

When metal diethyldithiocarbamates are extracted above pH 8, practically all the diethyldithiocarbamic acid is transferred to the aqueous phase[1,2] as the anion and it is not possible to determine the equilibrium concentration of HA in the organic phase. For this special case the extraction constant can be calculated from

$$K = q\,(1 + \beta_s[B^{n-}]^s)\,K_{HA}^N/c_{HA}^N P_{HA}^N \tag{5}$$

where $K_{HA} = [H^+]\,[A^-]/[HA]$, $P_{HA} = [HA]_{org}/[HA]$, and c_{HA} is the total concentration of HA in the aqueous phase present as anion A^-.

The value $K_{HA}\cdot P_{HA}^{-1}$ for diethyldithiocarbamic acid can be easily determined from its distribution ratio p_{HA} at various pH from the following equation[1,2]:

$$K_{HA}/P_{HA} = [H^+]/p_{HA} \tag{6}$$

The other methods for the determination of extraction constants are based on the investigation of the exchange reaction between the metal ion M^{N+} in the aqueous phase and the diethyldithiocarbamate of another metal $M'A_{N'}$ according to the equation:

$$N\,(M'A_{N'})_{org} + N'\,M^{N+} = N'\,(MA_N)_{org} + N\,M'^{N'+} \tag{7}$$

The equilibrium constant of this reaction

$$[MA_N]_{org}^{N'}\,[M'^{N'+}]^N/[M'A_{N'}]_{org}^N\,[M^{N+}]^{N'} = K^{N'}/K'^N \tag{8}$$

and

$$K = \frac{[MA_N]_{org}}{[M^{N+}]}\left(\frac{[M'^{N+'}]}{[M'A_{N'}]_{org}}\,K'\right)^{N/N'} = q_0\left(\frac{K'}{q_0'}\right)^{N/N'} \tag{9}$$

where q_0 and q_0' are the distribution ratios of metals M and M′ respectively

From eqn. (9) it follows that from the distribution ratios q_0 and q_0', it is possible to determine the extraction constant K if the second extraction constant K' is known.

In the presence of a masking agent which forms with the metals in question the non-extractable complexes MB_s and $M'B_{s'}$, eqn. (9) becomes more complicated:

$$K = q/1 + \beta_s[B^{n-}]^s\,(K'(1 + \beta_{s'}[B^{n-}]^{s'})/q'\,)^{N/N'} \tag{10}$$

where q and q' are the distribution ratios of metals M and M′ respectively, in the presence of masking agent H_nB.

For the case when more than 99% of the reagent HA liberated from the complex $M'A_{N'}$ is consumed to form the complex MA_N, then

$$N'\,[M'^{N'+}] = N\,[MA_N]_{org} \tag{11}$$

Equation (11) is valid when

$$N\,[MA_N]_{org} \geqslant 100\,([HA]_{org} + [A^-]) \tag{12}$$

From eqn. (2) and with the definitions of K_{HA} and P_{HA} given for eqn. (5), the concentration of free metal ion M^{N+} can be given by:

$$[M^{N+}] \geqslant (100/N\,K)\,(K'/q')^{N-1/N'}\,([H^+] + K_{HA}/p_{HA}) \tag{13}$$

When eqn. (13) is fulfilled, then the calculation of the extraction constant K can be done simply after determining the distribution ratio of one metal, for the distribution ratio of the second metal can be calculated from the original concentrations of the two metals.

Two-phase stability constant of metal diethyldithiocarbamates can be calculated from the extraction constant and from the value $P_{HA}.K_{HA}^{-1}$ of diethyldithiocarbamic acid according to the equation:

$$\beta_{N,\mathrm{org}} = [\mathrm{MA}_N]_{\mathrm{org}}/[\mathrm{M}^{N+}][\mathrm{A}^-]^N = K(P_{HA}/K_{HA})^N \qquad (14)$$

EXPERIMENTAL

Apparatus

pH-meter pHK-1 with glass electrode; Zeiss (Jena) Universal spectrophotometer; mechanical shaker; scintillation counter with well-type NaI(Tl) crystal; Geiger-Müller end-window counter.

Reagents

All the reagents used were of A.R. purity. Carbon tetrachloride was purified by distillation. The radioisotopes used were of radiochemical purity.

Diethyldithiocarbamic acid in carbon tetrachloride was prepared freshly before each set of experiments as follows: an aqueous solution of sodium diethyldithiocarbamate was shaken with an equal volume of carbon tetrachloride. During shaking, perchloric acid was added stepwise until pH 1–2 was reached. The organic phase was separated, filtered and stored in a dark bottle. The equilibrium concentration of diethyldithiocarbamic acid was spectrophotometrically determined as copper diethyldithiocarbamate at 436 nm after shaking the organic phase with an equal volume of 0.1 M copper chloride solution for 5 min.

Distribution of diethyldithiocarbamic acid between carbon tetrachloride and water

10 ml of acetate buffer (pH 6.0–6.5, $\mu = 0.1$) was shaken for 5 min with 10 ml of diethyldithiocarbamic acid in carbon tetrachloride. After measuring the pH value, the concentration of diethyldithiocarbamic acid in both phases was spectrophotometrically determined as copper diethyldithiocarbamate.

Distribution of metal diethyldithiocarbamates

Procedure I. A solution of diethyldithiocarbamic acid in carbon tetrachloride (20–50 ml) was shaken on a mechanical shaker with an equal volume of an aqueous phase containing the appropriate metal. The pH was adjusted by addition of sodium hydroxide and perchloric acid and sodium perchlorate was added to give a constant ionic strength of 0.10. After shaking for 5 min (this time was found to be sufficient for attaining the extraction equilibrium), the equilibrium concentration of diethyldithiocarbamic acid in the organic extract was spectrophotometrically determined as copper diethyldithiocarbamate. The distribution ratio of the metal in question was determined radiometrically and/or spectrophotometrically and the extraction constant was calculated according to eqn. (3).

All distribution experiments were carried out at 20°.

Procedure II. To the aqueous phase (20–50 ml), containing the appropriate metal and ethylenediaminetetraacetic acid as masking agent, sodium hydroxide and sodium perchlorate were added to obtain pH 12.0–12.5 and ionic strength $\mu = 0.1$. This solution was shaken on a mechanical shaker with an equal volume of diethyldithiocarbamic acid in carbon tetrachloride for some hours to reach the extraction equilibrium. Under these conditions all the diethyldithiocarbamic acid was transferred to the aqueous phase. The equilibrium concentration of the metal in the organic extract and the total concentration of diethyldithiocarbamic acid (c_{HA}) in the aqueous phase were spectrophotometrically determined as copper diethyldithiocarbamate. The equilibrium concentration of metal in the aqueous phase was determined as follows: to 5.0 ml of the aqueous phase were added an excess of sodium diethyldithiocarbamate and enough perchloric acid to give pH *ca.* 1. The metal diethyldithiocarbamate formed was quantitatively extracted into 5.0 ml of carbon tetrachloride. This prepared extract was washed with three portions (5 ml) of aqueous ammonia (*ca.* pH 10) to remove all free diethyldithiocarbamic acid from the organic phase. The concentration of the metal diethyldithiocarbamate remaining was determined spectrophotometrically as copper diethyldithiocarbamate.

Above pH 12, all ethylenediaminetetraacetic acid (H_4Y) is present in the aqueous phase as the anion Y^{4-}; however, a correction for formation of NaY^{3-} must be taken into account.

The extraction constant was calculated from the results obtained according to eqn. (5).

Procedure III. To 10 ml of metal salt solution of known concentration, sodium perchlorate and perchloric acid were added to give the ionic strength $\mu = 0.1$. The prepared solution was shaken for some hours with an equal volume of the other metal diethyldithiocarbamate in carbon tetrachloride which did not contain any free diethyldithiocarbamic acid. From the distribution ratio of one or both metals determined radiometrically and/or spectrophotometrically, the extraction constant was calculated from eqn. (9). If a masking agent was present in the aqueous phase eqn. (10) was used.

RESULTS AND DISCUSSION

Diethyldithiocarbamic acid

From the distribution ratio of diethyldithiocarbamic acid at various pH values, the value ($pK_{HA} + \log P_{HA}$) was determined according to eqn. (6). The mean value from 8 experiments ($pK_{HA} + \log P_{HA}) = 6.21 \pm 0.03$ is in excellent agreement with BODE's data[3].

Manganese

BODE[4] found that manganese can be extracted only in the absence of reducing agents. However, some preliminary experiments showed that even in the presence of hydrazine, manganese can be extracted as a violet complex with maximum absorbancy at 505 nm. The composition of the extractable complex was therefore determined first.

A solution of diethyldithiocarbamic acid in carbon tetrachloride was shaken with an excess of manganese chloride solution at pH *ca.* 7. The manganese diethyldithiocarbamate thus prepared contained no free diethyldithiocarbamic acid. The concentration of manganese in this complex was determined spectrophotometrically at 505 nm and the concentration of diethyldithiocarbamate anion was determined as the copper complex at 426 nm. From these experiments it was found that manganese is extracted as MnA_2.

The distribution of manganese (traced with ^{52}Mn) was studied by Procedure I. The mean value of the extraction constant was $\log K = -4.42 \pm 0.14$.

Iron

BODE[5] has shown that iron(II) and iron(III) are extracted as diethyldithiocarbamate in the same pH region; from BODE's work it can be concluded that in both cases only one type of extractable complex is formed. This assumption was verified by comparing the spectrum and composition of iron diethyldithiocarbamate formed from iron(II) and (III); in both cases only the FeA_2 complex was extracted.

The distribution of iron at pH 1.3–2.2 was studied spectrophotometrically at 600 nm (Procedure I). The mean value of the extraction constant was found to be $\log K = 1.20 \pm 0.14$. This value was verified by investigation of the exchange reaction

$$^{65}ZnA_{2,\mathrm{org}} + Fe^{2+} \rightleftharpoons FeA_{2,\mathrm{org}} + {}^{65}Zn^{2+}$$

as in Procedure III. At pH 4, the condition given by eqn. (13) was fulfilled and from the distribution of radiozinc between the two phases (equilibrium was reached in 1–2 h) the extraction constant $\log K = 1.28 \pm 0.13$ was calculated by means of eqn. (9) ($\log K' = 2.96$).

Cobalt

On basis of the distribution of radiocobalt (^{60}Co) at pH 2.0–2.6 (Procedure I) it was found that cobalt is extracted as CoA_2 with the extraction constant $\log K = 2.33 \pm 0.06$. Since BODE[1,4] assumed that cobalt is extracted as CoA_3, the exchange reaction between zinc-65 diethyldithiocarbamate in carbon tetrachloride and cobalt(II) chloride solution was investigated (Procedure III). From the results obtained it can be concluded that cobalt is primarily extracted as CoA_2 which is slowly transformed into the much more stable complex CoA_3.

Nickel

The extraction constant of nickel diethyldithiocarbamate was determined from investigation of the exchange reaction (Procedure III):

$$NiA_{2,\mathrm{org}} + Pb^{2+} \rightleftharpoons PbA_{2,\mathrm{org}} + Ni^{2+}.$$

The time of equilibration at pH *ca.* 3 was 15 h. The original and equilibrium concentration of NiA_2 in carbon tetrachloride was determined spectrophotometrically at 393 nm. From the values obtained the extraction constant $\log K = 11.58 \pm 0.16$ was calculated from eqn. (9) ($\log K' = 7.77$; eqn. (13) was fulfilled).

Palladium

In the case of palladium the exchange reaction

$$PdA_{2,\mathrm{org}} + {}^{204}Hg^{2+} \rightleftharpoons {}^{204}HgA_{2,\mathrm{org}} + Pd^{2+}$$

was investigated (Procedure III). The aqueous phase was 0.1 N hydrochloric acid; in this medium mercury forms a more stable chlorocomplex ($\log \beta_4 = 16.2$)[6] than palladium ($\log \beta_4 = 13.2$)[6]. From the results obtained it can only be concluded that the extraction constant of palladium is higher than that of mercury.

Copper

The distribution of copper in the presence of ethylenediaminetetraacetic acid (0.001–0.1 *M*) was studied spectrophotometrically at 436 nm (Procedure II). The time of equilibration was 0.5–4.0 h. The extraction constant, $\log K = 13.70 \pm 0.11$, was calculated from eqn. (5) ($\log \beta_1 = 18.9$; $pK_{HA} + \log P_{HA} = 6.21$).
The two-phase stability constant $\log \beta_{2,org} = 26.5–26.9$ determined by STILL[7] for chloroform is in agreement with the value $\log \beta_{2,org} = 26.12$ for carbon tetrachloride calculated from eqn. (14).

Silver

For the determination of the extraction constant sodium iodide, which forms a non-extractable complex, AgI_4^{3-}, with silver was used as a masking agent. The distribution of radiosilver (^{110m}Ag) at pH 1.0–1.5 was investigated (Procedure I). The time of equilibration was 1–2 h. The extraction constant $\log K = 11.90 \pm 0.13$ calculated from eqn. (4) ($\log \beta_4 = 14.2$) is in good agreement with the value $\log K = 11.52$ determined by metal chelate exchange reactions in the organic phase[8].

Zinc

The extraction constant of zinc diethyldithiocarbamate was determined by Procedure I with ^{65}Zn as a tracer. The mean value $\log K = 2.96 \pm 0.03$ agrees with the value $\log K = 2.54$ determined previously[8].

Cadmium

The distribution of cadmium in the presence of ethylenediaminetetraacetic acid ($\log \beta_1 = 16.46$)[6] was investigated by Procedure II. The time of shaking was 1.5–4 h. The mean value found, $\log K = 5.41 \pm 0.06$, is in very good agreement with the value $\log K = 5.13$ established previously[9].

Mercury

For determination of the extraction constant of mercury sodium iodide, which forms the non-extractable complex HgI_4^{2-} ($\log \beta_4 = 30.4$), was used as masking agent. The distribution of mercury was traced with ^{204}Hg at pH 1.0–1.5 (Procedure I); the time of equilibration was 0.15–2.0 h. The mean value found, $\log K = 31.94 \pm 0.11$ (eqn. (4)), was verified by investigation of the exchange reaction

$$CuA_{2,org} + {}^{204}Hg^{2+} \rightleftharpoons {}^{204}HgA_{2,org} + Cu^{2+}$$

in the presence of sodium iodide. From the results obtained the extraction constant was calculated from eqn. (10) to be $\log K = 32.33 \pm 0.03$. The value of this constant calculated from the exchange between mercury diethyldithiocarbamate and dithizone in carbon tetrachloride was rather lower ($\log K = 29.1$)[9].

Indium

The distribution of indium (^{114m}In tracer) in the presence of oxalic acid (log

$\beta_3 = 14.7$)[2] was studied by Procedure I; the time of shaking was 20–60 min. The value of the extraction constant log $K = 10.34 \pm 0.16$ calculated from eqn. (4) is in sufficient agreement with the value 9.59 found previously[9].

Thallium

The extraction of thallium(I) by (1–3) · 10^{-3} M diethyldithiocarbamic acid in carbon tetrachloride was studied with ^{204}Tl as tracer. From the distribution ratio at pH 3.4–4.4, a mean value for log $K = -0.53 \pm 0.02$ was calculated (log $K = 0.0$)[9].

Lead

From the distribution of lead in the presence of ethylenediaminetetraacetic acid (log $\beta_1 = 18.3$), the extraction constant log $K = 7.77 \pm 0.08$ was determined by Procedure III. This value differs from log $K = 5.74$ determined by exchange reactions of metal chelates in carbon tetrachloride[9].

Bismuth

The exchange reaction

$$^{210}\mathrm{BiA}_{3,\mathrm{org}} + 3\,\mathrm{Pb}^{2+} \rightleftharpoons 3\,\mathrm{PbA}_{2,\mathrm{org}} + 2\,{}^{210}\mathrm{Bi}^{3+}$$

formed the basis for the determination of the extraction constant of bismuth diethyldithiocarbamate. At pH *ca.* 1 and with 15 h of shaking, the bismuth complex was partially destroyed (*i.e.*, eqn. (13) was not fulfilled); for this reason, the distribution ratio of bismuth as well as of lead must be measured (radiometrically and spectrophotometrically). The mean value of the extraction constant found, log $K = 16.79 \pm 0.13$ (eqn. (9)), agrees very well with the value log $K = 16.48$ found previously[9].

CONCLUSIONS

In Table I, the extraction constants K and two-phase stability constants $\beta_{N,\mathrm{org}}$ are summarized. For comparison, the K values, determined by exchange

TABLE I

EXTRACTION DATA OF METAL DIETHYLDITHIOCARBAMATES

Metal ion	*Procedure*	*log K*	*1/N log K*	*log $\beta_{N,org}$*	*log K*[9]
Ag^+	II	11.90 ± 0.13	11.90	18.11	11.52
Bi^{3+}	III	16.79 ± 0.13	5.60	35.42	16.48
Cd^{2+}	II	5.41 ± 0.06	2.70	17.83	5.13
Co^{2+}	I	2.33 ± 0.06	1.16	14.75	—
Cu^{2+}	II	13.70 ± 0.11	6.85	26.12	
Fe^{2+}	I	1.20 ± 0.14	0.60	13.42	14.1
	III	1.28 ± 0.13	0.64	13.50	
Hg^{2+}	II	31.94 ± 0.11	15.97	44.36	29.10
	III	32.33 ± 0.03	16.16	44.75	
In^{3+}	II	10.34 ± 0.16	3.45	28.97	9.59
Mn^{2+}	I	-4.42 ± 0.14	-2.21	8 00	
Ni^{2+}	III	11.58 ± 0.16	5.79	24.00	
Pb^{2+}	II	7.77 ± 0.08	3.88	20.19	5.74
Pd^{2+}	III	>32	>16		
Tl^+	I	-0.53 ± 0.02	-0.53	5.68	0.0
Zn^{2+}	I	2.96 ± 0.03	1.48	15.38	2.54

reactions between metal diethyldithiocarbamates and dithizone in carbon tetrachloride[9], are included. It can be seen that in most cases (with the exceptions of lead and mercury) quite good agreement was reached.

The values of log $\beta_{N,\mathrm{org}}$ in carbon tetrachloride can be compared with the values log $\beta_{N,\mathrm{org}}$ in chloroform determined by STILL[7] for copper (26.5–26.9), lead (19.2–21.5), cadmium (16.9–18.8), zinc (16.1–16.5) and silver (19.3).

From the $1/N$ log K values it follows (see Table I) that the extractability of metal diethyldithiocarbamates decreases in the following order: Pd^{2+}, Hg^{2+}, Ag^{+}, Cu^{2+}, Ni^{2+}, Bi^{3+}, Pb^{2+}, In^{3+}, Cd^{2+}, Zn^{2+}, Co^{2+}, Fe^{2+}, Tl^{+} and Mn^{2+}. This order of extractability is very similar to that given by ECKERT[10].

SUMMARY

The extraction of metal diethyldithiocarbamates (Mn, Fe, Co, Ni, Pd, Cu, Ag, Zn, Cd, Hg, In, Tl, Pb and Bi) into carbon tetrachloride was investigated in order to establish the extraction constants and two-phase stability constants. The order of extractability of these chelates was determined.

RÉSUMÉ

On a examiné l'extraction de diéthyldithiocarbamates métalliques (Mn, Fe, Co, Ni, Pd, Cu, Ag, Zn, Cd, Hg, In, Tl, Pb et Bi) dans le tétrachlorure de carbone, afin d'établir les constantes d'extraction et les constantes de stabilité des 2 phases. On a déterminé l'ordre d'extratibilité de ces chélates.

ZUSAMMENFASSUNG

Die Extraktion von Metall-Diäthyldithiocarbamaten (Mn, Fe, Co, Ni, Pd, Cu, Ag, Zn, Cd, Hg, In, Tl, Pb und Bi) mit Tetrachlorkohlenstoff wurde untersucht, um ihre Extraktionskonstanten und Zweiphasen-Stabilitätskonstanten aufzustellen. Die Grössenordnung der Extrahierbarkeit dieser Chelate wurde bestimmt.

REFERENCES

1 H. BODE, *Z. Anal. Chem.*, 144 (1955) 165.
2 J. STARÝ, *The Solvent Extraction of Metal Chelates*, Pergamon Press, Oxford, 1964.
3 H. BODE, *Z. Anal. Chem.*, 142 (1954) 414.
4 H. BODE, *Z. Anal. Chem.*, 143 (1954) 182.
5 H. BODE, *Z. Anal. Chem.*, 172 (1960) 1.
6 J. BJERRUM, G. SCHWARZENBACH AND L. G. SILLÉN, *Stability Constants*, Part I, II, The Chemical Society, London, 1957.
7 E. STILL, *Finska Kemistsamfundets Medd.*, 73 (1964) 90.
8 J. RŮŽIČKA AND J. STARÝ, *Talanta*, in press.
9 J. STARÝ AND J. RŮŽIČKA, *Talanta*, in press.
0 E. ECKERT, *Z. Anal. Chem.*, 155 (1957) 23.

Analytica Chimica Acta
Elsevier Publishing Company, Amsterdam
Printed in The Netherlands

FRACTIONAL SUBLIMATION OF THE β-DIKETONE CHELATES OF THE LANTHANIDE AND RELATED ELEMENTS

EUGENE W. BERG AND J. JAIME CHIANG ACOSTA[*]
Coates Chemical Laboratories, Louisiana State University, Baton Rouge, La. 70803 (U.S.A.)
(Received April 26th, 1967)

STANIFORTH[1] reported in 1943 that some of the rare earth β-diketone chelates were non-volatile but the studies in recent years on the volatile character of various normal and transition metal β-diketone chelates suggested that there should be some observable volatility among the lanthanide β-diketone chelates. The volatilities of numerous β-diketone metal chelates have been reported[2–6] and the development of a fractional vacuum sublimator that effectively separated numerous multicomponent mixtures of various normal and transition metal β-diketone chelates has been described[7–9]. Simultaneously with the studies of BERG *et al.*[2–9], numerous workers (principally SIEVERS *et al.*)[10–24] were investigating the gas chromatography of metal β-diketone chelates.

In view of the success of the above-mentioned studies, the present authors

TABLE I

β-DIKETONES USED IN THIS STUDY

Trivial name and structural formula	*Systematic name*	*Adopted symbol*
Acetylacetone 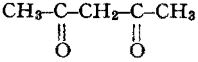 $CH_3\text{-}\underset{\underset{O}{\|}}{C}\text{-}CH_2\text{-}\underset{\underset{O}{\|}}{C}\text{-}CH_3$	2,4-Pentanedione	AA
Trifluoroacetylacetone 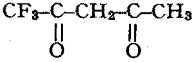 $CF_3\text{-}\underset{\underset{O}{\|}}{C}\text{-}CH_2\text{-}\underset{\underset{O}{\|}}{C}\text{-}CH_3$	1,1,1-Trifluoro- 2,4-pentanedione	TFAA
Hexafluoroacetylacetone 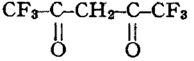 $CF_3\text{-}\underset{\underset{O}{\|}}{C}\text{-}CH_2\text{-}\underset{\underset{O}{\|}}{C}\text{-}CF_3$	1,1,1,5,5,5-Hexafluoro- 2,4-pentanedione	HFAA
Dipivaloylmethane 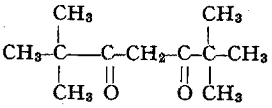 $CH_3\text{-}\overset{CH_3}{\underset{CH_3}{C}}\text{—}\underset{\underset{O}{\|}}{C}\text{-}CH_2\text{-}\underset{\underset{O}{\|}}{C}\text{-}\overset{CH_3}{\underset{CH_3}{C}}\text{-}CH_3$	2,2,6,6-Tetramethyl- 3,5-heptanedione	DPM

---

[*] Present address: Department of Chemistry, Universidad Technica Federico Santa Maria, Valparaiso, Chile.

decided to reinvestigate the volatile character of the β-diketone chelates of the lanthanides and a few closely related elements. The following ligands were chosen for study: acetylacetone, trifluoroacetylacetone, hexafluoroacetylacetone and dipivaloylmethane. The structural formula, trivial and systematic name of each of these ligands is given in Table I along with the symbol chosen to represent that ligand throughout this paper. The plan of study was to prepare and characterize the various β-diketone chelates of the lanthanides and related elements and establish whether they were sufficiently stable and volatile to be sublimed at low temperatures. If volatile chelates were found, then analytical separations were to be attempted or proposed based upon the fractional vacuum sublimation technique first proposed by BERG AND HARTLAGE[8]. Inasmuch as previous studies had suggested that chelate stability and volatility increased with an increase in the degree of fluorination of the ligand *and* an increase in the spherical nature of the chelate, it was anticipated that the most volatile and stable chelates would be formed with hexafluoroacetylacetone and dipivaloylmethane. The present study confirms this contention.

After much work had been done on the lanthanides in this laboratory, EISENTRAUT AND SIEVERS[25] reported the gas chromatographic separation of several lanthanide dipivaloylmethane chelates, thus confirming the soundness of the program of study. Work in this laboratory[26] had clearly demonstrated the volatility of numerous rare earth chelates prior to the publication of SIEVERS' work.

Although considerable work has been reported in the literature on the acetylacetonates of the Group IIIB and related elements, no systematic study of their volatility has been reported. Volatility data on the trifluoroacetylacetonates[1,27], hexafluoroacetylacetonates[28–30] and the dipivaloylmethanates[25] of the lanthanides are scarce. Furthermore, many discrepancies appear in the literature relating to melting points, degree of hydration and volatilities of these compounds which need to be clarified by a more thorough characterization of the chelates.

It is hoped that the study reported here will extend the knowledge of the lanthanide and related elements and suggest possible new approaches for separating mixtures of these elements.

EXPERIMENTAL

Reagents

Acetylacetone was distilled before use. The commercial trifluoroacetylacetone and hexafluoroacetylacetone (Peninsular Chem. Research, Inc.) and dipivaloylmethane (Pierce Chem. Co.) were used without further purification. All the lanthanide salts and metals (K and K Laboratories) had a stated purity of 99.9% or better. Scandium, yttrium, thorium and uranium salts were reagent grade.

Preparation of the various metal β-diketone chelates

Each of the chelates prepared was characterized by a carbon–hydrogen analysis, infrared spectrum and thermogravimetric analysis to verify or confirm the reported structure.

Acetylacetonates. The lanthanide acetylacetonates, were prepared by the method of STITES *et al.*[31]. The lanthanide chloride was dissolved in water and the solution pH was adjusted to a value of approximately 5.0. An aqueous solution of ammonium acetylacetonate was added to the lanthanide solution with constant stirring, while the pH of the reacting mixture was maintained at a value just below that of the pH of precipitation of the corresponding rare earth hydroxide[29]. The mixture was stirred for 12 h to insure the conversion of any basic acetylacetonate to the normal compound. The crystalline precipitate which was a trihydrate, was filtered and air-dried. Then the monohydrated chelate was prepared[32] by leaving the trihydrated form for 4 h in a desiccator over magnesium perchlorate.

Tetrakis(acetylacetonato)uranium(IV) was prepared by the method suggested by GRDENIĆ AND KOVPAR-COLIC[33]. The dark green crystalline compound melted at 177–178° (lit. 175–176°)[34] and was oxidized very easily in a normal atmosphere to the dioxouranium(VI) derivative with its characteristic yellow color.

Dioxouranium(VI) acetylacetonate was prepared as described by BILTZ AND CLINCH[35]. The orange crystalline product was recrystallized from methanol, and melted at 220–222° in a sealed capillary tube (lit. 225–250°)[34].

Tris(acetylacetonato)scandium(III) and tris(acetylacetonato)yttrium(III) were prepared by the method of STITES *et al.*[31]. The white crystalline compounds melted at 189–190° and 141–142° (in a sealed capillary tube) respectively.

Tetrakis(acetylacetonato)thorium(IV) was obtained from K and K Laboratories and purified by sublimation.

The physical properties of the various acetylacetonates prepared are summarized in Table II.

TABLE II

PHYSICAL PROPERTIES OF THE ACETYLACETONATE CHELATES

Compound	*Color*	*m.p. found (°)*	*m.p. literature (ref.) (°)*	*Probable state of hydration*
$La(AA)_3$	White	150–152	135–185[32]	Trihydrate
$Ce(AA)_3$	Yellow	148–150	131–147[32]	Trihydrate
$Sm(AA)_3$	White	143–145	143–147[32]	Trihydrate
$Er(AA)_3$	Pink	126–128	125–132[32]	Trihydrate
$Th(AA)_4$	White	172	172	
$U(AA)_4$	Dark green	177–178	175–176[34]	Anhydrous
$UO_2(AA)_2$	Orange	220–222	225–250[34]	Anhydrous
$Sc(AA)_3$	White	189–190		Anhydrous
$Y(AA)_3$	White	141–142		Trihydrate

Trifluoroacetylacetonates. All these chelates were prepared by the method suggested by YOUNG[36]. An aqueous solution of the ammonium salt of the trifluoroacetylacetone was added to the aqueous solution of lanthanide chloride. The mixture of the two solutions should be neutral to litmus. The trifluoroacetylacetonate chelate precipitated and was filtered. The precipitate was washed with water, air-dried and finally recrystallized from benzene as the dihydrate, except for the uranyl derivative which was recrystallized from methanol.

All these chelates were remarkably soluble in methanol. No sharp melting points were observed for the trifluoroacetylacetonate complexes. Upon heating, the solid slowly softened, and finally melted completely. This last temperature was taken as the melting point. The physical properties of the prepared trifluoroacetylacetonates are summarized in Table III.

TABLE III

PHYSICAL PROPERTIES OF THE PREPARED TRIFLUOROACETYLACETONE CHELATES

Compound	*Color*	*m.p. found (°)*	*m.p. literature (ref.) (°)*	*Probable state of hydration*
La(TFAA)$_3$	White	142–144	169[37]	Dihydrate
Ce(TFAA)$_3$	Dark-brown	127–129	130–131[37]	Dihydrate
Pr(TFAA)$_3$	Light-green	136–138	133–134[37]	Dihydrate
Nd(TFAA)$_3$	Lavender	147–149	133–134[37]	Dihydrate
Sm(TFAA)$_3$	Cream-white	147–149	—	Dihydrate
Eu(TFAA)$_3$	White	144–146	132–134[37]	Dihydrate
Gd(TFAA)$_3$	White	145–147	133–135[37]	Dihydrate
Tb(TFAA)$_3$	White Yellow Fluorescence	154–156	—	Dihydrate
Dy(TFAA)$_3$	White	152–154	—	Dihydrate
Ho(TFAA)$_3$	Cream-white	154–156	—	Dihydrate
Er(TFAA)$_3$	Pink	148–150	—	Dihydrate
Tm(TFAA)$_3$	White	156–158	—	Dihydrate
Yb(TFAA)$_3$	White	140–142	—	Dihydrate
Lu(TFAA)$_3$	White	188–190	—	Dihydrate
Sc(TFAA)$_3$	White	124–126	106–107[37]	Trihydrate
Y(TFAA)$_3$	White	146–148	132[37]	Anhydrous
Th(TFAA)$_4$	White	149–151	—	Anhydrous
UO$_2$(TFAA)$_2$	Yellow	210 dec.[a]	—	Monohydrate

[a] With evolution of gas.

Hexafluoroacetylacetonates. All the hexafluoroacetylacetonates were prepared by the method of Halverson *et al.*[28].

An aqueous solution of the lanthanide or related element chloride was shaken with a diethyl ether solution of ammonium hexafluoroacetylacetonate. The metal ion reacted with the ligand, and the chelate was extracted into the ether phase. The ether solution of the chelate was dried with sodium sulfate, and then the ether was evaporated. In this way, a solid chelate was obtained which was purified by recrystallization from a mixture of water-methanol (9:1). The hexafluoroacetylacetonates of lanthanum, cerium, praseodymium, holmium, erbium, and lutetium were purified by vacuum sublimation in a cold-finger type vacuum sublimator at a temperature of 180° and 0.05 mm mercury pressure.

Some anhydrous chelates were prepared by drying the hydrated compounds over phosphorus pentoxide at a pressure of 0.02 mm mercury for 72 h. The anhydrous chelates are normally darker than the hydrated ones and show a remarkable tendency toward hydration in the ambient atmosphere. On standing for only a short time in the atmosphere, they absorb moisture from the air and become once again the hydrated chelates.

A summary of the physical properties of the prepared hexafluoroacetylacetonates is shown in Table IV.

Dipivaloylmethanates. The dipivaloylmethanates were prepared as suggested by Eisentraut and Sievers[25]. A solution of the lanthanide or related element chloride in 1:1 ethanol–water was thoroughly mixed with an alcoholic solution of the sodium

TABLE IV

PHYSICAL PROPERTIES OF THE HEXAFLUOROACETYLACETONE CHELATES

Compound	*Color*	*m.p. found (°)*	*m.p. literature (ref.) (°)*	*Suggested degree of hydration*
$La(HFAA)_3$	White	143–146	—	Not certain
$Ce(HFAA)_3$	Yellow	125–126	—	Not certain
$Pr(HFAA)_3$	Light-green	148–151	—	Not certain
$Nd(HFAA)_3$	Lavender	141–142	117[38]	Not certain
$Sm(HFAA)_3$	Cream-white	144–145	—	Not certain
$Eu(HFAA)_3$	Light-yellow	176–177	125[39]	Not certain
$Gd(HFAA)_3$	White	170–173	—	Not certain
$Tb(HFAA)_3$	White Yellow Fluorescence	170–172	—	Not certain
$Dy(HFAA)_3$	Cream-white	185–188	—	Not certain
$Ho(HFAA)_3$	Cream-white	214–215	—	Not certain
$Er(HFAA)_3$	Pink	194–198	—	Not certain
$Tm(HFAA)_3$	White	194–196	—	Not certain
$Yb(HFAA)_3$	White	177–178	—	Not certain
$Lu(HFAA)_3$	White	222–223	—	Not certain
$Sc(HFAA)_3$	White	116–117[a]	—	Anhydrous
$Y(HFAA)_3$	White	142–144	—	Anhydrous
$Th(HFAA)_4$	White	122–123[a]	121–122[38]	Anhydrous

[a] Sharp melting point.

TABLE V

PHYSICAL PROPERTIES OF THE DIPIVALOYLMETHANE CHELATES[a]

Compound	*Color*	*m.p. Found (°)*	*m.p. literature (ref.) (°)*	*Probable state of hydration*
$La(DPM)_4$	White	239–245	238–248[25] 148–149[40]	Anhydrous
$Ce(DPM)_4$	Ruby red	276–278		Anhydrous
$Pr(DPM)_3$	Light green	222–224	222–224[25]	Anhydrous
$Nd(DPM)_3$	Lavender	218–219	215–218[25]	Anhydrous
$Sm(DPM)_3$	White	200–201	195.5–198.5[25] 143–144[40]	Anhydrous
$Eu(DPM)_3$	Yellow	190–191	187–189[25]	Anhydrous
$Gd(DPM)_3$	White	183–184	183–184[25]	Anhydrous
$Tb(DPM)_3$	White (yellow fluorescence)	150–152	177–180[25]	Anhydrous
$Dy(DPM)_3$	White	182–183	182–183[25]	Anhydrous
$Ho(DPM)_3$	Cream	178–180	180–182.5[25] 154–155[40]	Anhydrous
$Er(DPM)_3$	Pink	179–180	179–180[25] 153–154[40]	Anhydrous
$Tm(DPM)_3$	White	170–173	170–173[25]	Anhydrous
$Yb(DPM)_3$	White	165–167	166–169[25]	Anhydrous
$Lu(DPM)_3$	White	173–174	173–174[25]	Anhydrous
$Sc(DPM)_3$	Cream	154–156	152–155[25]	Anhydrous
$Y(DPM)_3$	White	145–155	169–172.5[25]	Anhydrous
$Th(DPM)_4$	White	308–310		Anhydrous
$Zr(DPM)_4$	Orange	330–332		Anhydrous

[a] All the dipivaloylmethanates were purified by vacuum sublimation at 0.1 mm mercury pressure at temperatures ranging from 144–200° and then recrystallized from *n*-hexane.

salt of dipivaloylmethane. The chelate precipitated immediately in the form of a well formed solid. This solid was filtered, washed and air-dried. The dried crystals were purified by sublimation in a cold-finger type vacuum sublimator at 0.1 mm mercury pressure and finally recrystallized from hexane. The sublimation temperatures varied from 144 to 200°. A summary of the physical properties of the prepared dipivaloylmethanates is given in Table V.

Fractional sublimation apparatus and procedure

A schematic diagram of, and specifications for, the fractional sublimator used in this work were reported earlier[8,9]. Briefly, the apparatus consists of a 1-m (11 mm O.D.) pyrex tube with a continuous temperature gradient maintained along its length and evacuated to 1 mm of mercury pressure with a carrier gas flowing from the high temperature to the low temperature end of the sublimator. Dry, deoxygenated nitrogen was used as the carrier. Dry commercial nitrogen was deoxygenated by bubbling the gas through a dilute sulfuric acid solution of vanadium(II) sulfate in the presence of amalgamated zinc[41].

TABLE VI

SUBLIMATION RECRYSTALLIZATION TEMPERATURE ZONES FOR VARIOUS METAL β-DIKETONE CHELATES

Metal	*Chelate ligand*				
	AA	*TFA*	*HFAA*	*HFAA*[a]	*DPM*[b]
La	Slightly volatile	123–93	116–82	96–88	132–92
Ce	nv	65–49	114–60	—	118–88
Pr		125–97	102–50	112–88	124–90
Nd		127–94	114–72	112–92	120–91
Sm	nv	134–97	130–50	—	116–66
Eu		126–92	104–60	124–88	116–65
Gd		118–94	94–50	110–88	138–66
Tb		132–100	97–60	110–88	97–61
Dy		118–76	80–46	122–88	94–57
Ho		123–104	92–50	122–86	92–50
Er	nv	nv	78–40	115–88	93–53
Tm		nv	88–60	121–88	86–49
Yb		nv	92–74	121–88	87–48
Lu		nv	80–46	115–86	92–50
Sc(III)	77–52	52–30	47–40	103–65	74–49
Y(III)	nv	nv	80–40	125–95	92–46
Th(IV)	134–82	74–50	55–44	103–48	120–88
U(IV)	129–92	nv			
UO_2^{2+}	146–114	139–56			
Zr(IV)					110–62

Sample size: 5–6 mg. Pressure: 1 mm mercury ([a] Pressure: 1 atm.; gas flow rate 4 ml/min). Temperature gradient: 50–150° ([b] Temperature gradient: 60–190°). Sublimation time: 2 h. Carrier gas: deoxygenated nitrogen. nv: non-volatile.

The sample of pure chelate (or mixture of chelates) was placed in a small glass boat and inserted into the high temperature end of the sublimator and carrier gas passed over the sample for 2h. The chelates recrystallized on the walls of the pyrex tube in discrete and reproducible temperature zones. The sublimation recrystallization temperature zones observed for the various chelates are reported in Table VI and Figs. 1–4. In cases where the recrystallization zone was divided into distinct areas, the greater concentration of chelate is shown as a thicker line.

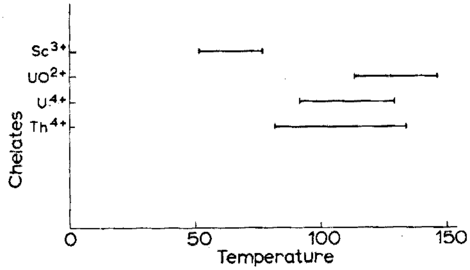

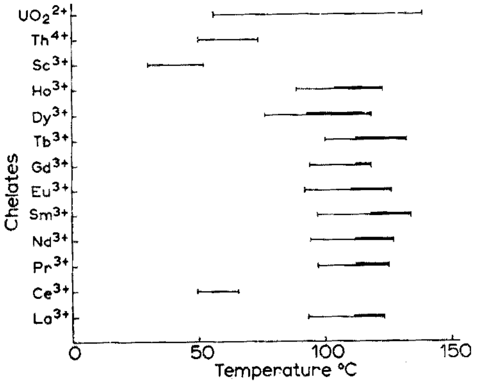

Fig. 1. Sublimation recrystallization temperatures for some acetylacetone chelates.

Fig. 2. Sublimation recrystallization temperatures for some trifluoroacetylacetone chelates.

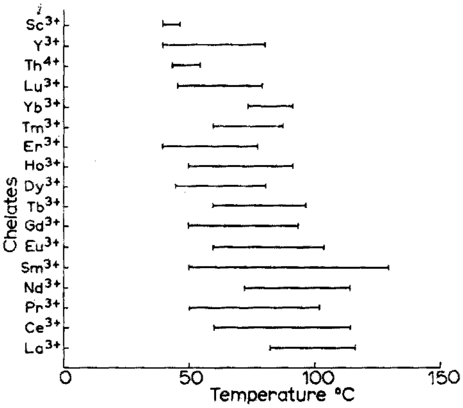

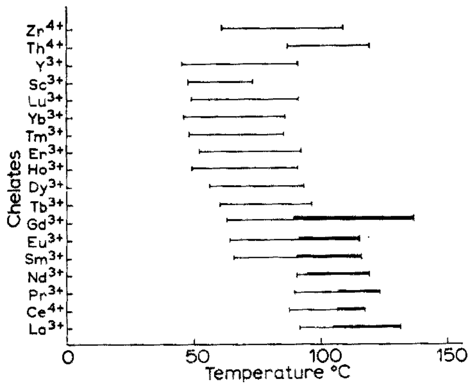

Fig. 3. Sublimation recrystallization temperatures for some hexafluoroacetylacetone chelates.

Fig. 4. Sublimation recrystallization temperatures for some dipivaloylmethane chelates.

DISCUSSION AND CONCLUSIONS

Acetylacetonates

It was found that the lanthanide and yttrium acetylacetonates do not sublime. Initially, this was considered surprising because it was well known that many of the normal and transition elements of both higher and lower atomic number than the lanthanides formed stable and volatile acetylacetonates. The lack of volatility of the lanthanide acetylacetonates is explained on the basis that the hydrates are too polar to sublime and that the corresponding anhydrous derivatives (which might be expected to sublime) are not formed under the conditions encountered in the vacuum sublimator.

The lanthanide acetylacetonates are prepared with no difficulty in the trihydrated form. The water of hydration is bound quite strongly, and efforts to obtain the anhydrous derivatives were unsuccessful. In fact, every attempt to form even the monohydrated derivatives by drying the trihydrated chelates, resulted in the formation of a basic compound. Apparently, when these hydrated chelates are heated in a normal atmosphere or in a vacuum, two processes occur simultaneously. First, the chelates undergo thermal decomposition with the loss of water and acetylacetone which results in the formation of basic compounds. Second, the basic compounds polymerize immediately to form polynuclear species which are not volatile. This same behavior has been observed by others[29,32,42].

Among the 4 lanthanide acetylacetonates studied extensively, only the lanthanum chelate was observed to sublime, and the quantity that sublimed was too small to be analytically significant. However, if the anhydrous lanthanide acetylacetonates could be formed they would probably exhibit a high degree of volatility.

The situation was completely different for the acetylacetonates of scandium(III), uranium(IV), thorium(IV) and dioxouranium(VI). Each of these chelates exhibited high volatility and thermal stability. Analyses indicated that each of these chelates were anhydrous.

Based upon the sublimation recrystallization temperature zones reported for these compounds in Fig. 1 and Table VI, it appears that scandium(III) could be separated without difficulty from thorium(IV), uranium(IV) and dioxouranium(VI) by the fractional vacuum sublimation of a mixture of the corresponding acetylacetonates.

It also is quite possible to separate scandium, uranium, and thorium from all of the lanthanides by taking advantage of the great difference in thermal stability between these two groups of elements. The scandium, uranium and thorium chelates are readily volatile whereas the lanthanides are thermally instable and non-volatile, so that they remain in the sample boat.

Trifluoroacetylacetonates

The lanthanide and yttrium trifluoroacetylacetonates exhibited a greater thermal stability than the corresponding acetylacetonates, and it was possible to determine sublimation recrystallization temperatures for some of these chelates. Unfortunately, thermal decomposition was so extensive among the trifluoroacetylacetonates as to eliminate any possibility of developing an effective separation of these chelates by fractional sublimation. Furthermore, for those chelates which were observed to sublime, their sublimation recrystallization temperatures were found in the temperature range of 76 to 134° (see Fig. 2 and Table VI). The only exception was the cerium chelate which recrystallized between 49° and 65°.

The same reasons given to explain the lack of volatility among the lanthanide acetylacetonates can be applied in the case of the trifluoroacetylacetonates.

The scandium and dioxouranium(VI) chelates showed a lower thermal stability than expected. Only thorium trifluoroacetylacetonate was completely volatile and had a good thermal stability. Thus, this group presents a case, where excellent separations can be achieved by utilizing differences in thermal stability rather than differences in volatility. For example, it should be possible to separate thorium quantitatively from all of the lanthanides, except cerium, and yttrium.

Hexafluoroacetylacetonates

As expected, these chelates exhibited high thermal stability and also a remarkable volatility, especially under vacuum conditions. When the sublimation recrystallization temperatures observed for these chelates are studied (see Fig. 3 and Table VI) it is apparent that mixtures of lanthanum and dysprosium; lanthanum and erbium; lanthanum and lutetium; and lanthanum and yttrium, can be successfully separated.

Also, it will be possible to separate scandium and thorium from all of the lanthanide hexafluoroacetylacetonates that recrystallize in the sublimator at temperatures higher than 48° and 56°, respectively. The only exceptions are the chelates of erbium and dysprosium which partially recrystallize at temperatures below 50°.

Although the thermal stability of the scandium hexafluoroacetylacetonate chelate is not appreciable, its sublimation recrystallization zone is short and separated from those of the lanthanide chelates, except erbium. Thus, one should be able to effect separations of scandium from the lanthanide hexafluoroacetylacetonates.

The very significant volatility shown by these compounds in the thermogravimetric analyses prompted a study of their fractional sublimation at atmospheric pressure. The sublimation recrystallization temperature zones observed for the lanthanide hexafluoroacetylacetonates at atmospheric pressure are listed in Table VI. Now, if these data are compared with the results obtained in vacuum, the following points become apparent.

(*a*) The recrystallization zones are shorter for the higher pressure. This is expected because under normal atmospheric pressure, the mean free path for the gaseous molecules is shorter, and in consequence there are more opportunities available to the molecules of the chelate to be directed toward the walls of the sublimation tube.

(*b*) The crystals are less numerous, bigger and better formed.

(*c*) All the sublimation recrystallization zones are located almost in the same temperature range.

This last fact is a clear indication that no fractional sublimation separations are possible under normal atmospheric pressure with the hexafluoroacetylacetonates although they are stable under these conditions.

Dipivaloylmethanates

All the dipivaloylmethane chelates investigated could be quantitatively sublimed and were thermally stable. A close scrutiny of the data in Table VI and Fig. 4 leads one to conclude that the lanthanide dipivaloylmethanates can be classified in two distinct groups. The least volatile group consists of the chelates from lanthanum through gadolinium. The more volatile group consists of the chelates from terbium through lutetium. Accordingly, it should be possible to separate the following mixtures:

La–Tm Pr–Tm Ce–Th Nd–Tm
La–Yb Pr–Yb Ce–Yb Nd–Yb

Lutetium should be separable from neodymium, praseodymium, cerium and lanthanum, but the experimental values for sublimation recrystallization temperatures suggest nonquantitative separations.

Scandium should be separable from lanthanum, cerium, praseodymium and neodymium; and finally, thorium should be separable from scandium, ytterbium and thulium.

Once again, yttrium behaves very similarly to the heavier lanthanides. This is not surprising because the identical oxidation state and similar ionic radii of the metal ions leads one to expect this kind of behavior.

An interesting phenomenon was found while checking the numerical values of the sublimation recrystallization temperatures of the hexafluoroacetylacetonates and dipivaloylmethanates of the lanthanide series. It was observed that the volatility of the chelates increased as the atomic weight (or molecular weight of the chelate) of the consecutive elements of the lanthanide series increased. This fact is shown in a graphical manner (see Fig. 5) in a plot of the atomic weight of the lanthanides *versus* the highest sublimation recrystallization temperature of the corresponding lanthanide chelate. The highest temperature of the recrystallization zone was taken as a relative measure of chelate volatility because the high temperature end of the zone was usually reproducible, sharp and easily defined. The variation of ionic radii with respect to atomic weight of the lanthanides is shown in this plot also. Granted certain irregularities, undoubtedly the general trend (shown in Fig. 5 by the curved line) indicates an increase in volatility with an increase in the atomic weight of the lanthanide. From Fig. 6, a plot of the highest recrystallization temperature as a function of

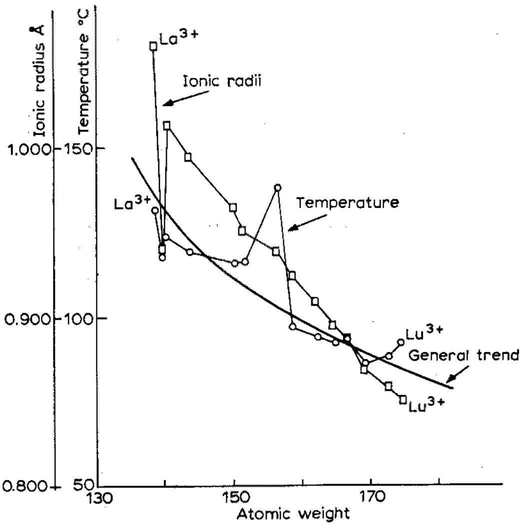

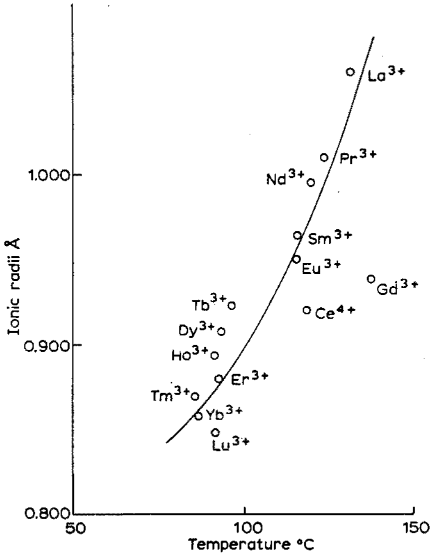

Fig. 5. Sublimation recrystallization temperature and ionic radius *versus* the atomic weight for the lanthanide dipivaloylmethanates.

Fig. 6. Sublimation recrystallization temperatures *versus* ionic radii for the lanthanide dipivaloylmethanates.

the ionic radius of the corresponding lanthanide, it is clear that the chelate volatility increases as the ionic radius of the metal decreases.

In spite of an increase in molecular weight the volatility of the chelates increases. This observation is contrary to what was expected, namely, that as the atomic weight of the lanthanide (or molecular weight of the chelate) increases, the volatility should decrease because the molecule will be heavier and less prone to enter the vapor phase. Such reasoning does not take into consideration the effects that the "lanthanide contraction" may have on molecular size and volatility. In fact, an increase in atomic weight of the lanthanide (or molecular weight of the chelate) will correspond to a decrease in chelate molecule size. Apparently the size of the chelate molecule is a more important factor in establishing chelate volatility than its molecular weight. Presumably, the smaller but heavier molecules can make the transition from the solid to the gaseous state more readily than the larger but lighter molecules. One can only speculate at the moment whether this difference in volatility is a function of chelate polarity or polarizability.

Some separations among the lanthanides have been performed by fractional vacuum sublimation to demonstrate the practicability of the technique. For example, equal amounts of $Tm(DPM)_3$ and $Nd(DPM)_3$ were thoroughly mixed and the mixture fractionally sublimed. The mixture was completely volatilized with no residue remaining in the sample boat and the individual chelates were recovered. Two sublimate zones, well separated, were observed at 118–88° and 84–48° which corresponded very closely to the previously observed sublimate zones for the pure Nd and Tm chelates, respectively. To confirm, at least qualitatively, that a good separation had been achieved, a sample of each sublimate zone was dissolved in hexane and its UV spectrum compared with that of the pure chelate. The spectra of the pure chelate and the corresponding sublimate fraction were identical with an absorption maximum exhibited at 274.3 nm and 282.6 nm for the $Nd(DPM)_3$ and $Tm(DPM)_3$, respectively. This separation and others effected are summarized in Table VII.

TABLE VII

SUMMARY OF FRACTIONAL SUBLIMATION SEPARATIONS CONFIRMED

Mixture	*Recrystallization temp. zones observed*	*% Recovery*
$Nd(DPM)_3$–$Tm(DPM)_3$	118–88°(Nd); 84–48°(Tm)	Quantitative
$Sc(DPM)_3$–$Pr(DPM)_3$	72–49°(Sc); 120–88°(Pr)	Quantitative
$La(DPM)_3$–$Yb(DPM)_3$	128–79°(La); 79–47°(Yb)	Quantitative—very slight overlap of zones
$Th(TFAA)_4$–$Gd(TFAA)_3$	70–47°(Th); 116–96°(Gd)[b]	Quantitative
$Th(HFAA)_4$–$La(HFAA)_3$[a]	52–42°(Th); 120–80°(La)	Quantitative

Sample size: 5 mg. Pressure: 1 mm mercury. Carrier gas: dry, deoxygenated nitrogen. Temperature gradient: 185–63° ([a] Temperature gradient: 154–56°). Sublimation time: 2 h.

[b] A great majority of the Gd remained in the sample boat because of the thermal instability and non-volatility of the $Gd(TFAA)_3$.

SUMMARY

Various β-diketone chelates of Sc(III), Y(III), Th(IV), U(IV), U(VI), Zr(IV) and the lanthanides have been prepared, characterized and investigated to determine if they were volatile and stable. The ligands employed were acetylacetone(AA), trifluoroacetylacetone(TFAA), hexafluoroacetylacetone(HFAA), and dipivaloylmethane(DPM). The chelates were sublimed in a fractional vacuum sublimator and the recrystallization temperature zones recorded for individual chelates. None of the lanthanide acetylacetonates are volatile but the Sc(III), Th(IV), U(IV) and dioxouranium(VI) acetylacetonates are thermally stable and quite volatile below 150° at 1 mm mercury pressure. The lanthanide, Sc(III), Y(III), and dioxouranium(VI) trifluoroacetylacetonates are volatile and can be vacuum-sublimed below 150°, but are thermally unstable; only the Th(IV) chelate is sufficiently stable to be quantitatively recovered by sublimation. The Sc(III), Y(III), Th(IV), and lanthanide hexafluoroacetylacetonates are thermally stable and easily sublimed below 125° *in vacuo* or at atmospheric pressure. All the dipivaloylmethanates studied were thermally stable and volatile and could be quantitatively recovered by vacuum sublimation below 140°.

The volatility of the HFAA and DPM lanthanide chelates increased with an increase in atomic weight (a decrease in ionic radii) of the lanthanides. The lack of volatility observed for the lanthanide AA and TFAA chelates is attributed to the fact that only hydrates of the chelates were formed, which decomposed at elevated temperatures *in vacuo* to form basic polymeric compounds,

Separations are proposed for numerous binary mixtures of the β-diketone chelates of the lanthanide and related elements. Recrystallization temperature zones are given for the following binary mixtures which were quantitatively resolved by the fractional sublimation technique: 118–88° for $Nd(DPM)_3$ and 84–48° for $Tm(DPM)_3$; 72–49° for Sc(DPM) and 120–88° for Pr(DPM); 128–79° for $La(DPM)_3$ and 79–47° for $Yb(DPM)_3$; 70–47° for $Th(TFAA)_4$ and 116–96° for $Gd(TFAA)_3$; 52–42° for $Th(HFAA)_4$ and 120–80° for $La(HFAA)_3$.

RÉSUMÉ

Divers chélates β-dicétone-Sc(III), Y(III), Th(IV), U(IV), U(VI), Zr(IV) et lanthanides ont été préparés, caractérisés et examinés pour déterminer leur volatilité et leur stabilité. Ligands utilisés: acétylacétone (AA), trifluoracétylacétone (TFAA), hexafluoracétylacétone (HFAA) et dipivaloylméthane (DPM). On propose des séparations de nombreux mélanges binaires des chélates β-dicétones des lanthanides et éléments parents.

ZUSAMMENFASSUNG

Verschiedene β-Diketon-Chelate von Sc(III), Y(IV), Th(IV), U(IV), U(VI), Zr(IV) und den Lanthaniden wurden hergestellt, charakterisiert und auf ihre Flüchtigkeit und Stabilität untersucht. Die verwendeten Liganden waren: Acetylaceton (AA), Trifluoroacetylaceton (TFAA), Hexafluoroacetylaceton (HFAA) und Dipivaloylmethan (DPM). Für zahlreiche binäre Mischungen von β-Diketon Chelaten werden Trennungen mit Hilfe der fraktionierten Sublimation vorgeschlagen.

REFERENCES

1 R. A. Staniforth, *Dissertation*, Ohio State University, 1943.
2 J. T. Truemper, *A Study of the Volatile Characteristics of Various Metal β-Diketone Chelate Compounds*, Ph. D. Dissertation, Louisiana State University, Baton Rouge, La., 1959.
3 E. W. Berg and J. T. Truemper, *J. Phys. Chem.*, 64 (1960) 487.
4 E. W. Berg and J. T. Truemper, *Anal. Chim. Acta*, 32 (1965) 245.
5 H. W. Dowling, *A Study of the Volatile Characteristics of Some Co(III) and Fe(II) β-Diketone Chelate Compounds*, M.S. Thesis, Louisiana State University, Baton Rouge, La., 1960.
6 E. W. Berg and H. W. Dowling, *J. Chem. Eng. Data*, 6 (1961) 556.
7 F. R. Hartlage, Jr., *Sublimation Separation Studies of Various Metal β-Diketone Chelate Compounds*, Ph. D. Dissertation, Louisiana State University, Baton Rouge, La., 1964.
8 E. W. Berg and F. R. Hartlage, Jr., *Anal. Chim. Acta*, 33 (1965) 173.
9 E. W. Berg and F. R. Hartlage, Jr., *Anal. Chim. Acta.*, 34 (1966) 46.
10 W. J. Biermann and H. Gesser, *Anal. Chem.*, 32 (1960) 1525.
11 R. E. Sievers, R. W. Moshier and M. L. Morris, *Inorg. Chem.*, 1 (1962) 966.
12 R. S. Juvet and R. P. Durbin, *J. Gas. Chromatog.*, 1 (1963) 14.
13 K. Yamakawa, K. Tanikawa and K. Arakawa, *Chem. Pharm. Bull. (Tokyo)*, 11 (1963) 1405.
14 T. Fujinaga, T. Kuwamoto and Y. Ono, *Bunseki Kagaku*, 12 (1963) 1199.
15 W. D. Ross, *Anal. Chem.*, 35 (1963) 1596.
16 W. D. Ross and G. Wheeler, Jr., *Anal. Chem.*, 36 (1964) 266.
17 J. E. Schwarberg, R. W. Moshier and J. H. Walsh, *Talanta*, 11 (1964) 1213.
18 D. K. Albert, *Anal. Chem.*, 36 (1964) 2034.
19 W. D. Ross, R. E. Sievers and G. Wheeler, Jr., *Anal. Chem.*, 37 (1965) 598.
20 T. Fujinaga, T. Kuwamoto and Y. Ono, *Nippon Kagaku Zasshi*, 86 (1965) 1294.
21 R. W. Moshier and R. E. Sievers, *Gas Chromatography of Metal Chelates*, Pergamon, New York, 1965.
22 R. W. Moshier and J. E. Schwarberg, *Talanta*, 13 (1966) 445.
23 T. Michino, Y. Ishihara, K. Saito and T. Nakazawa, *Bunseki Kagaku*, 15 (1966) 181.
24 G. Wheeler, Jr. and W. D. Ross, *Advan. Gas. Chromatog., Proc. Intern. Symp. 3rd, Houston, Texas, 1965*, published 1966, pp. 112–151.
25 K. J. Eisentraut and R. E. Sievers, *J. Am. Chem. Soc.*, 87 (1965) 5254.
26 J. J. Chiang A., *A Study on the Volatility of the β-Diketone Chelates of Group III B Elements*, Ph. D. Dissertation, Louisiana State University, Baton Rouge, La., 1967.
27 D. Purushotham, V. Ramachandra Rao and Bh. S. V. Raghava Rao, *Anal. Chim. Acta*, 33 (1965) 182.
28 F. Halverson, J. S. Brinen and J. R. Leto, *J. Chem. Phys.*, 40 (1964) 2790.
29 T. Moeller and H. E. Kremers, *Chem. Rev.*, 37 (1945) 114.
30 M. L. Bhaumik, *J. Inorg. & Nucl. Chem.*, 27 (1965) 261.
31 J. G. Stites, C. N. McCarty and L. L. Quill, *J. Am. Chem. Soc.*, 70 (1948) 3142.
32 G. W. Pope, J. F. Steinbach and W. F. Wagner, *J. Inorg. & Nucl. Chem.*, 20 (1961) 304.
33 D. Grdenić and B. Kovpar-Colic, *Inorg. Chem.*, 3 (1964) 1328.
34 H. I. Schlesinger, H. C. Brown, J. J. Katz, S. Archer and R. A. Lad, *J. Am. Chem. Soc.*, 75 (1953) 2446.
35 W. Biltz and J. A. Clinch, *Z. Anorg. Chem.*, 40 (1904) 221.
36 R. C. Young, in W. C. Fernelius, *Inorganic Synthesis*, Vol. 2, McGraw-Hill, New York, 1946.
37 J. K. Marsh, *J. Chem. Soc.*, Part 2 (1947) 1084.
38 K. Nakamoto, *Infrared Spectra of Inorganic and Coordination Compounds*, John Wiley and Sons, New York, 1963.
39 L. Sacconi and R. Ercoli, *Gazz. Chim. Ital.*, 731 (1949).
40 G. S. Hammond, D. C. Nonhebel and Chin-Hua, S. Wu, *Inorg. Chem.*, 2 (1963) 73.
41 L. Meites and T. Meites, *Anal. Chem.*, 20 (1948) 984.
42 W. F. Wagner, *Record Chem. Progr.*, 23 (1962) 155.

Analytica Chimica Acta
Elsevier Publishing Company, Amsterdam
Printed in The Netherlands

DETERMINATION OF ZIRCONIUM IN ZIRCONIUM-BEARING SANDS AND ZIRCONIUM CONCENTRATES BY A NONDISPERSIVE X-RAY FLUORESCENCE METHOD

B. HOŁYŃSKA AND L. LANGER
Institute of Nuclear Techniques, Academy of Mining and Metallurgy, Kraków (Poland)

(Received May 15th, 1967)

The chemical determination of zirconium in polymetallic silica matrices is difficult and lengthy, because of the necessary prior separations of interfering elements[1].

The analysis of sands is even more troublesome because the chemical composition of sands varies greatly and considerable amounts of iron and titanium are present as well as admixtures of calcium and rare-earth elements. The method presented below permits zirconium to be determined in the presence of varying amounts of iron and titanium.

ANALYSIS OF ZIRCONIUM-BEARING SANDS

Because of the presence of several metals in the test materials, a nondispersive X-ray fluorescence method was chosen. The characteristic X-ray K-series of zirconium was excited by a ^{109}Cd source emitting the characteristic KAg series of 22.6 keV. Such radiation, the energy of which is slightly above the absorption edge of zirconium (18.0 keV) gave a good excitation yield. The activity of the source amounted to *ca.* 30 or 100 μC depending on the particular procedure.

A simple standard apparatus was used, consisting of a H.V.-supply, a krypton-filled proportional counter with a resolution of about 18% at 6.4 keV, a pulse amplifier and scaler. A multichannel analyser was used in some measurements, but is not needed for routine work. The measurements were made in the normal compact geometry, *i.e.*, the source was placed on the counter window with the sample above this window[2]. The time of a single measurement was 1 min.

In the spectrum of sand samples, apart from peaks corresponding to the K-series of zirconium (15.7 keV), iron (6.4 keV) and the peak of scattered radiation (about 20.7 keV), several escape peaks are also present. Since the counting rate of pulses from zirconium for the applied source activity was sufficiently high, pulses in the range of escape peaks were eliminated by a suitable choice of discrimination level. This also allowed the characteristic radiation of iron and titanium to be cut off, so that the only radiation registered was due to the K-series of zirconium and the Compton-scattered primary radiation. The separation of these two radiation peaks was quite good, though not complete (Fig. 1).

Elimination of the matrix effect

In the determination of zirconium in sands, the matrix effect is due to varying contents of iron and titanium. The previous method[3] of eliminating this effect by measuring the transmitted radiation required the use of separate set-ups. In the present work, the matrix effect was eliminated by measuring the Compton-scattered primary radiation with the same apparatus. This type of procedure for dealing with matrix effects has been suggested by various authors[4,5], who have assumed that the ratio of fluorescence to scattered radiation is in a high degree independent of changes in the composition of the matrix. This assumption is in general not valid for large changes in the matrix; in such cases the ratio of fluorescence to scattered radiation does not permit an unambiguous determination of the element[6]. Figure 2 shows the dependence of the intensity ratio of fluorescence to scattered radiation on the zirconium content in sands for various concentrations of iron; no single calibration

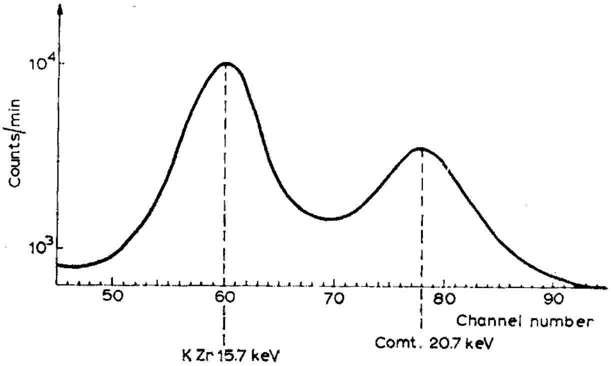

Fig. 1. X-Ray spectrum of a zirconium-bearing sand (zirconium content 1.8%).

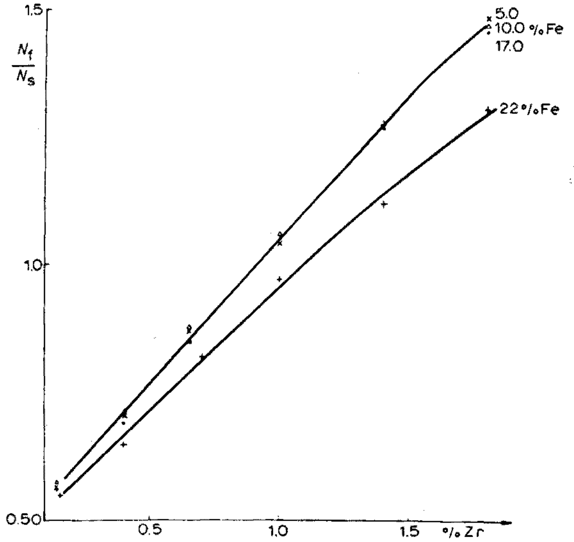

Fig. 2. Fluorescence to scattered radiation intensity ratio (N_f/N_s) for zirconium as a function of zirconium content in sands for different iron contents.

curve was valid over the whole concentration range, and the error in the determination of zirconium by such measurements could be as high as 20–30%. On the other hand, nomographic interpretation[7] of the data permitted zirconium to be determined independently even when there were large changes in the matrix composition.

The measurements made in order to establish the optimum conditions for zirconium determination were carried out with standard samples containing zirconium as $ZrSiO_4$, iron as Fe_3O_4, and silica; both zirconium and iron normally occur in natural sands in these forms. The zirconium and iron contents were in the ranges 0.15–2.0% and 5.0–22.0% respectively; such contents are typical for Polish zirconium-bearing sands. The standard samples did not contain titanium.

Determination of zirconium by the filter method

Two measurements were made: measurement of the intensity of the characteristic radiation of zirconium and measurement of the Compton-scattered primary radiation. Fluorescence radiation was selected with the help of a molybdenum filter (40 μ thick) which cut off the scattered radiation; the discrimination level was such that escape peaks were cut off. The scattered radiation was measured at another higher discrimination level in order to cut off the characteristic radiation of zirconium; an aluminum filter (1.0 mm thick) was used in order to improve the pre-

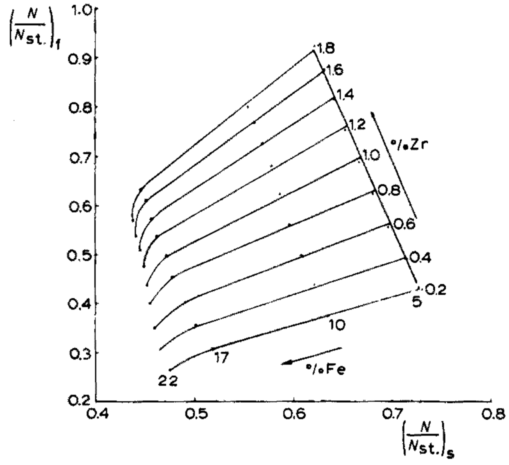

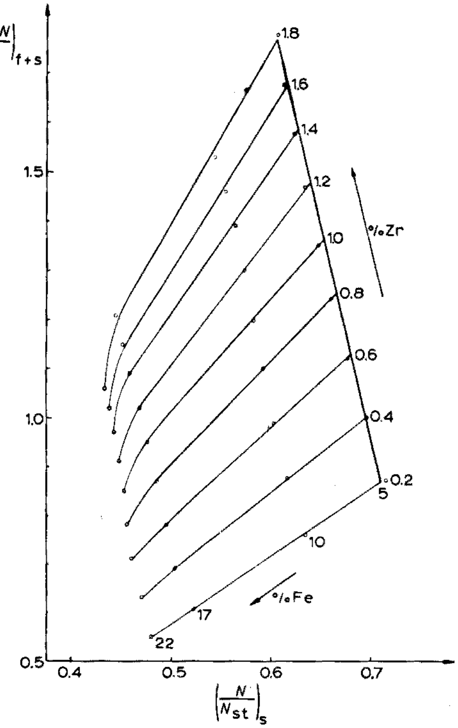

Fig. 3. A nomogram for zirconium determination by the filter method. N_{st}: count rate for standard sample. $(N/N_{st})_f$: relative intensity of characteristic zirconium radiation. $(N/N_{st})_s$: relative intensity of scattered radiation.

Fig. 4. A nomogram for zirconium determination by the method without filters.

cision. All measurements were standardized to a standard sample. The nomograph is shown in Fig. 3. The average relative error (s.d.) of the determination of zirconium, including statistical error, apparatus error and repeatability, was 1.5% for zirconium concentrations of 0.4–1.8% and 8.0% for zirconium contents below 0.2%. The time of a single determination was about 8 min. The activity of the source used in the measurements with the filters was 100 μC.

Determination of zirconium without the use of filters

In order to simplify the determination of zirconium, another method was worked out; this consisted of measuring the total count rate, *i.e.*, the sum of the characteristic radiation of zirconium and scattered radiation (N_{f+s}) at one discrimination level and then measuring the scattered radiation, N_s, only at a higher discrimination level. The results were again interpreted by a nomogram (Fig. 4). The average relative error was 2.8% for zirconium contents of 0.4–1.8% and 10% for zirconium contents less than 0.2%. Although this method decreased the time of measurement (5 min) even when the activity of the source was only 30 μC, the precision of the determination became significantly worse.

In both nomograms, the curves corresponding to the particular zirconium concentrations are bent for iron contents above 17%. This effect results in a considerable decrease in sensitivity and thus in a decrease in the precision of the results, especially for higher concentrations of zirconium, *i.e.* above 1%. The bends are probably due to incomplete separation of the characteristic radiation of zirconium from Compton-scattered primary radiation. When the scattered radiation is counted, some contribution from the characteristic radiation of zirconium is also measured. In the case of low iron contents, when the intensity of scattered radiation is large, the contribution of the fluorescence radiation of zirconium is small, but for higher iron

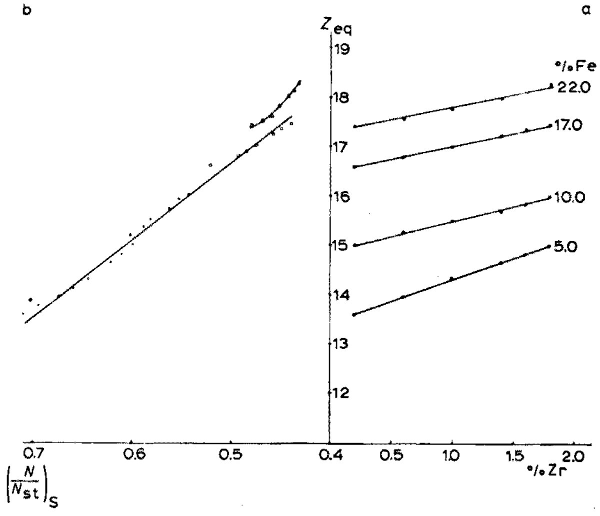

Fig. 5. (a) Dependence of equivalent atomic number Z_{eq} on zirconium content for different iron concentrations. (b) Dependence of measured scattered radiation intensity N_s on equivalent atomic number Z_{eq} for samples containing different concentrations of Fe. ● = 5% Fe. × = 10% Fe. ○ = 17% Fe. △ = 22% Fe.

and zirconium contents, when the intensity of scattered radiation decreases (with increasing equivalent atomic number Z_{eq} of the scatterer), the relative contribution of the fluorescence radiation of zirconium increases. This can be seen in Fig. 5; Fig. 5a shows the dependence of the equivalent atomic number Z_{eq} on the zirconium content for different constant concentrations of iron in sand samples. Z_{eq} is defined as the atomic number of a hypothetical element whose spectrum of scattered γ and X-ray quanta is identical with that of the composite medium considered[8]. The Z_{eq} value is obtained by calculation of the ratio $\mu_{phot.}/\mu_{Compt.}$, the energy being identical for both media. In Fig. 5b the dependence of the intensity of the scattered radiation measured on Z_{eq} is shown. It can be seen that for iron concentrations in the range 5.0–17.0%, this dependence is linear; for 22% of iron the dependence of N_s on Z_{eq} is not linear.

The application of a detector of better resolution, *e.g.* a semiconductor counter, would probably eliminate this disadvantage.

The effect of titanium

The synthetic standard samples used in the present work contained only iron as interelement, but natural sands also contain a considerable amount of titanium (3.0–10.0%). The effect of titanium on the zirconium results when only iron was present in the standards was therefore studied. Table I shows the results for zirconium in the presence of varying amounts of iron and titanium. The zirconium contents were obtained from the nomogram established without filters. Titanium had no significant effect on the results, when the matrix effect was eliminated by scattered radiation measurement.

TABLE I

THE DETERMINATION OF ZIRCONIUM IN SAMPLES CONTAINING VARYING AMOUNTS OF IRON AND TITANIUM

Fe cont. (%)	*Ti cont. (%)*	*% Zr obtained from nomogram*	*Relative error (%)*
10	—	0.86	1.0
6	4	0.85	
2	8	0.88	
5	5	0.87	
8	2	0.87	
17	—	0.86	
12	5	0.86	
5	12	0.86	
10	10	0.87	

Results for the determination of zirconium in several samples of natural sand by the classical chemical method and by both the proposed fluorescence methods (with and without filters) are given in Table II.

DETERMINATION OF ZIRCONIUM IN CONCENTRATES

The zirconium contents in concentrates before flotation in the technological procedure, are 25–35% and the total content of iron, titanium and rare-earth elements

TABLE II

DETERMINATION OF ZIRCONIUM IN NATURAL SANDS

Sample	*Chemical analysis*			*Fluorescence method with filters*		*Fluorescence method without filters*	
	% Fe	*% Ti*	*% Zr (A)*	*% Zr (B)*	*Differences (B-A)*	*% Zr (C)*	*Difference (C-A)*
1	9.56	4.50	0.95	0.63	−0.32	0.75	−0.20
2	17.70	9.43	0.91	0.93	+0.02	0.96	+0.05
3	20.6	8.53	1.38	1.33	−0.09	1.26	−0.12
4	13.75	5.33	0.48	0.48	0.00	0.45	−0.03
5	9.62	6.50	1.60	1.50	−0.10	1.58	−0.02
6	15.60	6.60	0.66	0.63	−0.03	0.67	+0.01

is *ca.* 20%. After flotation the corresponding values are 47–48.5% of zirconium while the admissible titanium content is 0.1%.

The sensitivity of the fluorescence method often decreases with an increase in the concentration of the element determined. In order to avoid this difficulty as well as the matrix effect, the well-known dilution method was used[9]. The dilution of concentrate samples with pure sand (of particle size less than 70 μ) in the ratio of 1:10 effectively decreased the concentration of iron and titanium to 0–3.5%. The matrix effect of these elements could be eliminated as in the case of sands, by measuring the scattered radiation. There was, however, no need to use the nomogram method, because with the concentration range of interelements involved, the fluorescence to scattered radiation ratio was essentially independent of matrix changes. A calibration

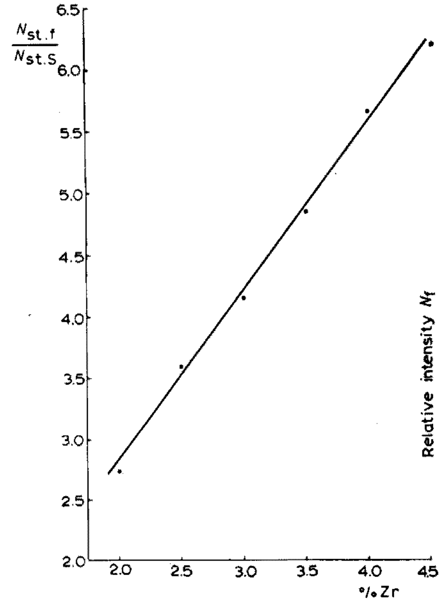

Fig. 6. Calibration curve for the determination of zirconium in concentrates.

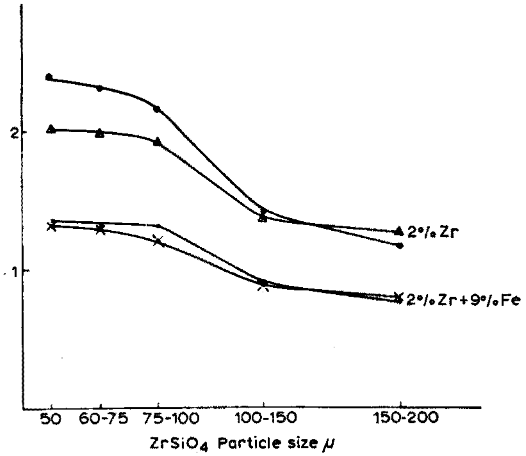

Fig. 7. Dependence of zirconium fluorescence radiation intensity on particle size of $ZrSiO_4$, for a zirconium content of 2.0% in a SiO_2 matrix. The four curves correspond to SiO_2 particle sizes of < 70 μ, 0% Fe (△); 150–200 μ, 0% Fe (○); < 70 μ, 9% Fe (×); 150–200 μ, 9% Fe (●).

curve (Fig. 6) could therefore be used in analysis of all concentrates. The average relative error of zirconium determination in concentrates was 2.0%.

THE PARTICLE SIZE EFFECT

In the case of the determination of zirconium in sands, the problem of the influence of particle size is important inasmuch as the particle size of zirconium silicate and pure sand as well as magnetite and ilmenite varies between 100 and 200 μ. The influence of the particle size of $ZrSiO_4$ and SiO_2 on the intensity of the fluorescence radiation of zirconium was therefore studied in the range between 50 and 200 μ. Artificially prepared samples containing two components ($ZrSiO_4+SiO_2$) and three components ($ZrSiO_4+SiO_2+Fe_3O_4$) were used. The intensity of the characteristic radiation of zirconium was measured for two particle sizes of silica (<70 μ and 150–200 μ) and varying particle sizes of zirconium silicate; typical results are shown in Fig. 7. As can be seen from the figures, there are two particle size ranges—one below 70 μ and the other above 150 μ—in which the intensity of the characteristic zirconium radiation is only slightly affected by the particle size of zirconium silicate. When iron is present in the sample, the general shape of the curves is not changed.

The general character of the dependence between the particle size of the compound containing the relevant element and the intensity of its fluorescence radiation is consistent with the results obtained by CLAISSE[10,11] and BERNSTEIN[12,13] who have obtained similar curves for other elements and matrices.

The range of large particle sizes, in which the characteristic radiation intensity is constant, corresponds to the particle size of zirconium silicate and silica in natural sands. However, judging from the repeatability of measurements it seems advantageous to reduce the particle size of the samples below 70 μ; with large particle sizes, the errors from the inhomogeneity of samples amount to about 25% (relative error). The grinding can easily be done by standard techniques.

It is a pleasant duty to express deep gratitude to Dr. L. GÓRSKI and Dr. J. CZUBEK for valuable discussions during the progress of this work.

SUMMARY

A nondispersive X-ray fluorescence method for the rapid, nondestructive determination of zirconium in zirconium-bearing sands and zirconium concentrates is described. A ^{109}Cd source of primary radiation and compact geometry for measurements were used. The matrix effect from iron and titanium in sands was eliminated by measuring the fluorescent radiation of zirconium and the scattered primary radiation, and interpreting the data with nomograms. For concentrates, dilution with pure sand and measurement of the ratio of fluorescence to scattered radiation were used to reduce a matrix effect; a calibration curve was then satisfactory. Particle size effects were avoided by grinding to below 70 μ.

RÉSUMÉ

On décrit une méthode de fluorescence aux rayons-X, non dispersive, pour le dosage rapide, non destructif du zirconium dans des sables et concentrés de zirconium. On utilise ^{109}Cd comme source de rayonnement primaire et la géométrie compacte de mesure. Etant donné l'apparition de l'effet de matrice dû à la présence du fer et du titane, on propose également une méthode d'élimination de cet effet. La méthode consiste à mesurer le rayonnement de fluorescence du zirconium et le rayonnement primaire diffusé par l'effet Compton, et en une interprétation à l'aide de nomogramme. Dans le cas des concentrés on procède par dilution de l'échantillon à l'aide de sable pur et mesure du rapport rayonnement de fluorescence/rayonnement diffusé; ce qui permet l'utilisation d'une courbe d'étalonnage. On examine également l'influence du broyage.

ZUSAMMENFASSUNG

Eine röntgenfluoreszenzanalytische Methode zur schnellen Bestimmung von Zirkonium in Sanden und Zirkoniumkonzentraten wird beschrieben, bei der mit einer ^{109}Cd-Quelle primär angeregt wird. Matrixeffekte, die durch Eisen und Titan im Sand hervorgerufen werden, wurden eliminiert, indem die Fluoreszenzstrahlung des Zirkoniums und die gestreute primäre Strahlung gemessen und die Daten mit Nomogrammen interpretiert wurden. Bei den Konzentraten wurde mit reinem Sand verdünnt und das Verhältnis von Fluoreszenz- zu gestreuter Strahlung benutzt, um Matrixeffekte zu reduzieren. Dadurch ergab sich eine zufriedenstellende Eichkurve. Einflüsse durch die Teilchengrösse wurden durch Mahlen bis auf eine Korngrösse von $< 70\ \mu$ vermieden.

REFERENCES

1 *Analyse der Metalle. Vol. II. Betriebs Analysen*, Part 2, Springer Verlag, Berlin, 1961, p. 998.
2 T. Florkowski, B. Dziunikowski, A. Kosiara and M. Wasilewska, *Proc. Salzburg Symp. Radiochem. Methods Anal., I.A.E.A., Vienna, 1965*, Vol. II. p. 419.
3 B. Dziunikowski, B. Holyńska and J. Stachurski, *Chem. Anal. (Warsaw)*, in press.
4 P. Martinelli and P. Blanquet, *Proc. Salzburg Symp. Radiochem. Methods Anal., I.A.E.A., Vienna, 1965*, Vol. II. p. 451.
5 K. G. Carr-Brion and J. R. Rhodes, *Proc. XII Colloq. Spectrosc. Intern., Exeter, 1965*, Hilger and Watts, London, p. 438.
6 A. Lubecki, M. Wasilewska and L. Górski, *Spectrochim. Acta*, in press.
7 B. Dziunikowski, *Nukleonika*, 9 (1964) 829.
8 J. Czubek, *Proc. Warsaw Symp. Radioisotop. Instrum. in Industry and Geophys., I.A.E.A., Vienna, 1966*, Vol. II, p. 246.
9 H. A. Liebhafsky, H. G. Pfeiffer, E. H. Winslow and P. D. Zemany, *X-Ray Absorption and Emission in Analytical Chemistry*, J. Wiley and Sons, New York, 1960, p. 173.
10 F. Claisse, *Accurate X-Ray Fluorescence Analysis without Internal Standards*, Dept. of Mines., Prov. Quebec, Canada, PR No. 327, 1956.
11 F. Claisse and C. Samson, *Advances in X-Ray Analysis*, Vol. 5, Plenum Press, New York, 1961, p. 335.
12 F. Bernstein, *Advances in X-Ray Analysis*, Vol. 5, Plenum Press, New York, 1961, p. 486.
13 F. Bernstein, *Advances in X-Ray Analysis*, Vol. 6, Plenum Press, New York 1962 p. 436.

Analytica Chimica Acta
Elsevier Publishing Company, Amsterdam
Printed in The Netherlands

THE PRECISE DETERMINATION OF ^{239}Np FOR THE EVALUATION OF ^{238}U CAPTURE CROSS-SECTIONS AT VARYING NEUTRON ENERGIES IN A ZERO-ENERGY FAST REACTOR

R. S. LARGE AND L. P. O'CONNOR
Atomic Weapons Research Establishment, Aldermaston, Berkshire (Great Britain)
(Received May 15th, 1967)

The reactor VERA (Versatile Experimental Reactor Assembly) is a zero-energy experimental fast reactor using plutonium or enriched uranium and a variety of moderators with a maximum output of 100 W[1]. As part of the reactor experimental programme it was necessary to determine the rate of neutron capture in ^{238}U in assemblies with neutron energy spectra in the range 1 keV to several MeV. Thin uranium metal foils of natural isotopic composition, each weighing 0.3–0.4 g, were used for this purpose. The arrangement of the foils in the reactor could be varied at will; it was expected that from 10^2 to 10^4 d.p.s. of neptunium-239 would be produced per g of uranium by the end of an irradiation. The results were required to have an absolute accuracy of $\pm 1\%$ with the best precision obtainable.

Owing to the low power of the reactor, the ratio of uranium to ^{239}Np was unusually high for this type of experiment, hence it was of importance to bear in mind the levels of the principal natural radioactive species concerned, which are:

^{238}U and ^{234}U	$2.5 \cdot 10^4\, \alpha$ sec^{-1} per g U
^{234}Th/^{234}Pa (24.1 d)	$2.5 \cdot 10^4\, \beta^-$ sec^{-1} per g U at equilibrium
^{234m}Pa (6.7 h)	80 β^- sec^{-1} per g U at equilibrium

In view of the large number of analyses required, the chemical separation and purification of the ^{239}Np had to be done in the shortest time consistent with the production of a radiochemically pure source. Additionally, the final solution should have negligible solid content so that sources could be prepared by evaporation, thus avoiding a lengthy electrodeposition stage and also ensuring negligible source self-absorption.

Published methods for the chemical separation of ^{239}Np with subsequent counting[2–5] do not give adequate precision (with the exception of the method of BARNETT *et al.*[4] who obtained a precision of 2% (2σ) for routine samples). Most methods, including the AWRE procedure[5], employ solvent extraction of neptunium(IV) by thenoyltrifluoracetone; this involves several extractions and back-extractions each requiring 10–20 min.

The ^{239}Np chemical yield is normally obtained by using ^{237}Np as tracer. ^{237}Np is an α-emitter with a half-life of $2.2 \cdot 10^6$ years, decaying to the β-emitter 27.0-d ^{233}Pa. The method must, therefore, include separation of ^{233}Pa from ^{237}Np at a known time in order that the ^{233}Pa contribution to the total β-count can be calculated. Also the amount of added ^{237}Np should be kept to the minimum consistent with obtaining reasonable counting statistics on the final source.

It was thought that coprecipitation of the neptunium as neptunium(IV) on lanthanum fluoride (to separate from the bulk of the uranium), followed by an anion-exchange stage to remove the lanthanum carrier, would give an efficient purification; additionally, some decontamination from protactinium would be obtained. Considerable variations have been encountered in studies of the coprecipitation behaviour of protactinium[6–8] especially on lanthanium fluoride; ELSON[6] states that the carrying results are always adversely affected by the presence of zirconium. Experiments were made, therefore, to determine the amount of ^{233}Pa carried on the lanthanum fluoride precipitate under the proposed analytical conditions.

Lanthanum fluoride precipitations

Experiments were made with 1 mg of lanthanum to carry *ca.* $2\cdot10^4$ d.p.m. of ^{237}Np; the fluoride precipitate was re-dissolved by complexing and then re-precipitated by the addition of further fluoride. The number of cycles was varied and the effect of the presence of 1 mg of zirconium was also investigated; full details of the procedure are as given below. The decontamination factor for ^{233}Pa was determined for the overall process, including the removal of lanthanum by anion exchange in concentrated hydrochloric acid. Typical results are given in Table I.

TABLE I

PROTACTINIUM DECONTAMINATION FACTORS FOR PRECIPITATION—ANION EXCHANGE STAGES

Number of fluoride precipitations	*One*	*One*	*Two*	*Two*	*Three*
1st	No Zr	Added Zr	No Zr	Added Zr	Added Zr
2nd	—	—	Added Zr	Added Zr	No Zr
3rd	—	—	—	—	No Zr
Decontamination factor for Pa	$3\cdot10^1$	$2\cdot10^2$	$1\cdot10^2$	$2\cdot10^4$	$4\cdot10^4$

From these and similar experiments, it was found that for ^{237}Np tracer at the 100 d.p.m. level, a negligible contribution to the total β^--activity from ^{233}Pa would be obtained using two reduced fluoride precipitations (in the presence of zirconium) followed by precipitation of the hydroxide and subsequent removal of the lanthanum carrier by anion exchange in concentrated hydrochloric acid. Any thorium present in solution would accompany the lanthanum, since thorium is not absorbed significantly by anion-exchange resins from hydrochloric acid.

When the procedure was used with 0.3–0.4 g of natural uranium without added neptunium, up to 1% of the thorium accompanied the neptunium; this arose from insufficient washing of the column with concentrated hydrochloric acid. The presence of 100–200 d.p.m. of uranium was attributed to the reduction of small amounts of uranium(VI) at the reduction stage (see *Recommended procedure*) which would then be eluted from the column with the neptunium[9].

Anion exchange in 3 M nitric acid

In order to remove residual uranium and ^{234}Th and to improve the purity of the neptunium both radiochemically and in respect of weighable inorganic impurities, an additional anion-exchange stage using nitric acid was employed. This would also serve to decontaminate from ^{233}Pa (if work on the samples was interrupted, after the fluoride precipitation, for more than a day) and from plutonium (if present in more highly irradiated samples).

A method in which neptunium(IV) is absorbed on an anion-exchange resin from 3 M nitric acid, is available[10] for the separation of ^{239}Np from freshly irradiated ^{238}U and associated plutonium isotopes. The distribution coefficient for neptunium(IV) is maximal in *ca.* 6 M acid solutions, but in practice acidities have to be restricted to 3 M, because the resin catalyses the normally slow reactions between nitric acid and reductant. Under the conditions recommended on p. 127, typical decontamination factors obtained are *ca.* 10^5 for plutonium, *ca.* 10^4 for uranium and *ca.* $3 \cdot 10^2$ for thorium. Recovery of neptunium is 85–100%. To determine the decontamination factor for protactinium, 10^4-d.p.m. of ^{237}Np (in equilibrium with ^{233}Pa) was added to the column in the appropriate solution; after elution the α- and β^--activity of the fraction was determined. Neptunium recovery was 90% and no β^--activity could be detected, so that the decontamination factor was of the order of 10^4 or greater.

Foil preparation

Early batches of irradiated uranium foils were received for analysis coated with an oxide film, so that the uranium content had to be determined by controlled potential coulometry in 0.5 M sulphuric acid. Subsequently, foils were cleaned in dilute acid before irradiation and the uranium weight was obtained by direct weighing of the foil after irradiation; some foils were also analysed for uranium content by coulometric analysis of the foil solution and the interim oxide formation was found to be negligible.

Source preparation

All sources for counting were prepared by evaporating a dilute nitric acid solution of the neptunium onto stainless steel discs with a little tetraethylene glycol present to spread the source. After the discs had been dried and lightly flamed, there was no visible residue from the second anion-exchange eluate and the sources were essentially weightless. Attention must be paid to the acids used, some batches having higher solid contents on evaporation than others.

To investigate the effect of source weight on the α-counting, several sources were prepared by direct evaporation of known weights of calibrated ^{237}Np tracer solution. The sources were counted in both an AERE type 1093 scintillation counter, and a gas flow proportional counter of 2π geometry using 90% argon/10% methane. A further series of discs was similarly prepared and varying amounts of lanthanum were added, as a solution in dilute nitric acid, to groups of the discs. The solution on each disc was evaporated to dryness, and the residue was dissolved, dried and flamed as described on p. 127. After counting, the disintegration rate of the tracer solution was calculated. The results (Table II) showed that up to an added weight of 65 μg, there was little evidence of a decline in the count rate. Amounts of 65 μg of lanthanum oxide were clearly visible, hence it was concluded that sources with negligible visible solid residue would not suffer appreciably from self-absorption losses in α-counting; this was borne out by later routine results (see DISCUSSION).

TABLE II

EFFECT OF ADDED SOLID ON COUNTING RATE OF ^{237}Np SOURCES

	α scintillation counting			*2πα proportional counting*		
	Mean d.p.m./g $^{237}Np \cdot 10^3$	*Coefficient of variation from counting statistics alone (%)*	*Overall coefficient of variation for sources (%)*	*Mean d.p.m./g $^{237}Np \cdot 10^3$*	*Coefficient of variation from counting statistics alone (%)*	*Overall coefficient of variation for sources (%)*
Direct evaporation of solution No added solid (12 sources)	2.20	1.9	1.9	2.20	0.3	0.9
Lanthanum solution added and source TEG spread (4 sources at each level). Weight added La_2O_3 (μg)						
6	2.21	0.5	1.7	2.22	0.4	0.6
10	—	—	—	2.19	0.3	2.6
15	2.20	0.5	1.9	2.19	0.4	2.2
65	2.19	0.5	1.8	2.17	0.3	1.7
120	2.11	0.5	2.4	2.14	0.4	1.8

Counting

The recovery of added ^{237}Np tracer was determined by counting in an AERE Type 1093 α-scintillation counter, standardised by reference to a low geometry counter of the type described by HURST *et al.*[11]. Examination of several sources by α-spectrometry indicated the presence of ^{237}Np alone, which gave peaks of essentially Gaussian shape similar to those obtained with thin uniform electrodeposited sources.

The ^{239}Np was β^--counted in an AWRE Type A2 gas flow proportional counter[12] having a 5.3-mg cm^{-2} aluminium window, against a standardised source[13] of ^{243}Am, correcting for the appreciable response of these counters to the conversion X-ray spectrum of ^{243}Am[14]. For low activity β^--sources, it is necessary to apply a similar correction for the conversion X-ray spectrum contribution of ^{237}Np to the β^- count[14].

In a number of cases where routine samples had been counted for a period equal to approximately three half-lives, the half-life of the ^{239}Np was computed from the counting data by the method of least squares (Table III); the weighted mean for the 6 values is 2.358 ± 0.015d which is in good agreement with the published value of 2.359 ± 0.010d[15].

TABLE III

CALCULATED HALF-LIFE OF ^{239}Np FROM ROUTINE SOURCES

Sample	$T_{\frac{1}{2}}d \pm 99\%$ *confidence limit*	*Decay*	
		No. of $T_{\frac{1}{2}}d$	*No. of points*
V31	2.364 ± 0.007	8.0	15
V59	2.361 ± 0.018	2.9	7
V60	2.372 ± 0.026	3.0	7
V81	2.348 ± 0.010	3.3	7
V111	2.354 ± 0.021	2.9	6
WB1	2.354 ± 0.026	3.3	7

EXPERIMENTAL

Reagents

Iron(II) sulphamate solution. Add 6 g of iron powder and 19.5 g of sulphamic acid to 30–40 ml of freshly boiled distilled water. When the reaction is complete, filter and dilute to 50 ml. The solution can be kept for several days in an airtight container.

Wash solution A. Mix 10 ml of 3 *M* nitric acid (freed from nitrogen oxides by boiling before dilution) with 0.1 ml of 50% hydrazine nitrate solution and 0.2 ml of iron(II) sulphamate solution.

Wash solution B. As for solution A omitting the sulphamate.

Lanthanum and zirconium carrier solutions. Prepare solutions containing 10 mg of the element (as nitrate) per ml in 3–4 *M* nitric acid.

Recommended procedure

Weigh the uranium foil. Add a known weight of ^{237}Np tracer (*ca.* 100 d.p.m.) and dissolve in 3–4 ml of concentrated nitric acid. Add 0.2 ml of 60% perchloric acid and evaporate to dryness. Wash down beaker with a few ml of water and re-evaporate. Redissolve in 2–3 ml of water.

Transfer to a 10-ml lusteroid centrifuge tube. Adjust the volume to *ca.* 4 ml. Add concentrated ammonia solution dropwise to give a permanent precipitate. Redissolve the precipitate in the minimum amount of 1 *M* nitric acid. Add 1 ml of 6 *M* nitric acid in excess, 1 mg each of lanthanum and zirconium carriers and 0.25 ml of 5% hydrazine nitrate solution. Dilute to *ca.* 6 ml. Place the tube in a hot water bath for 5 min. Cool, add 0.5 ml of 40% hydrofluoric acid, place the tube in a hot water bath for a few minutes, cool, centrifuge and reject the supernate. Wash the precipitate three times with 2 ml of 0.1 *M* nitric acid containing one drop of 12.5% ammonium fluoride solution. Dissolve the precipitate in 0.2 ml of saturated boric acid solution and 0.15 ml of concentrated nitric acid. Add 0.5 mg of zirconium carrier, dilute to *ca.* 1 ml and add 0.05 ml of 5% hydrazine nitrate solution. Add 0.25 ml of 12.5% ammonium fluoride solution. Warm in a water bath for several minutes. Cool, centrifuge and reject the supernate. Wash the precipitate twice with 2 ml of 0.1 *M* nitric acid containing one drop of 12.5% ammonium fluoride solution. Dissolve the precipitate in 0.2 ml of saturated boric acid solution and 0.5 ml of concentrated hydrochloric acid. Dilute to 4.5 ml and add ammonia solution to precipitate the hydroxide. Wash the precipitate twice with 1 ml of water.

Dissolve the precipitate in 0.5 ml of concentrated hydrochloric acid and transfer to a column (5 cm × 0.4 cm diameter) of DeAcidite FF anion exchange resin (7–9% DVB < 200 mesh) pretreated with concentrated hydrochloric acid. Wash the column with a further 9.5 ml of concentrated hydrochloric acid. Reject the eluate. Elute neptunium with 5 ml of 4 *M* hydrochloric acid and evaporate to dryness. Add 0.2 ml of concentrated nitric acid and re-evaporate to dryness.

Dissolve the residue in 1 ml of wash solution A and transfer to the top of a column (8 cm × 0.4 cm diameter) of the DeAcidite FF resin pretreated with 3 *M* nitric acid. Wash the column with the following solutions (*i*) 7 ml of wash solution A (note time of separation of ^{233}Pa), (*ii*) 4 ml of wash solution B, (*iii*) 1 ml of 1 *M* nitric acid. Discard these fractions. Elute neptunium with 5 ml of 1 *M* hydrochloric acid.

Evaporate the eluate to dryness. Add 0.1 ml of redistilled nitric acid and re-evaporate. No visible residue should be present (Note). Take up in 2–3 drops of 1 *M* nitric acid and mount totally on a 1-in. diameter stainless steel disc. Evaporate to dryness under an infrared lamp. Add 0.05 ml of 1 *M* nitric acid and 0.05 ml of aqueous 2% tetraethylene glycol solution and re-evaporate. Flame to a light straw colour.

Determine ^{239}Np by β-counting in a gas flow proportional counter calibrated for ^{239}Np against a standardised ^{243}Am source. Determine the yield by α-counting the ^{237}Np under the same conditions as the original ^{237}Np tracer.

Note. Extraneous contamination (*e.g.* iron) may be removed at this stage by the following procedure. Dissolve the residue in 1 *M* nitric acid. Add 1–2 drops each of iron(II) sulphamate solution and 5% hydrazine nitrate solution and sufficient solid ammonium nitrate to give a saturated solution in a final volume of 1–1.5 ml. Extract neptunium with an equal volume of methyl isobutyl ketone (MIBK). Wash the organic phase with an equal volume of saturated ammonium nitrate in 1 *M* nitric acid. Mount the MIBK extract directly on a stainless steel disc using the following technique. Place a metal nut or ring, the external diameter of which is greater than

1 inch, on a hot-plate maintained at 150–200°. The internal diameter of the nut should be slightly smaller than the disc. The disc, which is placed on the nut and must be horizontal, is then hotter at the circumference than at the centre. Careful addition of the MIBK extract to the disc results in an evaporated source confined to the disc centre.

DISCUSSION AND CONCLUSIONS

The arrangement of foils in the VERA reactor is generally in pairs, and ideally each member of a pair is considered to be identical with the other in respect of neutron flux and energy. In Table IV the agreement between the ^{239}Np analysis of foil pairs for each set of results for a number of reactor cores is expressed as the standard deviation of a single result from the mean, including counting statistics.

TABLE IV

AGREEMENT BETWEEN ^{239}Np ANALYSIS OF FOIL PAIRS

Core	*Number of pairs of foils*	*Coefficient of variation (%)*
3A	10	2.4
5A	9	3.1
7A	10	2.9
11A Series I	5	1.6
11A Series II	10	1.4

An improved arrangement for mounting the foils in the reactor was adopted for Core 11A. This appears to be reflected in an improvement in the results. No change in analytical procedure was made apart from a change from 2π α-proportional counting to α-scintillation counting (after Core 11A Series I) for convenience.

The method described has been in use at AWRE Aldermaston for over 4 years and has proved to be a satisfactory method which obviates prior separation of ^{233}Pa daughter from the ^{237}Np tracer used as yield indicator. The mean recovery of added ^{237}Np for one batch of 17 consecutive samples was 71.4% with a coefficient of variation of 9.9%. A later check on 10 consecutive samples gave a mean recovery of 70.9% with a coefficient of variation of 7.5%.

We wish to thank Mr. W. H. Davies for assistance with the chemical separations and samples, Mr. A. J. Hodge for counting the sources and Mr. J. Herrington and Mr. G. C. Goode for the coulometric analyses.

SUMMARY

A method is described for the determination of ^{239}Np in natural uranium metal foils irradiated in a zero-energy reactor. The foils are dissolved in nitric acid in the presence of ^{237}Np used for the determination of the yield of ^{239}Np. Neptunium is co-precipitated with lanthanum fluoride; lanthanum and thorium are removed by anion exchange in hydrochloric acid solution, and the neptunium is further purified by anion exchange in nitric acid solution. Sources for counting are prepared by direct evaporation of an aqueous solution onto a stainless steel disc. No corrections are necessary to the ^{237}Np α-count for absorption in the source. The method does not necessitate prior separation of daughter ^{233}Pa from the ^{237}Np tracer and gives sources of high purity in good yield.

RÉSUMÉ

On décrit une méthode pour le dosage de ^{239}Np dans de l'uranium métallique naturel irradié dans un réacteur à énergie zéro. Le métal est dissous dans l'acide nitrique en présence de ^{237}Np utilisé pour la détermination du rendement de ^{239}Np. Le neptunium est coprécipité avec du fluorure de lanthane. La et Th sont éliminés par échangeur d'anions en solution chlorhydrique; le neptunium est ensuite purifié par échangeur d'anions en solution nitrique. Les sources pour le comptage sont préparées par évaporation directe d'une solution aqueuse sur disque d'acier inox. Cette méthode ne nécessite pas de séparation de ^{233}Pa d'avec le traceur ^{237}Np et donne des sources très pures avec un bon rendement.

ZUSAMMENFASSUNG

Es wird eine Methode zur Bestimmung von ^{239}Np in Folien von natürlichem Uranmetall beschrieben, die in einem Nullenergie-Reaktor bestrahlt wurden. Die Folien werden in Salpetersäure in Gegenwart von ^{237}Np gelöst, das zur Bestimmung der Ausbeute an ^{239}Np verwendet wird. Das Neptunium wird mit Lanthanfluorid mitgefällt; Lanthan und Thorium werden mit einem Anionenaustauscher in salzsaurer Lösung abgetrennt, und das Neptunium wird weiterhin durch einen Anionenaustauscher in salpetersaurer Lösung gereinigt. Die Proben werden zum Zählen durch direktes Eindampfen einer wässrigen Lösung in einer Schale aus rostfreiem Stahl vorbereitet. Korrekturen für die Absorption der α-Strahlung des ^{237}Np sind nicht erforderlich. Die Methode erfordert keine vorhergehende Abtrennung der Tochter ^{233}Pa und ergibt Quellen von hoher Reinheit in guter Ausbeute.

REFERENCES

1 *Directory of Nuclear Reactors*, Vol. V, I.A.E.A., Vienna, 1964.
2 N. BAER, M. J. GALPERN AND W. CARBONNE, *Nucl. Sci. Eng.*, 3 (1958) 113.
3 F. L. MOORE, *Anal. Chem.*, 30 (1958) 1368.
4 G. A. BARNETT, W. A. V. BROWN AND D. J. FERRETT, *Reactor Sci. and Technol. (J. Nucl. Energy, Pts A/B)*, 17 (1963) 389.
5 F. H. CRIPPS, unpublished work.
6 R. E. ELSON, *The Actinide Elements*, National Nuclear Energy Series Div. III, 14A, McGraw-Hill, New York, 1954, p. 103.
7 A. G. MADDOCK AND L. MILES, *J. Chem. Soc.*, (1949) S248.
8 D. BROWN AND A. G. MADDOCK, *Quart. Rev. (London)*, 17 (1963) 289.
9 K. A. KRAUS AND F. NELSON, *Proc. U.N. Intern. Conf. Peaceful Uses At. Energy, Geneva, 1955*, Vol. 7, 1956, p. 113.
10 L. P. O'CONNOR, unpublished work.
11 R. HURST, G. R. HALL AND K. N. GLOVER, *AERE Report C/R 647*, 1951.
12 D. E. WATT AND F. J. BANNISTER, *AWRE Report NR/P-6/60*, 1960.
13 F. H. CRIPPS AND J. W. WEALE, *J. Inorg. & Nucl. Chem.*, 7 (1958) 339.
14 L. P. O'CONNOR AND R. S. LARGE, *Intern. J. Appl. Radiation Isotopes*, 14 (1963) 620.
15 D. COHEN, J. C. SULLIVAN AND A. J. ZIELEN, *J. Inorg. & Nucl. Chem.*, 11 (1959) 159.

Analytica Chimica Acta
Elsevier Publishing Company, Amsterdam
Printed in The Netherlands

DETERMINATION OF THORIUM AND URANIUM IN BIOLOGICAL MATERIALS

M. PICER AND P. STROHAL
Institute for Medical Research, Yugoslav Academy of Sciences and Arts and "Ruder Bošković" Institute, Zagreb (Yugoslavia)

(Received March 30th, 1967)

With the increasing use of thorium and uranium, the determination of these elements over a large scale of concentrations and in various materials has become of particular interest[1-7]. Because of possible contamination, it is necessary to control the concentrations of thorium and uranium in various organs and materials. Thus the development of a new method for an accurate routine determination in biological material, even at very low concentrations, is of interest. The determination of traces of thorium[8] is important because no satisfactory analytical procedure has been available for its submicro determination either in biological materials or in materials of biological origin, although there are some useful procedures for the determination of traces of uranium[9]; so far the most satisfactory of such methods appears to be the fluorimetric method.

The development[10] of new analytical procedures for the submicro determination of thorium and uranium is also of interest for the study of trace elements in human organisms. Since the toxic effects of uranium and thorium have been better understood than their biological effects, the determination of these elements in submicrogram concentrations should lead to a better understanding of their biological role. The extensive recent application of activation analysis[11] suggested the suitability of such a method for this determination. A chemical separation of the two elements from the bulk of inorganic ions present in biological materials, *i.e.* the separation of thorium and uranium from large amounts of sodium, calcium, magnesium, phosphorus, iron, etc., and from small amounts of various other elements, would also be necessary.

Nuclear data

The determination of thorium and uranium by neutron activation analysis can be made in two different ways, by measuring either the (n, γ) products or the fission products. Since neutron fluxes in reactors contain fast, intermediate and thermal neutrons, fission of ^{232}Th and ^{238}U can also be obtained, but this type of nuclear reaction cannot be applied in the present case because the thorium and uranium contents cannot be distinguished. The activity formed by the (n, γ) reaction followed by β decay was therefore utilized. Unlike the fission reaction, the (n, γ) reaction has no nuclear interference, so that the activities due to ^{233}Pa and ^{239}Np had to be separated and measured. The nuclear characteristics of the measured radionuclides are presented in Table I.

TABLE I

NUCLEAR DATA

Target	*Abundance in natural element (%)*	*Formation of measured radionuclides*	*Half-life of measured radionuclides*
^{232}Th	100	$^{232}Th\ (n, \gamma)^{233}Th \rightarrow {}^{233}Pa$	27.0 days
^{238}U	99.29	$^{238}U\ (n, \gamma)^{239}U \rightarrow {}^{239}Np$	2.36 days

Since no monoenergetic neutron flux was available, the real cross-sections could not be obtained. According to published data[12] the significance of large resonances for ^{238}U should be taken into account.

EXPERIMENTAL

Standard preparation

Standards solutions were prepared from analytical grade uranyl nitrate and thorium nitrate. The solutions were made up and diluted to give a final concentration of thorium or uranium of about 10 ng/ml. Standards were prepared for irradiation in the same way as samples. A quantity of pure silica powder approximately equal to the amount of biological sample was mixed with standard solutions, dried and sealed into silica ampoules. Standards were irradiated together with samples under the same irradiation conditions.

Sample preparation and irradiation

All biological samples were wet-ashed to avoid any possible loss of microconstituents during heating. Samples of water and acids were prepared by evaporation under an infrared lamp. The samples thus prepared were dried at 110°, placed into quartz ampoules and sealed.

Irradiations were performed in the RA reactor at the "Boris Kidrič" Institute for Nuclear Sciences, Belgrade, in a flux of about $3 \cdot 10^{13}$ n cm^{-2} sec^{-1}. The duration of irradiation was varied from several hours to 3 weeks.

Chemical treatment of irradiated samples

All samples were cooled after irradiation for about one day in order to allow ^{233}Th and ^{239}U to decay to ^{233}Pa and ^{239}Np. Quartz ampoules containing irradiated samples and standards were then boiled in aqua regia for about 20 min to decontaminate the outside walls from possible contaminants picked up during the handling before irradiation.

The ampoules were broken and their contents transferred to beakers containing 6 *N* nitric acid. The beakers were gently heated and after the samples had been dissolved, pieces of broken silica tubes were removed.

Since no isotope carriers could be applied in the case of protactinium and neptunium, the problem of chemical yield determination had to be solved after the separation procedure. Some experiments showed that if an equal quantity of non-irradiated material was added to the irradiated standard and if the separation procedures for both the standard and the sample were made under the same conditions, the error was negligible.

Separation of protactinium. Since none of the known analytical procedures for the protactinium separation has given satisfactory results for the separation of this element from irradiated biological samples, an attempt was made to introduce certain modifications. By means of modification of known procedures[13,14] for the protactinium separation from irradiated thorium targets and from certain geological samples, samples of satisfactory radiochemical purity were obtained. Irradiated samples were dissolved in nitric acid and then the solution was passed through a silica gel exchange column at a flow rate of about 0.2 ml/min to separate protactinium from the bulk of other activities. The column was then washed with three 20-ml portions of 6 *N* nitric acid. After washing, protactinium was eluted from the column with 50 ml of 0.5 *M* oxalic acid. To this eluate 10 ml of concentrated nitric acid and 5 ml of 30% hydrogen peroxide were added and then the solution was heated under an infrared lamp. After the oxalic acid present in the solution had been destroyed, 20 ml of concentrated hydrochloric acid was added to the solution and the solution was evaporated to a volume of a few milliliters. Protactinium was extracted from the 6 *N* hydrochloric acid solution with methyl isobutyl ketone. The solvent extraction procedure was repeated twice, and the protactinium was re-extracted with 1 *N* hydrochloric acid. The final purification of protactinium was performed by passing the 1 *N* hydrochloric acid solution through a silica gel column; the column was then washed with 6 *N* nitric acid and finally eluted with 15 ml of 0.5 *M* oxalic acid. Protactinium samples were placed on the counting planchettes, evaporated and counted.

Separation of neptunium. For the separation of neptunium from irradiated biological material the procedures described elsewere[15,16] had to be modified because of the low separation yields obtained. Yields as low as 18% were obtained by the procedure for the separation of neptunium by coprecipitation with lanthanum fluoride, probably because of the presence of various ions which interfere in the coprecipitation process. A modified procedure was therefore developed and yields above 70% were obtained.

The radiochemical separation was initiated by adding 10 drops of 1 *N* potassium permanganate to the nitric acid solution of the irradiated sample. The solution was gently heated and then manganese dioxide was precipitated by introducing 5 drops of 1 *N* sodium nitrite solution. The manganese dioxide precipitate was reduced with sodium nitrite and further neptunium separation was performed by coprecipitation with lanthanum hydroxide. For this purpose 1 ml of 5 *M* hydroxylamine hydrochloride solution and 10 mg of La^{3+} were added to the supernate. The precipitation of lanthanum hydroxide was performed by adding ammonia to the sample solution while stirring the solution vigorously. The precipitate which, besides lanthanum hydroxide, contained also other hydroxides, phosphates, etc., was separated from the solution by centrifugation and washed with distilled water. The precipitate thus prepared was dissolved in 6 *N* nitric acid and 2 ml of 1 *N* sulphuric acid and 2 ml of 0.05 *N* sodium bromate were added to oxidize neptunium to a higher oxidation state. The system was stirred and then lanthanum fluoride was precipitated by adding 1 ml of 0.6 *M* hydrofluoric acid. The precipitate was separated by centrifugation and wasted. Seven ml of saturated sulphur dioxide solution was added to the supernate to reduce neptunium to the lower oxidation state. Then the precipitation with lanthanum fluoride was repeated by adding hydrofluoric acid solution. The precipitate was separated from the supernate by centrifugation and washed several times with water. Lathanum fluoride precipitates were then dissolved by gentle heating in a saturated aluminium nitrate solution, to which 10 drops of concentrated nitric acid and 2 drops of 1 *M* sodium bromate were added. After a heating period of about 5 min, 3 g of ammonium nitrate and a few milliliters of water were added and ammonium nitrate was dissolved by heating on a water bath. The cooled solution was extracted twice with 2 ml of ether. Ether fractions were placed on aluminium counting planchettes, carefully evaporated, and the samples prepared for counting.

Measurement of activity

The γ-ray emissions of protactinium and neptunium were measured with a $3 \times 3''$ NaI(Tl) scintillation counter coupled to a 256-channel analyser. The spectra obtained were compared with those of the standards, which were taken in the same way. The decay of the photopeaks at 0.313 and 0.068 MeV was followed and half-lives of 27 days and 2.3 days for the protactinium and neptunium samples respectively, were obtained. The spectra were determined for a period of several half-lives and radiochemical purity was checked by detailed analysis of the spectra obtained.

The amounts of protactinium and neptunium were calculated by comparing the area under the photopeaks of the samples and the standards. Since the standards and the samples were measured under the same experimental conditions, no additional corrections were needed.

RESULTS AND DISCUSSION

The accuracy of the method was checked by adding known amounts of thorium and uranium to the samples to be analysed. This was done over a large scale of concentrations; typical results obtained are presented in Table II.

TABLE II

ACCURACY CHECKS BY THE ADDITION METHOD

Thorium added to sample (μg)	2.34	2.25	0.047	0.045
Thorium found (μg)	2.03	1.90	0.032	0.027
Uranium added to sample (μg)	0.42	0.39	0.046	0.047
Uranium found (μg)	0.37	0.32	0.038	0.028

The results of the analyses for uranium and thorium contents in various samples are presented in Table III. The relative standard error for urine samples for example was found to be 22% and 17% for thorium and uranium, respectively. These values are quite reasonable, considering that they correspond to concentrations as low as about 10^{-10} g/ml.

According to published data, thorium in quantities of only 10^{-7} g/l of urine[17] has been determined, but in such cases a preliminary concentration of thorium was necessary. In the present work as little as 10^{-11} g of thorium was determined, which shows the excellent sensitivity of the method described. In the case of uranium, the sensitivity of the method is in the range of a very sensitive fluorimetric method[18]. These sensitivities were obtained with a neutron flux of $5 \cdot 10^{13}$ n·cm^{-2}·sec^{-1}.

The chemical, physical and nuclear properties of microconstituents in biological material usually indicate that a pre-irradiation treatment of samples is needed. Any chemical or physical treatment of the sample before irradiation must be carried out in such a manner as to avoid the contamination of the sample. Accordingly, in the described procedures, the pre-irradiation treatment was performed with special care and all the reagents used were tested for thorium and uranium contents.

TABLE III

ANALYSES OF VARIOUS SAMPLES

Sample	*Concentration found*	
	Thorium	*Uranium*
Urine	$7.4 \cdot 10^{-11}$ g/ml	$3.1 \cdot 10^{-10}$ g/ml
Faeces	Not measured	$6.0 \cdot 10^{-6}$ g/day
Ashed bone	$2.3 \cdot 10^{-8}$ g/g	$4.1 \cdot 10^{-10}$ g/g
Blood	$5 \cdot 10^{-10}$ g/ml	$5 \cdot 10^{-10}$ g/ml
Water	$2.4 \cdot 10^{-10}$ g/ml	$5 \cdot 10^{-10}$ g/ml
Nitric acid (Merck, p.a.)	$1.7 \cdot 10^{-13}$ g/ml	$2.5 \cdot 10^{-12}$ g/ml

It should also be mentioned that the samples were not heated before irradiation and therefore no loss of trace elements by evaporation was possible.

The use of the (n, γ) reaction for the determination of thorium and uranium by the activation technique has several advantages. First, such a reaction is more sensitive than a fission reaction. Secondly, the (n, γ) reaction enables one to distinguish between radioactive products due to the ^{232}Th fission and those obtained by the ^{238}U fission. Moreover, the (n, γ) reactions have no nuclear interference. Since the (n, γ) products in both cases have short half-lives, the use of these radionuclides requires pneumatic facilities for prompt irradiation and delivery of samples. The measurement of their β-decay products with much longer half-lives is therefore desirable.

The results indicate that both thorium and uranium can be determined in samples analysed by the described procedures. They also show that the content of thorium and uranium in chemicals should be taken into account during the analytical procedure, but the influence of chemicals on the total thorium and uranium content will be significant only in cases when large amounts of acids are introduced. The proposed analytical procedures are suitable for the studies of metabolism of thorium and uranium under biological equilibrium conditions.

One of us (M.P.) expresses his thanks to the "Ruder Bošković" Institute for making available the facilities used.

SUMMARY

An activation method for the determination of traces of thorium and uranium in various biological samples after wet digestion is described. The (n, γ) and β-decay products of both thorium and uranium were separated and measured. Modified radiochemical separation procedures for protactinium and neptunium activities are described. The method was applied to determination of thorium and uranium in urine, faeces, bone, blood, water and some chemicals.

RÉSUMÉ

Une méthode est décrite pour le dosage de traces de thorium et d'uranium dans divers échantillons biologiques. Après minéralisation on procède à une analyse par activation. Les produits n, γ et β- du thorium et de l'uranium peuvent être séparés et mesurés. On décrit des procédés de séparation radiochimique pour les activités du protactinium et du neptunium. Cette méthode a été appliquée à l'urine, aux os, au sang, à l'eau et à quelques produits chimiques.

ZUSAMMENFASSUNG

Die Bestimmung von Spuren Thorium und Uran in verschiedenartigen biologischen Proben wird beschrieben. Die Proben wurden nass verascht und anschliessend aktiviert. Die β-Zerfallsprodukte von Thorium und Uran wurden abgetrennt und gemessen. Modifizierte radiochemische Trennungsverfahren für die Protactinium- und Neptunium-Aktivitäten werden beschrieben.

REFERENCES

1 A. A. SMALES, D. MAPPER AND A. P. SEYFANG, *Anal. Chim. Acta*, 25 (1961) 587.
2 L. A. HASKIN, H. W. FEARING AND F. S. ROWLAND, *Anal. Chem.*, 33 (1961) 1298.
3 J. W. MORGAN AND J. F. LOVERING, *Anal. Chim. Acta*, 28 (1963) 405.
4 D. DECAT, B. VAN ZANTEN AND H. LEUAERT, *Anal. Chem.*, 35 (1963) 845.
5 C. W. SILL AND C. P. WILLIS, *Anal. Chem.*, 36 (1964) 622.
6 H. STÄRK AND C. TURKOWSKY, *Radiochim. Acta*, 5 (1966) 16.
7 A. TRAVESI, J. PALOMARES AND G. DOMINIQUEZ, *Anal. Chim. Acta*, 35 (1966) 421.
8 D. I. RYABCHIKOV, *Analiticheskaya Khimia Toria*, Akademia Nauk USSR, Moscow, 1962.
9 A. A. NEMODRUK, *Himicheskie Methody Opredelenia Urana*, v sb. *Analiticheskaya Khimia Urana*, Akademia Nauk USSR, Moscow, 1962.
10 E. J. UNDERWOOD, *Trace Elements in Human and Animal Nutrition*, 2nd Edn., Academic Press, New York, 1962.
11 W. S. LYON, JR. (Editor), *Guide to Activation Analysis*, D. van Nostrand Company, Inc., New York, 1964.
12 D. J. HUGHES AND R. B. SCHWARTZ, *Neutron Cross Sections*, Report BNL-325, 2nd Edn., 1958.
13 A. V. DAVGDOV, *Metody Koncentrirovaniya Veschestv v Analitičeskoj Khimii*, Nauka, Moscow, 1965, p. 64.
14 S. J. LYLE, *Talanta*, 12 (1965) 573.
15 L. MAGNUSON, in W. W. MEINKE, *Chemical Procedures in Bombardment Work at Berkeley*, USAEC Rept. AECO-3084, 1951.
16 G. W. REED, *Geochim. Cosmochim. Acta*, 13 (1958) 248.
17 C. TESTA, Determination of Thorium in Urine by Means of Kel-F Column Supporting tri-N-octyl phosphine oxide, in *Radiological Health and Safety in Mining and Milling of Nuclear Materials*, Vol. II, I.A.E.A., Vienna, 1964.

Analytica Chimica Acta
Elsevier Publishing Company, Amsterdam
Printed in The Netherlands

DETERMINATION OF SUBMICROGRAM AMOUNTS OF SELENIUM(IV) BY MEANS OF THE CATALYTIC REDUCTION OF 1,4,6,11-TETRAAZANAPHTHACENE

TAKUJI KAWASHIMA* AND MOTOHARU TANAKA
Laboratory of Analytical Chemistry, Faculty of Science, Nagoya University, Chikusa-ku, Nagoya (Japan)

(Received April 18th, 1967)

Since 3,3′-diaminobenzidine was proposed as a specific reagent for selenium(IV)[1,2], a large number of *o*-diamines have been exploited and employed for the spectrophotometric and fluorimetric determination of microgram amounts of selenium(IV)[3–16]. On the other hand, the catalytic effect of selenium on the reduction of methylene blue has been studied in qualitative and quantitative analyses for this element[17,18].

A short communication by the present authors[19] has noted the possible analytical application of the catalytic effect of selenium in the following reaction[20,21]:

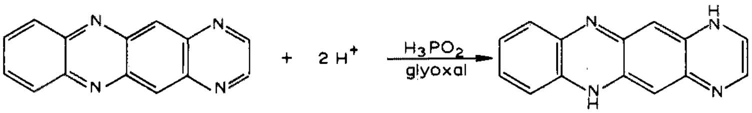

1,4,6,11-tetraaza-naphthacene (TAN)
(λ_{max}=478 nm)

1,6-dihydro-1,4,6,11-tetraazanaphthacene (DHTAN)
(λ_{max}=570, 600 nm)

The present paper describes details of the method, which allows the determination of submicrogram amounts of selenium(IV).

EXPERIMENTAL

Reagents

1.5·10⁻⁴ M 2,3-diaminophenazine solution. For the preparation of 2,3-diaminophenazine (DAP) the procedure given by ULLMANN AND MAUTHNER[22] was followed with a slight modification; 21.2 mg of DAP hydrochloride are dissolved in 500 ml of 0.1 *M* hydrochloric acid by gentle warming. The solution is stable for at least 2 weeks in a dark place at room temperature. If some crystals separate out, it is necessary to warm the solution before use.

Stock selenium solution (1 mg of Se/ml). Dissolve 2.20 g of anhydrous sodium selenite in 1 l of 0.1 *M* hydrochloric acid. Standardize the solution iodimetrically.

---

[*] Present address: Chemical Institute, Liberal Arts College, Kagoshima University, Kagoshima (Japan).

Prepare working solutions containing less than 1.5 μg of Se/ml by appropriate dilution with 0.1 *M* hydrochloric acid.

4% Glyoxal solution. Dilute 5 ml of commercial 40% glyoxal to 50 ml with 0.1 *M* hydrochloric acid. Prepare fresh daily. Standardize the 40% glyoxal gravimetrically with 2,4-dinitrophenylhydrazine.

50% Hypophosphorous acid. This is commercially available; the concentration of the acid was found to be 10.1 *M*.

Other reagents used were of general-reagent grade.

Apparatus

Beckman Model DU spectrophotometer with 1-cm Corex cells; Radiometer Type PHM 22 pH meter with glass electrode; Sharp Model TEB-10 thermoelectric circulating bath.

Preliminary test procedure

The sample solution (45 ml) containing 1 μg of selenium(IV), glyoxal and DAP was placed in a 100-ml reaction vessel; 5 ml of 50% hypophosphorous acid was placed in a glass-stoppered test tube. Both solutions were kept at 50° in a thermostat, to attain thermal equilibrium (about 10 min), and then mixed to initiate the reaction. At a definite reaction time several ml of the solution was pipetted into a dry test tube immersed in an ice-water bath. Then the absorbance was measured at 600 nm, the characteristic wavelength for the absorption of the 1,6-dihydro-1,4,6,11-tetraazanaphthacene.

RESULTS AND DISCUSSION

DAP ($\lambda_{max}=492$ nm) reacts with glyoxal to form 1,4,6,11-tetraazanaphthacene (TAN) ($\lambda_{max}=478$ nm)[20].

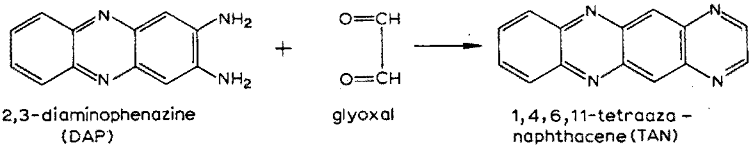

In the presence of hypophosphorous acid the latter is reduced to a blue compound, 1,6-dihydro-1,4,6,11-tetraazanaphthacene (DHTAN). This reduction is catalyzed by a minute amount of selenium(IV).

Absorption spectra

The absorption spectra of DAP, TAN and DHTAN are shown in Fig. 1; the absorption maxima are found at 492 and 478 nm for DAP and TAN respectively, and at 570 and 600 nm for DHTAN. The absorption spectrum of the latter conforms to the previous finding by DECHARY *et al.*[20].

Effect of temperature

As expected the reaction proceeds faster at higher temperature as illustrated in Fig. 2. Although in principle higher sensitivity can be realized at higher reaction

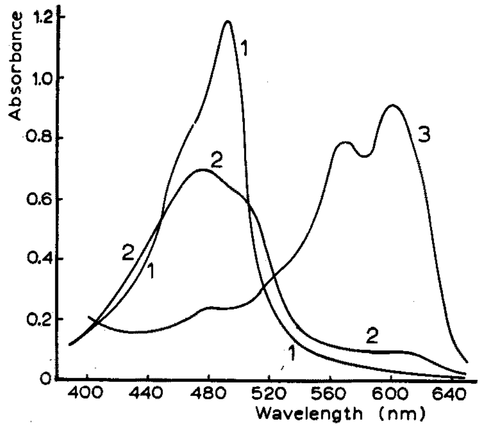

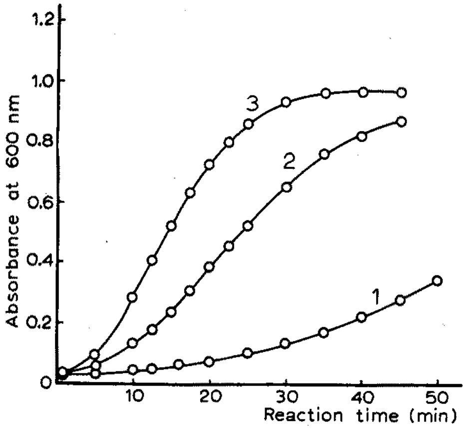

Fig. 1. Absorption spectra of 2,3-diaminophenazine (DAP) (1), 1,4,6,11-tetraazanaphthacene (TAN) (2) and 1,6-dihydro-1,4,6,11-tetraazanaphthacene (DHTAN) (3). Concentration of dyestuffs, $3.0 \cdot 10^{-5}$ *M*; [H^+], $3 \cdot 10^{-1}$ *M*.

Fig. 2. Effect of temperature. Curve 1, 40.0±0.2°; Curve 2, 49.4±0.2°; Curve 3, 55.4±0.2°. DAP, $3.0 \cdot 10^{-5}$ *M*; glyoxal, $1.8 \cdot 10^{-2}$ *M*; H_3PO_2, 1 *M*; [H^+], $3 \cdot 10^{-1}$ *M*; Se(IV), 0.98 μg/50 ml.

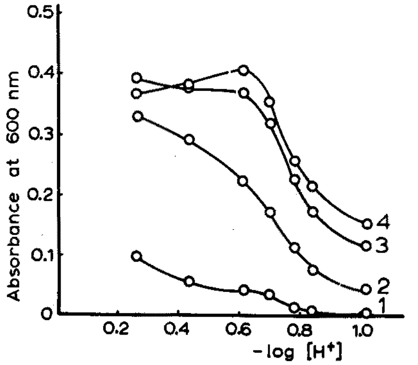

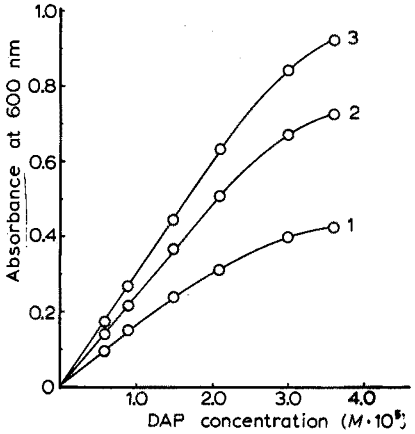

Fig. 3. Effect of hydrogen ion concentration. Reaction time: (1) 10 min; (2) 20 min; (3) 30 min; (4) 35 min. Reaction temperature, 49. 6±0.2°; DAP, $3.0 \cdot 10^{-5}$ *M*; glyoxal, $1.8 \cdot 10^{-2}$ *M*; H_3PO_2, 1 *M*; Se(IV), 0.98 μg/50 ml.

Fig. 4. Effect of 2,3-diaminophenazine concentration. Reaction time: (1) 20 min; (2) 30 min; (3) 40 min. Reaction temperature, 49.6±0.2°; glyoxal, $1.8 \cdot 10^{-2}$ *M*; H_3PO_2, 1 *M*; [H^+], $3 \cdot 10^{-1}$ *M*; Se(IV), 0.98 μg/50 ml.

temperature, the determination of selenium(IV) should preferably be carried out at a temperature between 50° and 55°, because the decomposition of the product (DHTAN) and the blank absorbance become appreciable at temperatures higher than 55°.

Effect of the hydrogen ion concentration

Figure 3 illustrates the effect of the hydrogen ion concentration on the rate of the reaction. The optimum conditions are found in the [H^+] range 3–$4 \cdot 10^{-1}$ *M* for reaction times of about 30 min. Thus the reaction was carried out at a hydrogen ion concentration of $3 \cdot 10^{-1}$ *M* for the determination of selenium.

Effect of 2,3-diaminophenazine concentration

As is evident from Fig. 4, the reaction is of the first order with respect to the DAP concentration. Taking into account the solubility of DAP and the attainable sensitivity, the concentration was fixed at $3.0 \cdot 10^{-5}$ *M*.

Effect of glyoxal concentration

TAN was reduced in the presence of various amounts of glyoxal. Glyoxal plays a role as a reactant not only in the formation of TAN but also in the reduction of this compound. And the role of glyoxal as a reductant differs to some extent in the presence and in the absence of selenium (see the rate law given below). The absorbance at 600 nm rose steeply as the glyoxal concentration was increased to $1.3 \cdot 10^{-2}$ *M* and decreased gradually with glyoxal concentrations above $3 \cdot 10^{-2}$ *M*. The optimum concentration of glyoxal was found to lie in the range of concentration from $1.3 \cdot 10^{-2}$–$2.5 \cdot 10^{-2}$ *M*. The reaction was carried out with a concentration of $1.8 \cdot 10^{-2}$ *M* glyoxal.

Effect of hypophosphorous acid concentration

The results for the effect of hypophosphorous acid concentration are shown in Fig. 5. In order to avoid the pH changes arising from the differences in the amount of hypophosphorous acid, the reaction was carried out at higher acidity ($[H^+]: 6 \cdot 10^{-1}$ *M*). As is evident from Fig. 5, the reaction is of the first order with respect to hypophosphorous acid concentration. The concentration was fixed at 1.0 *M*.

Stability of the color after quenching

When the reaction mixture was allowed to stand at room temperature(25°) after quenching in an ice-water bath, the reaction proceeded slowly and the absorb-

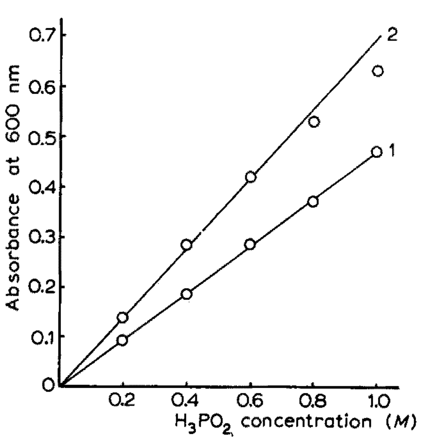

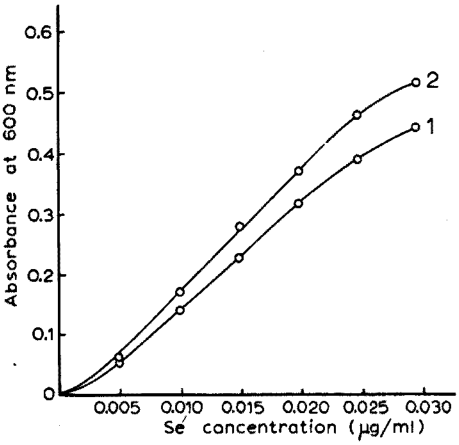

Fig. 5. Effect of hypophosphorous acid. Reaction time: (1) 15 min; (2) 20 min. Reaction temperature, 49.6±0.2°; DAP, $3.0 \cdot 10^{-5}$ *M*; glyoxal, $1.8 \cdot 10^{-2}$ *M*; $[H^+]$, $6 \cdot 10^{-1}$ *M*; Se(IV), 0.98 μg/50 ml.

Fig. 6. Working curves for selenium. Reaction time: (1) 25 min; (2) 30 min. Light path, 10 mm; wavelength, 600 nm.

ance increased gradually. But the absorbance remained unchanged for at least 40 min when the solution was kept in an ice-water bath. Thus the reaction mixture should be quenched and kept in an ice-water bath until the absorbance measurement.

Recommended procedure

Take 4.5 ml of sample solution (about 0.1 M in hydrochloric acid) containing not more than 0.15 μg of selenium(IV), 0.10 ml of 4% glyoxal and 1.0 ml of DAP ($1.5 \cdot 10^{-4} M$) in a glass-stoppered test tube. Maintain the solution for about 10 min at 50° in a thermostat, until thermal equilibrium is reached. Add 0.5 ml of hypophosphorous acid solution to initiate the reaction. At exactly 30 min after the addition of hypophosphorous acid, quench the reaction in an ice-water bath. Then measure the absorbance at 600 nm preferably within 30 min.

Typical working curves are shown in Fig. 6.

Effect of diverse ions

The following elements or compounds do not interfere with the determination of 0.1 μg of selenium at least up to the specified amount: magnesium(II) (1 mg), calcium(II) (1 mg), cobalt(II) (1 mg), nickel(II) (1 mg), aluminum(III) (1 mg), arsenic(III) (0.15 mg), arsenic(V) (0.15 mg), zinc(II) (0.1 mg), lead(II) (0.1 mg), cadmium(II) (0.1 mg), tin(IV) (0.1 mg), molybdenum(VI) (0.01 mg), sodium chloride (20 mg), potassium chloride (20 mg), ammonium chloride (20 mg), ammonium sulfate (20 mg), potassium nitrate (20 mg), tartaric acid (20 mg).

Barium(II) (1 mg), iron(III) (1 mg) and manganese(II) (0.01 mg) give rise to a negative interference (Table I). With copper(II) (0.01 mg), vanadium(V) (0.1 mg) and tungsten(VI) (0.1 mg), positive interferences are observed. These elements seem to act as catalysts in the color development. The positive interference of antimony(III) can effectively be eliminated by tartaric acid. Bismuth(III), tin(II), tellurium(IV) and iodide should be avoided because the mode of color development is different in

TABLE I

EFFECT OF INTERFERING IONS ON THE DETERMINATION OF 0.106 μg OF SELENIUM BY THE RECOMMENDED PROCEDURE

Ion added	μg	*Se found*(μg)	*Ion added*	μg	*Se found*(μg)
Sb(III)	240	0.145	Mn(II)	10	0.085
	240	0.105		1	0.095
Ba	1000	0.003	Te(IV)	10	>0.15
	100	0.075		1	0.047
	10	0.093		0.1	0.088
Bi(III)	10	0.078	Sn(II)	100	0.074
	10[a]	0.097		10	0.098
	1	0.103	V(V)	10	0.123
Cu(II)	10	0.123		1	0.115
	1	0.105	W(VI)	100	0.135
Fe(III)	1000	0.002		10	0.103
	100	0.093			
I^-	1000	>0.15			
	100	0.078			
	10	0.110			
	1	0.118			

[a] 20 mg of tartaric acid were added.

the presence of these elements. However, the presence of tin(II) and iodide together with selenium(IV) in a sample solution seems quite unlikely. Most of these interfering elements can be separated from selenium(IV) by solvent extraction with oxine and/or by ion exchange.

Since selenium(VI) does not give rise to any coloration, the method allows the determination of selenium(IV) in selenium(VI) compounds.

Mechanism of the reaction

The color formation is first order with respect to the concentration of DAP, hypophosphorous acid and selenium(IV). In the absence of selenium, the reaction is first order in glyoxal concentration, while lower glyoxal dependence is observed in the presence of selenium. Thus the role of glyoxal seems to be different in the presence and in the absence of selenium. The rate law for the reaction may therefore be expressed as:

$$v = \frac{\mathrm{d[DHTAN]}}{\mathrm{d}t} = \{k_1[\text{glyoxal}] + k_2[\text{Se}][\text{glyoxal}]^a\}[\text{DAP}][\text{H}_3\text{PO}_2]$$

where square brackets denote concentrations and a is about 2/3. An unidentified product of the reaction of glyoxal with hypophosphorous acid reduces TAN to DHTAN and selenium(IV) acts as a catalyst in the reaction.

Details of the kinetic study will be published elsewhere.

SUMMARY

In the presence of glyoxal and hypophosphorous acid 1,4,6,11-tetraazanaphthacene is reduced to 1,6-dihydro-1,4,6,11-tetraazanaphthacene. The reaction is catalyzed by selenium(IV). By means of this catalytic reaction, submicrogram amounts of selenium(IV) can easily be determined. The method is simple and sensitive, and there are few interferences.

RÉSUMÉ

En présence de glyoxal et d'acide hypophosphoreux le 1,4,6,11-tétrazanaphtacène est réduit en 1,6-dihydro-1,4,6,11-tétrazanaphtacène. La réaction est catalysée par le sélénium(IV). Cette réaction catalytique permet de doser facilement des teneurs en sélénium(IV) de l'ordre du submicrogramme. Cette méthode est simple et sensible et ne présente que peu d'interférences.

ZUSAMMENFASSUNG

In Gegenwart von Glyoxal und Hypophosphorsäure wird 1,4,6,11-Tetraazanaphthazen zu 1,6-Dihydro-1,4,6,11-Tetraazanaphthazen reduziert. Die Reaktion wird durch Selen(IV) katalysiert. Mittels dieser katalytischen Reaktion können Submikro-Mengen von Selen(IV) leicht bestimmt werden. Die Methode ist einfach, empfindlich und besitzt nur wenige Störungen.

REFERENCES

1 J. Hoste, *Anal. Chim. Acta*, 2 (1948) 402.
2 J. Hoste and J. Gillis, *Anal. Chim. Acta*, 12 (1955) 158.
3 K. Cheng, *Anal. Chem.*, 28 (1956) 1738; *Chemist-Analyst*, 45 (1956) 67.
4 T. Danzuka and K. Ueno, *Anal. Chem.*, 30 (1958) 1370.
5 J. H. Watkinson, *Anal. Chem.*, 32 (1960) 981.
6 W. J. Kelleher and M. J. Johnson, *Anal. Chem.*, 33 (1961) 1429.
7 P. W. West and Ch. Cimerman, *Anal. Chem.*, 36 (1964) 2013.
8 C. A. Parker and L. G. Harvey, *Analyst*, 86 (1961) 54; 87 (1967) 558.
9 P. F. Lott, P. Cukor, G. Moriber and J. Solga, *Anal. Chem.*, 35 (1963) 1159.
10 H. Ariyoshi, M. Kiniwa and K. Toei, *Talanta*, 5 (1960) 112.
11 L. J. Throop, *Anal. Chem.*, 32 (1960) 1807.
12 C. Le Peintre, *Compt. Rend.*, 253 (1961) 1696.
13 E. Sawicki, *Anal. Chem.*, 29 (1967) 1376.
14 D. Demeyere and J. Hoste, *Anal. Chim. Acta*, 27 (1962) 288.
15 P. Cukor, J. Walzcyk and P. F. Lott, *Anal. Chim. Acta*, 30 (1964) 473.
16 M. Tanaka and T. Kawashima, *Talanta*, 12 (1965) 211.
17 F. Feigl and P. W. West, *Brazil, Min. Agr., Dept. Nac. Prod. Mineral, Lab. Prod. Mineral*, Bol. No. 24 (1946) 13; *Anal. Chem.*, 19 (1947) 351.
18 H. Goto, T. Hirayama and S. Ikeda, *J. Chem. Soc. Japan, Pure Chem. Sect.*, 73 (1952) 652.
19 M. Tanaka, T. Kawashima and H. Miwa, *Bull. Chem. Soc. Japan*, 37 (1964) 1085.
20 J. W. Dechary, E. Kun and H. C. Pitot, *Anal. Chem.*, 26 (1954) 449.
21 E. Sawicki, T. R. Hauser and R. Wilson, *Anal. Chem.*, 34 (1962) 505.
22 F. Ullmann and F. Mauthner, *Ber.*, 35 (1902) 4302.

Analytica Chimica Acta
Elsevier Publishing Company, Amsterdam
Printed in The Netherlands

SEPARATION OF ALKALINE EARTH ELEMENTS BY CATION-EXCHANGE CHROMATOGRAPHY IN AMMONIUM MALONATE MEDIA

F. W. E. STRELOW AND C. R. VAN ZYL
National Chemical Research Laboratory, South African Council for Scientific and Industrial Research, Pretoria (South Africa)
AND C. R. NOLTE
Department of Inorganic Chemistry, University of Pretoria, Pretoria (South Africa)

(Received April 24th, 1967)

The separation of the elements of the alkaline earth group, Mg(II), Ca(II), Sr(II) and Ba(II) by ion-exchange chromatography has received considerable attention during the last decade. Eluants employed include hydrochloric acid[1], hydrochloric acid–methanol[2], ammonium chloride[3], ammonium acetate[4,5], ammonium formate[6], ammonium acetate or formate plus methanol[7], the ammonium salts of citrate[8], lactate[9] and α-hydroxyisobutyrate[10,11], and EDTA[12] and DCyTA[13,14] for cation exchange; ammonium citrate[15] and nitric acid–methanol or ethanol mixtures[16,17] have been used for anion-exchange chromatography. Hydrochloric acid would be the most attractive of these eluants because it can be removed most easily, but the separation factor for the calcium(II)–strontium(II) pair is rather small ($\alpha \approx 1.4$ for the concentration range 1 N to 2 N hydrochloric acid with Dowex 50W-X8 or an equivalent resin); thus only small amounts of strontium can be separated quantitatively and fairly large columns are required. The best eluants for calcium(II)–strontium(II)–barium(II) separations probably are lactate, α-hydroxyisobutyrate, EDTA and DCyTA, but the destruction of these reagents in the eluates is rather tedious and the magnesium(II)–calcium(II) separations are not very satisfactory. With α-hydroxyisobutyrate, magnesium forms an insoluble precipitate when present in larger than trace amounts, and with EDTA and DCyTA it appears in the eluate between calcium(II) and strontium(II). Anion exchange in citrate media or nitric acid–alcohol mixtures provides good Mg(II)–Ca(II)–Sr(II) separations; but the strontium(II)–barium(II) separation is not satisfactory—in citrate because the distribution coefficients for both strontium(II) and barium(II) are too low, and in nitric acid–alcohol because barium and to a lesser extent strontium tend to form insoluble nitrates in the resin matrix.

In ammonium acetate reasonable separations for Mg(II)–Ca(II)–Sr(II)–Ba(II) mixtures are possible[4], but the separation factors are small (between 1.9 and 2.6 in the relevant region of concentration) and fairly large columns have to be employed for the separation of major amounts. The addition of an organic solvent such as alcohol leads to considerably increased separation factors[7], but this is accompanied by slower exchange rates, peak broadening and increased tailing.

CANNAN AND KIBRICK[18] have shown that the stabilities of the alkaline earth association complexes with malonate decrease with increasing atomic weights from magnesium to barium. Increased separation factors compared with hydrochloric acid or ammonium chloride, therefore can be expected for cation exchange using ammonium malonate eluants. Also, the malonate ions can be destroyed without the formation of carbonaceous matter by heating at low temperatures.

$$CH_2[COONH_4]_2 \xrightarrow{\Delta} CH_3COOH\uparrow + CO_2\uparrow + 2NH_3\uparrow \qquad (1)$$

Alternatively, after separation, the eluates can be treated with a slight excess of hydrochloric acid (pH *ca.* 1.5), diluted to contain not more than 0.5 N ammonium chloride and passed through a column of AG50W-X8 resin in the hydrogen form. The malonate and ammonium ions can be eluted with 0.5 N hydrochloric acid, followed by elution of the alkaline earth metal with a suitable concentration of either hydrochloric or nitric acid.

Since the ion-exchange behaviour of the elements in the alkaline earth group in ammonium malonate media does not seem to have received attention in the literature, it was decided to determine the equilibrium distribution coefficients for these elements systematically and apply the results for the development of separations. Beryllium also was included in the investigation.

EXPERIMENTAL

Apparatus and reagents

Analytical-reagent grade chemicals were used throughout with the exception of malonic acid, which was obtained as a 99% pure reagent (Fluka AG, Bucks, Switzerland). It was further purified from traces of cations by passing a solution (about 2 N) through a cation-exchange column in the hydrogen form. This is very effective for removal of traces of alkaline earth elements because their distribution coefficients in 2 N malonic acid are around 1000 or higher.

The resin used was the AG50W-X8 sulphonated polystyrene; 100–200-mesh particle size was used for equilibrium studies and 200–400-mesh particle size for column experiments. Unless otherwise specified, the resin was used in the ammonium form. Borosilicate glass tubes of 2 cm inner diameter with fused-in glass sinter plates of No. 2 porosity and a burette tap at the bottom were used as columns.

A Perkin-Elmer 303 atomic absorption spectrophotometer was employed for determinations of low concentrations of the alkaline earth metals.

Equilibrium distribution coefficients

Coefficients were determined by equilibrating for 24 h in a mechanical shaking apparatus 2.718 g of dry AG50W-X8 resin in the ammonium form (equivalent to 2.500 g of resin in the hydrogen form) with 250 ml of a solution containing 1 mmol of the required element and the required concentration of ammonium malonate; 2.500 g of resin in the hydrogen form was used for determining coefficients in malonic acid. After the resin had been separated from the aqueous phase by filtration, the amounts of the elements in both phases were determined by suitable analytical methods and the coefficients

$$D = \frac{\overset{\text{Equivalents in resin phase}\,\cdot\,\text{ml solution}}{\cancel{\text{equivalents in resin phase}}}}{\underset{\text{Equivalents in aqueous phase}\,\cdot\,\text{g resin}}{\cancel{\text{equivalents in aqueous phase}}}} \cdot \frac{\cancel{\text{g resin}}}{\cancel{\text{ml solution}}}$$

were calculated from the results. All results refer to water-free resin in the H^+-form. The analytical methods are summarized in Table I and the distribution coefficients are presented in Table II.

From plots of distribution coefficients against ammonium malonate concentrations, separation factors, $\alpha = D_A/D_B$ for element pairs were estimated for D-values of 10 for the more weakly absorbed element. The separation factors and the corresponding eluant concentrations are given in Table III.

Coefficients in malonic acid also were determined and were found to be very high over the concentration range 0.1–2.0 N [$D > 10^3$ for Mg(II), Ca(II), Sr(II), Ba(II), and Be(II)].

TABLE I

ANALYTICAL METHODS USED

Element	*Method*
Be(II)	Gravimetrically as cupferron complex.
Mg(II)	Titration with EDTA; eriochrome black T indicator. Small amounts by atomic absorption spectrometry.
Ca(II)	Titration with EDTA; methylthymol blue indicator. Gravimetrically as $CaSO_4$ in resin phase (for equilibria). Small amounts by atomic absorption spectrometry.
Sr(II)	Gravimetrically as $SrSO_4$. Small amounts by atomic absorption spectrometry.
Ba(II)	Gravimetrically as $BaSO_4$. Small amounts by atomic absorption spectrometry; nitrous oxide flame, solution of chloride in 96% ethanol.

TABLE II

EQUILIBRIUM DISTRIBUTION COEFFICIENTS IN AMMONIUM MALONATE MEDIA

Element	*Normality of ammonium malonate*					
	0.1 N	*0.2 N*	*0.5 N*	*1.0 N*	*2.0 N*	*3.0 N*
Be(II)	7.8	5.1	3.3	<1.0	<1.0	<1.0
Mg(II)	205	49.3	8.0	3.2	1.6	0.8
Ca(II)	910	290	33.7	7.3	1.8	0.9
Sr(II)	1760	460	71	17.3	3.8	2.0
Ba(II)	4500	990	160	40.5	13.3	11.1

TABLE III

SEPARATION FACTORS

Separation	*Factor*	*Normality malonate*
Be(II)–Mg(II)	26	0.10
Mg(II)–Ca(II)	4.3	0.45
Ca(II)–Sr(II)	2.4	0.87
Sr(II)–Ba(II)	2.7	1.27

Elution curves

Favourable conditions for separation of element pairs were estimated from plots of D-values against eluant concentration and experimental elution curves were prepared at the estimated conditions. The elements were absorbed from a solution 0.1 N in ammonium malonate and 0.1 N in malonic acid on a column of AG50W-X8 resin in the ammonium form. They were washed on to the column with a solution containing the same concentration of these reagents. The elements were then eluted with the chosen concentration of ammonium malonate at a flow rate of 2.0 ± 0.2 ml/min; 25-ml fractions were taken with an automatic fractionator, and, after removal of the malonate, analysed by a suitable method.

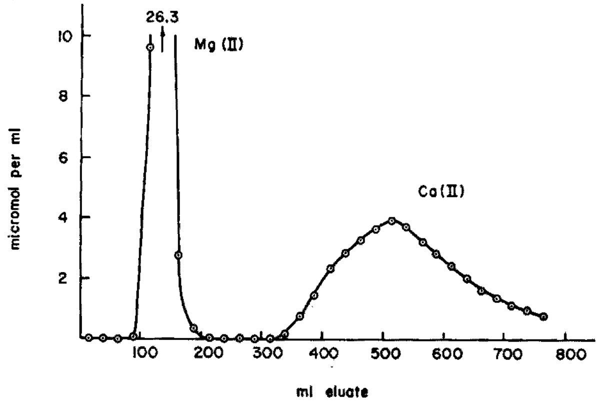

Fig. 1. Elution curve for Mg(II)–Ca(II) with 0.40 N ammonium malonate at pH 7. Column of 30-ml AG50W-X8 resin, 200–400 mesh, NH_4^+-form. Flow rate 3.0 ± 0.2 ml/min; 1 mmole Mg(II) + 1 mmole Ca(II).

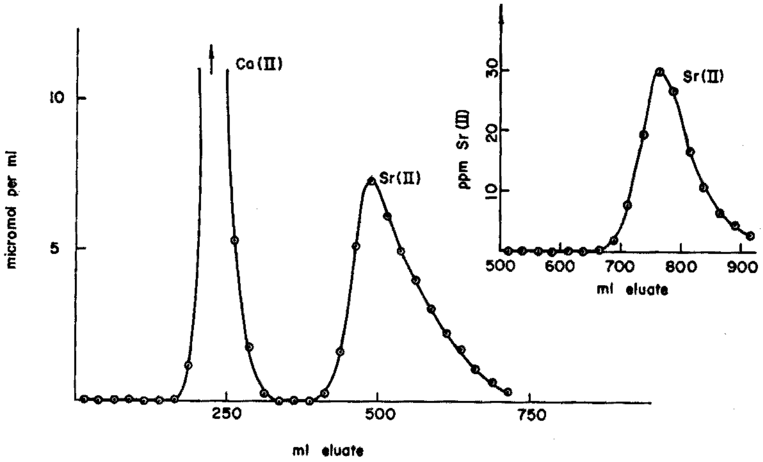

Fig. 2. Elution curve for Ca(II)–Sr(II) with 0.80 N ammonium malonate at pH 7. Column of 60-ml AG50W-X8 resin, 200–400 mesh, NH_4^+-form. Flow rate 2.0 ± 0.2 ml/min; 1 mmole Ca(II) + 1 mmole Sr(II).

Figure 1 presents the experimental elution curve for the magnesium(II)–calcium(II) pair (1 millimole of each element) with 0.40 N ammonium malonate as eluant.

Figure 2 shows an elution curve for the calcium(II)–strontium(II) pair with columns of 20 g resin and an eluant concentration of 0.80 *N*. An insert in this Fig. shows the position of the strontium elution peak when only small amounts (0.05 millimole) are present. Under the same conditions as those mentioned for Fig. 2 but with a 0.70 *N* malonate solution as eluant, calcium(II) was eluted in the 230–470-ml portion of the eluate and strontium(II) in the portion from 560 to *ca.* 900 ml, the separation thus being better than with 0.80 *N* malonate.

Figure 3 shows an elution curve for a Be(II)–Mg(II)–Ca(II)–Sr(II)–Ba(II) mixture containing 0.5 millimole of each element. The metal ions were absorbed from 50 ml of 0.20 *N* ammonium malonate solution containing 0.1 *N* free malonic acid and were eluted with a sequence of 200 ml of 0.20 *N* ammonium malonate + 0.10 *N* malonic acid for beryllium(II), 250 ml of 0.50 *N* ammonium malonate for magnesium(II), 800 ml of 0.80 *N* ammonium malonate for calcium(II) and strontium(II) and 200 ml of 3.0 *N* nitric acid for barium(II).

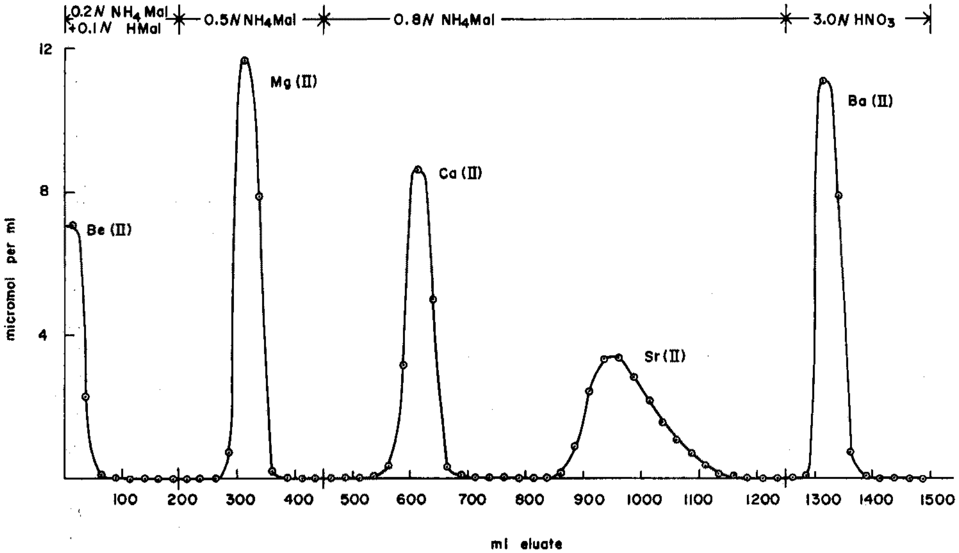

Fig 3. Elution curve for Be(II)–Mg(II)–Ca(II)–Sr(II)–Ba(II) with ammonium malonate at pH 7. Column of 60-ml AG50W-X8 resin, 200–400 mesh, NH_4^+-form. Flow rate 2.0 ± 0.2 ml/min; 0.5 mmole of each element.

Quantitative separations

Beryllium(II)–magnesium(II). The metal ions were absorbed from 100 ml of 0.20 *N* ammonium malonate + 0.1 *N* malonic acid on a column of 10 g (30 ml) of AG50W-X8 resin. Beryllium(II) was eluted with 200 ml of an eluant containing the same malonate–malonic acid concentrations, at a flow rate of 2.0 ml/min. About 100 ml of 0.50 *N* hydrochloric acid were passed through the column to remove the malonate and part of the ammonium ions and magnesium was then eluted with 200 ml of 2.0 *N* hydrochloric acid at a flow rate of 3.0 ± 0.2 ml/min.

Magnesium(II)–calcium(II). The metal ions were absorbed from 50 ml of a neutral chloride solution on a 10-g resin column. Magnesium(II) was eluted with 250 ml of 0.40 N ammonium malonate at 2.0±0.2 ml/min; the first 50 ml of eluate was discarded. Malonate and most of the ammonium ions were removed with 200 ml of 0.50 N hydrochloric acid, and calcium(II) was then eluted with 200 ml of 3.0 N hydrochloric acid at 3.0±0.2 ml/min.

Calcium(II)–strontium(II). The metal ions were absorbed from 50 ml of a neutral chloride solution on a 20-g resin column. Calcium(II) was eluted with 500 ml of 0.70 N ammonium malonate at a flow rate of 2.0±0.2 ml/min; the first 200 ml were discarded. Malonate and part of the ammonium ions were then eluted with 200 ml of 0.50 N hydrochloric acid and finally the strontium(II) with 300 ml of 3.0 N hydrochloric acid at 3.0±0.2 ml/min. When large amounts of calcium (10 mmole) and small amounts of strontium (<0.1 mmole) were present, 450 ml of 0.80 N malonate was used to elute the calcium(II) and the ammonium ions were removed with 500 ml of 0.50 N hydrochloric acid.

Strontium(II)–barium(II). The elements were absorbed as described for Ca(II)–Sr(II) and strontium(II) was eluted with 450 ml of 1.10 N ammonium malonate at a flow rate of 1.5±0.2 ml/min. The first 100 ml of eluate was discarded. Malonate and ammonium ions were removed as described above and barium was then eluted with 300 ml of 3.0 N nitric acid at 3.0±0.2 ml/min.

Be(II)–Mg(II)–Ca(II)–Sr(II)–Ba(II). One millimole of beryllium(II) plus 0.5 millimole of each of the other 4 elements in 100 ml of 0.20 N ammonium malonate containing 0.10 N free malonic acid were absorbed on a 20-g (60 ml) resin column. Beryllium(II) was eluted with 200 ml of 0.20 N ammonium malonate containing 0.10 N malonic acid. The eluate was taken from the beginning of the absorption step. The next metal ions were then eluted with stepwise increasing concentrations of ammonium malonate: 300 ml of 0.50 N for magnesium(II), 450 ml of 0.70 N for calcium(II), and 350 ml of 1.10 N for strontium(II). Malonate and ammonium ions were removed from the column by elution with 500 ml of 0.50 N hydrochloric acid, and barium(II) finally was eluted with 200 ml of 3.0 N nitric acid. A flow rate of 2.0±0.2 ml/min was maintained throughout.

Separation from malonate

The eluates of those elements which were eluted first contained ammonium malonate. In the case of beryllium this was removed by adding a slight excess of nitric acid (pH *ca.* 1.5) to the eluate and passing it through a 20-g columm of AG50 W-X8 resin in the H^+-form. After the malonate and ammonium ions had been eluted with 600 ml of 0.50 N nitric acid, the beryllium(II) could be eluted quantitatively with 250 ml of 2.0 N hydrochloric acid.

In the cases of the other elements the eluates were caught in teflon beakers and evaporated to dryness on a sand-bath or hot-plate, the final temperature being about 250°. This destroyed ammonium malonate, as described in eqn. (1), without the formation of carbonaceous matter. The residues were dissolved in hydrochloric acid and the metal ions were determined (Table I). In the case of microgram amounts of strontium(II) and barium(II), traces of interfering elements (mostly sodium and ammonium ions) sometimes were removed by cation exchange on a small column of AG50W-X8 resin before atomic absorption spectrometry was applied. The results of quantitative separations are shown in Table IV.

TABLE IV

RESULTS OF QUANTITATIVE SEPARATIONS

Taken				*Found*			
Element	*mg*	*Element*	*mg*	*Element*	*mg*	*Element*	*mg*
Be(II)	9.16	Mg(II)	24.13	Be(II)	9.13 ± 0.04	Mg(II)	24.15 ± 0.03
Mg(II)	24.13	Ca(II)	39.88	Mg(II)	24.14 ± 0.02	Ca(II)	39.90 ± 0.05
Mg(II)	0.241	Ca(II)	39.88	Mg(II)	0.239 ± 0.003	Ca(II)	39.89 ± 0.04
Mg(II)	120.7	Ca(II)	0.199	Mg(II)	120.6 ± 0.2	Ca(II)	0.200 ± 0.03
Ca(II)	39.88	Sr(II)	87.0	Ca(II)	39.89 ± 0.05	Sr(II)	86.9 ± 0.2
Ca(II)	0.199	Sr(II)	87.0	Ca(II)	0.201 ± 0.004	Sr(II)	87.0 ± 0.2
Ca(II)	398.8	Sr(II)	0.174	Ca(II)	398.9 ± 0.2	Sr(II)	0.172 ± 0.003
Sr(II)	87.0	Ba(II)	137.2	Sr(II)	87.1 ± 0.3	Ba(II)	137.1 ± 0.2
Sr(II)	0.174	Ba(II)	137.2	Sr(II)	0.172 ± 0.03	Ba(II)	137.2 ± 0.2
Sr(II)	870.0	Ba(II)	0.274	Sr(II)	870.6 ± 1.1	Ba(II)	0.272 ± 0.006
		Be(II)	18.31	Be(II)	18.34 ± 0.07		
		Mg(II)	12.07	Mg(II)	12.06 ± 0.03		
		Ca(II)	19.94	Ca(II)	19.96 ± 0.04		
		Sr(II)	43.5	Sr(II)	43.4 ± 0.2		
		Ba(II)	68.6	Ba(II)	68.5 ± 0.1		

DISCUSSION

The elements of Group 2A from beryllium to barium can be separated from each other quantitatively in a single column run by elution with stepwise increasing concentrations of ammonium malonate from a column of AG50W-X8 resin in the ammonium form. Separation factors are larger than those in hydrochloric acid, ammonium chloride and ammonium formate or acetate for all the ion pairs involved. The separation factor for the calcium–strontium pair, which is the smallest (Table III), is smaller than the factors obtained in lactate and α-hydroxyisobutyrate media, but the total selectivity spread from magnesium(II) to barium(II) or from beryllium(II) to barium(II) as given by the separation factor at a distribution coefficient of 10 for the least strongly absorbed element is distinctly larger: $\alpha^{Ba}_{Mg} = 23$ and $\alpha^{Ba}_{Be} \approx 450$ for malonate as compared with $\alpha^{Ba}_{Mg} = 11$ and $\alpha^{Ba}_{Be} = 27$ for lactate.

Exchange rates are slower than those in hydrochloric or nitric acid solutions. Slow flow rates and small resin particle sizes therefore can improve separations considerably by reducing tailing and giving sharper elution peaks, especially for the heavier alkaline earths. Under the right conditions, separations are sharp and adjacent pairs of elements can be separated and recovered quantitatively in weight ratios from 1:1000 to 1000:1 and above. The eluant can easily be destroyed without charring by simple heating; for accurate work, this thermal decomposition has to be carried out in teflon or platinum vessels because glass is slightly attacked by the hot concentrated reagent which in this respect resembles oxalic acid. The malonate also can be separated by cation exchange as described for berryllium.

When microgram amounts of one element are separated from large amounts of others, the contribution of the reagents to the amount of the minor element has to be determined carefully. This is especially serious in the cases of magnesium(II) and calcium(II), where it also becomes advisable to carry out separations in a dust-free room to exclude random contributions by airborne particles.

The best eluant concentration for the separation of the larger amounts of calcium(II) and strontium(II) is 0.70 N. At lower eluant concentrations the D-values for calcium(II) become too large and large elution volumes and increased tailing result, while at higher concentrations the element-free volume between the peaks becomes increasingly smaller; but when only small amounts of strontium(II) are present, this element appears much later in the eluate and an eluant concentration of 0.80 N, which provides a faster elution of calcium(II), is preferable. Similarly, the concentrations for the Mg(II)–Ca(II) and Sr(II)–Ba(II) separations can be increased from 0.40 to 0.50 N and from 1.10 to 1.20 N, respectively, for smaller amounts of the more strongly absorbed element.

SUMMARY

Be(II), Mg(II), Ca(II), Sr(II) and Ba(II) can be separated by elution from a cation-exchange column in the ammonium form with increasing concentrations of ammonium malonate. A typical elution sequence for a 60-ml column (volume in H^+-form) of AG50-X8 resin is: 200 ml of 0.20 N ammonium malonate plus 0.10 N malonic acid for Be(II); 300 ml of 0.50 N, 450 ml of 0.70 N, 350 ml of 1.10 N ammonium malonate for Mg(II), Ca(II) and Sr(II), respectively, and 200 ml of 3.0 N nitric acid for Ba(II). Separations are sharp and quantitative for element pairs in weight ratios from 1:1000 to 1000:1. Distribution coefficients, elution curves and quantitative separations are presented.

RÉSUMÉ

Be, Mg, Ca, Sr et Ba peuvent être séparés par élution d'une résine échangeuse de cations sous forme ammonium, avec des concentrations croissantes de malonate d'ammonium. Les séparations sont nettes et quantitatives. Les coefficients de partage sont donnés ainsi que les courbes d'élution et des séparations quantitatives.

ZUSAMMENFASSUNG

Be(II), Mg(II), Ca(II), Sr(II) und Ba(II) können durch Elution von einer Kationenaustauscherkolonne mit steigenden Konzentrationen von Ammoniummalonat getrennt werden. Die Trennungen sind scharf und quantitativ bis zu Gewichtsverhältnissen von 1:1000 bis 1000:1 für ein Elementpaar. Verteilungskoeffizienten, Elutionskurven und Ergebnisse der quantitativen Trennungen werden angegeben.

REFERENCES

1 L. MAZZA, L. SARDO AND R. FRACHE, *Gazz. Chim. Ital.*, 95 (1965) 509; *Chem. Abstr.*, 63 (1965) 17115.
2 M. TANAKA, *J. Chem. Soc. Japan, Pure Chem. Sect.*, 85 (1964) 117.
3 H. HOLZAPFEL AND W. TISCHER, *J. Prakt. Chem.*, 27 (1965) 91; *Chem. Abstr.*, 62 (1965) 12422.
4 M. HONDA, *Japan Analyst*, 3 (1953) 132; *Chem. Abstr.*, 48 (1954) 9868.
5 G. EULITZ, *Z. Anal. Chem.*, 178 (1961) 360.
6 H. TSUBOTA AND Y. KITANO, *Bull. Chem. Soc. Japan*, 33 (1960) 765, 770.
7 H. TSUBOTA, *Bull. Chem. Soc. Japan*, 38 (1965) 159; *Chem. Abstr.*, 62 (1965) 12482.

8 E. Hantabal, M. Fojtik, V. Rusek and T. Trnovec, *Chem. Zvesti*, 18 (1964) 203; *Chem. Abstr.*, 61 (1964) 2454.
9 M. Lerner and W. Rieman, *Anal. Chem.*, 26 (1954) 610.
10 L. Wish, *Anal. Chem.*, 33 (1961) 53.
11 F. H. Pollard, G. Nickless and D. Spincer, *J. Chromatog.*, 13 (1964) 224.
12 J. J. Bouquiaux and J. H. C. Gillard, *Anal. Chim. Acta*, 30 (1964) 273.
13 Z. Sulcek, P. Povondra, R. Přibil and R. Stangl, *Talanta*, 9 (1962) 647.
14 P. Povondra and R. Přibil, *Talanta*, 10 (1963) 713.
15 F. Nelson and K. A. Kraus, *J. Am. Chem. Soc.*, 77 (1953) 801.
16 J. S. Fritz and H. Waki, *Anal. Chem.*, 35 (1963) 1079.
17 J. S. Fritz, H. Waki and B. B. Garralda, *Anal. Chem.*, 36 (1964) 900.
18 R. K. Cannan and A. Kibrick, *J. Am. Chem. Soc.*, 60 (1938) 2314.

Analytica Chimica Acta
Elsevier Publishing Company, Amsterdam
Printed in The Netherlands

CHROMATOGRAPHY OF LEAF CHLOROPLAST PIGMENTS ON ION-EXCHANGE PAPERS*

JOSEPH SHERMA
Department of Chemistry, Lafayette College, Easton, Pa. 18042 (U.S.A.)
HAROLD H. STRAIN
Chemistry Division, Argonne National Laboratory, Argonne, Ill. 60439 (U.S.A.)

(Received April 17th, 1967)

One-way chromatography on pure cellulose paper (*e.g.*, Whatman No. 1) is not very effective for the separation of the chloroplast pigments. With many different wash liquids, pigments in spots of the leaf extracts are incompletely separated, the chlorophylls yielding double-tailing zones[1,2]. Carotenoid pigments in the saponified leaf extracts (without chlorophylls) are also incompletely separated by many wash liquids[1,3]. Because chromatography on commercial ion-exchange papers has served to separate various classes of organic compounds[4–6], it was decided to evaluate these papers for the pigment separations.

EXPERIMENTAL

The following papers were employed as received from the manufacturer: Amberlite SA-2 paper (Rohm and Haas) containing 45% of sulfonic acid cation exchanger IRA-120 in the sodium form; Amberlite SB-2 paper (Rohm and Haas) containing 45% of quaternary ammonium anion exchanger IRA-400 in the chloride form; MN-Ionenaustauscherpapier (Macherey, Nagel and Co.), a strongly-acid cellulose sulfonic-acid exchanger in the sodium form; MN-Ionenaustauscherpapier (Macherey, Nagel and Co.), a strongly-basic cellulose quaternary ammonium exchanger in the chloride form.

The first two papers are cellulose interspersed with ion-exchange resin and have an exchange capacity of 1.5–2.0 meq/g. The latter two consist of chemically modified cellulose with an exchange capacity of 0.4–0.5 meq/g.

Ascending development was carried out as previously described[1] in Unitkit tanks (Shandon Co.) lined with Whatman No. 1 paper and wrapped in aluminum foil. Sheets of ion-exchange paper, 20 × 20 cm, were spotted 1″ from the bottom with pigment, air-dried, formed into a cylinder, fastened with tongued clips, and developed in a tank which had been equilibrated with 50 ml of wash liquid for at least 15 min. After the solvent had risen 15 cm past the origin, the paper was removed and the zones observed.

Separated zones were detected by visual observation and by color reactions with hydrochloric acid. The pigments eluted from the individual zones were identified

---

[*] Work performed in the Chemistry Department, Lafayette College.

by their spectral absorption properties, with a Beckman DK-2A recording spectrophotometer.

Leaf extracts were prepared by disintegrating 2.0 g of fresh spinach in a blender with acetone, centrifuging and salting the pigments into petroleum ether (60–110°). The solvent was evaporated and the residue dissolved in 1 ml of petroleum ether (60–110°). Alternatively, the green acetone extract was saponified with methanolic potassium hydroxide before the pigments were transferred to 1:1 ether–petroleum ether (60–110°). The solvent was then evaporated and the residue dissolved in 1 ml of 1:1 ether–petroleum ether (60–110°). This procedure[1] removed the green pigments and some colorless material so that the separation of the carotene and xanthophylls could be studied.

The wash liquids were those most effective in the separation of leaf extracts and saponified leaf extracts on cellulose[1-3]. Their compositions are expressed in volume percentages. Low-boiling (20–40°) petroleum ether was used to prepare the wash liquids containing that component.

RESULTS AND DISCUSSION

Figure 1 shows the clearest separations achieved for leaf extracts on the SA-2, MN cation-exchange and SB-2 ion-exchange papers. In each paper, 5 zones were resolved. Chlorophylls *a* and *b* were well separated from each other, but only 3 of the 4 principal carotenoid pigments were found. Small amounts of pheophytin were also noted. These results are very similar to those on Whatman No. 1 with the same wash liquids and level of loading[1]. The developed zones have double-tailing portions[1] characteristic of separations in cellulose paper. This double tailing was eliminated

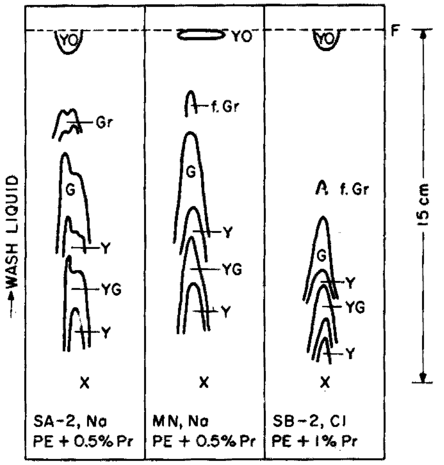

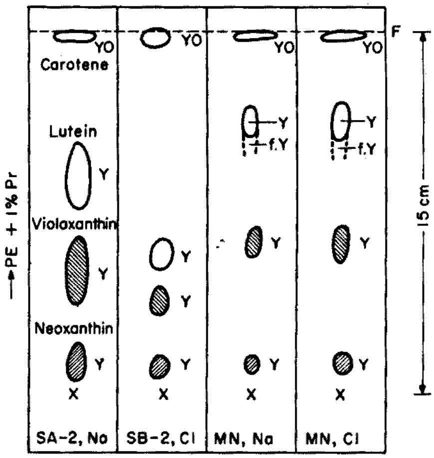

Fig. 1. Pigments in 2 μl of leaf extract separated on various ion-exchange papers with various wash liquids.
F = front, wash liquid; f = faint; G = green; Gr = grey; O = orange; PE = petroleum ether; Pr = *n*-propanol; X = starting point; Y = yellow; \\\ = blue by HCl vapor; /// = green by HCl vapor.

Fig. 2. Pigments in 2 μl of saponified leaf extract separated on various ion-exchange papers with petroleum ether plus 1% propanol as the wash liquid. For abbreviations, see legend to Fig. 1.

when narrow initial zones of the mixture were spread uniformly across the paper, but the separations were identical with those in the central region of the migrating spots. Other ion-exchange papers and wash liquids yielded poorer separations. Under the conditions tested, ion-exchange papers, at best, are no better than Whatman No. 1 paper for the one-way chromatography of the pigments in spots of the leaf extracts.

With saponified leaf extracts, however, ion-exchange papers gave some separations quite superior to those in pure cellulose paper. Figures 2 and 3 show 8 chromatographic systems which yielded a complete separation of the 4 principal carotenoid pigments[7] present in leaves. Compared to earlier results on Whatman No. 1 paper[1,3], the migration order is the same (*i.e.*, neoxanthin (most sorbed), violaxanthin, lutein ± zeaxanthin, carotene (least sorbed)), but the separations are superior.

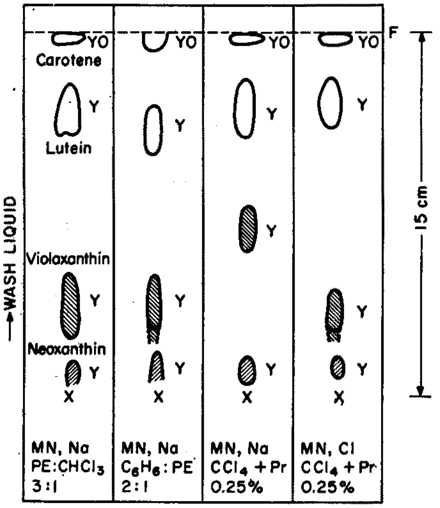

Fig. 3. Pigments in 2 µl of saponified leaf extract separated on ion-exchange papers with various wash liquids. For abbreviations see legend to Fig. 1.

Figure 2 shows results on all 4 ion-exchange papers with petroleum ether plus 1% propanol as the wash liquid. In each case the 4 principal yellow zones were well resolved. Except for the trailing of the lutein zone in the MN papers, no minor zones were observed. The ion-exchange papers dried at 80° for 0.5 h before addition of the pigments gave essentially the same result as the unheated papers. By contrast, Whatman No. 1 paper with this same petroleum ether plus 1% propanol wash liquid served only to separate the carotene from the xanthophylls[1].

Figure 3 shows the results in other systems which resolved the principal carotenoid pigments. On Whatman No. 1 paper, petroleum ether–chloroform did not give a complete separation of neoxanthin and violaxanthin at the same loading[1], and the benzene–petroleum ether and CCl$_4$–propanol wash liquids gave distinguishable but not completely resolved zones[3].

Many other systems involving the 4 ion-exchange papers in combination with various wash liquids were studied, but these gave separations inferior to those shown in Figs. 2 and 3. All of these systems partially resolved the carotenoid pigments, and most of them completely resolved all but two of the pigments. With a few of these wash liquids, however, results on Whatman No. 1 paper were better than corresponding separations on the ion-exchange papers.

When the developed chromatograms were exposed to the vapors of concentrated hydrochloric acid, carotene and lutein remained yellow, violaxanthin turned blue and neoxanthin became blue-green or green[1]. For further identification of the separated pigments, the zones formed by the chromatography of five 10-μl spots were cut out. The individual pigments were eluted with ethanol, and their spectral absorption curves were determined. The wavelengths of the maxima[7,8] corresponded to those of the pigments named in Figs. 2 and 3, and the shapes of the curves were identical with those of pigments from zones resolved by 3:1 petroleum ether–chloroform on Whatman No. 1 paper. Consequently, the ion-exchange papers had not rearranged any of the yellow pigments, as occurs with acids, nor was there any indication of additional major pigments, as reported by other workers[9,10].

Loadings of 2, 5, and 10 μl were tested in each system (1 μl corresponds to 1/1000 of the pigment extracted from 2.0 g of leaves). A loading of 2 μl was found to be best for optimum separation and visual detection of all the principal zones. When the loading was 5 μl, the xanthophyll zones were larger and less well separated; at 10 μl, the xanthophyll zones were even larger and the separations still less.

Another advantage of some ion-exchange papers is the high rate of solvent flow. A typical development of 15 cm required only 15–25 min with SA-2 and SB-2 paper, compared with flow times usually greater than 1 h for Whatman No. 1 and both MN papers.

In most cases, the ion-exchange papers sorbed the carotenoid pigments less strongly than did Whatman No. 1 paper. This was especially pronounced with 1:1 ethyl ether–petroleum ether plus 1% propanol, which carried all the pigments with the solvent front on all 4 ion-exchange papers, but which permitted adsorption on the cellulose paper. This result indicates that ion exchangers, themselves, have a low affinity for the pigments, and several column experiments proved this to be true.

Columns (20 × 1.0 cm) of Dowex 1-X8 (chloride form) resin and Dowex 50-X8 (sodium form) resin (both 50–100 mesh) were prepared with water and petroleum ether plus 1% propanol was passed through until the interstitial water was replaced and the column appeared uniform (50–100 ml). When 500-μl portions of the leaf extract or saponified leaf extracts were applied to either column and eluted with petroleum ether plus 1% propanol, the pigments passed through without sorption. Similar results were obtained when the column ion exchanger was dehydrated with acetone, ether and petroleum ether before addition of the pigments. The results were the same in a column of Amberlyst A-26 resin, a macro-pore anion exchanger specifically designed for nonaqueous solvents.

These results suggest that the cellulose in the ion-exchange papers is mainly responsible for the separations obtained, but that the ion exchanger in the paper is in some cases advantageous, because it distinguishes, more sharply, the yellow pigments, an effect that is undoubtedly complicated. The MN papers with their lower ion-exchange capacity often have even less affinity for a given yellow pigment with a given solvent than do the SA-2 or SB-2 papers. Besides this, the cellulose in the ion-exchange papers might become altered in various ways during the manufacture of the papers, so that more than the dilution of the cellulose with ion-exchanger is involved.

SUMMARY

For the separation of leaf carotenoid pigments, some ion-exchange papers are more effective than pure cellulose papers. Separations of the major pigments on ion-exchange paper are superior to those obtained by uni-dimensional paper chromatography. For green-leaf extracts, ion-exchange papers offer no advantage. Ion-exchange columns do not separate the chloroplast pigments. On ion-exchange paper, there is no major yellow pigment in addition to neoxanthin, violaxanthin, lutein, and carotene.

RÉSUMÉ

Certains papiers échangeurs d'ions sont plus efficaces que ceux de cellulose pure pour la séparation des pigments caroténoïdes des feuilles. Les séparations de la plupart des pigments sur papier échangeur d'ions sont supérieures à celles obtenues par chromatographie uni-dimensionnelle sur papier. Pour les extraits de feuilles vertes les papiers échangeurs d'ions n'offrent aucun avantage. Les colonnes échangeuses d'ions ne permettent pas de séparer les pigments chloroplasts. Sur papier échangeur d'ions, il n'y a pas de pigment jaune à côté de néoxanthine, violaxanthine, lutéine et carotène.

ZUSAMMENFASSUNG

Zur chromatographischen Trennung von Blatt-Carotenoide sind einige Ionenaustauscher-Papiere wirksamer als reine Zellulosepapiere. Trennungen der Hauptpigmente sind auf Ionenaustauscher-Papier denen überlegen, die mit der eindimensionalen Papierchromatographie erhalten wurden. Für die grünen Blattextrakte bieten die Ionenaustauscher-Papiere keinen Vorteil. Ionenaustauscher-Kolonnen trennen die Chloroplast-Pigmente nicht. Auf dem Ionenaustausch-Papier gibt es kein Gelbpigment zusätzlich zum Neoxanthin, Violaxanthin, Lutein und Carotin.

REFERENCES

1 H. H. STRAIN, J. SHERMA, F. L. BENTON AND J. J. KATZ, *Biochim. Biophys. Acta*, 109 (1965) 1.
2 H. H. STRAIN, J. SHERMA AND M. GRANDOLFO, unpublished results.
3 H. H. STRAIN AND M. K. BECK, unpublished results.
4 J. SHERMA AND L. H. PIGNOLET, *Anal. Chim. Acta*, 34 (1966) 185.
5 J. SHERMA AND D. W. THOMPSON, *Anal. Chim. Acta*, 32 (1965) 181.
6 D. LOCKE AND J. SHERMA, *Anal. Chim. Acta*, 25 (1961) 312.
7 H. H. STRAIN, *Ann. Priestley Lectures*, 32 (1958).
8 H. H. STRAIN, *Carnegie Inst. Wash. Publ.*, 490 (1938).
9 A. K. KHUDAIRI, *Biochim. Biophys. Acta*, 46 (1961) 344.
10 F. T. WOLF, *Plant Physiol.*, 38 (1963) 649.

Analytica Chimica Acta
Elsevier Publishing Company, Amsterdam
Printed in The Netherlands

DÜNNSCHICHTCHROMATOGRAPHISCHE TRENNUNG UND BESTIMMUNG VON URONSÄUREN UND URONSÄURELACTONEN

W. ERNST
Chemische Abteilung, Institut für Meeresforschung, Bremerhaven

(Eingegangen am 4. April, 1967)

Im Zusammenhang mit der Untersuchung von Polysaccharidfraktionen benötigten wir ein Verfahren zur Trennung und Bestimmung verschiedener Uronsäuren im Mikrogramm-Bereich in Gegenwart neutraler Monosaccharide. Kleine Mengen von Salzen und Säuren, die durch den Gang der Aufarbeitung in die Analysenprobe gelangen, sollten ohne Einfluss sein. Im Hinblick auf die geringen zur Verfügung stehenden Mengen sowie auf eine rasche Durchführbarkeit der Trennung kam eine dünnschichtchromatographische Methode in Betracht.

Eine den gestellten Anforderungen genügende Trennung war mit den bisher in der Literatur beschriebenen dünnschichtchromatographischen Trennverfahren an borsäurehaltigem Kieselgel G[1] und an Cellulose[2] nicht möglich. Erfolgversprechend erschien jedoch die Trennung an Kieselgur G-Schichten, die mit Phosphatpuffer imprägniert waren. Eine gute Trennung verschiedener Kohlenhydratkomponenten wurde von WALDI[3] an derartigen Schichten erzielt, nachdem von JAYME UND KNOLLE[4] die Brauchbarkeit von phosphatimprägniertem Glasfaserpapier zur Trennung von Kohlenhydraten vorgeschlagen worden war. Durch Standardisierung der phosphatgepufferten Kieselgur G-Schichten sowie der Auftragetechnik konnten wir auch für Uronsäuren gute Trennungen erzielen, die auch zu ihrer quantitativen Bestimmung mit Hilfe von Naphthoresorcin geeignet waren. Die quantitative Bestimmung wurde zunächst für Galacturon- und Glucuronsäure ausgearbeitet.

VERSUCHSERGEBNISSE

Trennungen

Gute Trennungen an phosphatgepufferten Kieselgur G-Schichten werden mit Aceton–Butanol–Natriumphosphat-Puffer (0.1 M NaH_2PO_4) = 40:25:35 bei Kammerübersättigung und Raumtemperatur erhalten. Mit diesem Fliessmittel liegen Galacturonsäure, Guluronsäure, Glucuronsäure und Mannuronsäure bei 15 cm Laufstrecke im Mittelfeld des Chromatogramms mit R_F-Werten von 0.4–0.6. Die untere Nachweisgrenze liegt bei ca. 0.5 μg. Glucuronsäure und Galacturonsäure lassen sich bis zu 50 μg in jedem beliebigen Verhältnis trennen. Ähnliche Mengenverhältnisse ergeben sich bei der Trennung von Guluron- und Mannuronsäure. Eine einwandfreie Trennung aller vier Uronsäuren wird bis zu 5 μg je Uronsäure erreicht. Die Lactone von Glucuronsäure, Guluronsäure und Mannuronsäure lassen sich mit demselben Fliessmittel gut trennen und haben R_F-Werte zwischen 0.76 und 0.94.

Die in Polysaccharidfraktionen häufig vorkommenden Kohlenhydratkomponenten wie Glucose, Mannose, Galactose, Arabinose, Xylose, Fucose und Rhamnose liegen oberhalb der Uronsäureflecken und stören die Trennung der Uronsäuren nicht, wenn ihre Gesamtmenge nicht mehr als 100 μg je aufgetragene Analysenprobe auf 2 cm Startlänge beträgt. Die Versuche wurden mit einer Zuckermischung durchgeführt, in der die genannten Komponenten in etwa äquimolarer Mischung vorlagen. In Gegenwart derartiger Kohlenhydratkomponenten ist eine Trennung der Uronsäurelactone wegen der gleichartigen R_F-Werte nicht möglich.

Die Trennschichten sollen möglichst gleichmässig sein, da grössere Schichtdickenunterschiede Veränderungen der R_F-Werte zur Folge haben. Zu stark getrocknete Trennschichten wirken sich nachteilig auf die Trennschärfe aus. Aus diesem Grunde empfiehlt sich eine Aufbewahrung der Platten über Wasser im Exsiccator, wenn sie längere Zeit gelagert werden sollen. Weiterhin ist aus dem gleichen Grunde während des Zwischentrocknens der Schicht beim Auftragen der Substanzlösung nur Kaltluft anzuwenden, wobei die Trennplatte oberhalb der Startlinie mit einer Schablone abgedeckt wird. Keinen wesentlichen Einfluss auf die Qualität der Trennung haben Schwefelsäure, Essigsäure, Barium- und Natriumacetat in einer Konzentration von 0.1 N. Natriumchlorid und Salzsäure stören in Konzentrationen über 0.05 N. Abbildung 1 gibt die Trennqualität für verschiedene Substanzmischungen wieder.

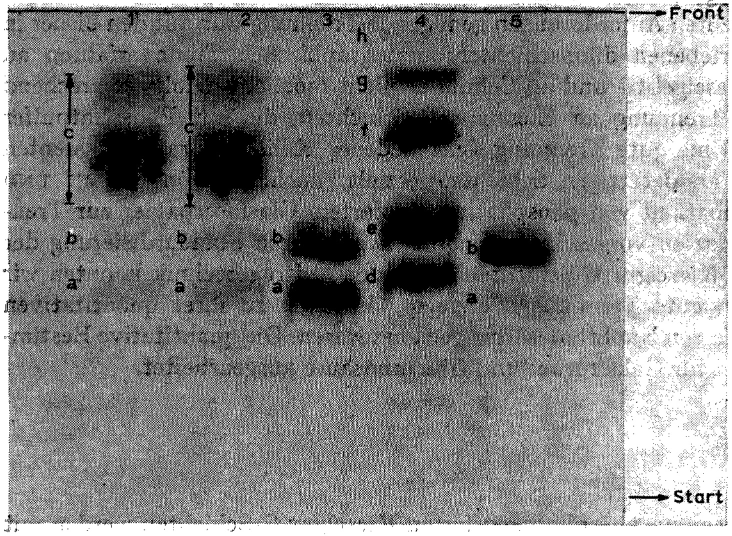

Abb. 1. Auftrennung verschiedener Uronsäuregemische. (1) 2.5 μg Galacturonsäure (a) + 2.5 μg Glucuronsäure (b) + 110 μg neutrales Monosaccharidgemisch (s. Text) (c); (2) wie (1), aber je 5.0 μg Uronsäure; (3) 40.0 μg Galacturonsäure (a) + 40.0 μg Glucuronsäure (b); (4) Alginsäurehydrolysat: Guluronsäure (d), Manuronsäure (e), Manuronlacton (f), Guluronlacton (h), + Glucuronlacton (g); (5) 1.25 μg Galacturonsäure (a) + 50.0 μg Glucuronsäure (b).

Sichtbarmachung und quantitative Auswertung der Substanzflecken

Als Reagens zur Detektion und quantitativen Bestimmung der Uronsäuren eignet sich Naphthoresorcin, das bekanntlich mit Uronsäuren, Uronsäurelactonen, aber auch mit anderen Kohlenhydratkomponenten beim Erwärmen vorwiegend blaue Farbstoffe bildet. Das Reagens wurde in wässrig-schwefelsaurer Lösung und in alkoholisch-phosphorsaurer Lösung verschiedener Konzentration verwendet. Die besten Werte ergaben sich bei Anwendung einer ca. 0.5%igen alkoholisch-phosphorsauren Lösung, die sich gleichmässig aufsprühen lässt. Der auf den Trennschichten erzeugte Farbstoff lässt sich leicht mit Essigsäureäthylester extrahieren. Die blauvioletten Farbstoffextrakte wurden bei 565 nm photometriert. Es zeigte sich in zahlreichen Versuchen, dass auf jeweils einer Trennplatte im Bereich von 0–15 µg für Galacturonsäure und Glucuronsäure das Beersche Gesetz erfüllt ist. Die Farbausbeute kann jedoch von Platte zu Platte stärkeren Schwankungen unterliegen, so dass auf jeder Trennplatte zur Festlegung der Eichgeraden ein Testgemisch beider Uronsäuren mitentwickelt werden muss. Die unterschiedlichen Farbausbeuten sind zurückzuführen auf Unterschiede bei der Erwärmung der Platten sowie unterschiedliche Reagenschargen. Auch sind die Farbausbeuten für beide Uronsäuren unterschiedlich. Galacturonsäure liefert eine um 25% höhere Farbausbeute als Glucuronsäure. Die Ausdehnung der quantitativen Bestimmung auf den Bereich von 20–50 µg ist möglich, wenn man eine Testmischung von 30 µg je Uronsäure mitverarbeitet. Durch die Verwendung einer Testmischung kann auf besondere Massnahmen bei der Erwärmung der besprühten Trennplatten bei der Farbstoffentwicklung verzichtet werden. Als günstig hat sich ein Temperaturbereich von 105–110° im Trockenschrank erwiesen. Bei dieser Temperatur genügt eine Erhitzungsdauer von 15 Min. Kürzere Zeiten ergeben keine genügende Farbstoffbildung, während längere Zeiten eine stärkere Untergrundverfärbung und damit höhere Leerwerte zur Folge haben. Bei der Bestimmung der Uronsäuren in Gegenwart neutraler Monosaccharide müssen die Uronsäurelactone vor der Trennung entlactonisiert werden.

ARBEITSVORSCHRIFT ZUR BESTIMMUNG DER URONSÄUREN

Erforderliche Reagenzien

Fliessmittel: Aceton–Butanol–Phosphatpuffer = 40:25:35 (V/V). Aceton, p.a., Butanol, p.a. Merck, wässrige 0.1 *M* NaH_2PO_4.

Sprühreagens: 0.5 g Naphthoresorcin, Merck, + 100 ml Äthanol + 10 ml 85%ige H_3PO_4.

Testlösung: 10 µl Lösung enthalten je 10 µg Galacturonsäure und Glucuronsäure bzw. 30 µg beider Säuren.

Beschichtung der Trennplatten

Zur Beschichtung von fünf 20 × 20 cm Glasplatten werden 25 g Kieselgur G (Merck) mit 50 ml Phosphatpuffer (wässrige 0.1 *M* NaH_2PO_4, p.a.) verrieben und mit einem Streichgerät in einer Schichtdicke von 0.25 mm aufgetragen. Die Schichten werden bei Raumtemperatur über Nacht getrocknet und am anderen Tage benutzt oder über Wasser in einem Exsiccator aufbewahrt.

Auftragen der Probelösungen

Mit einer 25-µl Hamiltonspritze werden 10 µl Lösung in zwei Portionen von je 5 µl auf eine Startlinie von 2 cm aufgetragen. Nach Auftragung der ersten 5 µl wird mit Kaltluft zwischengetrocknet, wobei die Platte oberhalb der Startlinie mit einer Schablone abgedeckt wird. Der Abstand zwischen Startlinie und unterem Plattenrand beträgt 1.5–2 cm. Vor der Entwicklung müssen die Flecken vollkommen trocken sein. Auf eine Platte können vier Analysenlösungen und eine Testlösung aufgetragen werden.

Entwicklung

Die Trennkammer wird mit Fliesspapier ausgekleidet und mindestens 15 Min vor dem Einstellen der Platte mit 100 ml Fliessmittel beschickt, wobei die Papierauskleidung vollständig benetzt werden muss. Die Entwicklung wird bei Raumtemperatur mit einer Laufstrecke von 15 cm durchgeführt und ist nach ca. 110–130 Min beendet. Die Trennplatten werden nach dem Herausnehmen 10 Min an der Luft und anschliessend 10 Min im Trockenschrank bei 105–110° getrocknet. Nach dem Abkühlen wird mit Reagenslösung besprüht. Hierzu werden auf den mittleren Teil der Lauffläche von 9 x 20 cm (3 cm über der Startlinie bis 3 cm unterhalb der Frontlinie) durch strichweises horizontales Besprühen 8–10 ml Reagenslösung unter gleichmässiger Befeuchtung der Platte aufgetragen. Die so behandelte Platte wird noch 5 Min bei Raumtemperatur liegengelassen und dann 15 Min bei 105–110° im Trockenschrank erwärmt. Danach lässt man 15–20 Min bei Raumtemperatur abkühlen. Die Uronsäuren erscheinen als blaue Flecken.

Quantitative Auswertung

Zur quantitativen Bestimmung der getrennten Uronsäuren wird die Platte aufrecht gestellt, der betreffende Substanzfleck mit der Schmalseite eines Objektträgers ausgeschabt und in ein kleines Reagensglas übergeführt. Die ausgeschabte Fläche beträgt ca. 2–3 cm². Der isolierte Fleck wird mit 3 ml Essigsäureäthylester (DAB 6, Merck) durchgeschüttelt und nach Zusatz von 0.2 ml 2 *N* Schwefelsäure nochmals gut geschüttelt. In gleicher Weise werden die Flecken der Testmischung sowie ein als Leerwert dienendes flächengleiches Stück des Untergrundes behandelt. Die Extrakte werden durch ein kleines Faltenfilter in 1 cm Küvetten filtriert und bei 565 nm gegen den Leerwert gemessen. Zur Berechnung wird die gefundene Extinktion mit dem Eichwert multipliziert. Als Ergebnis erhält man die im aufgetragenen Probevolumen enthaltenen µg Uronsäure. Der Eichwert wird mit Hilfe der jeweils mitent-

TABELLE I

(A–C) Trennung und Bestimmung von 11 Mischungen von Galacturon- und Glucuronsäure in verschiedenen Mischungsverhältnissen; (D) Bestimmung von Glucuronlacton nach vorheriger Entlactonisierung und chromatographischer Entwicklung; (E) wie D, aber in Gegenwart von 110 µg eines Gemisches von Monosacchariden (Glucose, Mannose, Galactose, Fructose, Rhamnose, Xylose u. Arabinose in etwa äquimolarer Mischung). In µg.

Uronsäure	*A*		*B*		*C*		*D*		*E*	
	geg.	*gef.*	*geg.*	*gef.*	*geg.*	*gef.*	*geg.*	*gef.*	*geg.*	*gef.*
Galacturon	1.25	1.2	12.0	12.5	20.0	20.6				
Glucuron	1.25	1.1	46.0	42.8	20.0	20.2				
Galacturon	2.50	2.7	50.0	46.5	40.0	39.2				
Glucuron	2.50	2.5	1.25	0.9	40.0	40.7				
Galacturon	5.0	5.4	2.5	2.6	50.0	47.0				
Glucuron	5.0	5.2	15.0	15.0	50.0	46.3				
Galacturon	15.0	15.1	5.0	5.3						
Glucuron	15.0	15.0	30.0	27.9						
							2.4	2.3	2.4	2.2
							9.5	9.6	4.7	5.2
							14.2	14.8	9.5	9.6

wickelten bekannten Menge Testsubstanz bestimmt. Hierzu wird die µg-Menge der betreffenden Test-Uronsäure durch die hierfür gefundene Extinktion dividiert. Der Eichwert gilt jeweils für eine Platte und muss für jede Platte und jede Uronsäure gesondert bestimmt werden. Für den Bereich von 0–20 µg je Uronsäure werden je 10 µg Testsubstanz, für 20–50 µg je 30 µg Testsubstanz mitentwickelt. Ergibt sich beispielsweise für 10 µg Glucuronsäuretest eine Extinktion von 0.210, so beträgt der Eichwert 10 : 0.210 = 47.6.

Arbeitsweise bei Anwesenheit von Lactonen. In Gegenwart von neutralen Monosacchariden müssen Uronsäurelactone zu ihrem Nachweis und zur quantitativen Bestimmung entlactonisiert werden: 1 ml der neutralen Probelösung mit maximal 5 mg Uronsäure werden mit 25 µl 2 *N* NaOH versetzt, nach 15 Min. Stehen bei Raumtemperatur mit 30 µl 2 *N* Essigsäure angesäuert und anschliessend für die beschriebene Uronsäurebestimmung verwendet. In Abwesenheit von neutralen Monosacchariden kann die Lactonzone gesondert bestimmt werden, wobei die Besprühung mit dem Reagens bis zur Frontlinie erfolgt.

Beleganalysen

In Tab. I sind die Ergebnisse einiger Beleganalysen von verschiedenen Uronsäuregemischen zusammengestellt.

DISKUSSION

Durch die relativ hohe Beladbarkeit der Schichten von 1–50 µg im Falle von Galacturon- und Glucuronsäure bzw. Guluron- und Mannuronsäure ergibt sich eine grosse Variabilität hinsichtlich der zu untersuchenden Substanzmischungen. Die Bestimmung der Uronsäuren in Polysacchariden ist ohne Abtrennung der neutralen Monosaccharide nach der hydrolytischen Spaltung noch möglich, wenn der Uronsäuregehalt 2–3% beträgt. Die in Polysaccharidfraktionen des Meeresbodens in geringen Mengen vorkommenden Uronsäuren[5] konnten mit diesem Verfahren bestimmt werden, worüber an anderer Stelle berichtet werden wird. Sollen die neutralen Monosaccharide vor der Bestimmung der Gesamt-Uronsäuren an Anionenaustauschern abgetrennt werden, so ist vorher eine Entlactonisierung eventuell vorhandener Uronsäurelactone erforderlich. Da sich mit demselben Fliessmittel auch die Uronsäurelactone sehr gut trennen lassen, bietet einerseits die Überführung der Uronsäuren in ihre Lactone eine weitere Möglichkeit zu ihrer Identifizierung. Andererseits kann hierdurch das Mengenverhältnis von Lacton zu freien Uronsäuren in ihren Mischungen auf ein und derselben Platte bestimmt werden. Beispielsweise geben Alginsäurehydrolysate bei der Auftrennung nach dem beschriebenen Verfahren im allgemeinen vier Flecken, die, nach steigendem R_F-Wert geordnet, mit Guluronsäure, Mannuronsäure, Mannuron- und Guluronlacton identisch sind.

Frau R. Ernst und Frl. I. Johannsen danke ich für ihre Mitarbeit. Der Deutschen Forschungsgemeinschaft danke ich für die Gewährung von Sachmitteln.

ZUSAMMENFASSUNG

Es wird eine neue Methode zur dünnschichtchromatographischen Trennung

von Galacturon-, Glucuron-, Mannuron- und Guluronsäure sowie der entsprechenden Uronsäurelactone mitgeteilt. Die quantitative Bestimmung der Galacturon- und Glucuronsäure in beliebigen Mischungen von 1–50 µg wird beschrieben. Neutrale Monosaccharide in Mengen bis zu 100 µg sowie geringere Konzentrationen anorganischer Verbindungen stören die Trennung nicht.

SUMMARY

A new method for the separation of galacturonic, glucuronic, mannuronic and guluronic acid and the corresponding lactones by thin-layer chromatography is described. The determination of mixtures of galacturonic and glucuronic acid (1–50 µg) is described. Neutral monosaccharides up to 100 µg and lower concentrations of inorganic materials do not interfere with the separation.

RÉSUMÉ

Une nouvelle méthode par chromatographie en couches minces est décrite pour la séparation des acides galacturonique, glucuronique, mannuronique et guluronique, et des lactones correspondantes. On propose un dosage quantitatif des acides galacturonique et glucuronique dans des mélanges de 1–50 µg.

LITERATUR

1 G. Pastuska, *Z. Anal. Chem.*, 179 (1961) 427.
2 A. Schweiger, *J. Chromatog.*, 9 (1962) 374.
3 D. Waldi, *J. Chromatog.*, 18 (1965) 417.
4 G. Jayme und H. Knolle, *Angew. Chem.*, 68 (1956) 243.
5 W. Ernst, *Veroeffentl. Inst. Meeresforsch. Bremerhaven*, 10 (1966) 81.

Analytica Chimica Acta
Elsevier Publishing Company, Amsterdam
Printed in The Netherlands

SHORT COMMUNICATIONS

On the form of the curves of continuous variation

The form of the curves of continuous variation has been discussed by different authors. An equation describing the curves of complexes of the type AB has been given by Schwarzenbach[1]. This group of complexes is characterized by their convex curves without inversions or concave parts, the gradient at each end having a finite value. Asmus[2] plotted theoretical curves for some complexes of the general form AB_n; for values of $n \geqq 2$ he obtained curves with an inversion, a corresponding concave curve part and a parabolic approach to the end-point. Klausen and Langmyhr[3] plotted theoretical curves for A_2B_2 complexes.

In a recent paper, Buděšínský[4] discussed the method of continuous variation and the molar ratio method, with particular regard to the forms of the curves obtained by these methods and their use for determining the conditional constants of very stable complexes. Buděšínský maintained that previous publications by himself, Asmus and the present authors are erroneous in regard to the form of the curves of continuous variation.

The present, rather confusing, discrepancies concerning the form of the curves

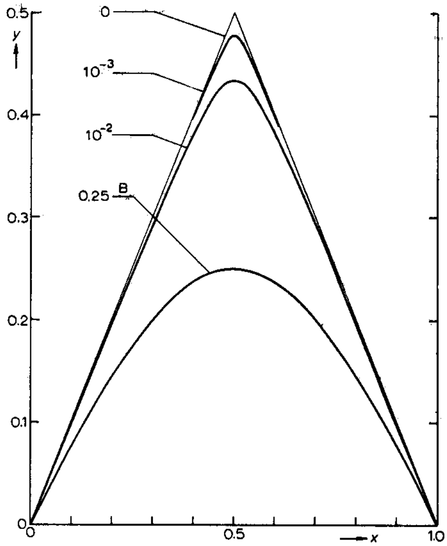

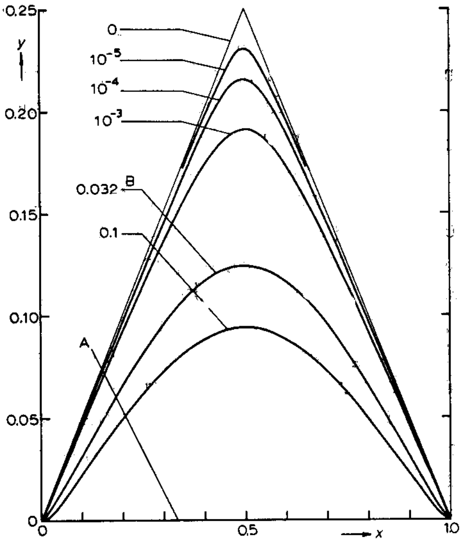

Fig. 1. Theoretical curves of continuous variation for a series of AB complexes with different values of $1/Kc$. The curve for $1/Kc = 0.25$ was obtained from earlier data[4] for the total molar concentration (c) of the reactants and the lower limiting value of the stability constant.

Fig. 2. Theoretical curves of continuous variation for a series of A_2B_2 complexes with different values of $1/Kc^3$. A = tangential line (see text). The curve B ($1/Kc^3 = 0.032$) was obtained from earlier data[4] for the total molar concentration (c) of the reactants and the lower limiting value of the stability constant.

of continuous variation made it seem desirable to construct a new series of theoretical curves, preferably with the use of a computer.

Theoretical curves of continuous variation

With the aid of a computer, theoretical curves were plotted for complexes of the composition AB, A_2B_2, AB_2 and AB_3, and for each composition curves were calculated for different values of $1/Kc$, $1/Kc^3$, $1/Kc^2$ and $1/Kc^3$, respectively (K representing the stability constant and c the total molar concentration of the reactants). The curves were constructed from the following equation[3]:

$$(1-x-my)^m\,(x-ny)^n-(1/Kc^{m+n-1})\,y=0, \quad \text{where } y=[A_mB_n]/c.$$

From this equation it can be seen that $1/Kc^{m+n-1}$ is the parameter that determines the deviation from the curve of the infinitely stable complex. The curves obtained are reproduced in Figs. 1–4, in which the straight lines representing the infinitely stable complexes are also given.

In accordance with the previous theoretical curves given by ASMUS[2] and by KLAUSEN AND LANGMYHR[3], and in contrast to the other results[4], the curves for the A_2B_2, AB_2 and AB_3 complexes exhibit inversions with corresponding concave curve parts and parabolic approaches to the end-points. These characteristic features are thus present in all theoretical and experimental curves of all complexes of the type A_mB_n, m and/or $n \geqq 2$. (It should be noted, however, that the inversions, the concave parts and the parabolic approaches to the end-points are less easily observed as the stability of the complex increases.)*

Accordingly, the statement[4] that the only reason for the appearance of inversions, concave parts and parabolic approaches to the end-points is the presence of unwanted species or side reactions, is not correct. This statement is based upon theoretical considerations, but when the calculations are made as recommended[4], the equations become indeterminate so that no definite conclusions can be drawn.

The theoretical curves given in the above figures may be used to evaluate the applicability of the methods of BUDĚŠÍNSKÝ[4] and of SCHAEPPI AND TREADWELL[5] for determining stability constants from curves of continuous variation. These methods are based on drawing tangents to the curve from both end-points, so that the curve representing the infinitely stable complex is established. However, these authors were probably not aware of the fact that complexes of low stability of the form A_mB_n (m and/or $n \geqq 2$) exhibit curves with end branches of pronounced parabolic form; in these cases the tangents from the end-points do not represent the infinitely stable compound.

In order to obtain reasonably accurate data by the methods of BUDĚŠÍNSKÝ, and of SCHAEPPI AND TREADWELL, it is necessary that the stability be above a certain limiting value.

---

* From an unpublished mathematical treatment, one of the present authors (KSK) showed that for each of the above set of curves of a complex of a given composition, *e.g.* as found in one of the Figs. 2–4, the points obtained by drawing tangents to the curves from the left end-point lie on a straight line defined by the equation:

$$y=-(1/m)x+(n-1)/m(m+n-1) \quad (n \geqq 2)$$

This tangential line is shown on each of the Figs. 2–4; the line was found to be parallel to the right branch of the hypothetical curve of the infinitely stable complex.

The following approximate lower limiting values for the stability constant were estimated from the theoretical curves plotted in the Figs. 1–4:

$$K_{AB}=10^3/c,\quad K_{A_2B_2}=10^5/c^3,\quad K_{AB_2}=10^5/c^2,\quad \text{and}\quad K_{AB_3}=10^7/c^3$$

(where c again represents the total molar concentration of the reactants).

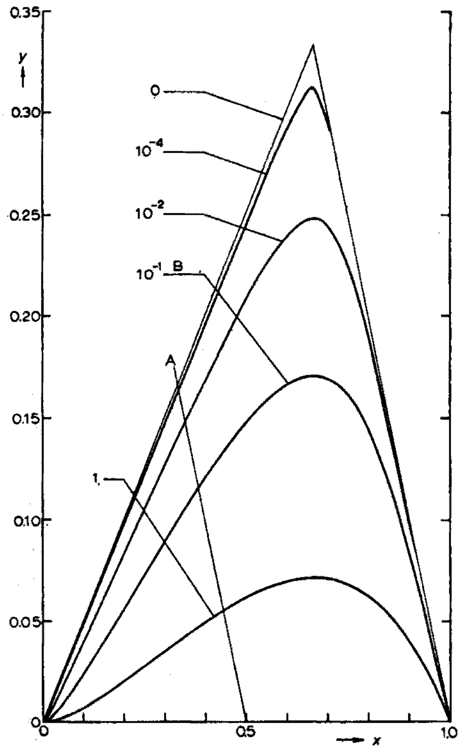

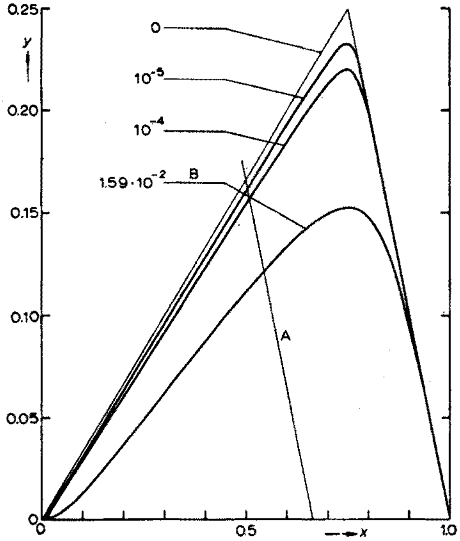

Fig. 3. Theoretical curves of continuous variation for a series of AB_2 complexes with different values of $1/Kc^2$. A = tangential line (see text). The curve B ($1Kc^2=10^{-1}$) was obtained from earlier data[4] for the total molar concentration (c) of the reactants and the lower limiting value of the stability constant.

Fig. 4. Theoretical curves of continuous variation for a series of AB_3 complexes with different values of $1/Kc^3$. A = tangential line (see text). The curve B ($1/Kc^3=1.59\cdot 10^{-2}$) was obtained from earlier data[4] for the total molar concentration (c) of the reactants and the lower limiting value of the stability constant.

Chemical Institute A,
University of Oslo,
Blindern (Norway)

K. S. KLAUSEN
F. J. LANGMYHR

1 G. SCHWARZENBACH, *Helv. Chim. Acta*, 32 (1949) 839.
2 E. ASMUS, *Z. Anal. Chem.*, 183 (1961) 321.
3 K. S. KLAUSEN AND F. J. LANGMYHR, *Anal. Chim. Acta*, 28 (1963) 335.
4 B. BUDĚŠÍNSKÝ, *Collection Czech. Chem. Commun.*, 32 (1967) 235.
5 Y. SCHAEPPI AND W. D. TREADWELL, *Helv. Chim. Acta*, 31 (1948) 577.

(Received May 1st, 1967)

The spectrophotometric determination of hyponitrite

A spectrophotometric method for the determination of hyponitrite ($N_2O_2^{2-}$) in alkaline solution has been proposed by ADDISON *et al.*[1], who reviewed the previous literature on the absorption spectra of hyponitrites; these investigators found $\log \varepsilon_{max} = 3.60$ for the species $N_2O_2^{2-}$ at 248 nm but this value seems to require revision.

Moderate concentrations of hyponitrous acid in acidic solution can be determined[2] by the old precipitation method. No spectrophotometric method for this species seems to have been available; a procedure is suggested below.

Reagents and equipment

Sodium hyponitrite and pure $Ag_2N_2O_2$ were prepared by published methods[3]. To obtain a stable solution of hyponitrous acid by the interaction of hydrochloric acid and silver hyponitrite, it is essential to use an excess of as pure as possible silver hyponitrite. The first filtrate usually contains colloidal silver chloride. A convenient method of removing the colloidal suspension is to let the solution pass through the same filter repeatedly.

The concentration of the hyponitrous acid solution (usually around 0.04 *M*) was determined by the precipitation method[2] with the normal titrimetric accuracy. The room temperature was kept at 20°. To check for the stability of the solutions, each time 4 precipitations were made within a few minutes (the back-titrations could be performed later). Between the second and third precipitations, a sample of the hyponitrous acid solution was diluted, or dropped into 50 ml of 2 *M* sodium hydroxide and then diluted to the appropriate concentration.

Three U.V.-spectrophotometers were used in order to establish the reproducibility of the results: Hilger H.700, Cary M14, and Zeiss PM QII.

Absorption spectra

The species $N_2O_2^{2-}$ in alkaline solution shows a normally shaped peak. The maximum has been reported as lying at 248 nm[1,4] and at 247 nm[5]. In the present work, this maximum was found at 247 nm, and the half band width, $\Delta\nu$, was 36 nm.

The spectra of $H_2N_2O_2$ and $HN_2O_2^-$ exhibit a peak accompanied by a weak shoulder. The spectra of the following mixtures were studied: (*a*) $H_2N_2O_2$ in pure aqueous solution, (*b*) $H_2N_2O_2$ in 10^{-2} and 10^{-3} *M* hydrochloric acid, and (*c*) $HN_2O_2^-$ in 10^{-2} *M* borax (pH 9.2). The peak maximum of $H_2N_2O_2$ was found at 208 nm with $\Delta\nu = 27$ nm, and its shoulder at 242 ± 2 nm when hydrochloric acid was present. Pure aqueous solutions of hyponitrous acid have a pH around 4. In such solutions the ratio $(HN_2O_2^-)/(H_2N_2O_2)$ becomes appreciable and the peak of $HN_2O_2^-$ overlaps with the shoulder of $H_2N_2O_2$. At pH 9.2, the peak maximum of $HN_2O_2^-$ was found at 232 nm with $\Delta\nu = 47$ nm, and its shoulder at 280 ± 3 nm. BUCHHOLZ *et al.*[5] reported the peak maximum of $H_2N_2O_2$ at 207 nm and that of $HN_2O_2^-$ at 232 nm.

Molar extinction coefficients

In the acidic solutions of hyponitrous acid, a little ethanol was added (1%, v/v) to secure stabilization[5]. For the peak of hyponitrous acid at 208 nm, ε_{max} was found to be $4.61\ (\pm 0.02) \cdot 10^3$. This value is not affected by a variation in the hydrochloric acid concentration in the region 10^{-3}–10^{-2} *M*. Beer's law is obeyed up to hyponitrous acid concentrations of at least $3 \cdot 10^{-4}$ *M*. Higher concentrations of hyponitrous acid in acidic solution can be measured at 240 nm, where ε_{240} was found to be 2.4 (±0.1) · 10^2. These two values of ε are based on the determination of the hyponitrous acid concentration by the precipitation method. The value given for ε_{240} expresses the resultant absorption caused by both the bands with λ_{max} 208 nm (strong) and 242 nm (very weak) respectively. The latter seems to have ε_{max} considerably less than ε_{240}. This makes the analysis of the shoulder into components unreliable.

Owing to the very well known instability of $HN_2O_2^-$ there can be no question of accurate measurement of the ε_{232} value of this species. For general spectroscopic considerations the value $\varepsilon_{232} = 7.7\ (\pm 0.4) \cdot 10^3$ is satisfactory. This was estimated by extrapolation of the measurements back to the moment when 10 ml of a standard aqueous solution of hyponitrous acid were added to a borax solution. If the shoulder is analyzed into a component band with $\lambda_{max} = 280$ nm, this weak band seems to have a molar extinction coefficient equal to $0.25 \cdot \varepsilon_{232}$ and a $\Delta\nu$ of 41 nm.

Two independent methods were used (each in triplicate) to determine the molar extinction coefficient of the species $N_2O_2^{2-}$.

Method I. 20.00 ml of an aqueous *ca.* 0.04 *M* hyponitrous acid solution (accurately determined by 4 precipitations as described above) were added dropwise and with good agitation to a 100-ml volumetric flask containing 50 ml of 2 *M* sodium hydroxide. This was diluted to obtain a series of appropriate concentrations of sodium hyponitrite in 1 *M* sodium hydroxide.

Method II. Single perfectly grown crystals[6] of $Na_2N_2O_2 \cdot 6H_2O$ were used as a standard.

Both methods gave the same results: $\varepsilon_{max} = 6.55\ (\pm 0.2) \cdot 10^3$ for $N_2O_2^{2-}$.Beer's law was obeyed up to a concentration of $1.5 \cdot 10^{-4}$ *M*.

To ensure stability and suppress hydrolysis of $N_2O_2^{2-}$ to $HN_2O_2^-$, alkali concentrations as high as 1 *M* are recommended. In 0.2 *M* sodium hydroxide, ε_{max} was found to be smaller by 4%.

Discussion

ADDISON *et al.*[1] reported $\log \varepsilon_{max} = 3.60$, which corresponds to $\varepsilon_{max} = 4.0 \cdot 10^3$ for the hyponitrite ion; this value is less than two-thirds of the value found in this work. These investigators used as a standard pure anhydrous sodium hyponitrite. However, when this anhydrous salt is mixed with water, heat is evolved (calorimetric measurements on this reaction are not available); some of the hyponitrite may thus decompose during dissolution and this may be the reason why ADDISON *et al.* found low values for the extinction coefficient. Presumably hyponitrite does not decompose during the dissolution of $Na_2N_2O_2 \cdot 6H_2O$ because it is hydrated already.

Another partial cause for the discrepancy may be that ADDISON *et al.* used 0.1 *M* sodium hydroxide as solvent. Technical instrumental defects can be ignored, because their results for sodium nitrite agree with those found in the present work ($\varepsilon_{max} = 23.0$ and 22.64(±0.1) in 0.1–1 *M* sodium hydroxide, respectively).

The precipitation method is not likely to produce high values for hyponitrous acid in acidic solution by a coprecipitation of atmospheric carbon dioxide; silver carbonate cannot coprecipitate with silver hyponitrite at pH 4.5–5[2], unless the carbonate concentration exceeds 0.01 *M*. Low results might be expected because of the slight solubility of silver hyponitrite, but this is suppressed by the excess of silver(I).

Finally, the concordance of the molar extinction value of hyponitrite, as determined by the precipitation method, with that based on the theoretical composition of $Na_2N_2O_2 \cdot 6H_2O$, suggests that the precipitation method is sufficiently accurate, within the limits of its precision (1%)[2].

The authors gratefully acknowledge the support of this work by the Royal Hellenic Research Foundation. They are also indebted to the Greek Atomic Energy Committee for permission to use their equipment.

Laboratory of Physical Chemistry,
University of Athens,
Navarinou 13 A.,
Athens-144(Greece)

C. N. Polydoropoulos
S. D. Voliotis

1 C. C. Addison, G. A. Gamlen and R. Thompson, *J. Chem. Soc.*, (1952) 338.
2 C. N. Polydoropoulos and M. Pipinis, *Chim. Chronika (Athens, Greece)*, 28A (1963) 107.
3 C. N. Polydoropoulos, *Chem. Ind. (London)*, (1963) 1686.
4 G. Kortüm and B. Finckh, *Z. Physik. Chem.*, B48 (1941) 32.
5 J. R. Buchholz and R. E. Powell, *J. Am. Chem. Soc.*, 85 (1963) 509.
6 C. N. Polydoropoulos and S. D. Voliotis, to be published.

(Received May 31st, 1967)

BOOK REVIEW

Organometallic Compounds. Methods of Synthesis, Physical Constants, and Chemical Reactions. Vol. II. Compounds of Germanium, Tin and Lead, Edited by M. Dub, 2nd Edn., Springer-Verlag, Berlin, 1967, xix+697 pp., price DM 98,—; $24.50.

This second volume in the series covers the literature on germanium, tin and lead compounds from 1937 to 1964. As in the first volume, the survey is comprehensive and uncritical. In addition to references covering methods of preparation, properties and reactions, there are various references to biological and physiological activity and to commercial applications. These last serve to emphasize the practical importance of these compounds and the intensive industrial work which has been done in this area of chemistry.

The production is up to the standard set by the first volume and the series is clearly a "must" for reference libraries.

E. J. Forbes (Birmingham)

Journal of

RADIOANALYTICAL CHEMISTRY

An International Journal Dealing with all
Aspects of Nuclear Analytical Chemistry

JOURNAL OF RADIOANALYTICAL CHEMISTRY intends to serve as the organ for collecting from all sources original papers, notes, letters to the editor and preliminary notes in the field of nuclear analytical chemistry which up till now have been published in various general analytical and radiochemical journals.

The main subjects covered are:

- Activation analysis
- Radiometric analysis
- Radioreagent analysis and radiometric titration
- Isotope dilution analysis
- Beta-, gamma- and X-ray and neutron absorption and back-scattering
- Analytical separations involving isotopes
- Instrumentation for radioanalytical chemistry

A Bibliography Section will also be included.

PUBLICATION will be in one volume of six issues per year.

LANGUAGES will be English, French and German, but manuscripts should preferably be submitted in English.

MANUSCRIPTS should be sent to the Co-ordinating Editor: Dr. T. Braun, Institute of Inorganic and Analytical Chemistry, L. Eötvös University, Múzeum krt. 4/b, Budapest VIII, Hungary.

SUBSCRIPTION price is £8.5.0, US$22.50, Dfl. 82.50 per volume plus postage. Subscription orders and requests for specimen copies may be sent to your usual supplier or to

ELSEVIER PUBLISHING COMPANY

P.O. BOX 211 - AMSTERDAM - THE NETHERLANDS

VOL. 40 NO. 1 ANALYTICA CHIMICA ACTA JANUARY 1968

CONTENTS

Pigments

An Introduction to their Physical Chemistry

edited by David Patterson

Senior Lecturer, Department of Colour Chemistry, University of Leeds, Great Br

5½ × 8½", ix + 210 pages, 93 illus., 1967, Dfl. 32.50, 65s., US $ 12.00

In this book the principles of physical chemistry are applied to the problems of making using the insoluble organic and inorganic pigments manufactured for use in paints, prin inks, plastics and synthetic fibres. Development over many years has resulted in a high de of technical quality in many of these pigments, achieved by purely empirical methods, bu use of such methods means that each case must be judged on its merits. On the other h the application of physico-chemical theories can bring unifying concepts to a wide rang phenomena, and provide a deeper understanding of the processes involved.
It is quite insufficient to treat the making of pigments as the synthesis of certain compou and to emphasize this the purely preparative chemistry of pigments has been left outside scope of this book. Instead, pigments are regarded as substances produced to exert partic optical effects on certain media by colouring and opacifying them. The ways in which ments can be prepared to carry out these functions, together with the appropriate technic for appraising their performance of them are consequently the main content of the book the problems cannot be solved at present, but this book by showing what can be achi and attempting to provide signposts to some of the unexplored areas, will undoubtedly sti late and encourage further work in a field that is of considerable industrial importance.

Contents

ELSEVIER PUBLISHING COMPANY
AMSTERDAM LONDON NEW YOR]

121E

2 3 H.A. 2511